Polyethylenimine- and lipid- based nanoparticles as gene and drug delivery systems for aerosol therapy to the lung

Dissertation

zur

Erlangung des Doktorgrades

der Naturwissenschaften

(Dr. rer. nat.)

dem

Fachbereich Pharmazie

der Philipps Universität Marburg

vorgelegt von

Elke Kleemann

aus Leipzig

Marburg/Lahn 2005

Vom Fachbereich Pharmazie

der Philipps-Universität Marburg als Dissertation am 24. Mai 2005 angenommen.

Erstgutachter: Prof. Dr. Thomas Kissel

Zweitgutachter: Prof. Dr. Werner Seeger

Tag der mündlichen Prüfung am 25.Mai 2005

Die vorliegende Arbeit

entstand auf Anregung und unter Anleitung von

Herrn Prof. Dr. Thomas Kissel

am Institut für Pharmazeutische Technologie und Biopharmazie

der Philipps-Universität Marburg

und in enger Zusammenarbeit mit der Arbeitsgruppe von

Herrn Prof. Dr. Werner Seeger

im Fachbereich Innere Medizin / Pneumologie,

Justus-Liebig-Universität Gießen

meinen Eltern

Angelika & Thomas Kleemann

in Liebe und Dankbarkeit

Danksagung

Table of Contents

Chapter 1

General introduction

INHALATION – A BRIEF OVERVIEW OF PULMONARY DRUG DELIVERY

Aerosol inhalation as a route for pulmonary drug delivery is currently experiencing a period of tremendous growth. Indeed, the combination of a better understanding of lung pathogenesis and the overcoming of a number of issues related to aerosol delivery has presented new opportunities in the field of inhalation therapy [1, 2]. The significant growth in new technologies for drug delivery via inhalation has fuelled interest in employing aerosolized drugs for the treatment of respiratory diseases as well as systemic disorders [3, 4]. A large number of topical, respiratory drugs for an inhalation therapy already exists encompassing different classes (Table 1), and still the number of such formulations is rising [5, 6]. The disadvantages associated with the parenteral administration of drug substances, such as high doses or injection-related side reactions, pain, patient compliance and cost, have motivated researchers and manufacturers to develop pulmonary delivery systems for systemic drugs. In this respect, different non-peptide and peptide-based drugs such as insulin or the human growth hormone (hGH) have been reported to reach the systemic circulation following aerosol administration (Table 2). One recent breakthrough in pulmonary drug delivery, causing local and systemic reaction, is the development of cyclosporine, which was recently approved by the FDA as an immunosuppressant for post-lung transplantation patients [7].

Controlled drug delivery systems are becoming increasingly attractive options for inhalation therapies. The rationale of controlled drug delivery is to change the pharmacokinetic and pharmacodynamic behaviour of a drug substance by controlling its liberation, absorption and distribution [8]. Traditionally, the successful delivery of complex biomolecules, such as proteins, peptides or nucleotides, was only possible parenterally as such molecules are often temperature sensitive, instable at physiological pH and display a short half life. However, the development of novel drug carrier systems such as lipid- and polymer-based particles, chemical and biological drug-modification have been proposed to obtain controlled drug delivery systems for the lung [9-11]. It was demonstrated that the pulmonary administration of such new micro- and nano- scaling delivery systems is a suitable alternative to injection, even though the drugs must overcome numerous barriers in the lung to reach the site of action.

Utilizing such novel technologies, the lung as been recently explored as an important target organ for gene therapy of many acute and chronic diseases, including cancer, asthma, cystic fibrosis, alpha-1-antitrypsin deficiency and respiratory distress syndrome, among others [12, 13]. Of particular interest in this respect, is the polycation polyethylenimine, since it was

observed to serve as effective and protective vehicle for nucleotides. More detailed information concerning these topics will be introduced further on in this chapter.

Table 1. Aerosol drugs for topical treatment of pulmonary diseases (Abbreviations see page 185), approved or under development in human trials (*).

drug	drug class	trade name	diseases	references
tiotropium-bromid	anticholinergic-bronchodilator	Spiriva	COPD	[14]
budesonide	corticosteroid	Pulmicort	asthma, COPD	[15-17]
fenoterol	ß$_2$-sympathomimetic	Berodual	asthma	[18]
iloprost	prostaglandins	Ventavis	PAH	[19]
cromolyn sodium	mast cells stabilizer	Intal	allergic asthma	[20]
tobramycin	aminoglycoside-antibiotic	TOBI	CF, PAI	[21, 22]
pentamidine	chemotherapeutic	Pentacarinat	HIV, PCP	[23]
ribavirin	virus-static	Virazole	respiratory virus infection	[24, 25]
surfactant	phospholipid, protein mixture	Alveofact	ARDS	[26-28]
colistin	cyclopeptide-antibiotic	*	CF, PAI	[21, 23]
amphotericin B	peptide-fungicide	Amphotericin B	CF, HIV, fungal pneumonia	[4, 23]
alpha 1-antitrypsin	alpha 1-protease inhibitor	*	lung emphysema, CF, ARDS	[27, 29]

Table 2 Aerosol drugs for systemic treatment, approved or under development in human trials (*).

drug	drug class	trade name	diseases	references
insulin	peptide-hormone	Exubera	diabetes	[30, 31]
heparin	anticoagulants	*	thrombosis, emphysema	[32]

cyclosporine	immunosuppressant	Pulminiq	lung transplantation	[7, 33]
alpha 1-antitrypsin	alpha 1-protease inhibitor	*	alpha 1-anti-trypsin deficiency, congenital emphysema	[34, 35]
calcitonin	peptide-hormone	*	osteoporosis	[2, 36]
ergotamin	vasoconstrictor	*	migraine	[37]
hGH	peptide-hormone	*	growth hormone deficiency	[38]
leuprolide acetate	synthetic analogue of GnRH	*	infertility, breast & prostate cancer	[39, 40]

CELLULAR AND EXTRA CELLULAR BARRIERS IN PULMONARY DRUG DELIVERY – AN OVERVIEW OF THE LUNG ANATOMY AND PHYSIOLOGY

The lung is a complex organ, which forms a border between the external and internal environment. Its primary function is to enable rapid uptake of oxygen, required for metabolic processes, and the elimination of the toxic product carbon dioxide. The respiratory tract consists of a conducting region and a respiratory area, and is anatomically characterized by extensive bifurcations. According to Weibel's bronchial tree (Figure 2), the conducting airways are classified into 16 bifurcations, comprising the trachea, the bronchi and the bronchioles [41]. The terminal bronchioles represent the passage to the respiratory region, which is classified into other 6 bifurcations. The respiratory region includes the respiratory bronchioles, from which the alveolar ducts with alveolar sacs branch off. The human lung consists of approximately 30000 terminal bronchioles and each of those branches into 10000-15000 alveoli. This region comprises a surface area of approximately 100 m^2 where air and blood come into intimate contact and gas-exchange takes place across a thin epithelial and endothelial barrier (~ 0.5 µm) [42]. Although the bronchial and alveolar epithelia display high permeability to water, various gases and lipophilic substances, whereas the permeation of many hydrophilic substances of large molecular size and ionic species is limited [43].

Bronchial tree	Bifurcations	Area [cm2]
Trachea	0	2,54
Main Bronchie	1	2,33
Small bronchie	2	2,13
	3	
	4	2,48
Bronchioles		
Terminal bronchioles	16	180,0
Respiratory bronchioles	17 / 19	944,0
Alveolar ducts		5880,0
Alveolar sacs	23	
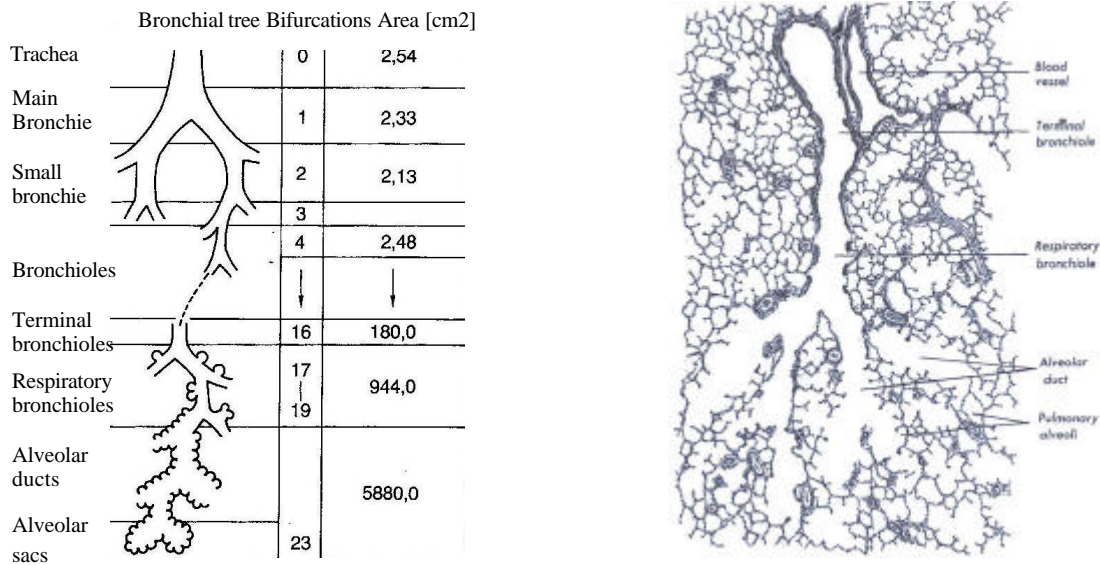
Figure 2. Left: Schematic of the bronchial tree [41]. Right: section through terminal bronchioles and the following bifurcations [42].

The conduction airways consist of the epithelial lining, the basement membrane, the sub-epithelial connective tissue and the smooth muscles. Three cell types predominate in the stratified bronchial epithelia of the conducting region: ciliated, secretory and basal cells. Whilst the goblet cells and the submucosal gland cells are responsible for the secretion of mucus (100 ml per day), the major function of the ciliated cells is the propulsion of mucus upwards and out of the lung. Each ciliated cell contains circa 40 cilia of 3- 6 µm length. The mucus consists of oligomeric mucin glycoproteins as the major component, and it forms two layers - a gel like layer on the outside and a more fluid layer on the cell side. During the cilia beat in direction to the pharynx the cilia are stretched and thus they reach the gel layer. The backwards movement of the cilia occurs in the curved position in the fluid layer. Due to this propulsion the mucus moves 2.5 mm per minute in direction to the pharynx and thus the lung will be cleared of foreign substances.

The bronchioles represent the passage to the respiratory airways and the epithelium transit to single cell layer, consisting of ciliated cells and Clara cells that are the progenitors of the bronchial epithelium. The thick mucus lining (1 – 10 µm) fades to the surfactant lining (0.1 – 0.2 µm), and constitutes the physical barriers to pulmonary absorption [42].

The alveolar epithelium is primarily composed of type I and type II pneumocytes. Type I cells have a very thin cell body (0.2 µm) with long membranous extensions. Due to their large cell diameter of approximately 200 µm, they occupy an area of approximately 95 % of the

alveolar surface even though they represent only 33 % of the total number of alveolar epithelia cells. The type I pneumocytes border on a single layer of basal membrane that is connected to the capillary endothelium on the opposite side. Because of their thin cell body, the distance between alveolar lumen and blood is lowest (0.5 to 0.6 µm), making their main function the gas-exchange and transport of molecules possible. The type II pneumocytes are characterized by a more cuboidal morphology, and due to their small diameter (~ 15 µm) they cover only 5 % of the total alveolar surface. Their main functions are the production of surfactant and the differentiation into type I cells when the epithelium is damaged. Furthermore, it was reported that pneumocytes express a variety of transport proteins such as calveolin or clathrin, which are able to internalize macromolecules or even nanoparticles by endocytosis [44].

In the respiratory airways the alveolar epithelium is covered by the surfactant lining layer which is composed of phospholipids and proteins. Beside its function in the host defence, the surfactant is primarily responsible for the stabilization of the alveoli structure. Due to the surface tension between alveolar air and the wet cell surface the alveolar sacs run the risk of collapsing (the smaller sacs) or bursting (larger sacs). The phospholipids of the surfactant are bipolar molecules and act as an interface between a myelin containing hypophase (on the cell surface) and the alveolar air, thus reducing the surface tension and stabilizing the alveoli [45]. The surfactant proteins (A, B, C & D) have been identified as playing a fundamental role in innate immunity (A & D) and lipid packing of the interface (B & C) [46].

Among the different respiratory cells, the ciliated epithelia cells of the larger and smaller airways and the type I and type II pneumocytes are the key players in the pulmonary drug transport [3]. The transport of drugs into the pulmonary circulation occurs through different routes. Whereas lipophilic drugs pass the epithelium via the transcellular transport, hydrophilic drugs are transported mainly via the intercellular passage. The small pore sizes between the alveolar cells (0.6-1nm) and the tight junction depth (0.261 µm) limiting their drug transport. The mechanisms of macromolecular transports are the subject of genuine interest and vesicular trafficking was studied intensively [47]. Recently, a putative alternative transport pathway within the type I pneumocytes has been described comprising plasma membrane vesicles or invaginations called caveolae. The key structural and functional protein for the caveolae is the caveolin. Caveolae are morphologically evident as omega-shaped invaginations of the plasma membrane and form discrete functional vesicles with a diameter of 50-100 nm within the cell cytoplasm. Caveolae undertake transport functions including that of the endocytic and transcytotic movement of macromolecules, and indeed microbes and

microbial toxins [47, 48]. Therefore, caveolae might permit vascular targeting to achieve theoretical expectations of tissue-specific pathway for overcoming key cell barriers to many drug and gene therapies in vivo [49].

Approximately 80-85 % of the alveolar walls are covered with capillaries and these receive the first passage of the whole cardiac output of venous blood to assure the oxygen supply of the body [42]. With respect to these considerations, studies were undertaken to use the pulmonary endothelium as targeting tissue for pulmonary drug delivery from the vascular side. In support of this notion, native and modified antibodies to angiotensin-converting enzyme, thrombomodelin, intercellular adhesion molecule and platelet endothelial cell adhesion molecule were studied and it was postulated that they possibly could serve as carriers for drug/gene targeting to the pulmonary endothelium [50, 51]. Whereas calveolae forms recycling endosomes in particular for transcellular transport, the clatrin-coated pits ensure to uptake of molecules into the cells by endocytosis [52].

The mucociliary clearance represents the first barrier in the lung for inhaled substances and is particularly successful in the clearance of larger particles. In the respiratory tract the pulmonary barrier consist of pulmonary enzymes and alveolar macrophages. Pulmonary enzymes, such as proteases and peptidases, will be excreted by pneumocytes type II cells as component of the surfactant (protein A & D) or they are located inside macrophages, lymphocytes, neutrophils and mast cells and they readily degrade inhaled macromolecules. Alveolar macrophages play an important role in the host defence, and are strategically located in the alveolar ducts and sacs. The human lung is estimated to contain 2.3×10^{10} macrophages, with 50-100 per alveolus. Several types of receptor on the macrophage cell surface identify and mediate the internalization of inhaled substances and particles. Macrophages may also phagocytose particles or molecules opsonized by the surfactant proteins, immunoglobulins and complement components. Once internalized foreign substances are targeted to the phagolysomal compartment and destroyed [53].

The immune response generated in the respiratory system is confined to the region exposed to antigen stimulation. The upper and lower respiratory tract are associated with their own specialized immune surveillance system. Whereas the conducting airways are associated with the nasal associate lymphoid tissue (NALT), the respiratory area encompasses the bronchus associate lymphoid tissue (BALT). The BALT contains lymphoreticular aggregates with B cells and T cells situated under the lung epithelium. The lung is also comprised of non-lymphoid cells, such as dentritic cells and alveolar macrophages and they are mainly found in the areas of maximum antigen presentation. Macrophages, dentritic cells and also B

lymphocytes are antigen presenting cells and the immune response of the lung depends on the interaction between those and T- and B-lymphocytes respectively. Dentritic cells are regarded as the main antigen presenting cells involved in the stimulation of antigen specific native T lymphocytes, whereas macrophages (by secretion of interleukin 1) and B cells my be involved in restimulating pre-existing or memory T-lymphocytes [54].

INHALATION DEVICES

Aerosolization devices have to fulfil several requirements to ensure safe and efficient drug transport to the site of action: reproducible dosing, high efficiency of drug delivery, ease of device operation, short duration of treatment, minimized risk to patient, environmental protection and cost-effectiveness [55]. Three types of devices are commonly used for the administration of drugs to the respiratory tract: pressurized metered dose inhalers (MDI), dry powder inhalers (DPI) and nebulizers. An adequate understanding of the advantages and disadvantages of the different systems is required to make a proper choice between them [56]. A MDI contains the drug in suspension, emulsion or solution to which a propellant has been added. When the device is activated, a metered dose is released at high velocity, which requires a simultaneous inhalation by the patient. To overcome this challenge, more recent developments, require a breath actuated drug release [57]. A DPI consists of a dry powder formulation, a dosing principle and an inhaler device. It operates by using the inspiratory flow of the patient for dose entrainment and disintegration of the powder formulation [58]. Nebulizers are used to aerosolize drug solutions and sometimes drug suspension for inhalation. They are typically used in situations when severe obstruction of the airways or insufficient coordination by the patient does not allow the use of other systems. A significant advantage of nebulizers in comparison to MDIs and DPIs, is their universal availability, hence, the same device can be employed for different drug solutions or dispersions.

There are two basic types of nebulizers, the air-jet and the ultrasonic nebulizer. For a typical air-jet nebulizer (Figure 1A) compressed air (1) passes through a narrow hole (2) and entrains the drug solution (3) from one or more capillaries (4) mainly by momentum transfer. The aerosol droplets are formed by a break-up process of the liquid from the liquid column and their size is mainly dependent on the design of the capillaries. Large droplets impact on one or more baffles (5), in order to refine the droplet size distribution to the required range for inhalation. Only smaller droplets with less inertia can follow the streamlines of air (6) and pass the baffle. In practise, there exists a wide variation in the performance of different types

of nebulizers [59, 60]. PARI GmbH is the world's leading manufacturer of aerosol delivery apparatuses. They manufacture numerous air-jet nebulizers for infants and adults for use in hospitals or at home, e.g. Pari boy®, Pari LC® or Pari Sole® [61].

In an ultrasonic nebulizer (Figure 1B), droplets are produced by a rapid vibrating piezoelectric crystal (1). The frequency of the vibrating crystal determines the droplet size for a given solution. In the most nebulizers the ultrasonic vibrations are transferred directly to the surface of the drug solution in a drug reservoir. In some ultrasonic nebulizers, such as the illustrated Optineb® (Nebu-tec) apparatus, the vibrations are transferred to a connecting liquid (2) before reaching the drug reservoir (3). Hence, these nebulizers reduce the shear forces applied to the drug, and minimize any heat applied to the formulation in the process of nebulization [62]. As previously described, whilst the smaller droplets follow the airstreams (4) the larger impact on the baffle (5).
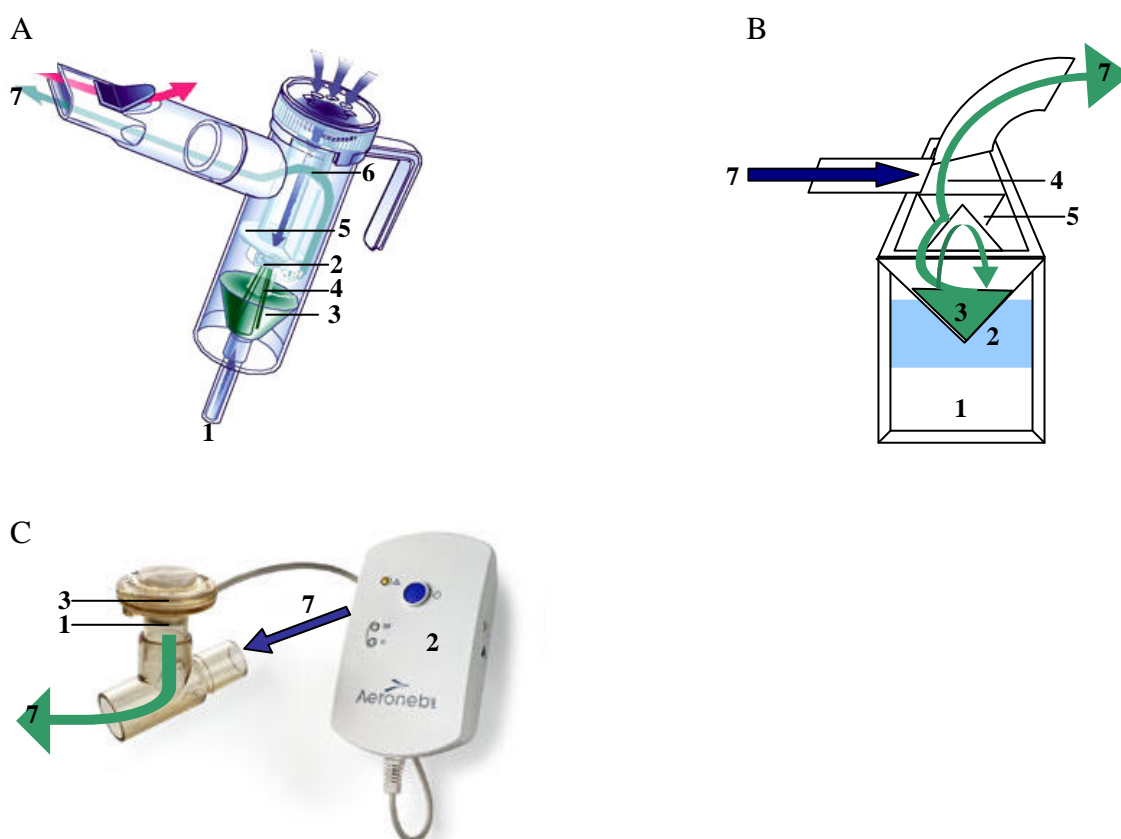
Figure 1. A schematic presentation of the nebulizers utilized in this work: A) Pari LC® [61], B) Optineb® and C) Aeroneb® [63]. The working principles are detailed in the text.

Several manufacturers, such as Aerogen(Figure 1C), Omron, ODEM and Pari, have developed new aerosol devices that utilize a vibrating mesh or plate (1) with multiple apertures to produce a liquid aerosol. Such devices display a number of beneficial features including: the generation of fine aerosol particles, no internal baffling system is required, they are portable and battery operated (2), they efficiently aerosolize solutions and suspensions, and they have minimal residual volume of medication left in the drug reservoir (3). As a consequence thereof, their efficiency of delivering drugs to the respiratory tract is higher than conventional air-jet or ultrasonic nebulizers [64]. The Aeroneb$^{®}$ (Aerogen), utilized in the studies of this thesis, was developed for the nebulization of sensitive drugs such as proteins or peptides. In contrast to common ultrasonic nebulizers, the frequency is low and the temperature in the Aeroneb$^{®}$ is constant and thus there is a minimal risk of denaturing biomolecules such as proteins, peptides or nucleotides [63].

There are two main parameters that determine the nebulizer performance: the droplet size distribution of the aerosol and the drug output rate. However, it should be taken into account that the performance of the nebulizer is also influenced by the patient's inspiration flow (7), the air flow rate from the compressor, and the physical properties of the drug solution [56].

The droplet size distribution is important for the actual deposition in the lung. Therefore, aerosol particle sizes are commonly characterised by the mass median aerodynamic diameter, which can be determined using e.g. laser diffraction analysis [65]. Diameters measured by laser diffraction technique are based upon geometric particle dimension. For the spherical droplets in the aerosol cloud from nebulizers, the equivalent volume diameter equals the measured mass median geometric diameter. The aerodynamic particle diameter is the diameter of a unit density sphere that has the same terminal settling velocity in still air as the considered particle. From spherical particles of aqueous drug solution, also the dynamic shape factor and droplet density have unity, and so the aerodynamic diameter equals the measured geometric diameter. No corrections are necessary and the volume distribution curve from laser diffraction analysis yields a correct mass median aerodynamic diameter [57].

The three principal mechanisms that lead to pulmonary deposition are internal impaction, sedimentation and diffusion. Internal impaction occurs during the passage through the oropharynx and the large conducting airways for particles that pose a size > 3 µm, or have a high mass and velocity. Due to the small diameter of the alveoli, particles < 3 µm sediment mainly by gravitational force in the respiratory airways. Additionally, sedimentation increases by breath-holding. In the range below 0.5 – 1 µm, particles are deposited by diffusion, which is based on Brownian motion.

Besides the aerosol droplet size, particle geometry and charge, lung morphology as well as ventilatory parameters can all influence the site, extent and efficiency of drug deposition. Therefore, particle features such as source (solution, powder or suspension), diameter, density, electrical charge, hygroscopy or shape are often determining parameters for the aerosol deposition [57, 66].

In respect to achieve drug deposition in the lower airways and circumvent macrophageal clearance porous microparticles have been developed. These are characterized by a large geometric diameter, which acts to both improve drug loading and circumvent clearance by alveolar macrophages. However, due to their hollow porous structure the aerodynamic diameter of these microparticles is much smaller than the geometric diameter. Therefore, the amount and the retention period of the particles deposed in the respiratory airways could be improved [9, 67, 68].

The drug output rate is another important factor in regard to confine the nebulization time and thus improving the patient compliance. The output rate (mg/min) is the mass of drug converted to aerosol per unit time. It can be determined either by weighing the nebulizer before and after use, or more exactly by measuring the drug concentration in the nebulized fraction [69].

Taken together, the knowledge of the cellular aspects, the pulmonary clearance and immune response, the characterization of delivery devices and the pulmonary deposition display major targets to pulmonary drug delivery. An optimal delivery system would transport the drug safely and specifically to its pulmonary target region or into the systemic circulation and than realize the drug at the side of action in a given kinetic. To optimize current delivery systems or developing novel systems, future studies addressing the unique molecular, biological and physiological characterization of both the various respiratory regions and the drug formulations have to be carried out.

GENE THERAPY

The treatment of disease at the genetic level was first proposed over 30 years ago [70, 71]. The "gene therapy rollercoaster" started in1990 with the treatment of the first patient in a gene therapy clinical trial for sever combined immunodeficiency using a retroviral vector [72]. Since then, gene therapy has reached a point of serious pharmaceutical developments as evidenced by the 1020 clinical trials that have already been initiated worldwide [73]. The

genetic material of interest can be either DNA or RNA, and the altered function can be an increase or decrease in the production of a protein. Fundamental problems involved in gene therapy are (i) the selection and isolation of the appropriate gene, (ii) the delivery to and into the cells of interest, and (iii) the efficient gene expression or suppression [74]. A typical gene delivery protocol utilises plasmid DNA (pDNA) amplified and isolated from bacteria that contains the sequence of interest, a viral promoter for expression in the eukaryotic cells and an antibiotic resistance gene for selection stringency and amplification of the bacterial host [75, 76]. In the present work, pDNA under the promoter control of Cytomegalovirus, containing 4000-5000 base pairs was utilized. From a technological point of view, the physico-chemical properties of pDNA, such as high molecular weight (= 2500 kDa), hydrophilicity, extensive anionic charge density, and susceptibility to enzymatic degradation makes it a difficult compound for delivery across several cellular barriers [77, 78]. Obviously, delivery of naked DNA would lead to poor transfection efficiency. Therefore, the development of gene delivery vehicles play a predominate role in gene therapy. These vehicles have to fulfil several requirements including minimal side effects, providing effective DNA condensation and protection, transport through the cell membrane and finally DNA release and nuclear entry [52, 79].

Gene delivery vehicles

On the whole two different approaches have been utilized to achieve delivery of nucleic acid to cell nuclei, namely viral and non-viral vectors. Viral vectors represent the majority of gene delivery vehicles employed in published studies and clinical trials to date (Figure 3), since they are known to be extremely efficient in effecting transgene expression [73, 80]. Such vectors have their genome altered to prevent viral replication, reduce their cytotoxicity and permit incorporation of the resulting therapeutic transgene [81]. In early 2004, the world's first human gene therapy product, Gendicine®, an adenoviral vector expressing the tumor-suppressor gene p53, obtained market approval by the Chinese FDA for the treatment of head and neck squamous cell carcinoma [78]. However, the problems of low-virus titer, inability to transfect non-dividing cells, induction of strong immune response and significant toxicity must still be overcome and have led to the development of alternative approaches in gene delivery, including non-viral vectors [82].
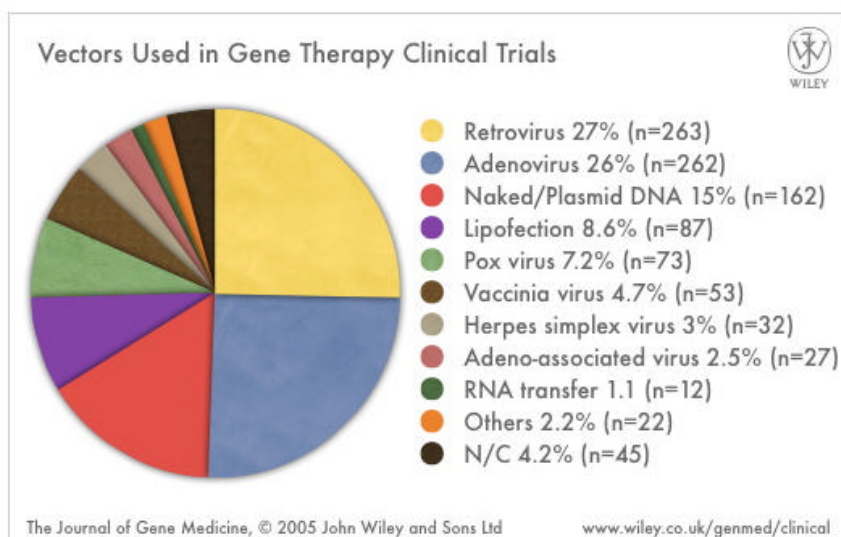
Figure 3. Gene delivery vehicles employed in clinical trials since 1989.

Non-viral gene delivery vehicles are receiving increasing attention as they hold several advantages over other approaches, such as ease of manipulation, stability, low cost, safety and high flexibility regarding the size of the transgene delivered [83]. A variety of effective non-viral gene delivery approaches have been developed including: naked DNA injection [84-86], biological techniques such as hybridized DNA (bioplexes) [87] or peptides [88], physical techniques such as electroporation [89, 90], sonoporation [91], laser irradiation [91], gene gun [92] or magnetofection [91], and synthetic transfection reagents including polymer based nanoparticles [93-95], cationic lipids (lipoplexes) [96-98] or cationic polymers (polyplexes) [99]. Among the cationic polymers employed, polyethylenimines (PEIs) have exhibited particularly promising results in both transgene delivery and the following transfection efficiency in many cell culture models, as well as in numerous in vivo applications [100, 101].

Polyethylenimine mediated gene transfer

PEI is a synthetic cationic polymer that was first described in 1995 as non-viral gene delivery vehicle [102]. Since then, it has gained significant popularity due to its ability to form nanoscale complexes with DNA, and subsequently releasing these polyplexes into the cytosol. As depicted in Table 3, such polyplexes have been utilized over a broad spectrum of applications. In an attempt to improve the efficiency and biocompatibility of the vector, numerous modifications have been synthesized and studied for a variety of therapeutic applications (Table 3).

Table 3: In vivo delivery of different PEI/pDNA polyplexes.

gene delivery vector	transgene	targeting tissue/ therapeutic applications	reference
25 kDa branched polyethylenimine (BPEI)	p53, IL-12	lung metastases, inhibition of tumor growth	[103-106]
	reporter gene	lung	[107]
	reporter gene	brain	[108]
	porphobilinogen deaminase	liver, hepatic porphyria	[109]
	IL-2, Hepatitis B Ag	muscle, vaccination	[110]
25 kDa linear polyethylenimine (linPEI)	reporter gene	lung, cystic fibrosis	[107, 111, 112]
	somastatin receptor protein	pancreatic cancer	[113]
polyethylenglycol-graft PEI (PEGPEI)	reporter gene	tumor targeting	[114]
	reporter gene	spinal cord disorders	[115]
	reporter gene	lung	[116, 117]
transferin-PEI or -PEGPEI	reporter gene	tumor targeting	[118, 119]
	reporter gene	lung	[116]
	TNF-alpha	tumor necrosis, inhibition of tumor growth	[120]
epithelial growth factor -PEGPEI	reporter gene	tumor targeting, liver	[120]
galactosylated PEI	reporter gene	liver	[121]
cyclodextrin-PEI	marker gene	liver	[122]

PEI is highly water soluble and positively charged due to its high density of protonatable amino groups. Every third atom in the molecule is a nitrogen, with approximately 20% of these being protonated under physiological conditions [123]. As a result, the polymer can change ionization state over a broad pH range thus providing a high buffer capacity. This property is a considerable advantage of PEI over other cationic polymers in terms of gene delivery into the cytoplasm, as explained below.

The interaction of pDNA with PEI to form a gene delivery system is demonstrated schematically in Figure 4. Condensation of the anionic DNA with the cationic PEI is based on electrostatic interactions, and leads to the formation of compact particles of approximately 100 nm in diameter, depending upon the PEI modification [100]. The degree of condensation, and thus the net charge of the resulting particle, is strongly dependant on the cation-to-anion ratio, or more precisely the PEI nitrogen-to-DNA phosphate ratio (N/P ratio). Complete condensation of DNA (fully exploit cation-anion interactions) seems to occur at N/P ratios of 3-5 depending upon the PEI modification [124]. However, maximum accessible DNA condensation is obtained only with a high PEI extend at N/P ratios > 6, resulting in small polyplexes that exhibit a strong positive net charge. This charge induces the polyplexes to bind to the negatively charged glycosaminoglycans, which are present on cell membranes, and leads to the subsequent polyplex internalization by endocytosis [125]. Post endocytotic uptake, the complexed PEI acts as so called proton sponge. The amino groups buffer the protons in the endo-lysosomal compartment, leading to an influx of chloride anions, a subsequent increase in the osmolarity and eventually to endosomal rupture [126]. The released polyplexes must then either enter the nucleus whole, or release the DNA to enter the nucleus alone. The precise mechanisms involved in the DNA migration to the nucleus through the cytoplasm and passage through the nuclear membrane are still unknown. Recent localization experiments suggest that the pDNA-PEI polyplexes can penetrate into the nucleus, suggesting that dissociation of the polycation DNA may not be prerequisite for nuclear translocation [127, 128]. In contrast energy-dependent uptake of pDNA alone into the nucleus via the nuclear pore complexes was shown recently [129]. However, transport of the DNA from the cytosol into the nucleus is certainly one of the major limitations for efficient gene transfer mediated by non-viral vectors [52, 83]. Recent studies have proposed a mechanism for PEI polyplexes that involves protein-driven transport through the cytoplasm towards the nucleus on microtubules. This active transport led to efficient perinuclear accumulation within minutes, suggesting PEI displays nuclear targeting activity [130]. The passage of polyplexes through the nuclear membrane is also poorly understood and it was discussed that the passage appears only in dividing cells [83, 131]. The in vivo investigations presented in chapter 4 of this thesis suggest pDNA released from PEI enter the nucleus of pulmonary epithelial cells alone.
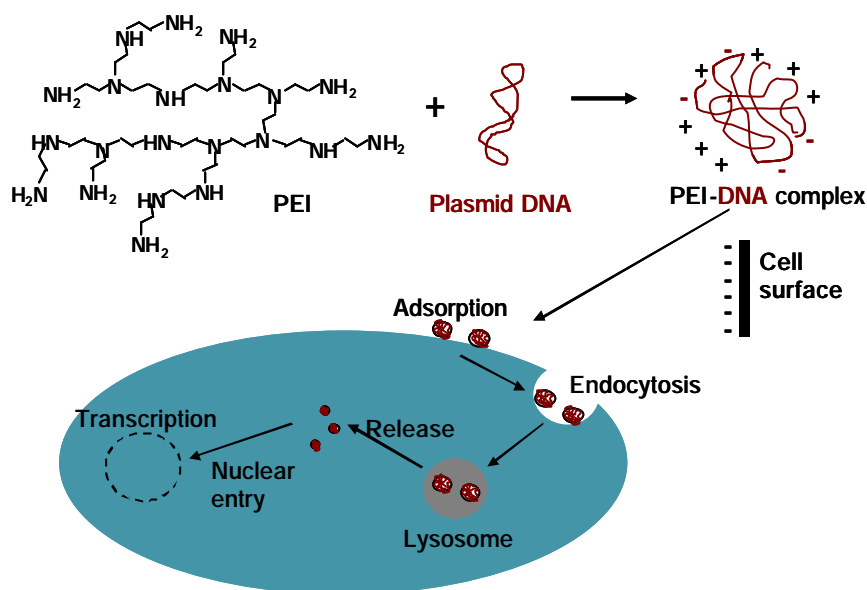
Figure 4. Formation of PEI-DNA polyplexes and their cellular uptake.

Pulmonary gene therapy

The lung possesses inherent advantages for gene therapy since it is easily accessible via the airways, offers a large surface area for transfection and reduces the risk of systemic side effects. Pulmonary gene therapy may lead to new treatment strategies for life-threatening respiratory diseases such as cystic fibrosis, lung cancer, asthma, pulmonary fibrosis and pulmonary hypertension. However, the gene delivery systems have to overcome considerable barriers (Figure 5) before cell binding and entry can take place, as described in detail above. Various strategies, including the route of administration, have been evaluated to overcome these barriers and ensure an efficient gene transfer to the lung cells. In an attempt to bypass the pulmonary barriers, several lung targeting vectors, as described in detail below, have been administered intravenously. However, this route inevitably precludes some of the advantages associated with pulmonary administration, such as the reduced side effects.
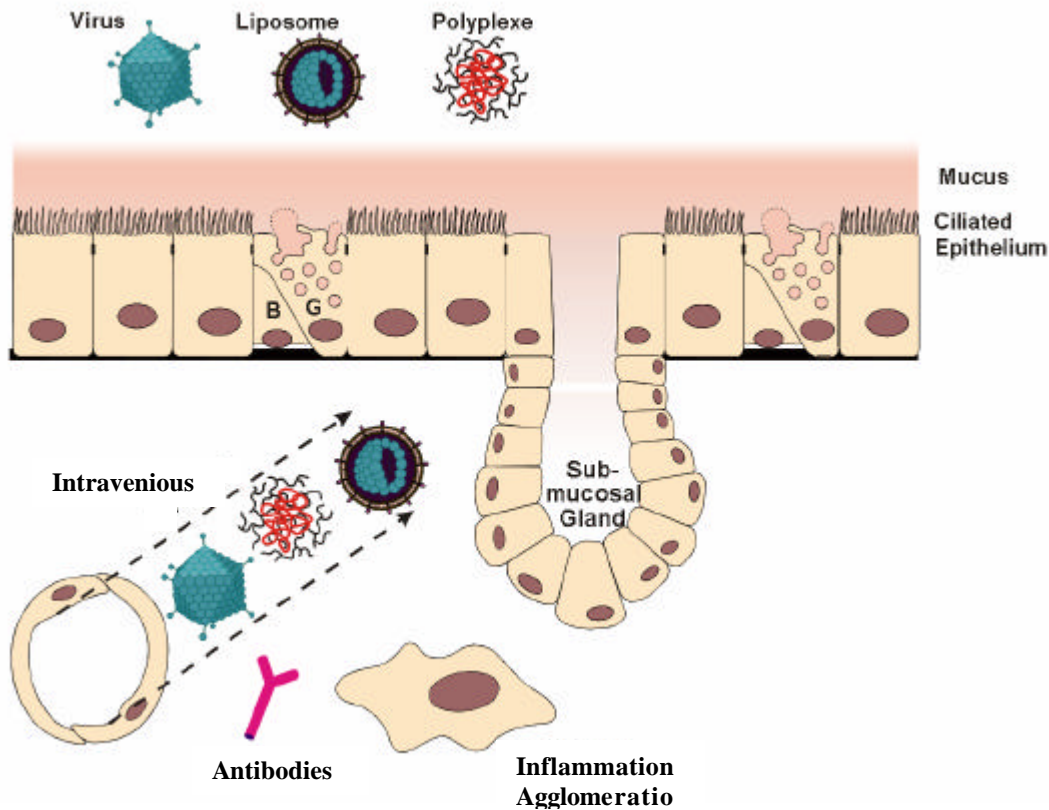
Figure 5. Routes and barriers of pulmonary gene delivery. Gene delivery system administered to the airways have to pass the lung bifurcations, than the mucus layer (produced by the goblet cells (G)) and the cilia of the bronchial epithelium or the surfactant of the alveolar epithelium before cell uptake can occur. Via the intravenous route the vectors come in contact with the blood corpuscles and sever agglomeration or inflammation can be induced. The continuous endothelium and the basement membrane have to be overcome by the delivery systems before reaching the lung cells.

Pulmonary gene delivery by viral vectors

Viral vectors are generally particularly efficient in mediating gene transfer and expression in vivo [81]. However, results of clinical trials have demonstrated the inefficiency of adenoviral and adeno-associated virus (AAV) vectors mediating gene expression in airway epithelial cells [132, 133]. This was explained by the low transduction efficiency of these vectors due to the pulmonary defence and the lack of viral receptors at the apical surface of the airways [134-136]. Recombinant AAV vectors are unique among viral vectors, since they commonly inhabit a human host without causing any pathology. Therefore, intensive efforts have been undertaken to identify new types of AAV. Such studies have resulted in the recent

development of AAV2 vectors, which appeared to be safe and have superior duration profiles of the expressed genes [137, 138]. Therefore, AAV2 have been applied in clinical trials phase I and II for the inhalation therapy of cystic fibrosis. The trials indicated a lack of any vector-mediated toxicity, a surprisingly efficient DNA transfer and an increase in pulmonary function. However the effect lasted only 30 days and repeated administration did not appear to be capable of sustaining the positive effects [139].

The recombinant Sendai virus (SeV) is currently the most efficient viral vector for airway gene transfer in vivo. SeV has been demonstrated to produce efficient transfection throughout the respiratory tract of animals, as well as in human nasal epithelial cells in vitro [140-142]. Unfortunately, a lack of efficiency after repeated administration was also observed for this vector, demonstrating again the limitation of viral vectors as a consequence of the activation of the immune system. Therefore, several strategies have been adopted in order to limit immune response. In the lung this can be obtained either through pharmacological interventions aimed at reducing the host immune responses, or through modifications of the viral vector in order to make it less immunogenic [54, 81].

The development of lentiviral vectors has been a recent advance in the field of viral gene transfer. These integrating vectors appear to be promising vehicles for gene delivery into respiratory epithelial cells by virtue of their ability to infect non-dividing cells and mediate long-term persistence of transgene expression. Studies in human airway tissues and animal models have highlighted the possibility of achieving gene expression by lentiviral vectors, which outlasted the normal lifespan of the respiratory epithelium, indicating targeting of a 'stem cell' compartment [143, 144]. Thus, re-administration would not be necessary, making it the most interesting viral vector for pulmonary therapy of inherent diseases to date.

Pulmonary gene delivery by non-viral vectors - a brief overview

Generally, non-viral vectors are less efficient gene delivery vehicles than viral vectors. However, due to challenges involved in the use of viral vectors in the lung, non-viral vectors have been considered as realistic alternatives.

Cationic liposomes complexed with DNA (lipoplexes) have been extensively studied as transfection agent of lung epithelial cells both in vitro and in vivo. As a consequence of their low toxicity and immunogenicity they have been utilized in several clinical trials for the treatment of cystic fibrosis (CF) [145-150]. Three double-blind studies demonstrated efficiency and safety of dipalmitoyl-phosphatidylcholin/cholesterol [145, 147] and dioleoyl-trimethyl-ammonium-propane [148] liposomes in the nasal epithelium of cystic fibrosis

patients. In addition to detecting vector-specific DNA and mRNA, all three studies showed partial corrections of CF transmembrane conductance regulator defect in the nose, in one case extending out to 15 days post-administration [147]. Importantly, one study evaluated the effects of three doses lipoplex doses to the nose at one month intervals, and recorded no evidence of lung inflammation or immune response [146]. In addition, the efficiency after the third dose was comparable to earlier doses, suggesting that unlike viral vectors, repeated delivery of lipoplexes was effective, at least in the nose. Due to their low efficiency in the lung of cystic fibrosis patients, new cationic lipids have been designed. Significantly improved gene expression was evaluated in the patient's lung post-inhalation of lipoplexes between pDNA and Genenzyme lipid 67® (GL-67®) [151, 152]. However, both studies reported side-effects in the form of lung inflammation consisting of fever and increased levels of TNF-alpha as well as IL-6 in the bronchial and alveolar lining fluid.

Nanoparticles, peptides and a variety of cationic polymers such as PEI, poly-L-lysine or polyamidoamines, complexed with plasmid DNA have all been explored for pulmonary gene therapy. The suitability of nanoparticles synthesised from porcine gelatin, human serum albumin and polyalkylcyanoacrylate as drug and gene carriers for pulmonary application was investigated on airway epithelium cells in vitro. Such nanoparticles displayed low cytotoxicity and no inflammation, in combination with an efficient uptake in human bronchial epithelial cells, indicating their suitability as gene carriers for pulmonary application [153].

Several advantages in mediating gene transfer to lung epithelial cells were demonstrated for protein transduction domains. As such, numerous TAT peptides were applied to lung epithelial cells in cell culture, either alone, in combination with lipids or BPEI, or covalently linked to liposomes. TAT was able to improve transfection efficiency, although the mechanism remains controversial, and energy independent as well as endocytotic pathways were discussed. [154-157]

The group of Davies et al. developed polylysine conjugates for targeting to the airway epithelium. They generated small sized anti-pIg Fab-polylysine polyplexes, resulting in successful transgene expression in lung epithelial cells of rats. However, the immunoglobulin fragment led to immunological response in the animals lung, thus reducing the transfection efficiency [158]. In an alternative approach they developed a polylysine conjugate as targeting structure to the serpin-enzym complex receptor by utilizing a new synthetic peptide, derived from alpha-1-antitrypsin. These polyplexes led to partial correction of the chloride transport defect in nose epithelium of cystic fibrosis mouse model [159, 160]. Recently, they described the development of a PEG-substituted polylysine. This new polymer was able to form discrete

unimolecular (with respect to pDNA) stable nanoparticles with a small diameter < 20 nm. Intrapulmonary application of these particles in mice resulted in transgene expression in the airway epithelium and endothelium, whereas unmodified polylysine did not result in pulmonary gene expression [161].

Beyond the non-viral approaches, PEI holds particular advantages in pulmonary gene delivery since it was observed to both, overcome the pulmonary barriers unspoiled and encourages high levels of gene expression [12, 162-164].

Pulmonary gene delivery by polyethylenimine

The linear form of PEI (linPEI) has been successfully implemented in systemic gene delivery, resulting in very high levels of gene expression in the mouse lung [165]. These polyplexes were observed to cross the endothelial barrier, resulting in transgene expression in bronchial and alveolar epithelium [166]. When utilizing the intravenous route, linPEI mediated far higher levels of transfection activity than the branched form (BPEI). However, as discussed at length above, a positive charge ratio for PEI polyplexes is required, and this can lead to the formation of aggregates with blood bodies and to interactions with the endothelium of the small lung vessels, both of which can result in toxic side effects [167, 168]. Orson et al. developed a novel intravenous method to deliver small quantities of plasmid to lung tissue by using non-toxic quantities of polyethylenimine conjugated to serum albumin. The resulting aggregates led to highly efficient gene expression in lung interstitial and endothelial tissues when injected intravenously in mice. Using human growth hormone as the encoded foreign antigene for immunization, administration of the particle-bound plasmid elicited both pulmonary mucosal and systemic immune responses [169-171].

The delivery of polyplexes to the airways is a relatively new field, being less than a decade old. In this short period of time significant developments in aerosol delivery systems and vectors have resulted in major advances toward potential applications for a variety of pulmonary diseases [12]. Numerous PEIs have been investigated in vitro in order to prove their stability during nebulization and in the airways surface liquid [124, 172, 173]. In comparison to lipid vectors and polyamidoamines, PEI was observed to be more stable, indicating it may be more suitable in overcoming the lung barriers [172]. In fact, linPEI and BPEI have been observed to be more efficient in gene transfer to lung epithelial cells than cationic lipids or polyamidoamines [107, 112, 174-176]. Furthermore, distribution studies of BPEI polyplexes administered to mice via inhalation or instillation demonstrated effective pulmonary delivery of these vehicles, whilst intravenous application caused unspecific

distribution in different organs and short half lives [174, 177]. Various genes, formulated with BPEI, were expressed at high levels in the lung epithelial cells of mice upon aerosol administration [178, 179]. Furthermore, aerosol administration led to significant inhibition of tumor growth when plasmid DNA, coded for the apoptosis-inducing protein p53 [104, 180, 181] or interleukin IL-12 [105, 106], was utilized in experimental lung tumor models. However, this delivery system was limited by the lung inflammation observed in mice treated with lnPEI or BPEI polyplexes. The inflammation, evidenced by neutrophil infiltration and cytokine response, was more pronounced when polyplexes were administered via instillation compared to inhalation [111, 176, 182].

In an attempt to reduce the toxicity of PEI vectors, PEGPEI copolymers have been investigated as possible pulmonary gene transporters. The application of these vectors to the mouse lung resulted in improved lung compatibility due to a reduced interaction with the airways surface liquid [116, 117]. However, the levels of gene expression remained at the level of naked DNA, indicating the need for further developments, such as ligand targeting to improve the uptake into lung epithelial cells [99, 183].

Consequently, clinical trials have indicated that transgene expression is limited and declines over time for both viral and non-viral vectors. The re-administration of viral vectors leads to a less pronounced degree of corrections [54]. Cationic lipids can be re-administrated, but suffer from low transfection efficiency. In contrast, PEI-based polymers are considerably more stable and efficient for pulmonary gene therapy. However, their use in animal models has only recently begun and requires further developmental work, particularly with a view to decreasing their cytotoxicity. Rudimental advances in the design of targeting structures for receptor mediated gene delivery have been made, and represent another challenge in efficient and safe pulmonary gene therapy.

LIPOSOMAL DRUG DELIVERY SYSTEMS

Liposomes, first mentioned in 1968 [184], consist of lipid bilayers that form spherical particles with diameters in the range of 50-5000 nm. The lipids can either be naturally occurring substances, or synthetic modifications of these. Commonly used liposomes are prepared using lipids that occur naturally in biomembranes of living cells, such as phospholipids, making the liposomes biocompatible and thus ideal drug carriers in pharmaceutical technology. The first drug loaded liposomes were developed in 1972, and

intravenous application to rats demonstrated their potential in improving the pharmacodynamics and biocompatibility of the encapsulated drug [185]. Since then, interest in the field of liposomal drug delivery has increased, with the first products now being on the market [186-189]. Besides medical application, liposomes have become widely used in the cosmetic industry, where less strict regulations for stability and reproducibility permit a greater number of products to reach the market [190].

The level of liposomal stability and permeability to both hydrophilic and hydrophobic ions or molecules is strongly dependent on the chemical structure of the lipids utilized for their preparation. The most commonly used lipids in liposomal preparation are phospholipids. These have been studied extensively as they are one of the major components of cell membranes in animal, plant and bacterial cells. Biological membranes contain a complex mixture of a variety of lipids, whereas the liposomes used in pharmaceutical applications are normally composed of either a single lipid, or a mixture of two or three different lipids. Figure 6 displays the typical structures of liposomal formulations. The amphiphilic phospholipid molecules are arranged in one or more concentric bilayers separated by aqueous channels, surrounding an aqueous core. Hydrophilic drug molecules are dissolved in the aqueous phase, whereas lipophilic drug molecules reside inside the bilayers.
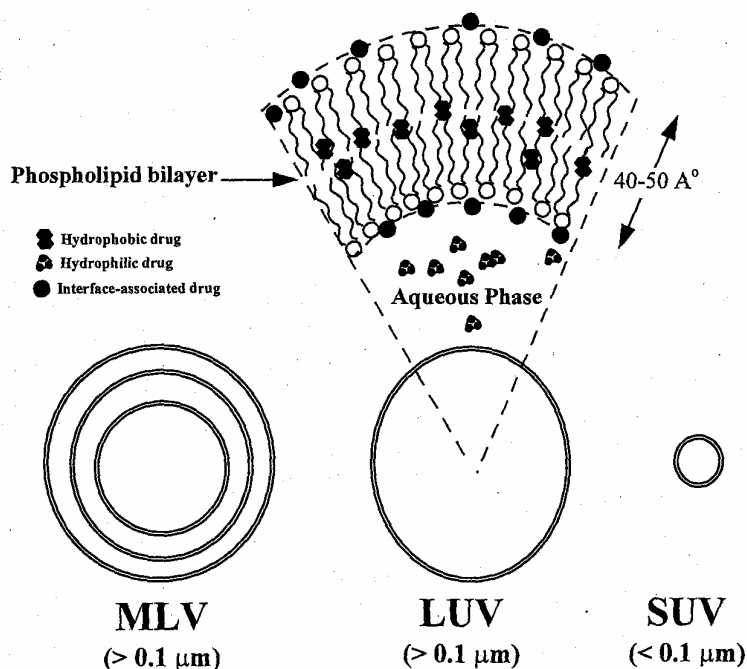
Figure 6. Types of liposomes, depending on size and number of bilayers [191].

There are literally an infinite number of lipids that could be used to prepare liposomes. Within these, there exist many different categories, including cationic, neutral, and anionic

lipids. The lipid chosen for use in a liposomal formulation is dependant on what will be encapsulated, and the therapeutic approach taken. As explained above, cationic lipids are commonly used in the field of gene therapy, whereas anionic and neutral lipids are generally employed in the preparation of drug-loaded vehicles. Neutral lipids are particularly important for intravenous and pulmonary applications as they reduce unspecific interactions with blood corpuscles, proteins or proteolipids of the blood and the lung lining fluid respectively. Thus, there are a number of phospholipids that may be used to manufacture liposomes. These are broadly classified into natural phospholipids (e.g. phosphatidylcholine, phosphatidylserin and phosphatidylglycerol from egg yolk or soya beans and sphingomyelin) and synthetic phospholipids (e.g. dipalmitoyl-phosphatidylcholin or dipalmitoyl-phosphatidylethanol-amine). The lipids used in this work are depicted in Figure 7. Cholesterol has often been included in liposomal formulations as a number of positive effects have been recorded including increased in vitro and in vivo stability and the ability to control the release of entrapped hydrophilic materials [192, 193]. Non-ideal mixing or immiscibility of lipids can lead to liposomal bilayers those are highly permeable. Therefore, differential scanning calorimetry is a very helpful tool to study their thermotropic behaviour, and thus the liposomal stability [194].
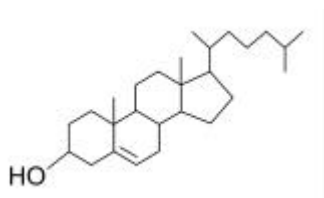
cholesterol   dipalmitoyl-phosphatidylcholin
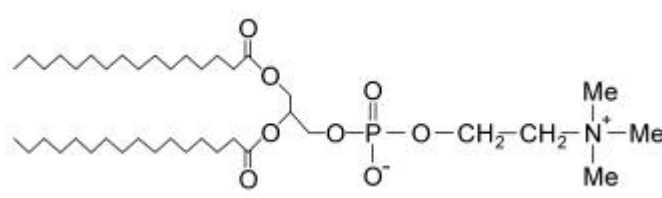
[methoxy (polyethylenglycol)-2000]-pipalmitoyl-phosphatidylethanolamin
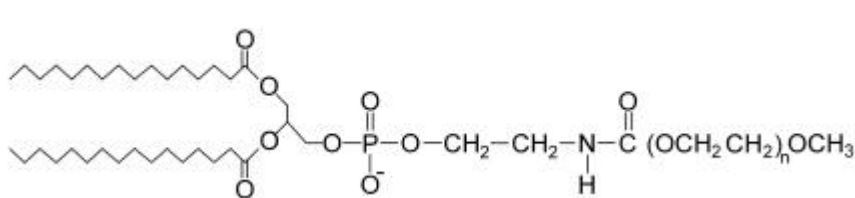
Figure 7. Lipids utilized in the present work (Chapter 6).

The most common method of liposome production requires the preparation of a thin lipid film by vacuum evaporation, prior to the addition of an aqueous medium containing the drug compound to the film at an appropriate temperature [195]. Agitation results in the generation

of multilamellar vesicles (MLVs), which have more than one bilayer surrounding the aqueous core (Figure 6). These liposomes are comparatively large, having diameters ranging between 0.5 µm and 5 µm. Other types of liposome include small unilamellar vesicles (SUVs), which contain only one lipid bilayer and have diameters between 20 nm and 100 nm and may be produced by sonicating MLVs. Large Unilamellar vesicles (LUVs) range in size between 0.1 µm and 1 µm and may be produced by extrusion of MLVs through defined filter pores [195].

We can distinguish four mechanisms of liposomes-cell interaction by which liposomes can deliver their contents to cells (Figure 8). The occurrence of any of these interactions depends largely on the liposomes characteristics, such as the lipid composition, the size, the charge, and the presence of targeting structures. For example, by altering the lipid components, and thus the liposomal membrane stability, the release kinetics of the lipid vehicle can be controlled. Other major factors that determine the type of mechanism involved in liposome-cell interaction are the cell and environmental factors such as the presence of blood, serum or lung lining fluid [195].
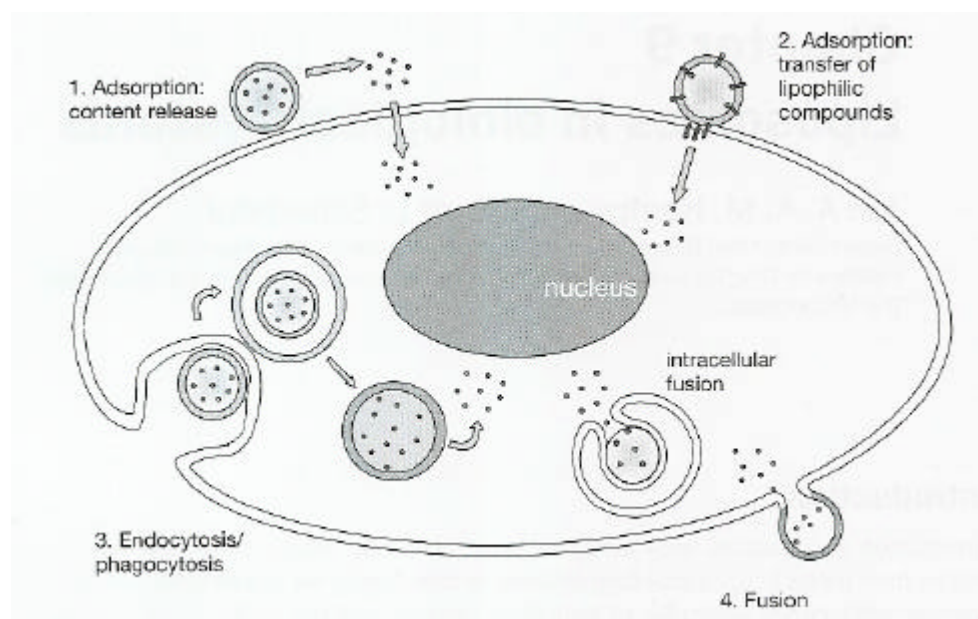
Figure 8. Possible mechanisms by which liposomes can interact with cells and deliver their contents. 1. Adsorption followed by extracellular release of the liposome contents and subsequent transport of these into the cell. 2. Adsorption followed by transfer of the lipophilic compounds from the liposomal bilayer to the plasma membrane. 3. Endocytotic internalization followed by endolysosomal degradation and intracellular drug release. 4. Fusion of the liposomal membrane with the cell or endosomal membrane, thereby releasing the contents into the cytoplasm [195].

A primary objective in the recent developments of liposomes as drug carriers has been to achieve selective localization of the drug at a specific site of action. With this aim in mind, both passive and active targeting structures have been linked to the liposomes (Figure 9). Similar to the approach in gene therapy with PEGPEI copolymers, liposomes were also modified with PEG as a passive targeting structure. Lipids with a PEG residue linked to the lipid headgroup were used to formulate liposomes that displayed an increased circulation time in the blood stream. This was achieved as a consequence of the sterically stabilized liposomes being able to circumvent the reticuloendothelial system [189, 196, 197]. Cationic lipids, which are generally utilized in gene transfer, significantly increase the interactions of the liposomes with the cell membrane, thus increasing unspecific cellular uptake (passive targeting). In contrast, active targeting can be achieved with antibodies or antibody fragments, which can increase the cellular uptake into defined cells. Active targeting structures, such as antibodies [198], antibody fragments [199, 200], lectines [201], folate [202] or peptides [203] attached to the liposome surface have the potential to become low toxic, highly specific and potent drug carriers.
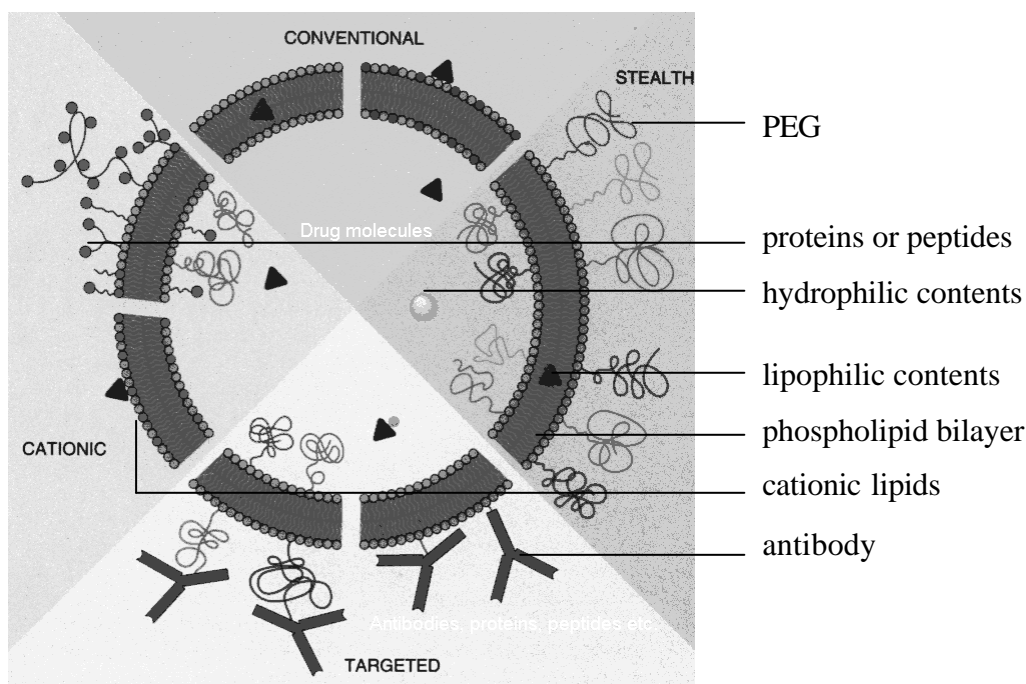
Figure 9. Different approaches of liposome modification and passive or active targeting [204].

Liposomes as pulmonary drug delivery vehicles

Aerosolized liposomes offer the advantages of controlled drug release for both local and systemic therapy with much reduced systemic side effects. When liposomes were first applied to the animal lung via instillation, extended drug release combined with high biocompatibility was reported [205]. The first aerosolization, using a commercial air-jet nebulizer, was the proof-of-principle that liposomes can serve as colloidal drug carriers for sustained release in pulmonary therapy [206]. Neither acute nor chronic effects of inhaled liposomes on pulmonary function in animals and healthy human volunteers were detected [207, 208]. Furthermore, in contrast to the rapid clearance of soluble drug from the lung, 50–60 % of phosphatidylcholine liposomes are retained in the lung for up to 24 hours after inhalation and thus can sustain the drug release [209]. As such, research in the field of liposome nebulization attained significant growth making it an important, highly biocompatible method of drug therapy for the lung [210-213].

Different therapeutic approaches led to the development of various liposomal formulations, encapsulating drugs such as amikacin [214], beclomethasone [215], ciprofloxacin [216], salbutamol [216], triamcinolone [217, 218], fentanyl [219], interleukin-2 [220, 221], amphotercin B [222] and morphine [223]. The influences of numerous liposomes upon the nebulizer characteristics of a number of air-jet and ultrasonic nebulizers were investigated. The influence of different nebulizers upon the liposome stability were also studied, since sheer forces (air-jet) and frequency (ultrasonic) can alter aerosolized compounds [218, 224, 225]. Depending upon the lipid composition and concentration, the liposomal stability varied, and drug release during the aerosolization process was sometimes observed [214]. Such liposomal leakage was more pronounced during nebulization with ultrasonic apparatus, and for liposomes containing only phosphatidylcholine [214, 226]. When cholesterol was used in the liposome preparation, improved bilayer stability was observed [201, 225, 226]. Lyophilization of the liposomes led to increased drug encapsulation efficiency and improved nebulization stability, however the formation of larger aggregates (1-5 µm) was observed, indicating reduced deposition in respiratory airways [215, 227].

Hung et al. reported a significant advance in aerosol therapy using liposomes. They developed an inhalative liposomal formulation encapsulating fentanyl (AeroLEF^{TM}) [219], which was recently approved for Phase IB clinical trial [228]. Saari et al. observed a sustained release kinetic for nebulized beclomethasone liposomes in humans [229]. However, not all

liposomal formulations accomplished the expectations of controlled drug release for inhalation therapy [220, 230].

Interesting developments in aerosol delivery of liposomes are described in the studies of Desai et al. Their approach involves dispersion of the physical mixture of phospholipid(s) and drug in saline, which results in spontaneous formation of liposomes and, thus, drug encapsulation in the lung lining fluid. Various phospholipids containing antimicrobial agents were investigated. Encouraging results were obtained in terms of high levels of lipid/drug nebulization in a short period of time and lower levels of drug leakage. This facile approach is expected to overcome problems associated with stability upon aerosolization, storage and high production costs [216].

Inhalative liposomes reveal the potential of sustaining and controlling the release of drugs for local and systemic therapy. Thus, systemic side effects could be reduced, drug distribution could be better controlled and the compliance of the patient is likely to be enhanced due to the non-invasive route and the low application frequency. However, before the full promise of such formulations can be revealed, many hurdles must be overcome such as the need for improved nebulizer techniques and apparatus, and improved liposome formulations that reveal more efficient drug loading, better stability during storage and nebulization, and a better understanding of the mechanisms of drug release from such formulations.

AIMS OF THIS THESIS

The respiratory tract is a barrier that exists between an organism and its environment that can be exploited for the aerosol administration of synthetic or biologically active drug substances. The administration of nanoscale carriers containing drugs or nucleic acids to the lung is an important, rapidly expanding field in the treatment of various pulmonary diseases. The overall aim of this thesis was to develop a number of effective polycationic- and lipid-based nano-carriers to act as delivery systems in aerosol therapy. Such nanoparticles should fulfil several requirements, including: (i) efficient encapsulation of the active drug molecule, (ii) providing sufficient protection of this drug, both during the aerosolization process and in the airways lining fluid, and (iii) to efficiently deposit the active molecule into the conducting and respiratory airways. Three different nebulizers will be employed throughout this work with a view to identifying device most suitable to achieving our aims, depending upon the material to be nebulized.

The first four chapters in this thesis will concentrate on the investigation of numerous polyethylenimine modifications as vehicles for pulmonary gene therapy, with the fifth study centred on the use of liposomal formulations in aerosol therapy.

Whilst it is well known that nebulization can alter the properties of macromolecules and PEI is able to transport DNA into the lung cells of mice, it is not well understood exactly how the aerosolization process effects the morphology of PEI polyplexes. In Chapter 2, a number of PEI modifications will be employed to investigate how effectively they condense and protect DNA. This will be achieved by utilizing atomic force microscopy to study any alterations that occur in polyplex morphology post-aerosolization. Alongside this, we will investigate if the physico-chemical properties of the polyplexes (hydrodynamic diameter & particle charge) have been altered post-nebulization.

Low toxicity has been reported for both low molecular weight PEI and the PEGPEI [231, 232]. As such, chapter 3 focuses on the in vitro and in vivo study of these polymers as prospective pulmonary gene vectors.We believe that these PEI modifications might display improved biocompatibility when compared to the commonly used BPEI polymer. Prior to transfection studies in the mouse lung, the PEI polyplexes will be investigated in terms of their size, structure, charge, DNA protection, cytotoxicity and transfection efficiency in a lung epithelial cell line.

The work contained in chapter 4 builds on the studies discussed in chapter 3. Our aim here will be to investigate the in vivo toxicity of low molecular weight PEI and PEGPEI in

the mouse lung. This will be achieved by investigating typical indicators of inflammatory response in the mouse lung post-administration of the polyplex formulation. In an attempt to identify the type of cells targeted by the different PEIs, the distribution of the gene vectors and the location of the gene expression will be determined. The development of a nebulization system for the application of polyplexes into the mouse lung will also be investigated, as previous studies utilized whole body nebulization systems, making the application of a definite dose impossible.

Recent advances have demonstrated that utilizing protein transduction domains, such as TAT peptides, as gene vectors may result in highly efficient, non-toxic gene transfer [155, 157]. Therefore, we will attempt to synthesise a novel polymer containing TAT peptide linked to PEGPEI (Chapter 5). As it is assumed that the TAT peptide could lead to an enhanced cell uptake thus improving transgene expression in lung epithelial cells. A range of in vitro and in vivo studies will be undertaken in an attempt to investigate the pDNA condensation and protection, the transfection efficiency, the distribution and the toxicity of this new gene vector.

The work in Chapter 6 of this thesis describes the development of liposomes as sustained release formulations for an aerosol therapy of pulmonary hypertension. The aim of this study is to uncover liposomal formulations that are stable during nebulization, and are able to encapsulate high quantities of a prostacyclin.

REFERENCES

1. R. Dhand. Aerosol therapy during mechanical ventilation: getting ready for prime time. *Am J Respir Crit Care Med* **168**: 1148-1149 (2003).
2. R. U. Agu, M. I. Ugwoke, M. Armand*, et al.* The lung as a route for systemic delivery of therapeutic proteins and peptides. *Respir Res* **2**: 198-209 (2001).
3. D. A. Groneberg, C. Witt, U. Wagner*, et al.* Fundamentals of pulmonary drug delivery. *Respir Med* **97**: 382-387 (2003).
4. R. J. Kuhn. Formulation of aerosolized therapeutics. *Chest* **120**: 94S-98S (2001).
5. E. Kondili and D. Georgopoulos. Aerosol medications. *Respir Care Clin N Am* **8**: 309-334 (2002).
6. P. J. Barnes and T. T. Hansel. Prospects for new drugs for chronic obstructive pulmonary disease. *Lancet* **364**: 985-996 (2004).
7. A. T. Iacono, T. E. Corcoran, B. P. Griffith*, et al.* Aerosol cyclosporin therapy in lung transplant recipients with bronchiolitis obliterans. *Eur Respir J* **23**: 384-390 (2004).
8. S. Conti, L. Polonelli, R. Frazzi*, et al.* Controlled delivery of biotechnological products. *Curr Pharm Biotechnol* **1**: 313-323 (2000).
9. A. I. Bot, T. E. Tarara, D. J. Smith*, et al.* Novel lipid-based hollow-porous microparticles as a platform for immunoglobulin delivery to the respiratory tract. *Pharm Res* **17**: 275-283 (2000).
10. K. M. Taylor and J. M. Newton. Liposomes for controlled delivery of drugs to the lung. *Thorax.* **47**: 257-9 (1992).
11. J. Fiegel, J. Fu, and J. Hanes. Poly(ether-anhydride) dry powder aerosols for sustained drug delivery in the lungs. *J Control Release* **96**: 411-423 (2004).
12. A. Gautam, J. C. Waldrep, and C. L. Densmore. Aerosol gene therapy. *Mol Biotechnol* **23**: 51-60 (2003).
13. D. R. Gill, L. A. Davies, I. A. Pringle*, et al.* The development of gene therapy for diseases of the lung. *Cell Mol Life Sci* **61**: 355-368 (2004).
14. S. J. Keam and G. M. Keating. Tiotropium bromide. A review of its use as maintenance therapy in patients with COPD. *Treat Respir Med* **3**: 247-268 (2004).
15. B. H. Rowe, M. L. Edmonds, C. H. Spooner*, et al.* Corticosteroid therapy for acute asthma. *Respir Med* **98**: 275-284 (2004).
16. E. J. O'Connell. Review of the unique properties of budesonide. *Clin Ther* **25 Suppl**: 42-60 (2003).
17. D. D. Sin and S. F. Man. Inhaled corticosteroids in the long-term management of patients with chronic obstructive pulmonary disease. *Drugs Aging* **20**: 867-880 (2003).
18. F. Kassner, R. Hodder, and E. D. Bateman. A review of ipratropium bromide/fenoterol hydrobromide (Berodual) delivered via Respimat Soft Mist Inhaler in patients with asthma and chronic obstructive pulmonary disease. *Drugs Aging* **64**: 1671-1682 (2004).
19. H. Olschewski, H. A. Ghofrani, D. Walmrath*, et al.* Inhaliertes Prostazyclin und Iloprost bei schwerer sekundärer pulmonaler Hypertonie durch Lungenfibrose. *Pneumologie* **54**: 133 - 142 (2000).
20. T. J. Kallstrom. Evidence-based asthma management. *Respir Care* **49**: 783-792 (2004).
21. M. E. Klepser. Role of nebulized antibiotics for the treatment of respiratory infections. *Curr Opin Infect Dis* **17**: 109-112 (2004).
22. S. M. Cheer, J. Waugh, and S. Noble. Inhaled tobramycin (TOBI): a review of its use in the management of Pseudomonas aeruginosa infections in patients with cystic fibrosis. *Drugs Aging* **63**: 2501-2520 (2003).

23. P. Diot, P. F. Dequin, B. Rivoire, *et al.* Aerosols and anti-infectious agents. *J Aerosol Med* **14**: 55-64 (2001).

24. E. De Clercq. Antiviral drugs in current clinical use. *J Clin Virol* **30**: 115-133 (2004).

25. H. Dimich-Ward, M. L. Wymer, and M. Chan-Yeung. Respiratory health survey of respiratory therapists. *Chest* **126**: 1048-1053 (2004).

26. J. Lewis and R. A. Veldhuizen. Surfactant: current and potential therapeutic application in infants and adults. *J Aerosol Med* **9**: 143-154 (1996).

27. A. M. Cantin, D. E. Woods, D. Cloutier, *et al.* Leukocyte elastase inhibition therapy in cystic fibrosis: role of glycosylation on the distribution of alpha-1-proteinase inhibitor in blood versus lung. *J Aerosol Med* **15**: 141-148 (2002).

28. J. E. Gadek. Consensus on surfactant and inhaled nitric oxide for ARDS. *J Aerosol Med* **9**: 155-162 (1996).

29. C. Vogelmeier and R. Buhl. Therapy of lung diseases with antiproteases. *Pneumologie* **48**: 57-62 (1994).

30. T. Quattrin. Inhaled insulin: recent advances in the therapy of Type 1 and 2 diabetes. *Expert Opin Pharmacother* **5**: 2597-2604 (2004).

31. Pfizer/Nektar Therapeutics. Insulin inhalation. Pfizer/Nektar Therapeutics: HMR 4006. *Drugs R D* **5**: 166-170 (2004).

32. Y. Qi, G. Zhao, D. Liu, *et al.* Delivery of therapeutic levels of heparin and low-molecular-weight heparin through a pulmonary route. *Proc Natl Acad Sci U S A* **101**: 9867-9872 (2004).

33. G. J. Burkart, G. C. Smaldone, M. A. Eldon, *et al.* Lung deposition and pharmacokinetics of cyclosporine after aerosolization in lung transplant patients. *Pharm Res* **20**: 252-256 (2003).

34. J. Kropp, M. Wencker, A. Hotze, *et al.* Inhalation of [123I]alpha1-protease inhibitor: toward a new therapeutic concept of alpha1-protease inhibitor deficiency? *J Nucl Med* **42**: 744-751 (2001).

35. M. L. Ellett. Alpha 1-antitrypsin deficiency. *Gastroenterol Nurs* **14**: 138-141 (1991).

36. H. K. Chan, A. R. Clark, J. C. Feeley, *et al.* Physical stability of salmon calcitonin spray-dried powders for inhalation. *J Pharm Sci* **93**: 792-804 (2004).

37. D. Kohler. Aerosols for systemic treatment. *Lung* **168**: 677-684 (1990).

38. C. Bosquillon, V. Preat, and R. Vanbever. Pulmonary delivery of growth hormone using dry powders and visualization of its local fate in rats. *J Control Release* **96**: 233-244 (2004).

39. J. Y. Zheng, M. Y. Fulu, D. Y. Lee, *et al.* Pulmonary peptide delivery: effect of taste-masking excipients on leuprolide suspension metered-dose inhalers. *Pharm Dev Technol* **6**: 521-530 (2001).

40. A. Adjei, D. Sundberg, J. Miller, *et al.* Bioavailability of leuprolide acetate following nasal and inhalation delivery to rats and healthy humans. *Pharm Res* **9**: 244-249 (1992).

41. E. R. Weibel. *Morphology of the human lung*, Springer-Verlag, Berlin, 1963.

42. R. Ferlinz. *Pneumologie in Praxis und Klinik*, Thieme Verlag, Stuttgart, 1994.

43. C. Mobley and G. Hochhaus. Methods used to assess pulmonary deposition and absorption of drugs. *DDT* **6**: (2001).

44. D. A. Groneberg, M. Nickolaus, J. Springer, *et al.* Localization of the peptide transporter PEPT2 in the lung: implications for pulmonary oligopeptide uptake. *Am J Pathol* **158**: 707-714 (2001).

45. W. Schoedel, H. Slama, and E. Hansen. Time-dependent behaviour of lung alveolar surfactant film. *Pflugers Arch* **322**: 336-346 (1971).

46. J. Vadolas, R. Williamson, and P. A. Ioannou. Gene therapy for inherited lung disorders: An insight into pulmonary defence. *Pulm Pharmacol Therapeutics* **15**: 61-72 (2002).

47. M. Gumbleton. Caveolae as potential macromolecule trafficking compartments within alveolar epithelium. *Adv Drug Deliv Rev* **49**: 281-300 (2001).

48. M. Gumbleton, A. J. Hollins, Y. Omidi, *et al.* Targeting caveolae for vesicular drug transport. *J Control Release* **87**: 139-151 (2003).

49. D. P. McIntosh, X. Y. Tan, P. Oh, *et al.* Targeting endothelium and its dynamic caveolae for tissue-specific transcytosis in vivo: A pathway to overcome cell barriers to drug and gene delivery. *Proc Natl Acad Sci USA* **99**: 1996-2001 (2002).

50. S. M. Danilov, V. D. Gavrilyuk, F. E. Franke, *et al.* Lung uptake of antibodies to endothelial antigens: key determinants of vascular immunotargeting. *Am J Physiol Lung Cell Mol Physiol* **280**: 1335-1347 (2001).

51. S. Li, Y. Tan, E. Viroonchatapan, *et al.* Targeted gene delivery to pulmonary endothelium by anti-PECAM antibody. *Am J Physiol Lung Cell Mol Physiol* **278**: 504-511 (2000).

52. D. Lechardeur, A. S. Verkman, and G. L. Lukacs. Intracellular routing of plasmid DNA during non-viral gene transfer. *Adv Drug Deliv Rev* **57**: 755-767 (2005).

53. T. Thepen, G. Kraal, and P. G. Holt. The role of alveolar macrophages in regulation of lung inflammation. *Ann N Y Acad Sci* **725**: 200-206 (1994).

54. S. Ferrari, U. Griesenbach, D. M. Geddes, *et al.* Immunological hurdles to lung gene therapy. *Clin Exp Immunol* **132**: 1-8 (2003).

55. R. Dhand. New frontiers in aerosol delivery during mechanical ventilation. *Respir Care* **49**: 666-677 (2004).

56. S. Pedersen. Inhalers and nebulizers: which to choose and why. *Respir Med* **90**: 69-77 (1996).

57. P. P. Le Brun, A. H. de Boer, H. G. Heijerman, *et al.* A review of the technical aspects of drug nebulization. *Pharm World Sci* **22**: 75-81 (2000).

58. S. P. Newman. Dry powder inhalers for optimal drug delivery. *Expert Opin Biol Ther* **4**: 23-33 (2004).

59. D. T. Loffert, D. Ikle, and H. S. Nelson. A comparison of commercial jet nebulizers. *Chest* **106**: 1788-1792 (1994).

60. A. H. Kendrick, E. C. Smith, and R. S. Wilson. Selecting and using nebuliser equipment. *Thorax* **52**: 92-101 (1997).

61. PARI GmbH. Product information, www.pari.com (2004).

62. Nebu-Tec GmbH. Optineb Product information, www.nebu-tec.de (2004).

63. Aerogen Technologie. Review and performance report for the Aerogen professional nebulizer system, www.aerogen.com (2002).

64. R. Dhand. Nebulizers that use a vibrating mesh or plate with multiple apertures to generate aerosol. *Respir Care* **47**: 1406-1416 (2002).

65. G. Einberg and S. Holmberg. Characteristics of particles and their behaviour in ventilation air. *Int J Ventilation* **2**: 45-54 (2003).

66. T. B. Martonen and I. M. Katz. Deposition patterns of aerosolized drugs within human lungs: effects of ventilatory parameters. *Pharm Res* **10**: 871-878 (1993).

67. J. Fiegel, C. Ehrhardt, U. F. Schaefer, *et al.* Large porous particle impingement on lung epithelial cell monolayers--toward improved particle characterization in the lung. *Pharm Res* **20**: 788-796 (2003).

68. K. Koushik and U. B. Kompella. Preparation of large porous deslorelin-PLGA microparticles with reduced residual solvent and cellular uptake using a supercritical carbon dioxide process. *Pharm Res* **21**: 524-235 (2004).

69. P. P. Le Brun, A. H. de Boer, D. Gjaltema, *et al.* Inhalation of tobramycin in cystic fibrosis. Part 1: the choice of a nebulizer. *Int J Pharm* **189**: 205-214 (1999).

70. T. Friedmann and R. Roblin. Gene therapy for human genetic disease? *Science* **175**: 949-955 (1972).

71. E. Freese. Prospects of gene therapy. *Science* **175**: 1024-1025 (1972).

72. R. M. Blaese, K. W. Culver, A. D. Miller, *et al.* T lymphocyte-directed gene therapy for ADA- SCID: initial trial results after 4 years. *Science* **270**: 475-480 (1995).

73. http://www.wiley.com/legacy/wileychim/genmed/clinical/ (2005).

74. T. Friedmann. Overcoming the obstacles to gene therapy. *Sci Am* **276**: 96-101 (1997).

75. D. M. Prazeres, G. A. Monteiro, G. N. Ferreira, *et al.* Purification of plasmids for gene therapy and DNA vaccination. *Biotechnol Annu Rev* **7**: 1-30 (2001).

76. C. Toniatti, H. Bujard, R. Cortese, *et al.* Gene therapy progress and prospects: transcription regulatory systems. *Gene Ther* **11**: 649-657 (2004).

77. M. Nishikawa, Y. Takakura, and M. Hashida. Theoretical considerations involving the pharmacokinetics of plasmid DNA. *Adv Drug Deliv Rev* **57**: 675-88 (2005).

78. A. Rolland. Gene medicines: The end of the beginning? *Adv Drug Deliv Rev* **57**: 669-673 (2005).

79. D. Luo and W. M. Saltzman. Synthetic DNA delivery systems. *Nature Biotechnology* **18**: 33-37 (2000).

80. T. Friedmann. Clinical gene therapy: lessons from the ether dome. *Mol Ther* **10**: 205-206 (2004).

81. Z. L. Xu, H. Mizuguchi, F. Sakurai, *et al.* Approaches to improving the kinetics of adenovirus-delivered genes and gene products. *Adv Drug Deliv Rev* **57**: 781-802 (2005).

82. T. Friedmann. Stanfield Rogers: insights into virus vectors and failure of an early gene therapy model. *Mol Ther* **4**: 285-288 (2001).

83. C. M. Wiethoff and C. R. Middaugh. Barriers to nonviral gene delivery. *J Pharm Sci* **92**: 2003-217 (2003).

84. A. J. Comerota, R. C. Throm, K. A. Miller, *et al.* Naked plasmid DNA encoding fibroblast growth factor type 1 for the treatment of end-stage unreconstructible lower extremity ischemia: preliminary results of a phase I trial. *J Vasc Surg* **35**: 930-936 (2002).

85. R. Morishita, M. Aoki, N. Hashiya, *et al.* Safety evaluation of clinical gene therapy using hepatocyte growth factor to treat peripheral arterial disease. *Hypertension* **44**: 203-209 (2004).

86. A. Matsuki, S. Yamamoto, H. Nakagami, *et al.* No influence of tumor growth by intramuscular injection of hepatocyte growth factor plasmid DNA: safety evaluation of therapeutic angiogenesis gene therapy in mice. *Biochem Biophys Res Commun* **315**: 59-65 (2004).

87. M. G. Svahn, K. E. Lundin, R. Ge, *et al.* Adding functional entities to plasmids. *J Gene Med* **6 Suppl 1**: S36-44 (2004).

88. W. Li, F. Nicol, and F. C. Szoka, Jr. GALA: a designed synthetic pH-responsive amphipathic peptide with applications in drug and gene delivery. *Adv Drug Deliv Rev* **56**: 967-985 (2004).

89. Y. Yamashita, M. Shimada, R. Minagawa, *et al.* Muscle-targeted interleukin-12 gene therapy of orthotopic hepatocellular carcinoma in mice using in vivo electrosonoporation. *Mol Cancer Ther* **3**: 1177-1182 (2004).

90. Genetronics Biomedical. Bleomycin - electrical pulse delivery: electroporation therapy, MedPulser-bleomycin-Genetronics. *Drugs R D* **5**: 293-296 (2004).

91. S. Mehier-Humbert and R. H. Guy. Physical methods for gene transfer: Improving the kinetics of gene delivery into cells. *Adv Drug Deliv Rev* **57**: 733-753 (2005).

92. C. Trimble, C. T. Lin, C. F. Hung, *et al.* Comparison of the CD8+ T cell responses and antitumor effects generated by DNA vaccine administered through gene gun, biojector, and syringe. *Vaccine* **21**: 4036-4042 (2003).

93. M. Koeping-Hoeggard, K. M. Varum, M. Issa, *et al.* Improved chitosan-mediated gene delivery based on easily dissociated chitosan polyplexes of highly defined chitosan oligomers. *Gene Ther* **11**: 1441-1452 (2004).

94. F. Chellat, A. Grandjean-Laquerriere, R. Le Naour, *et al.* Metalloproteinase and cytokine production by THP-1 macrophages following exposure to chitosan-DNA nanoparticles. *Biomaterials* **26**: 961-970 (2005).

95. J. Panyam and V. Labhasetwar. Biodegradable nanoparticles for drug and gene delivery to cells and tissue. *Adv Drug Deliv Rev* **55**: 329-247 (2003).

96. S. Madhusudan, A. Tamir, N. Bates, *et al.* A multicenter Phase I gene therapy clinical trial involving intraperitoneal administration of E1A-lipid complex in patients with recurrent epithelial ovarian cancer overexpressing HER-2/neu oncogene. *Clin Cancer Res* **10**: 2986-2996 (2004).

97. I. Tranchant, B. Thompson, C. Nicolazzi, *et al.* Physicochemical optimisation of plasmid delivery by cationic lipids. *J Gene Med* **6 Suppl 1**: S24-35 (2004).

98. N. S. Templeton. Cationic liposome-mediated gene delivery in vivo. *Biosci Rep* **22**: 283-295 (2002).

99. E. Wagner. Strategies to improve DNA polyplexes for in vivo gene transfer: will "artificial viruses" be the answer? *Pharm Res* **21**: 8-14 (2004).

100. R. Kircheis, L. Wightman, and E. Wagner. Design and gene delivery activity of modified polyethylenimines. *Adv Drug Deliv Rev* **53**: 341-358 (2001).

101. G. F. Lemkine and B. A. Demeneix. Polyethylenimines for in vivo gene delivery. *Curr Opin Mol Ther* **3**: 178-182 (2001).

102. O. Boussif, F. Lezualcho, M. A. Zanta, *et al.* A versatile vector for gene and oligonucleotide transfer into cells in culture and in vivo: polyethylenimine. *Proc Natl Acad Sci U S A* **92**: 7297-7301 (1995).

103. A. Gautam, C. L. Densmore, S. Melton, *et al.* Aerosol delivery of PEI-p53 complexes inhibits B16-F10 lung metastases through regulation of angiogenesis. *Cancer Gene Ther* **9**: 28-36 (2002).

104. A. Gautam, J. C. Waldrep, C. L. Densmore, *et al.* Growth inhibition of established B16-F10 lung metastases by sequential aerosol delivery of p53 gene and 9-nitrocamptothecin. *Gene Ther* **9**: 353-357 (2002).

105. S. F. Jia, L. L. Worth, C. L. Densmore, *et al.* Aerosol gene therapy with PEI: IL-12 eradicates osteosarcoma lung metastases. *Clin Cancer Res* **9**: 3462-3468 (2003).

106. S. F. Jia, L. L. Worth, C. L. Densmore, *et al.* Eradication of osteosarcoma lung metastases following intranasal interleukin-12 gene therapy using a nonviral polyethylenimine vector. *Can Gene Ther* **9**: 260-266 (2002).

107. J. W. Wiseman, C. A. Goddard, D. McLelland, *et al.* A comparison of linear and branched polyethylenimine (PEI) with DCChol/DOPE liposomes for gene delivery to epithelial cells in vitro and in vivo. *Gene Ther* **10**: 1654-1662 (2003).

108. A. C. Hirko, D. D. Buethe, E. M. Meyer, *et al.* Plasmid delivery in the rat brain. *Biosci Rep* **22**: 297-308 (2002).

109. A. Johansson, G. Nowak, C. Moller, *et al.* Non-viral delivery of the porphobilinogen deaminase cDNA into a mouse model of acute intermittent porphyria. *Mol Genet Metab* **82**: 20-26 (2004).

110. Y. K. Oh, J. S. Park, M. J. Kang, *et al.* Enhanced adjuvanticity of interleukin-2 plasmid DNA administered in polyethylenimine complexes. *Vaccine* **21**: 2837-2843 (2003).

111. A. N. Uduehi, U. Stammberger, B. Kubisa, *et al.* Effects of linear polyethylenimine and polyethylenimine/DNA on lung function after airway instillation to rat lungs. *Mol Ther* **4**: 52-57 (2001).

112. S. Ferrari, A. Pettenazzo, N. Garbati, *et al.* Polyethylenimine shows properties of interest for cystic fibrosis gene therapy. *Biochim Biophys Acta* **1447**: 219-225 (1999).

113. F. Vernejoul, P. Faure, N. Benali, *et al.* Antitumor effect of in vivo somatostatin receptor subtype 2 gene transfer in primary and metastatic pancreatic cancer models. *Cancer Res* **62**: 6124-6131 (2002).

114. M. Ogris, S. Brunner, S. Schuller, *et al.* PEGylated DNA/transferrin-PEI complexes: reduced interaction with blood components, extended circulation in blood and potential for systemic gene delivery. *Gene Ther* **6**: 595-605 (1999).

115. L. Shi, G. P. Tang, S. J. Gao, *et al.* Repeated intrathecal administration of plasmid DNA complexed with polyethylene glycol-grafted polyethylenimine led to prolonged transgene expression in the spinal cord. *Gene Ther* **10**: 1179-1788 (2003).

116. C. Rudolph, U. Schillinger, C. Plank, *et al.* Nonviral gene delivery to the lung with copolymer-protected and transferrin-modified polyethylenimine. *Biochim Biophys Acta* **1573**: 75-83 (2002).

117. A. Kichler, M. Chillon, C. Leborgne, *et al.* Intranasal gene delivery with a polyethylenimine-PEG conjugate. *J Control Release* **81**: 379-388 (2002).

118. I. J. Hildebrandt, M. Iyer, E. Wagner, *et al.* Optical imaging of transferrin targeted PEI/DNA complexes in living subjects. *Gene Ther* **10**: 758-764 (2003).

119. R. Kircheis, T. Blessing, S. Brunner, *et al.* Tumor targeting with surface-shielded ligand-polycation DNA complexes. *J Control Release* **72**: 165-170 (2001).

120. M. Ogris, G. Walker, T. Blessing, *et al.* Tumor-targeted gene therapy: strategies for the preparation of ligand-polyethylene glycol-polyethylenimine/DNA complexes. *J Control Release* **91**: 173-181 (2003).

121. K. Morimoto, M. Nishikawa, S. Kawakami, *et al.* Molecular weight-dependent gene transfection activity of unmodified and galactosylated polyethyleneimine on hepatoma cells and mouse liver. *Mol Ther* **7**: 254-261 (2003).

122. S. H. Pun, N. C. Bellocq, A. Liu, *et al.* Cyclodextrin-modified polyethylenimine polymers for gene delivery. *Bioconjug Chem* **15**: 831-840 (2004).

123. D. Fischer, A. v. Harpe, and T. Kissel. Polyethylenimine: Polymer Structure Influences the Physicochemical and Biological Effects of Plasmid/PEI Complexes. *Biomaterials* 195-211 (2000).

124. E. Kleemann, L. A. Dailey, H. G. Abdelhady, *et al.* Modified polyethylenimines as non-viral gene delivery systems for aerosol gene therapy: Investigations of the complex structure and stability during air-jet and ultrasonic nebulization. *J Control Release* **100**: 437-450 (2004).

125. M. Ruponen, P. Honkakoski, S. Ronkko, *et al.* Extracellular and intracellular barriers in non-viral gene delivery. *J Control Release* **93**: 213-217 (2003).

126. J. P. Behr. The proton sponge: A trick to enter cells the viruses did not exploit. *Chimia* **51**: 34-36 (1997).

127. W. T. Godbey, K. K. Wu, and A. G. Mikos. Tracking the intracellular path of poly(ethylenimine)/DNA complexes for gene delivery. *Proc Natl Acad Sci USA* **96**: 5177-5181 (1999).

128. T. Bieber, W. Meissner, S. Kostin, *et al.* Intracellular route and transcriptional competence of polyethylenimine-DNA complexes. *J Control Release* **82**: 441-54 (2002).

129. M. Brisson and L. Huang. Liposomes: conquering the nuclear barrier. *Curr Opin Mol Ther* **1**: 140-6 (1999).

130. J. Suh, D. Wirtz, and J. Hanes. Efficient active transport of gene nanocarriers to the cell nucleus. *Proc Natl Acad Sci U S A* **100**: 3878-3882 (2003).

131. S. Brunner, E. Furtbauer, T. Sauer, *et al.* Overcoming the nuclear barrier: Cell cylce independent nonviral gene transfer with linear polyethylenimine or electroporation. *Mol Ther* **5**: 80-86 (2002).

132. T. R. Flotte and B. L. Laube. Gene therapy in cystic fibrosis. *Chest* **120**: 124S-131S (2001).

133. T. R. Flotte, P. L. Zeitlin, T. C. Reynolds, *et al.* Phase I trial of intranasal and endobronchial administration of a recombinant adeno-associated virus serotype 2 (rAAV2)-CFTR vector in adult cystic fibrosis patients: a two-part clinical study. *Hum Gene Ther* **14**: 1079-1088 (2003).

134. D. K. Meyerholz, B. Grubor, J. M. Gallup, *et al.* Adenovirus-mediated gene therapy enhances parainfluenza virus 3 infection in neonatal lambs. *J Clin Microbiol* **42**: 4780-4787 (2004).

135. M. F. Tosi, A. van Heeckeren, T. W. Ferkol, *et al.* Effect of Pseudomonas-induced chronic lung inflammation on specific cytotoxic T-cell responses to adenoviral vectors in mice. *Gene Ther* **11**: 1427-1433 (2004).

136. D. Duan, Y. Yue, Z. Yan, *et al.* Endosomal processing limits gene transfer to polarized airway epithelia by adeno-associated virus. *J Clin Invest* **105**: 1573-1587 (2000).

137. C. L. Halbert and A. D. Miller. AAV-mediated gene transfer to mouse lungs. *Methods Mol Biol* **246**: 201-212 (2004).

138. A. C. Fischer, S. E. Beck, C. I. Smith, *et al.* Successful transgene expression with serial doses of aerosolized rAAV2 vectors in rhesus macaques. *Mol Ther* **8**: 918-926 (2003).

139. T. R. Flotte. Gene therapy progress and prospects: recombinant adeno-associated virus (rAAV) vectors. *Gene Ther* **11**: 805-810 (2004).

140. Y. Yonemitsu, C. Kitson, S. Ferrari, *et al.* Efficient gene transfer to airway epithelium using recombinant Sendai virus. *Nat Biotechnol* **18**: 970-973 (2000).

141. S. Ferrari, U. Griesenbach, R. Farley, *et al.* Recombinant Sendai virus mediates CFTR gene transfer to airway epithelium both ex vivo and in vivo. *Thorax* **58**: 19-20 (2003).

142. S. Ferrari, U. Griesenbach, T. Shiraki-Iida, *et al.* A defective nontransmissible recombinant Sendai virus mediates efficient gene transfer to airway epithelium in vivo. *Gene Ther* **11**: 1659-1664 (2004).

143. L. Bao, V. Jaligam, X. Y. Zhang, *et al.* Stable transgene expression in tumors and metastases after transduction with lentiviral vectors based on human immunodeficiency virus type 1. *Hum Gene Ther* **15**: 445-456 (2004).

144. E. Copreni, M. Penzo, S. Carrabino, *et al.* Lentivirus-mediated gene transfer to the respiratory epithelium: a promising approach to gene therapy of cystic fibrosis. *Gene Ther* **11 Suppl 1**: S67-75 (2004).

145. N. J. Caplen, E. W. F. W. Alton, P. G. Middleton, *et al.* Liposome-mediated CFTR gene-transfer to the nasal epithelium of patients with cystic-fibrosis. *Nature Medicine* **1**: 39-46 (1995).

146.   S. C. Hyde, K. W. Southern, U. Gileadi, *et al.* Repeat administration of DNA/liposomes to the nasal epithelium of patients with cystic fibrosis. *Gene Ther* **7**: 1156-1165 (2000).

147.   D. R. Gill, K. W. Southern, K. A. Mofford, *et al.* A placebo-controlled study of liposome-mediated gene transfer to the nasal epithelium of patients with cystic fibrosis. *Gene Ther* **4**: 199-209 (1997).

148.   D. J. Porteous, J. R. Dorin, G. McLachlan, *et al.* Evidence for safety and efficacy of DOTAP cationic liposome mediated CFTR gene transfer to the nasal epithelium of patients with cystic fibrosis. *Gene Ther* **4**: 210-218 (1997).

149.   P. G. Noone, K. W. Hohneker, Z. Q. Zhou, *et al.* Safety and biological efficacy of a lipid-CFTR complex for gene transfer in the nasal epithelium of adult patients with cystic fibrosis. *Mol Ther* **1**: 105-114 (2000).

150.   J. Zabner, B. W. Ramsey, D. P. Meeker, *et al.* Repeat administration of an adenovirus vector encoding CFTR to the nasal epithelium of patients with cystic fibrosis. *J Invest Med* **44**: A319-A319 (1996).

151.   E. W. F. W. Alton, M. Stern, R. Farley, *et al.* Cationic lipid-mediated CFTR gene transfer to the lungs and nose of patients with cystic fibrosis: a double-blind placebo-controlled trial. *Lancet* **353**: 947-954 (1999).

152.   F. E. Ruiz, J. P. Clancy, M. A. Perricone, *et al.* A clinical inflammatory syndrome attributable to aerosolized lipid-DNA administration in cystic fibrosis. *Hum Gene Ther* **12**: 751-761 (2001).

153.   M. Brzoska, K. Langer, C. Coester, *et al.* Incorporation of biodegradable nanoparticles into human airway epithelium cells-in vitro study of the suitability as a vehicle for drug or gene delivery in pulmonary diseases. *Biochem Biophys Res Commun* **318**: 562-570 (2004).

154.   L. Hyndman, J. L. Lemoine, L. Huang, *et al.* HIV-1 Tat protein transduction domain peptide facilitates gene transfer in combination with cationic liposomes. *J Control Release* **99**: 435-444 (2004).

155.   C. Rudolph, C. Plank, J. Lausier, *et al.* Oligomers of the arginine-rich motif of the HIV-1 TAT protein are capable of transferring plasmid DNA into cells. *J Biol Chem* **278**: 11411-11418 (2003).

156.   J. S. Wadia, R. V. Stan, and S. F. Dowdy. Transducible TAT-HA fusogenic peptide enhances escape of TAT-fusion proteins after lipid raft macropinocytosis. *Nat Medicine* **10**: 310 - 315 (2004).

157.   V. P. Torchilin, T. S. Levchenko, R. Rammohan, *et al.* Cell transfection in vitro and in vivo with non-toxic TAT peptide-liposome-DNA complexes. *Proc Natl Acad Sci U S A* **100**: 1972–1977 (2003).

158.   T. Ferkol, A. Pellicena-Palle, E. Eckman, *et al.* Immunologic responses to gene transfer into mice via the polymeric immunoglobulin receptor. *Gene Ther* **3**: 669-678 (1996).

159.   A. G. Ziady, T. Ferkol, D. V. Dawson, *et al.* Chain length of the polylysine in receptor-targeted gene transfer complexes affects duration of reporter gene expression both in vitro and in vivo. *J Biol Chem* **274**: 4908-4916 (1999).

160.   A. G. Ziady, T. J. Kelley, E. Milliken, *et al.* Functional evidence of CFTR gene transfer in nasal epithelium of cystic fibrosis mice in vivo following luminal application of DNA complexes targeted to the serpin-enzyme complex receptor. *Mol Ther* **5**: 413-419 (2002).

161.   A. G. Ziady, C. R. Gedeon, T. Miller, *et al.* Transfection of airway epithelium by stable PEGylated poly-L-lysine DNA nanoparticles in vivo. *Mol Ther* **8**: 936-947 (2003).

162. C. L. Densmore. Polyethyleneimine-based gene therapy by inhalation. *Expert Opin Biol Ther* **3**: 1083-1092 (2003).
163. A. Gautam, C. J. Waldrep, and C. L. Densmore. Delivery systems for pulmonary gene therapy. *Am J Respir Med* **1**: 35-46 (2002).
164. C. M. Rudolph, R.H.; Rosenecker, J. Jet nebulization of PEI/DNA polyplexes: physical stability and in vitro gene delivery efficiency. *J Gene Med* **4**: 66-74 (2002).
165. D. Goula, C. Benoist, S. Mantero, *et al.* Polyethylenimine-based intravenous delivery of transgenes to mouse lung. *Gene Ther* **5**: 1291-1295 (1998).
166. D. Goula, N. Becker, G. F. Lemkine, *et al.* Rapid crossing of the pulmonary endothelial barrier by polyethylenimine/DNA complexes. *Gene Ther* **7**: 499-504 (2000).
167. L. Wightman, R. Kircheis, V. Rossler, *et al.* Different behaviour of branched and linear polyethylenimine for gene delivery in vitro and in vivo. *J Gene Med* **3**: 362-372 (2001).
168. P. Chollet, M. C. Favrot, A. Hurbin, *et al.* Side-effects of a systemic injection of linear polyethylenimine-DNA complexes. *J Gene Med* **4**: 84-91 (2002).
169. F. M. Orson, B. M. Kinsey, B. S. Bhogal, *et al.* Targeted delivery of expression plasmids to the lung via macroaggregated polyethylenimine-albumin conjugates. *Methods Mol Med* **75**: 575-590 (2003).
170. F. M. Orson, B. M. Kinsey, P. J. Hua, *et al.* Genetic immunization with lung-targeting macroaggregated polyethyleneimine-albumin conjugates elicits combined systemic and mucosal immune responses. *J Immunol* **164**: 6313-6321 (2000).
171. F. M. Orson, L. Song, A. Gautam, *et al.* Gene delivery to the lung using protein/polyethylenimine/plasmid complexes. *Gene Ther* **9**: 463-471 (2002).
172. N. Ernst, S. Ulrichskötter, W. A. Schmalix, *et al.* Interaction of liposomal and polycationic transfection complexes with pulmonary surfactant. *J Gene Med* **1**: 331-340 (1999).
173. L. A. Dailey, E. Kleemann, T. Merdan, *et al.* Modified Polyethylenimines as Non Viral Gene Delivery Systems for Aerosol Therapy: Effects of Nebulization on Cellular Uptake and Transfection Efficiency. *J Control Release* **100**: 425-436 (2004).
174. A. Bragonzi, G. Dina, A. Villa, *et al.* Biodistribution and transgene expression with nonviral cationic vector/DNA complexes in the lung. *Gene Ther* **7**: 1753-1760 (2000).
175. S. Ferrari, E. Moro, A. Pettenazzo, *et al.* ExGen 500 is an efficient vector for gene delivery to lung epithelial cells in vitro and in vivo. *Gene Ther* **4**: 1100-1106 (1997).
176. C. Rudolph, J. Lausier, S. Naundorf, *et al.* In vivo gene delivery to the lung using polyethylenimine and fractured polyamidoamine dendrimers. *J Gene Med* **2**: 269-278 (2000).
177. N. V. Koshkina, I. Y. Agoulnik, S. L. Melton, *et al.* Biodistribution and pharmacokinetics of aerosol and intravenously administered DNA-polyethyleneimine complexes: optimization of pulmonary delivery and retention. *Mol Ther* **8**: 249-254 (2003).
178. C. L. Densmore, F. M. Orson, B. Xu, *et al.* Aerosol delivery of robust polyethylenimine-DNA complexes for gene therapy and genetic immunization. *Mol Ther* **1**: 180-188 (2000).
179. A. Gautam, C. L. Densmore, B. Xu, *et al.* Enhanced gene expression in mouse lung after PEI-DNA aerosol delivery. *Mol Ther* **2**: 63-70 (2000).
180. A. Gautam, C. L. Densmore, and J. C. Waldrep. Inhibition of experimental lung metastasis by aerosol delivery of PEI-p53 complexes. *Mol Ther* **2**: 318-323 (2000).

181. A. Gautam, C. L. Densmore, S. Melton, *et al.* Aerosol delivery of PEI-p53 complexes inhibits B16-F10 lung metastases through regulation of angiogenesis. *Cancer Gene Ther* **9**: 28-36 (2002).

182. A. Gautam, C. L. Densmore, and J. C. Waldrep. Pulmonary cytokine responses associated with PEI-DNA aerosol gene therapy. *Gene Ther* **8**: 254-257 (2001).

183. E. Kleemann, N. Jekel, L. A. Dailey, *et al.* Enhanced gene expression in mice using polyplexes of low-molecular weight poly (ethylene imine) for pulmonary gene therapy. *J Gene Med* **submited**: (2005).

184. G. Sessa and G. Weissmann. Phospholipid spherules (liposomes) as a model for biological membranes. *J Lipid Res* **9**: 310-318 (1968).

185. G. Gregoriadis and B. E. Ryman. Lysosomal localization of enzyme-containing liposomes injected into rats. *Biochem J* **128**: 142P-143P (1972).

186. G. J. R. Charrois and T. M. Allen. Drug release rate influences the pharmacokinetics, biodistribution, therapeutic activity, and toxicity of pegylated liposomal doxorubicin formulations in murine breast cancer. *Biochim Biophys Acta Biomem* **1663**: 167-177 (2004).

187. C. E. Swenson, L. E. Bolcsak, G. Batist, *et al.* Pharmacokinetics of doxorubicin administered i.v. as Myocet (TLC D-99; liposome-encapsulated doxorubicin citrate) compared with conventional doxorubicin when given in combination with cyclophosphamide in patients with metastatic breast cancer. *Anticancer Drugs* **14**: 239-246 (2003).

188. K. Mross, B. Niemann, U. Massing, *et al.* Pharmacokinetics of liposomal doxorubicin (TLC-D99 ; Myocet) in patients with solid tumors: an open-label, single-dose study. *Canc Chemother Pharmacol* **54**: 514-524 (2004).

189. S. Faivre, H. Alsabe, L. Djafari, *et al.* Locoregional effects of pegylated liposomal doxorubicin (Caelyx (R)) in irradiated area: a phase I-II study in patients with recurrent squamous cell carcinoma of the head and neck. *Europ J Cancer* **40**: 1517-1521 (2004).

190. D. D. Lasic. Novel applications of liposomes. *Trends Biotechnol* **16**: 307-321 (1998).

191. A. Sharma and U. S. Sharma. Liposomes in drug delivery: progress and limitation. *Int J of Pharm* **154**: 123-140 (1997).

192. M. Anderson and A. Omri. The effect of different lipid components on the in vitro stability and release kinetics of liposome formulations. *Drug Deliv* **11**: 33-39 (2004).

193. Y. Barenholz. Liposome application: problems and prospects. *Curr Opin Coll Interface Sci* **6**: 66-77 (2001).

194. K. M. G. Taylor and R. M. Morris. Thermal-analysis of phase-transition behaviour in liposomes. *Thermochim Acta* **248**: 289-301 (1995).

195. V. P. Torchilin and V. Weissig. *Liposomes - A practical approach*, Oxford University Press, Oxford, 2003.

196. D. D. Lasic and D. Needham. The Stealth Liposomes: A Prototypical Biomaterial. *Chem Rev* **95**: 2601-2627 (1995).

197. T. Ishida, H. Harashima, and H. Kiwada. Liposome clearance. *Biosci Rep* **22**: 197-224 (2002).

198. M. J. Fonseca, J. C. Jagtenberg, H. J. Haisma, *et al.* Liposome-mediated targeting of enzymes to cancer cells for site-specific activation of prodrugs: comparison with the corresponding antibody-enzyme conjugate. *Pharm Res* **20**: 423-428 (2003).

199. T. Hamaguchi, Y. Matsumura, Y. Nakanishi, *et al.* Antitumor effect of MCC-465, pegylated liposomal doxorubicin tagged with newly developed monoclonal antibody GAH, in colorectal cancer xenografts. *Cancer Science* **95**: 608-613 (2004).

200. R. M. Abra, R. B. Bankert, F. Chen, *et al.* The next generation of liposome delivery systems: recent experience with tumor-targeted, sterically-stabilized immunoliposomes and active-loading gradients. *J Liposome Res* **12**: 1-3 (2002).

201. R. Abu-Dahab, U. F. Schäfer, and C. M. Lehr. Lectin-functionalized liposomes for pulmonary drug delivery: effect of nebulization on stability and bioadhesion. *Eur J Pharm Sci* **14**: 37-46 (2001).

202. A. Gabizon, H. Shmeeda, A. T. Horowitz, *et al.* Tumor cell targeting of liposome-entrapped drugs with phospholipid-anchored folic acid-PEG conjugates. *Adv Drug Deliv Rev* **56**: 1177-1192 (2004).

203. P. Holig, M. Bach, T. Volkel, *et al.* Novel RGD lipopeptides for the targeting of liposomes to integrin-expressing endothelial and melanoma cells. *Protein Eng Des Sel* **17**: 433-441 (2004).

204. http://www.unizh.ch/onkwww/lipos.htm. (2005).

205. R. L. Juliano and H. N. McCullough. Controlled delivery of an antitumor drug: localized action of liposome encapsulated cytosine arabinoside administered via the respiratory system. *J Pharmacol Exp Ther* **214**: 381-387 (1980).

206. S. G. Woolfrey, G. Taylor, I. W. Kellaway, *et al.* Pulmonary Absorption of Liposome-Encapsulated 6-Carboxyflurescein. *J Control Release* **5**: 203-209 (1988).

207. D. A. Thomas, M. A. Myers, B. Wichert, *et al.* Acute effects of liposome aerosol inhalation on pulmonary function in healthy human volunteers. *Chest* **99**: 1268-1270 (1991).

208. M. A. Myers, D. A. Thomas, L. Straub, *et al.* Pulmonary effects of chronic exposure to liposome aerosols in mice. *Exp Lung Res* **19**: 1-19 (1993).

209. A. Pettenazzo, A. Jobe, M. Ikegami, *et al.* Clearance of phosphatidylcholine and cholesterol from liposomes, liposomes loaded with metaproterenol, and rabbit surfactant from adult rabbit lungs. *Am Rev Respir Dis* **139**: 752-758 (1989).

210. R. N. Niven, T. M. Carvajal, and H. Schreier. Nebulization of liposomes III - The effects of operating conditions and local environment. *Pharm Res* **9**: 515-520 (1992).

211. R. N. Niven and H. Schreier. Nebulization of lLiposomes I - Effects of lipid compositon. *Pharm Res* **7**: 1127-1133 (1990).

212. R. W. Niven, M. Speer, and H. Schreier. Nebulization of liposomes II - The effects of size and modeling of solute release profiles. *Pharm Res* **8**: 217-221 (1991).

213. H. Schreier. Liposome Aerosols. *J of Lip Res* **2**: 145-184 (1992).

214. B. V. Wichert, R. J. Gonzalez-Rothi, L. E. Straub, *et al.* Amikacin liposomes: characterization, aerosolization, and in vitro activity against Mycobacterium avium-intracellulare in alveolar macrophages. *Int J Pharm* **78**: 227-235 (1992).

215. Y. Darwis and I. W. Kellaway. Nebulisation of rehydrated freeze-dried beclomethasone dipropionate liposomes. *Int J Pharm* **215**: 113-121 (2001).

216. T. R. Desai, R. E. Hancock, and W. H. Finlay. A facile method of delivery of liposomes by nebulization. *J Control Release* **84**: 69-78 (2002).

217. R. J. Gonzalez-Rothi, S. Suarez, G. Hochhaus, *et al.* Pulmonary targeting of liposomal triamcinolone acetonide phosphate. *Pharm Res* **13**: 1699-1703 (1996).

218. S. Suarez, R. Gonzalez-Rothi, H. Schreier, *et al.* Effect of dose and release rate on pulmonary targeting of liposomal triamcinolone acetonide phosphate. *Pharm Res* **15**: 461-465 (1998).

219. O. R. Hung, S. C. Whynot, J. R. Varvel, *et al.* Pharmacokinetics of inhaled liposome-encapsulated fentanyl. *Anesthesiology* **83**: 277-284 (1994).

220. C. Khanna, J. C. Waldrep, P. M. Anderson, *et al.* Nebulized interleukin 2 liposomes: Aerosol charakteristics and biodistribution. *J Pharm Pharmacol* **49**: 960-971 (1997).

221. R. M. Ten, P. M. Anderson, N. N. Zein, *et al.* Interleukin-2 liposomes for primary immune deficiency using the aerosol route. *Int Immunopharm* **2**: 333-334 (2001).
222. M. P. Lambros, D. W. A. Bourne, S. A. Abbas, *et al.* Disposition of Aerosolized Liposomal Amphotericin B. *J of Pharm Sci* **86**: 1066-1069 (1997).
223. T. L. Yaksh, J. C. Provencher, M. L. Rathbun, *et al.* Safety assessment of encapsulated morphine delivered epidurally in a sustained-release multivesicular liposome preparation in dogs. *Drug Deliv* **7**: 27-36 (2000).
224. P. A. Bridges and K. M. G. Taylor. An investigation of some of the factors influencing the jet nebulization of liposomes. *Int J Pharm* **204**: 69-79 (2000).
225. K. K. M. Leung, P. A. Bridges, and K. M. G. Taylor. The stability of liposomes to ultrasonic nebulization. *Int J Pharm* **145**: 95-102 (1996).
226. P. A. Bridges and K. M. G. Tayler. Nebulisers for the generation of liposomal aerosols. *Int J Pharm* **173**: 117-125 (1998).
227. P. A. Bridges and K. M. G. Taylor. The effect of freeze-drying on the stability of liposomes to jet nebulization. *J Pharm and Pharmacol* **53**: 393-398 (2001).
228. O. R. Hung, E. M. Sellers, H. L. Kaplan, *et al.* Phase IB clinical trial of aerosolized liposome encapsulated fentanyl (AeroLEF (TM). *Clinical Pharmacol Therapeutics* **75**: P4-P4 (2004).
229. M. Saari, M. T. Vidgren, M. O. Koskinen, *et al.* Pulmonary distribution and clearance of two beclomethasone liposome formulations in healthy volunteers. *Int J Pharm* **181**: 1-9 (1999).
230. E. J. Ruijgrok, A. G. Vulto, and E. W. M. van Etten. Aerosol delivery of amphotericin B desoxycholate (fungizone) and liposomal amphotericin B (AmBisome): Aerosol characteristics and in-vivo amphotericin B deposition in rats. *J Pharm and Pharmacol* **52**: 619-627 (2000).
231. D. Fischer, T. Bieber, Y. Li, *et al.* A novel non-viral vector for DNA delivery based on low molecular weight, branched polyethylenimine: effect of molecular weight on transfection efficiency and cytotoxicity. *Pharm Res* **16**: 1273-1279 (1999).
232. H. Petersen, M. F. Fechner, A. L. Martin, *et al.* Polyethylenimine-graft-poly(ethylene glycol) copolymers: Influence of copolymer block structure on DNA complexation and biological activities as gene delivery system. *Bioconjug Chem* **13**: 845-854 (2002).

Chapter 2

Modified polyethylenimines as non-viral gene delivery systems for aerosol gene therapy: Investigations of the complex structure and stability during air-jet and ultrasonic nebulization

ABSTRACT

Polyelectrolyte complexes between plasmid DNA and polyethylenimine (PEI) are promising non-viral delivery systems for pulmonary inhalation gene therapy and thus require sufficient stability during nebulization. The structure and stability of four different PEI/DNA polyplexes, namely branched (BPEI), linear (linPEI), poly(ethylene glycol)-grafted-PEI (PEGPEI), biodegradable PEI (bioPEI) with DNA, were investigated. Using atomic force microscopy the morphology of DNA and polyplexes before and after both air-jet and ultrasonic nebulization was characterized. The influence of nebulization on the physico-chemical properties, particle size and zeta potential, was studied. Efficient DNA condensation to spherical particles was achieved with BPEI (90 nm) and PEGPEI (110 nm). By contrast, incomplete DNA condensations, seen as flower structures were observed with linPEI (110 nm) and bioPEI (105 nm). Air-jet nebulization altered the polyplex structure to a greater extent than ultrasonic nebulization and resulted mainly in smaller and non-spherical particles (30-200 nm). Ultrasonic nebulization did not change the spherical structure or particle size of the polyplexes. In particular, the shape and size of the PEGPEI polyplexes did not change. We conclude that ultrasonic nebulization is a milder aerosolization method for gene delivery systems based on PEI. Additionally, PEGPEI/DNA polyplexes seem to be more stable than their counterparts, which may be advantageous in pulmonary inhalation gene therapy.

INTRODUCTION

Pulmonary gene therapy holds great promise for the treatment of many incurable lung diseases, such as cystic fibrosis, asthma or lung cancer [1, 2]. A number of delivery systems to target the peripheral lung tissues have been investigated, for example viral vectors including retro- or adeno-viruses, as well as non-viral gene delivery systems which include cationic polymers, cationic lipids or liposomes and peptides [3-7]. Polyethylenimine (PEI) has been proven to be a promising cationic polymeric delivery system, which complexes DNA by electrostatic interactions and can transfect cells under in vitro, as well as in vivo conditions [8-10].

Different application methods for gene therapy to the lung have been investigated, such as intravenous, intratracheal or even nasal administration [7, 11, 12]. Aerosol inhalation represents a non-invasive route for gene transport into the lung. Nebulization, in particular, can target gene carriers to the peripheral regions of the respiratory tract. A problem associated with gene delivery by aerosol inhalation of naked DNA, viruses or liposomes is their marked loss in transfection efficiency due to the nebulization process [5, 13]. Successful transfection of lung tissue after the aerosol application of PEI/DNA using an air-jet nebulizer was reported recently in mice, showing that PEI/DNA complexes are resistant to nebulizer-induced reduction of transfection efficiency [14, 15]. However, to our knowledge, structural investigations of aerosolized PEI/DNA complexes have not yet been reported in the literature.

Air-jet and ultrasonic nebulizations are the two predominant methods utilized therapeutically to aerosolize drug solutions. Air-jet nebulizers operate with compressed air, transporting liquid through nozzles creating small aerosol droplets, whereas ultrasonic nebulizers use the piezoelectric effect to generate high-frequency acoustic energy which generates aerosol droplets by cavitation. Both types of nebulizers offer various advantages and disadvantages. Air-jet nebulization can affect gene carrier systems as a result of the high shear forces applied during nebulization. Ultrasonic energy is notorious for altering or damaging some aerosolized drug substances [16, 17]. Furthermore, ultrasonic nebulizers are usually more expensive and have not yet been investigated for the aerosolization of gene delivery systems based on cationic polymers. To date only air-jet nebulizers have been used in inhalative gene therapy studies [5, 13, 18]. A significant disadvantage of air-jet nebulizers is the lower output, which results in a prolonged exposure time of the DNA to shear forces.

In this study we prepared complexes consisting of plasmid DNA and four different PEI-derivatives (polyplexes): A branched form, a linear form, a poly(ethylene) glycol-grafted and

a biodegradable PEI. The polymer-DNA complexes were nebulized with commercially available air-jet and ultrasonic nebulizers and the polyplex stabilities before and after nebulization were evaluated. Atomic force microscopy (AFM) was used to characterize the morphology of these gene delivery systems. AFM is a comparatively new technique for studying events involving DNA, such as condensation or degradation, and has recently been used to visualize the morphology of gene delivery systems [19, 20]. The AFM technique allows polyplex structures to be investigated under liquid conditions, which are more relevant to the physiological milieu, in contrast to electron microscopy studies, which frequently require fixation and sample preparation prone to artefacts. Furthermore, we used AFM to study the effect of jet and ultrasonic nebulization on the structure of naked DNA and compared this to the PEI/DNA complexes. We also investigated physico-chemical properties of the four PEI modifications regarding their ability to condense DNA, the complex size, zeta-potential, and their stability against DNase digestion, parameters which are important for efficient gene expression in vitro and in vivo [21-25].

Further investigations of the polyplexes were performed, mainly to prove the biological activity after nebulization. The transfection efficiency and cellular association in primary alveolar cells (AEC), A549 cells, and primary bronchial cells (BEC) was studied [26].

METHODS AND MATERIALS

Materials

Branched polyethylenimine (BPEI) with a molecular weight (MW) of 25 kDa was purchased from Sigma-Aldrich (Seelze, Germany). Plasmid DNA pBR322 (4 MDa, 4363 bp) was purchased for the AFM experiments from Sigma-Aldrich (Poole, Dorset, UK). For all other studies the plasmid DNA pgl3CMV-Luc (4.4 MDa, 4800 bp) was propagated in E. coli and purified using a Maxi Prep kit from Promega (Mannheim, Germany). DNase 1 for the DNase digestion study was purchased from Boehringer Mannheim (Mannheim, Germany).

Synthesis

Linear polyethylenimine (linPEI) with MW of 22 kDa was synthesized as previously reported [8]. The poly(ethylene glycol)-grafted-polyethylenimine (PEGPEI) and the biodegradable PEI (bioPEI) were synthesized as previously described [27, 28]. Briefly, PEG-PEI (45 kDa) was obtained by activating PEG-monomethyl ether (5 kDa) with a hexamethylene diisocyanate. The coupling of PEG to the amino groups of BPEI was carried

out in anhydrous chloroform at 60 °C, which led to a PEI copolymer containing 10 PEG 2000 Da molecules per molecule PEI. BioPEI (8 kDa) was synthesized by linking 4 molecules low molecular weight PEI (1.2 kDa) blocks to 3 molecules oligo(L-lactic acid-co-succinic acid) (1 kDa).

Polyplex formation

All polyplexes consisting of DNA and PEI were prepared in isotonic glucose solution at pH 7. The DNA concentration in the resulting complex solution was 1.5 µg/ml for the AFM investigations and 20 µg/ml for all other experiments. An optimal nitrogen-phosphorous ratio (N/P) of 10 for BPEI/DNA complexes has been previously described for intrapulmonary in vivo transfection [5, 15]. Therefore, the complexes of branched and linear PEI were formulated at N/P 10. It was reported, that modifications of PEI, like PEG-grafted or biodegradable PEIs, lead to a decrease in complex charges and significant less cytotoxicity than BPEI after applying them at high concentration to mouse fibroblasts [28, 29]. Transfection experiments for further studies in mind, an higher N/P ratio of 30 for PEGPEI and bioPEI was chosen to improve the cellular uptake and endosomal escape. The appropriate amount of polymer was added to the solution of plasmid, mixed by vigorous pipetting, and incubated for 10 minutes at room temperature.

DNA condensation

The efficiency of DNA condensation by the PEIs was examined using a fluorescence quenching method [30]. The fluorescence of ethidium bromide, a DNA-intercalating agent, is enhanced upon binding to DNA and quenched when displaced by higher affinity compounds. Briefly, complex preparation and the subsequent addition of ethidium bromide were carried out in isotonic glucose solution at pH 7. Increasing amounts of PEI were added to 0.4 µg plasmid to reach final N/P ratios of 0.5, 1, 1.5, 2, 3 and 10 for the BPEI and linPEI complexes and 0.5, 1, 1.5, 2, 3, 4, 6 and 30 for the PEGPEI and bioPEI complexes. The resulting 200 µl polyplex were incubated for 10 minutes prior to the addition of 300 µl of a 0.3 µg/ml ethidium bromide solution. The mixture was analyzed with a Perkin-Elmer LS 50 B fluorescence reader using an excitation wavelength of 518 nm (15 nm slit and 515 nm emission filter), and emission wavelength of 605 nm (20 nm slit). Relative fluorescence of the samples is reported as the sample values in relation to the fluorescence obtained in the absence of PEI (= 100 %). Data are presented as a mean of three measurements (± SD) and the values were fitted to a Bolzmann sigmoidal function using Microcal Origin® v 7.0.

Nebulization

PEI/DNA polyplexes were aerosolized using the air-jet nebulizer Pari LC$^{®}$ star (Pari, Starnberg, Germany) operated with the Pari Boy$^{®}$ compressor and the ultrasonic nebulizer Optineb$^{®}$ (Nebutec, Elsenfeld, Germany) operated with a frequency of 2.4 MHz and 12 l/min air flow rate. The filling volumes of the nebulizer were 4 ml and the nebulization to residual volume was performed in approximately 10-20 minutes. The nebulized samples were collected by aerosol deposition on a glass plate and subsequent collection in 1.5 ml Eppendorf tubes. All nebulizations for the investigations conducted were repeated twice.

Atomic force microscopy

Images of DNA and the PEI/DNA polyplexes were obtained using a Nanoscope IIIa Multimode Atomic Force Microscope (Veeco, Santa Barbara, CA, USA), operating in tapping mode in a liquid environment. All imaging was carried out at a scan speed of approximately 3 Hz with a 256 x 256 or 512 x 512 pixel resolutions. Silicon nitride oxide-sharpened cantilevers were selected, operating at resonance frequencies of approximately 10 kHz. The experiments were repeated twice to ensure reproducibility. A sample volume of 40 µl was placed onto a 1 cm^2 disk of freshly cleaved mica. Initially, non-nebulized and nebulized plasmid samples were imaged in absence of polymer. 10 mM nickel chloride was added to the plasmid solution to facilitate immobilization of the plasmid at the mica surface. The freshly prepared non-nebulized as well as the polyplexes 10 minutes after ultrasonic and air-jet aerosolization were imaged. To determine the mean particle size from these images, the diameters at about half-height of at least 30 polyplexes were analyzed.

Dynamic light scattering

Particle sizes of non-nebulized and nebulized PEI/DNA polyplexes were measured using a Zetasizer 3000 HS (Malvern Instruments, Worcester, UK). The instrument was calibrated with Nanospheres Size Standards (polymer microspheres in water, 220 nm +/- 6 nm) from Duke Scientific (Palo Alto, CA). The scattered light was detected at a 90° angle through a 400 µm pinhole. Measurements were performed at 25°C with count rates between 50 and 300 kCps in 5 runs of 60 sec duration each and analyzed in CONTIN mode. The size measurements of each non-nebulized and nebulized PEI/DNA were repeated twice with a newly prepared sample.

Laser Doppler anemometry

The zeta-potential measurements of DNA, as well as that of non-nebulized and nebulized PEI/DNA complexes, were carried out in the standard capillary electrophoresis cell of a Zetasizer 3000 HS (Malvern Instruments, Worcester, UK). The measurements were performed at 25 °C with automatic duration. The average values were calculated in three independent measurements (five runs each) of the plasmid DNA and all PEI/DNA polyplexes.

DNase digestion

Protection of DNA by the four different PEI modifications against DNase was examined in a DNase digestion experiment as published previously [31]. Polyplexes were formed as described above. The reaction mixture for the DNase digestion study contained 30 µl digestion buffer, 0.25 units DNase I and either 0.5 µg DNA or PEI/DNA polyplexes including 0.5 µg DNA. The reaction was carried out for 30 minutes at 37 °C and was then stopped by the addition of 5 µl stop solution. The digestion buffer for this experiment contained 0.1 M sodium acetate, 5 mM magnesium sulphate and was titrated to pH 8.0. The DNase stop solution contained equal volumes of 0.5 M EDTA, 2 M NaOH and 0.5 M NaCl. To separate the DNA from the polymer, 0.2 mg dextran sulphate per 1 µg DNA were added to the polyplexes. This experiment was performed three times and one representative gel was chosen to present the results.

Agarose gel electrophoresis

The electrophoresis gels contained 1 % agarose and 2 µg ethidium bromide. The gel electrophoresis was run in TBE buffer at pH 8 for 1.5 hours at a voltage of 80 V. To visualize the DNA, the fluorescence of intercalated ethidium bromide was detected using a transilluminometer (Biometra, Göttingen, Germany). The experiments were performed at least three times.

Statistics

Statistical calculations were carried out with SPSS 9.0 for Windows (SPSS GmbH, Munich, Germany). The results are reported as mean ± standard deviation (SD) and, in the case of AFM size measurements, the size range is also provided. Nonparametric statistical tests were performed using the Mann-Whitney-Test. Comparisons for analyzing hydrodynamic diameters measured by PCS and zeta-potential were performed using unpaired

Student's *t*-tests. In the case of multiple testing, the Bonferroni correction was applied [32]. Probability values $P<0.05$ were considered to be significant.

RESULTS AND DISCUSSION

DNA condensation

The nitrogen to phosphorous (N/P) ratio between PEI and DNA has been shown to critically affect lung tissue transfection [5, 33]. To quantify DNA condensation at different N/P ratios, we utilized the ability of PEI to quench DNA/ethidium bromide fluorescence. If DNA is condensed by the cationic polymer, ethidium bromide can no longer intercalate and fluorescence intensity decreases measurably. In Figure 1, the relative fluorescence is presented as a function of the N/P ratio. The comparison of the curves inflection points (point on a curve at which the sign of the concavity changes) give evidence about the interactions between polymer and DNA.

The relative fluorescence of all polyplexes decreased with increasing N/P ratios, due to increased DNA condensation. Unmodified BPEI condenses DNA at low N/P ratios efficiently (inflection point at N/P = 1.58 ± 0.19) and ratios > N/P 6 exhibit a maximum ethidium bromide exclusion with a residual fluorescence of approximately 6 %. The curve obtained with linPEI shows that efficient DNA condensation also commences at relatively low N/P ratios, the inflection point was observed at N/P = 1.63 ± 0.17. However, the maximum extent of DNA condensation is lower than that of BPEI; at N/P ratio > 4 a residual fluorescence of 12 % was observed. It is worth noting, that the linPEI/DNA at N/P = 0.5 showed a higher fluorescence (120 %) than the DNA alone. This is probably due to the configuration of DNA in the polyplexes (c. f. AFM results), which might even enhance ethidium bromide intercalation at low N/P ratios as compared to the free plasmid alone. It is conceivable that at low N/P ratios (< 1.5) in the linPEI/DNA polyplexes the plasmid strands are presented in wide loops, which makes an ethidium bromide intercalation easier as compared to supercoiled DNA. With an N/P ratio increase the DNA will be more incorporated in the polyplexes, however, not completely seen as residual fluorescence of 12 %. In contrast, both PEGPEI and bioPEI did not exhibit complete DNA condensation until much higher N/P ratios were attained. The inflection point in the quenching curve of the PEGPEI polyplexes was reached at the N/P ratio of 3.26 ± 0.22 and that of bioPEI polyplexes at 3.73 ± 0.26. At N/P 30, the ratio we used in all PEGPEI/DNA experiments, a complete quenching of ethidium bromide

fluorescence could be observed. The lowest extent of DNA condensation among all four PEIs was shown by bioPEI with a residual fluorescence of 15 % at N/P 30.
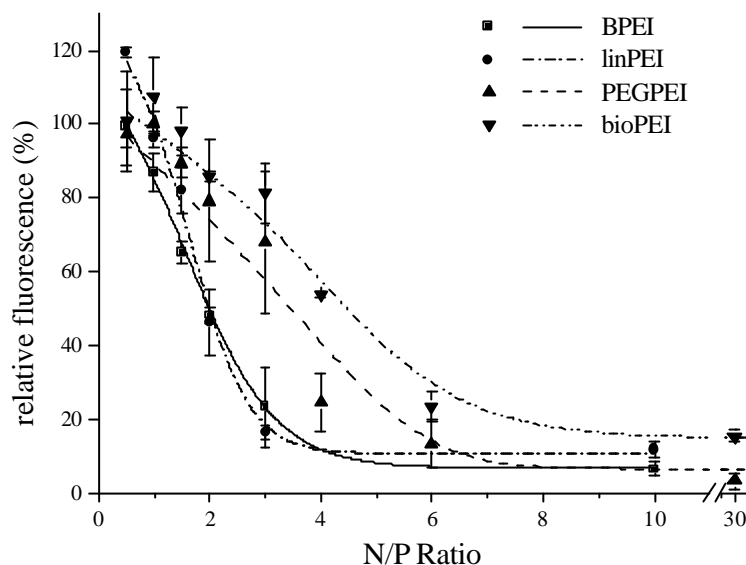
Figure 1. DNA condensation of the PEIs by increasing the N/P ratio measured as ethidium bromide quenching. Relative fluorescence of 100 % represents the fluorescence of DNA alone, while 0 % represents the residual fluorescence of ethidium bromide.

The four different derivatives of PEI exhibited highly variable effects with respect to DNA condensation. The fluorescence quenching assay suggests that unmodified PEIs (BPEI and linPEI) condense DNA at lower N/P ratios. At higher N/P ratios BPEI and PEGPEI in particular, exhibit a high extent of DNA condensation, whereas linPEI and bioPEI were not able to fully condense plasmid DNA.

Atomic force microscopy

Atomic force microscopy (AFM) in liquid media was used to study the morphology of DNA and PEI/DNA polyplexes, as well as to examine the influence of aerosolization on these structures. AFM is well suited for studying the morphology and size of polymer-DNA complexes in an aqueous environment [20]. However, it should be noted this technique examines individual polyplexes and only a fraction of the PEI/DNA complexes can be investigated. To document the prevalent polyplex morphology we selected one representative image. Furthermore, we measured the particle sizes of 30-50 polyplexes from different images (Table 1).

Table 1. Particle sizes of the non-nebulized and nebulized PEI/DNA were measured by using AFM and DLS. The size obtained from AFM images were measured by using the commercial available Digital Instruments section analyzer software. The values are given in nm ± SD (n=30). The mean hydrodynamic diameter (HD) and the polydispersity index (PDI) measured by using DLS were determined from 3 samples and repeating the measurement 5 times. The hydrodynamic diameters are given as z-average in nm ± SD. The significant differences in particle size and in polydispersity between the non-nebulized and nebulized complexes are marked with an asterisk (p<0.05).

method	polyplexe	BPEI/DNA	linPEI/DNA	PEGPEI/DNA	bioPEI/DNA
	non-nebulized				
AFM	mean	78.2 ± 15.6	64.5 ± 13.7	97.1 ± 19.5	79.3 ± 18.9
	range	58.6 - 128.0	48.8 - 94.5	64.5 - 138.2	48.5 - 133.4
DLS	HD	90.6 ± 13.4	110.9 ± 18.7	109.7 ± 7.3	105.0 ± 11.2
	PDI	0.49 ± 0.11	0.50 ± 0.06	0.60 ± 0.05	0.51 ± 0.15
	air-jet nebulized				
AFM	mean	33.1 ± 29.5*	27.7 ± 19.1*	133.5 ± 80.0*	181.1 ± 89.2*
	range	10.7 – 134.0	9.3 – 93.0	29.3 - 263.7	23.1 - 348.8
DLS	HD	109.2 ± 11.4	166.2 ± 40.0*	209.6 ± 21.6*	147.8 ± 72.5
	PDI	0.53 ± 0.05*	0.64 ± 0.26*	0.87 ± 0.13*	0.56 ± 0.12
	ultrasonic nebulized				
AFM	mean	209.5 ± 118.2*	121.9 ± 71.9*	87.8 ± 34.1	55.6 ± 20.7*
	range	70.3 - 459.6	60.6 - 251.9	36.7 - 162.7	25.7 - 94.0
DLS	HD	109.0 ± 14.2	145.4 ± 8.6*	123.2 ± 13.6	110.4 ± 14.3
	PDI	0.53 ± 0.09	0.46 ± 0.1	0.61 ± 0.08	0.5 ± 0.08

To evaluate the differences between uncondensed and condensed DNA we first imaged uncomplexed DNA (Figure 2). Non-nebulized plasmid DNA (Figure 2A) showed a relaxed, open loop structure with little twisting of the strands. The open loop structures and supercoiled forms are characteristic morphologies for uncondensed plasmids [19, 34]. After air-jet nebulization (Figure 2B), the plasmid is still relaxed, but many of the circular strands are fragmented. This DNA fragmentation may be explained by strong shear forces generated during this process. DNA fragmentation resulting from air-jet nebulization has also been reported before using gel electrophoresis [18]. Ultrasonic nebulization (Figure 2C) led not

only to the formation of DNA fragments, but also to the appearance of aggregated structures (blue arrows).
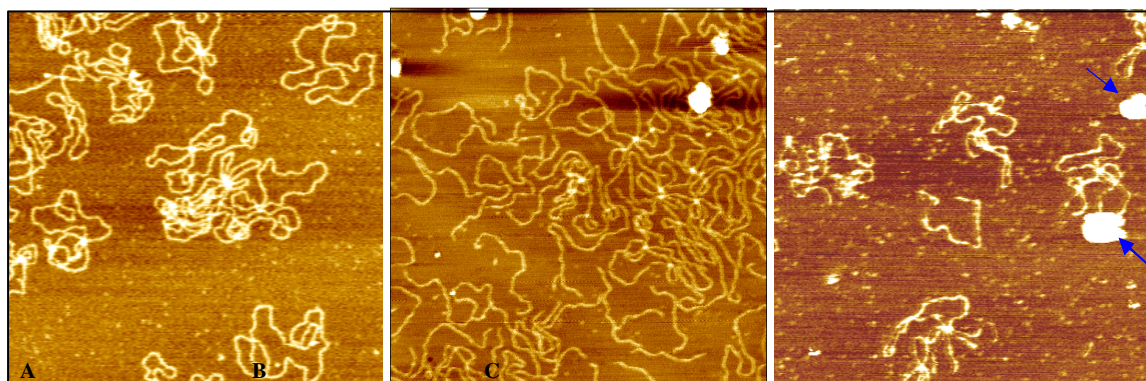
Figure 2. AFM images of DNA alone (scan sizes 1 µm x 1 µm, z-ranges 5 nm): A = non-nebulized, B = after air-jet nebulization, C = after ultrasonic nebulization. The DNA was solved in water and imaged on mica surface before and after the aerosolization processes. The addition of 10 mM nickel chloride solution to both the non-nebulized and air-jet nebulized DNA was necessary to encourage attraction at the mica surface. The blue arrows distinguish plasmid aggregates.

Representative AFM images of non-nebulized PEI/DNA polyplexes are shown in the Images A, D, G and J of Figure 3. The complexes of BPEI and DNA (Figure 3A) are highly condensed, forming spherical particles with sizes of approximately 80 nm. Condensates of linPEI/DNA displayed open loops of DNA outside the polyplex core (Figure 3D). This morphology is also known as a "flower structure" and indicates incomplete DNA condensation. The linPEI/DNA polyplex cores had a mean size of approximately 65 nm. PEGPEI/DNA polyplexes (Figure 3G) are fully condensed particles with a size of approximately 100 nm. Most of the bioPEI/DNA polyplexes (Figure 3J) are not fully condensed and plasmid loops outside the actual particle were observed. The morphology of the bioPEI/DNA polyplexes varied, and in addition to spherical particles often flower structures or rod like structures were noted. The AFM images suggest differing interactions between plasmid DNA and the PEI modifications leading to polyplex structures as outlined in Scheme 1.
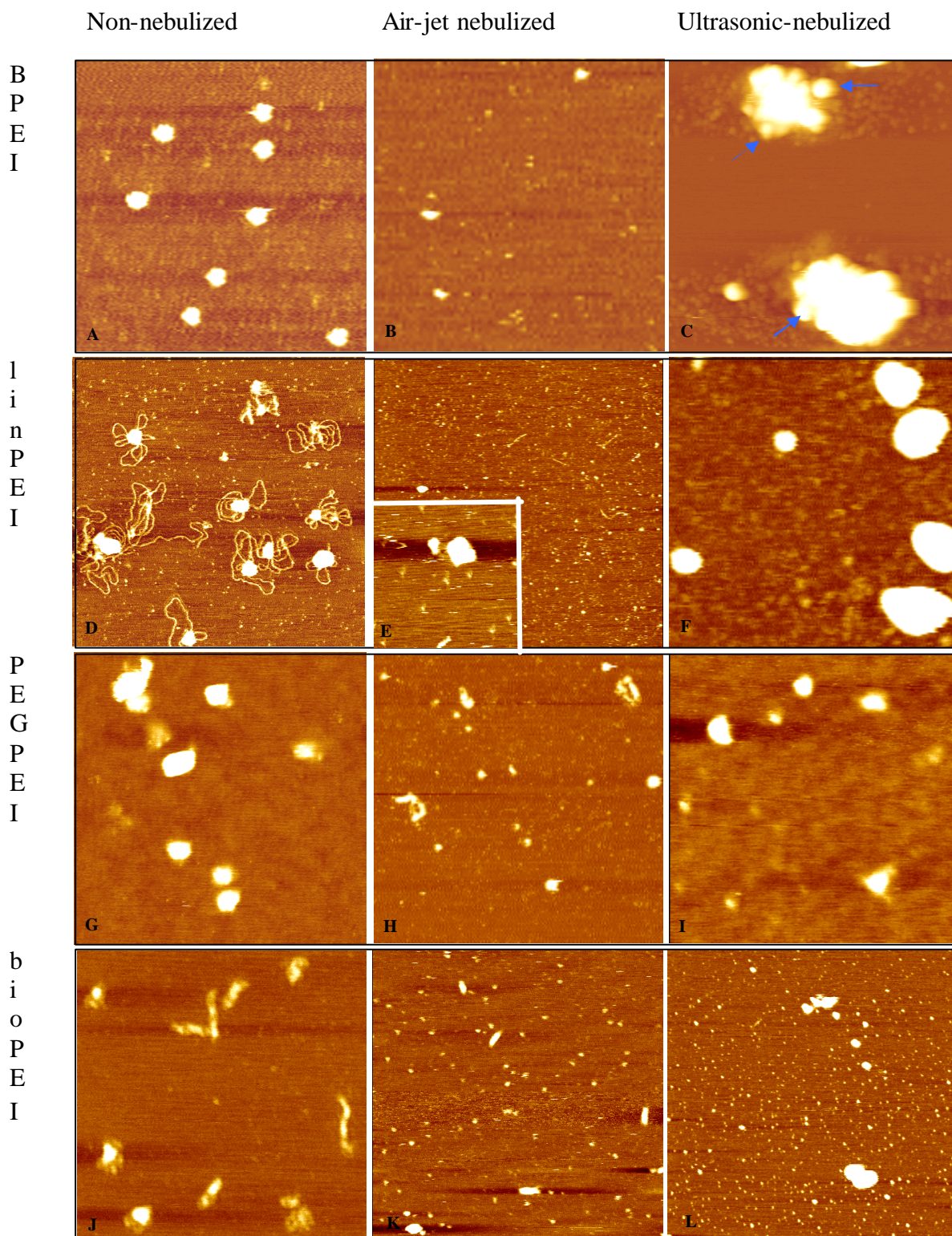
Figure 3. AFM images of PEI/DNA polyplexes (scan sizes 1 µm x 1 µm; z-ranges 10 - 50 nm). The polyplexes were formulated in isotonic glucose solution and imaged after the incubation time of ten minutes. Images were also taken immediately after the nebulization processes. The blue arrow distinguishes single particles in the polyplex agglomerate.

Scheme 1. Schematic representation of the four polyethylenimine modifications and their condensation with plasmid DNA.
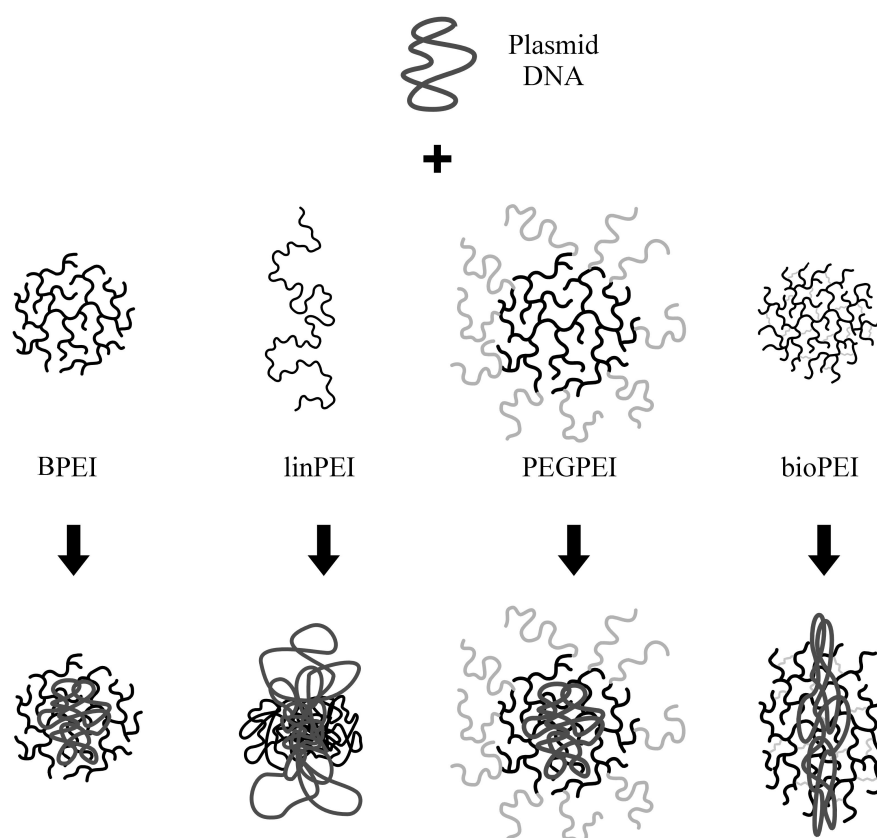
AFM images showed that only BPEI and PEGPEI form highly condensed spherical particles with plasmid DNA, which was confirmed by the high extent of DNA condensation seen for BPEI and PEGPEI in the ethidium bromide exclusion assay. Due to the branched structure of both PEGPEI and BPEI these molecules have a higher density of protonable amino groups than the linear PEI form or the bioPEI (see synthesis). A higher density of amino groups enables better interaction with phosphate groups of the DNA and thus might explain the better DNA condensation of BPEI and PEGPEI compare to linPEI and bioPEI. Incomplete DNA condensation with non-nebulized linear PEI was also observed by Dunlap et al. using AFM [20]. Complexes of DNA and linear PEI seem to be excellent non-viral transfection reagents under in vitro conditions, as well as in vivo gene transfer experiments, even surpassing the efficiency of BPEI [8, 11, 35, 36] This discrepancy might be evidence supporting the argument that efficient transfection does not require spherical particles. Furthermore, it seems to be important that the degree of condensation is not too strong to hinder the release of DNA from the complex inside the cell nucleus.

Figures 3B and C show AFM images of nebulized BPEI/DNA polyplexes. After air-jet nebulization (Figure 3B) smaller particles with sizes of approximately 33 nm (Table 1) and occasionally aggregates (not shown in the image) were observed, whereas after ultrasonic nebulization (Figure 3C) spherical particles and aggregates ranging from 70 nm to 460 nm were found. Within these aggregates single polyplexes can be distinguished (blue arrows in Figure 3C) therefore we assume these are agglomerates. Images of air-jet nebulized linPEI/DNA (Figure 3E) showed disrupted polyplexes as well as some spherical particles (small image). In contrast, the ultrasonic nebulization of linPEI/DNA (Figure 3F) led mainly to the formation of polyplexes and aggregates in a size range of 60-250 nm. After air-jet nebulization of PEGPEI/DNA (Figure 3H) we observed spherical, as well as rod-like particles and occasionally aggregates, with sizes ranging from 30 nm to 264 nm. A representative image of the ultrasonic nebulized PEGPEI/DNA polyplexes (Figure 3I) shows mainly spherical particles which have a size of 90 nm, similar to the non-nebulized PEGPEI/DNA polyplexes. Air-jet nebulization of bioPEI/DNA (Figure 3K) increased the amount of smaller particles. Ultrasonic nebulization of bioPEI/DNA (Figure 3L) seemed to have promoted a complete condensation of DNA resulting in condensed spherical particles with sizes ranging from 26 to 94 nm. In both images (Figure 3 K, L) free polymer can be seen probably due to the high N/P ratio of 30.

Due to high N/P ratios, polyplex suspensions can contained free polymer, in addition to polymer which is bound to the plasmid via electrostatic interactions. During the nebulization smaller polyplexes can be obtained either through rearrangement of the polyplexes/polymer or through fragmentation. Supercoiled plasmid has a size of 10 nm [37] and PEI alone approximately 5 nm. The smallest polyplexes we obtained after air-jet nebulization were 10 to 30 nm. Therefore we conclude both could be possible some polyplexes were disrupted and some could be still intact. Transfection of lung epithelial cells was successfully achieved after polyplex nebulization, suggesting that they retained their biological activity [26].

In all cases, the AFM investigations indicated that ultrasonic nebulization influenced the polyplex structure to a lesser extent than air-jet nebulization, because the images of polyplexes exposed to ultrasonic nebulization displayed primarily spherical particles and aggregates. In case of linPEI and bioPEI we assume that cavitation induced interactions between the uncondensed amino groups and the DNA, thus leading to the formation of condensed, spherical particles and aggregates.

Gel electrophoresis

Agarose gel electrophoresis was used to determine whether the strands or disrupted particles observed in the AFM images of nebulized polyplexes consisted of uncomplexed DNA. We expected only a small amount of DNA fragments and, therefore, we used 10 times concentrated solutions. The gel in Figure 4 shows the polyplexes: non-nebulized in lane 4-7, air-jet nebulized lane 8-11 and ultrasonic nebulized lane 12-15. A part of the plasmid in lane 4-6 was retained at the application point due to incomplete separation from the polymer by dextran sulphate. The gel demonstrated that in all cases of nebulized polyplexes, DNA fragments were generated to a higher (air-jet) or lower (ultrasonic) extent. Due to solvent evaporation during nebulization, concentration changes could not be determined in a quantitative manner. Nevertheless DNA fragmentation was observed using both nebulization techniques. Thus gel electrophoresis of the polyplexes confirms the finding of DNA fragmentation seen in some AFM images, especially those of air-jet nebulization. In case of naked DNA aerosolization, it could be shown here and in the AFM images, that the formation of DNA fragments during air-jet nebulization is more pronounced than during ultrasonic nebulization. Both gel electrophoresis and AFM confirm unexpectedly that ultrasonic energy does not alter or damage plasmid DNA and polyplexes severely in contrast to other ultrasonic aerosolized drug substances [16, 17].
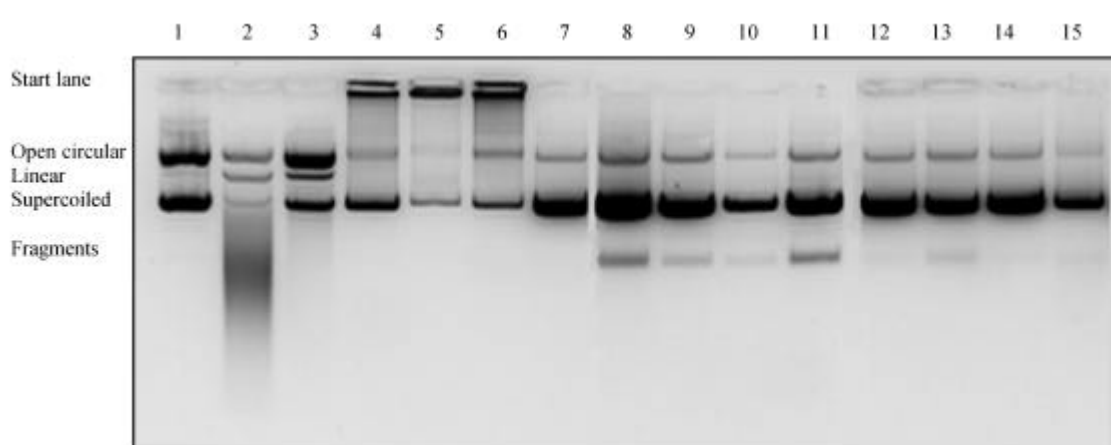
Figure 4. Agarose gel of non-nebulized and nebulized DNA and PEI/DNA: lane 1-3 showing DNA: non-nebulized (1), air-jet nebulized (2), ultrasonic nebulized (3); lane 4-7 showing non-nebulized polyplexes: BPEI (4), linPEI (5), PEGPEI (6), bioPEI (7); lane 8-11 showing air-jet nebulized polyplexes: BPEI (8), linPEI (9), PEGPEI (10), bioPEI (11); lane 12-15 showing ultrasonic nebulized polyplexes: BPEI (12), linPEI (13), PEGPEI (14), bioPEI (15).

Dynamic light scattering

In addition to the polyplex sizes determined from AFM images, the mean hydrodynamic diameters (HD) and the polydispersity index (PDI) of the non-nebulized and nebulized polyplexes was measured using DLS (Table 1 at page 51) to validate these results with an independent method. In the case of non-nebulized polyplexes, we observed that the smallest particles were formed between BPEI and DNA with mean hydrodynamic diameters of approximately 91 nm. The linPEI/DNA exhibited a particle size of 111 nm. Polyplexes consisting of DNA and PEGPEI (110 nm), or bioPEI (105 nm), yielded similar hydrodynamic diameters. As demonstrated by DLS and AFM, BPEI was able to form the smallest particles with DNA probably because of the branched molecule structure. PEGPEI formed the largest complexes with DNA probably because of the high molecular weight of the PEGPEI molecule.

After both air-jet, as well as ultrasonic nebulization, the hydrodynamic diameters of all investigated polyplexes increased. The differences of non-nebulized to air-jet nebulized polyplexes were higher than these of non-nebulized to ultrasonic nebulized polyplexes. The fact that particle sizes for the same complex measured by DLS were larger than those measured by AFM was particularly pronounced for the linPEI and the bioPEI polyplexes. This observation can be explained by the incomplete complexation process for linPEI and bioPEI, which let to a lower diffusivity and thus to a considerable increase in hydrodynamic diameter, as measured by DLS.

To understand the differences in particle size measurements obtained by AFM and DLS the following considerations should be taken into account. The method of DLS is a reliable size analysis technique for spherical particles, which measures the diffusivity of the particles by means of the scattered light and calculates their corresponding diameter. The major advantage of this method as compared to AFM is that a large number of particles are measured and thus subjective selection criteria cannot influence the results. Therefore, many studies have used DLS to investigate the particle size alteration to prove the polyplex stability [18, 38]. A considerable disadvantage of DLS is the fact that non-spherical particles show a lower diffusivity compare to spherical particles of the same volume equivalent diameter. This leads to a nominally larger diameter for non-spherical particles compared to spherical particles of the same volume equivalent diameter. Therefore, we think it is necessary to use both AFM and DLS to compensate the disadvantages of both methods and thus achieve more detailed information about the polyplex structure. In present study, both methods could demonstrate that air-jet nebulization alters the size of the PEI/DNA complexes to a greater

extent than ultrasonic nebulization. The images of air-jet nebulized polyplexes demonstrated that not only larger particles were formed, as the DLS measurements have shown, but that also many fragments were formed. Using CONTIN analyses for DLS data fitting we were not able to detect bimodal particle size distributions. However, in all cases the particle size polydispersity index increased after air-jet nebulization and it did not increase during ultrasonic nebulization. Thus the polydispersity increase after the air-jet nebulization supported the AFM results, which showed that particles with different particle sizes were formed.

The size of the polyplexes has been reported to be an important factor in facilitating gene transfer in cells [22, 24, 38]. Beside this the lung describes a more complex system to deliver polyplexes to and into the cells. Substances which are transported into the respiratory tract undergo two major clearance processes, the mucociliary and the alveolar macrophage clearance. Particles larger than 5 µm will be deposit mainly in the upper airways and bronchioles, hence such particles can be removed by the beating cilia. Particles which have been deposit in the alveolar space can be cleared by alveolar macrophages. A particle diameter less than 0.26 µm prevents from macrophageal phagocytosis [39]. Furthermore, endocytotic processes occur to formations smaller than 0.2 µm [37] and it is known that polyplexes based on PEI will be uptake by endocytosis and be released into the cytoplasm by lysosomal rupture according to the proton sponge theory [21]. These considerations make clear, that PEI/DNA particles should have a size smaller than 0.2 µm to ensure the uptake by pulmonary epithelial cells and according to the sizes measured by AFM and PCS the majority of the investigated polyplexes are smaller. However, some aggregates were formed (air-jet nebulized PEGPEI/DNA and bioPEI/DNA; ultrasonic nebulized BPEI/DNA and linPEI/DNA) which can not be uptake by endocytosis and could be cleared due to macrophages activity.

Laser Doppler anemometry

Interactions between PEI/DNA polyplexes and cell surfaces are dependent upon the particle surface charge [21]. To estimate the surface charge of the PEI/DNA polyplexes, we measured their respective zeta-potentials. The results of the zeta-potential analysis for DNA alone and the PEI/DNA polyplexes are depicted in Figure 5. The zeta-potential of the plasmid changed from approximately -33 mV for the non-nebulized to -20 mV after both air-jet and ultrasonic nebulization. This observation implies that strong structural alterations occurred and thus confirm the AFM and gel electrophoresis results.

For all four non-nebulized PEI/DNA polyplexes a highly positive charge was observed. A slightly lower zeta-potential of 25 mV was seen with PEGPEI/DNA compared to 30 mV for the other three PEI/DNA polyplexes. In the case of polyplex aerosolization, no statistically significant alterations in zeta-potentials were found, although PEGPEI/DNA did show an increase in zeta-potential from 25 mV (non-nebulized) to 33 mV for the air-jet nebulized and to 28 mV for the ultrasonic nebulized polyplexes. The increase was, however, not significant and the reason for this slight zeta-potential increase might be due to structural changes of the nebulized complexes which decreased the shielding effect of the PEG groups. For all other complexes the change in zeta-potential was minimal. This implies that the transfection efficiency of the aerosolized complexes might be comparable to that of non-nebulized complexes.
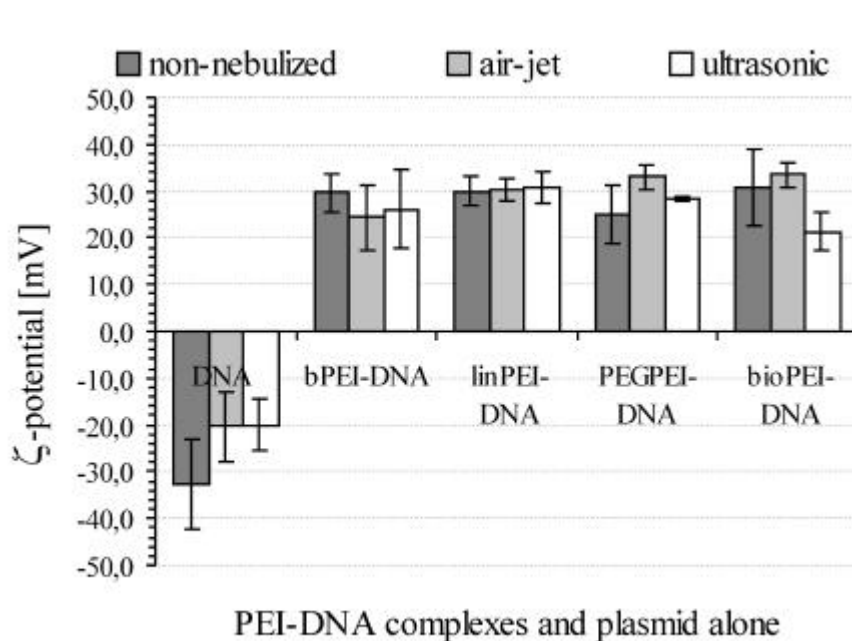
Figure 5. Zeta-potential measurements of non-nebulized and nebulized PEI/DNA polyplexes and naked DNA. For each PEI/DNA polyplex, three samples and five measurements for each sample were taken. The differences between the non-nebulized and nebulized polyplexes were not significant. Between non-nebulized and nebulized DNA the differences were significant at $p < 0.05$.

DNase digestion

The ability of the gene carrier to protect DNA against enzymatic degradation by DNase I, which is located in the cytoplasm, can be demonstrated by DNase digestion studies [12, 30].

Agarose gel electrophoresis was carried out after the digestion experiment (Figure 6). Untreated plasmid DNA (lane 1) can be differentiated in the supercoiled, open circular and linear form. During digestion, the DNase first unwinds the supercoiled DNA form and then cuts it into small DNA fragments of different lengths. The linear plasmid form was not present in the untreated DNA samples, but was formed due to the DNase digestion (lane 2). As low as 0.05 units DNase per one µg DNA caused DNA degradation to occur, as shown by the smear beneath the last band. Digestion with 0.5 units DNase (lane 3) led to a complete fragmentation and very short fragments were seen as a smear at the running front. Lanes 4 to 7 display the DNA of non-digested polyplexes. Insufficient separation of BPEI and DNA (lane 4) was observed probably because dextran sulphate did not separate these strongly condensed complexes completely. The DNase digestion is shown in lane 8 to 11. In all cases of the PEI/DNA polyplexes no smear in the top lane was observed, which means DNA was not degraded by the DNase. In lane 10 (PEGPEI/DNA) the supercoiled DNA form decreased and the open circular as well as the linear form increased. Thus, the enzyme seemed to have an effect on these polyplexes, however DNA was not degraded. The linPEI and bioPEI have shown incomplete complexation and less protection against DNase would be conceivable. However, no fragmented DNA was found after the digestion. It is probably, that the DNase enzymes are sterically hindered by the polyplex core. It can be concluded, that all four investigated PEIs were able to protect the DNA against DNase digestion.
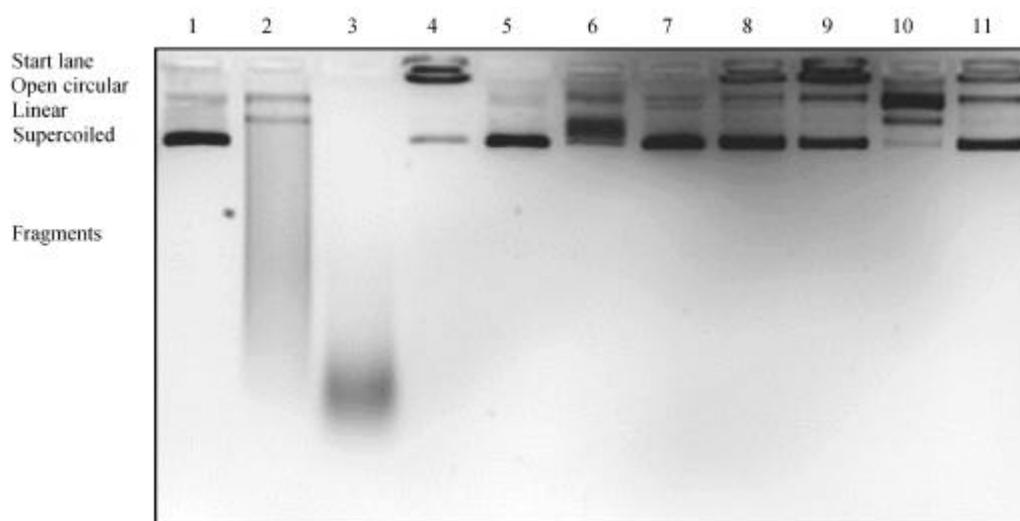
Figure 6. DNase digestion: agarose gel showing DNA non-digested (1), digested for 15 minutes with 0.05 Units (2) and 0.5 Units (3) DNase per 1 µg DNA; the four different complexes (in the order BPEI, linPEI, PEGPEI, bioPEI) non-digested (4-7), digested with 0.5 Units DNase per 1 µg DNA for 30 minutes (8-11).

CONCLUSIONS

PEGPEI was the only polymer of the four investigated PEIs, which was able to form spherical complexes that are stable during nebulization, particularly after ultrasonic nebulization. Furthermore, previous studies of Petersen et al. [27] have demonstrated superior transfection efficiency in vitro for PEGPEI modifications compare to BPEI. Due to these observations and the superior stability seen in this study, PEGPEI showed the most promising properties for pulmonary gene delivery. Methods like DLS and gel electrophoresis are often used to demonstrate the stability of gene carrier systems during nebulization. These methods are, of course, necessary; however, they cannot provide complete information about the polyplex structure. In the present study, AFM was used for the first time to investigate the morphology of PEI polyplexes before and after nebulization. The size of non-spherical particles, which may be generated during aerosolization, cannot be measured reliably by DLS alone. We could show that it is necessary to use independent imaging methods to obtain more information about polyplexes alterations generated during aerosolization. Polyplex morphology, particles size measurement and the polyplex stability studies have demonstrated a higher stability, in the meaning of fewer alterations, of all polyplexes during ultrasonic nebulization, as compared to air-jet nebulization. Therefore, we conclude that ultrasonic nebulization is a milder method to aerosolize gene delivery systems based on PEI. Studies of polyplex nebulization for gene therapy in the lung, which can be found in the current literature, were all undertaken using air-jet nebulizers [14, 15]. We believe that ultrasonic nebulization should not be neglected for polyplex aerosolization. Ultrasonic nebulization of PEGPEI/DNA polyplexes merits further investigations as delivery system for pulmonary gene therapy [26].

REFERENCES

1. U. Griesenbach, S. Ferrari, D. M. Geddes, *et al.* Gene therapy progress and prospects: cystic fibrosis. *Gene Ther* **9**: 1344-1350 (2002).
2. J. Vadolas, R. Williamson, and P. A. Ioannou. Gene therapy for inherited lung disorders: An insight into pulmonary defence. *Pulm Pharmacol Therapeutics* **15**: 61-72 (2002).
3. S. L. Hart, C. V. Arancibia-Cárcamo, M. A. Wolfert, *et al.* Lipid-Mediated Enhancement of Transfection by a Nonviral Integrin-Targeting Vector. *Hum Gene Ther* **9**: 575-585 (1998).
4. A. Gautam, J. C. Waldrep, C. L. Densmore, *et al.* Growth inhibition of established B16-F10 lung metastases by sequential aerosol delivery of p53 gene and 9-nitrocamptothecin. *Gene Ther* **9**: 353-357 (2002).
5. C. L. Densmore, F. M. Orson, B. Xu, *et al.* Aerosol delivery of rRobust polyethylenimine-DNA complexes for gene therapy and genetic immunization. *Mol Ther* **1**: 180-188 (2000).
6. W. Budts, P. Pokreisz, Z. Nong, *et al.* Aerosol Gene Transfer with inducible nitric oxide synthase reduces hypoxic pulmonary hypertension and pulmonary vascular remodeling in rats. *Circulation* **102**: 2880-2885 (2000).
7. A. Bragonzi, G. Dina, A. Villa, *et al.* Biodistribution and transgene expression with nonviral cationic vector/DNA complexes in the lung. *Gene Ther* **7**: 1753-1760 (2000).
8. S. Ferrari, E. Moro, A. Pettenazzo, *et al.* ExGen 500 is an efficient vector for gene delivery to lung epithelial cells in vitro and in vivo. *Gene Ther* **4**: 1100-1106 (1997).
9. G. F. Lemkine and B. A. Demeneix. Polyethylenimines for in vivo gene delivery. *Curr Opin Mol Ther* **3**: 178-182 (2001).
10. T. Merdan, J. Kopecek, and T. Kissel. Prospects for cationic polymers in gene and oligonucleotide therapy against cancer. *Adv Drug Deliv Rev* **54**: 715-758 (2002).
11. D. Goula, N. Becker, G. F. Lemkine, *et al.* Rapid crossing of the pulmonary endothelial barrier by polyethylenimine/DNA complexes. *Gene Ther* **7**: 499-504 (2000).
12. A. Kichler, M. Chillon, C. Leborgne, *et al.* Intranasal gene delivery with a polyethylenimine-PEG conjugate. *J Control Release* **81**: 379-388 (2002).
13. A. Gautam, C. L. Densmore, E. Golunski, *et al.* Transgene expression in mouse airway epithelium by aerosol gene therapy with PEI-DNA complexes. *Mol Ther* **3**: 551-556 (2001).
14. A. Gautam, C. L. Densmore, and J. C. Waldrep. Pulmonary cytokine responses associated with PEI-DNA aerosol gene therapy. *Gene Ther* **8**: 254-257 (2001).
15. A. Gautam, C. L. Densmore, B. Xu, *et al.* Enhanced gene expression in mouse lung after PEI-DNA aerosol delivery. *Mol Ther* **2**: 63-70 (2000).
16. J. L. Rau. Design principles of liquid nebulization devices currently in use. *Respir Care* **47**: 1257-1275 (2002).
17. O. N. M. McCallion, K. M. G. Taylor, M. Thomas, *et al.* Nebulization of fluids of different physicochemical properties with air-jet and ultrasonic nebulizers. *Pharm Res* **12**: 1682-1688 (1995).
18. C. M. Rudolph, R.H.; Rosenecker, J. Jet nebulization of PEI/DNA polyplexes: physical stability and in vitro gene delivery efficiency. *J Gene Med* **4**: 66-74 (2002).
19. H. G. Hansma. Surface biology of DNA by atomic force microscopy. *Annu Rev Phys Chem* **52**: 71-92 (2001).
20. D. D. Dunlap, A. Maggi, M. R. Soria, *et al.* Nanoscopic structure of DNA condensed for gene delivery. *Nucl Acid Res* **25**: 3095-3101 (1997).

21.   O. Boussif, F. Lezualcho, M. A. Zanta, *et al.* A versatile vector for gene and oligonucleotide transfer into cells in culture and in vivo: polyethylenimine. *Proc Natl Acad Sci U S A* **92**: 7297-7301 (1995).

22.   R. Kircheis, L. Wightman, and E. Wagner. Design and gene delivery activity of modified polyethylenimines. *Adv Drug Deliv Rev* **53**: 341-358 (2001).

23.   W. T. Godbey, K. K. Wu, and A. G. Mikos. Tracking the intracellular path of poly(ethylenimine)/DNA complexes for gene delivery. *Proc Natl Acad Sci USA* **96**: 5177-5181 (1999).

24.   D. Fischer, A. v. Harpe, and T. Kissel. Polyethylenimine: polymer structure influences the physicochemical and biological effects of plasmid/PEI complexes. *Biomaterials* 195-211 (2000).

25.   H. Petersen, K. Kunath, A. L. Martin, *et al.* Star-shaped poly(ethylene glycol)-block-polyethylenimine copolymers enhance DNA condensation of low molecular weight polyethylenimines. *Biomacromolecules* **3**: 926-936 (2002).

26.   L. A. Dailey, E. Kleemann, T. Merdan, *et al.* Modified Polyethylenimines as non viral gene delivery systems for aerosol therapy: effects of nebulization on cellular uptake and transfection efficiency. *J Control Release* **100**: 425-436 (2004).

27.   H. Petersen, P. M. Fechner, D. Fischer, *et al.* Synthesis, characterisation, and biocompatibility of polyethylenimine-graft-poly(ethylene glycol) block copolymers. *Macromol* **35**: 6867-6874 (2002).

28.   H. Petersen, T. Merdan, K. Kunath, *et al.* Poly(ethylenimine-co-L-lactamide-co-succinamide): a biodegradable polyethylenimine derivative with an advantageous pH-dependent hydrolytic degradation for gene delivery. *Bioconjug Chem* **13**: 812-821 (2002).

29.   H. Petersen, M. F. Fechner, A. L. Martin, *et al.* Polyethylenimine-graft-poly(ethylene glycol) copolymers: influence of copolymer block structure on DNA complexation and biological activities as gene delivery system. *Bioconjug Chem* **13**: 845-854 (2002).

30.   K. Kunath, A. von Harpe, D. Fischer, *et al.* Low-molecular-weight polyethylenimine as a non-viral vector for DNA delivery: comparison of physicochemical properties, transfection efficiency and in vivo distribution with high-molecular-weight polyethylenimine. *J Control Release* **89**: 113-125 (2003).

31.   W. T. Godbey, M. A. Barry, P. Saggau, *et al.* Poly(ethylenimine)-mediated transfection: a new paradigm for gene delivery. *J Biomed Mater Res* **51**: 321-328 (2000).

32.   L. Sachs. Angewandte Statistik. *Springer Verlag* (2002).

33.   D. Goula, C. Benoist, S. Mantero, *et al.* Polyethylenimine-based intravenous delivery of transgenes to mouse lung. *Gene Ther* **5**: 1291-1295 (1998).

34.   D. J. Ellis, D. T. F. Dyden, T. Berge, *et al.* Direct observation of DNA translocation and cleavage by EcoKI endonuclease using atomic force. *Nature structural biology* **6** (1999).

35.   A. Bragonzi, A. Boletta, A. Biffi, *et al.* Comparison between cationic polymers and lipids in mediating systemic gene delivery to the lung. *Gene Ther* **6**: 1995-2004 (1999).

36.   L. Wightman, R. Kircheis, V. Rossler, *et al.* Different behavior of branched and linear polyethylenimine for gene delivery in vitro and in vivo. *J Gene Med* **3**: 362-372 (2001).

37.   I. Mellman. Endocytosis and molecular sorting. *Annu Rev Cell Dev Biol* **12**: 575-625 (1996).

38. M. Ogris, P. Steinlein, M. Kursa, *et al.* The size of DNA/transferrin-PEI complexes is an important factor for gene expression in cultured cells. *Gene Ther* **5**: 1425-1433 (1998).

39. D. A. Groneberg, C. Witt, U. Wagner, *et al.* Fundamentals of pulmonary drug delivery. *Respir Med* **97**: 382-387 (2003).

Chapter 3

Enhanced gene expression in mice using polyplexes of low-molecular weight polyethyleneimine

for pulmonary gene therapy

ABSTRACT

Non-viral gene delivery using polyethyleneimine (PEI) as a carrier have previously been demonstrated to successfully mediate gene transfer to the mouse lung. The aim of this study was to elicit improved gene expression and decreased cytotoxicity for pulmonary gene therapy by replacing the commonly used carrier 25 kDa branched PEI (BPEI) by two PEI derivatives, low molecular weight PEI (LMWPEI) and poly(ethylene glycol)-graft-PEI (PEGPEI). Polyplexes, generated with different N/P ratios, were characterized by studying their structure, size and zeta-potential using atomic force microscopy, dynamic light scattering and laser Doppler anemometry respectively. Polymer and polyplex cytotoxicity was investigated using LDH and MTT assays. Polyplex transfection efficiencies studied in vitro on A549 and in vivo in the mouse lung were quantified via measurement of luciferase expression. Finally, by employing a modified fluorescence quenching assay, the polyplex stability was studied in an in vitro assay mimicking the alveolar lining layer. All polymers were shown to condense DNA to spherical particles of approximately 100 nm in size with positive zeta-potentials (+32 mV for BPEI, +17 mV for LMWPEI & PEGPEI polyplexes). LMWPEI demonstrated the lowest membrane damage and cell viability reduction, while BPEI was observed to be the most cytotoxic. Luciferase expression in vitro was approximately three times higher for PEGPEI/DNA when compared to BPEI/DNA. Although LMWPEI/DNA was shown to be less efficient in vitro, it caused the highest luciferase expression in the mouse lung after intratracheal instillation. The maximum efficiency was observed at N/P 8 for LMWPEI/DNA. Whilst PEGPEI polyplexes demonstrated the highest stability in the alveolar lining layer, a significantly higher transfection compared to naked DNA was not observed in the mouse lung. In conclusion, LMWPEI combines low cytotoxicity with high transfection efficiency in lung under in vivo conditions, rendering it a promising strategy for pulmonary gene delivery.

INTRODUCTION

Gene therapy is a relatively new approach for the treatment of lung disorders by replacement of defective genes or the introduction of new protein-based functions into pulmonary cells. Recently, gene therapy has been successfully implemented in the treatment of severe disorders, such as cystic fibrosis and tumors [1, 2]. However, several clinical trials using adenoviruses or adeno-associated viruses as gene carriers for the treatment of cystic fibrosis demonstrated a number of limitations for their clinical use. These include the lack of vector persistence in proliferating cells and immune responses, which inevitably precludes repeated administration. Clinical trials using cationic lipids as non-viral gene carriers have demonstrated that gene transfer to the upper airway epithelium is safe, but also transient and inefficient [3-5]. Thus, it is clear that more efficient and safe gene delivery systems are necessary to exploit gene therapy for the treatment of pulmonary diseases.

A variety of non-viral gene carriers, including polycationic polymers, cationic lipids, nanoparticles, peptides, proteolipidic and bacterial vectors have been developed for administration of DNA to the airway epithelium [6-10]. Of these, the polycation polyethyleneimine (PEI) has shown potential for lung gene therapy. After the first reported use of PEI as a pulmonary gene delivery system, numerous improvements were achieved regarding the efficiency of this non-viral carrier [11]. Polymer-DNA-complexes (polyplexes) formed of plasmid DNA and linear PEI (22 kDa) have shown high transfection levels in the lung epithelium via the intravenous, as well as intratracheal route [12, 13]. However, systemic side effects, such as blood cell aggregation (intravenous route) and deterioration of the lung function (intratracheal route), highlighted the limits of linear PEI in lung gene therapy [14, 15]. Polyplexes of branched PEI (25 kDa) (BPEI) with DNA resulted in significantly higher levels of pulmonary transgene expression compared to linear PEI after inhalation [16]. Additionally, minimal inflammatory effects and no immune response were recorded [17]. Furthermore, aerosol delivery of polyplexes containing BPEI and p53 DNA resulted in a significant reduction in the tumor burden and inhibition of lung metastasis in mouse models [18, 19]. Also, IL-12 transferred to the mouse lung using BPEI resulted in a therapeutic response of pulmonary osteosarcoma metastases [20].

Recently, we synthesized a branched low molecular weight PEI (LMWPEI), with a molecular weight of 5 kDa [21]. In several cell types, polyplexes of LMWPEI displayed a significantly lower toxicity combined with a high transfection efficiency when compared to high molecular weight PEI [22]. Furthermore, the stability and transfection efficiency post-

nebulization of polyplexes using the commercially available BPEI and a poly(ethylene glycol)-graft-PEI copolymer (PEGPEI) was shown to be dependant on polymer structure and composition [23, 24].

Consequently, the aim of this study was to compare different PEI derivatives, LMWPEI and PEGPEI, with the commercially available BPEI and assess their suitability for pulmonary gene therapy. This was achieved by studying various physico-chemical properties of the polyplexes, including their structure and dimensions by atomic force microscopy (AFM) and dynamic light scattering (DLS), as well as their charge by measuring the zeta-potential. The transfection efficiency and the cytotoxicity of the different polyplexes were studied in alveolar epithelial cells in vitro (A549). The stability in the alveolar compartment was addressed by in vitro studies in alveolar lining fluid (lavage) and natural lung surfactant (Alveofact®) in a fluorescence quenching assay. Finally, the transfection efficiencies in the mouse lung were investigated under in vivo conditions.

METHODS AND MATERIALS

Materials

Branched polyethyleneimine (BPEI) with a molecular weight of 25 kDa was purchased from Sigma-Aldrich (Seelze, Germany). The plasmid DNA pGL3 carrying luciferase coding region under the promoter control of cytomegalovirus (CMV) was kindly provided by J. Hänze (Department of Molecular Biology, University of Giessen, Germany), was propagated in E.coli and purified by PlasmidFactory (Bielefeld, Germany). Standard quality control performed by the manufacturer resulted in the following data: supercoiled content 92 %, bacterial DNA and RNA not detectable by AGE, identity confirmed by restriction fragment length. Alveofact® was purchased from Boehringer-Ingelheim (Germany). Bronchial alveolar lining fluid was freshly obtained form C57BL/6 mice via intratracheally instillation 1 hour prior to use. For removal of the cells, the BALF was centrifuged at 300 g at 4°C, and the pellet was discarded. All other materials were of analytical grade.

Synthesis

The low molecular weight PEI (LMWPEI) was synthesised and extensively characterized as described by von Harpe et al. [25]. The synthesis was carried out in aqueous solution from aziridine using HCl as a catalyst. The resulting molecular weight was approximately 5 kDa [22]. Ppoly(ethylene glycol)-graft-polyethyleneimine (PEGPEI), was synthesized as

previously described [26]. Briefly, PEGPEI was obtained by activating PEG-monomethyl ether (5 kDa) with a hexamethylene diisocyanate. The coupling of PEG to the amino groups of BPEI was carried out in anhydrous chloroform at 60 °C, which led to a PEI copolymer containing 2 PEG 5 kDa molecules per molecule of BPEI.

Polyplex Formation

All polyplexes consisting of DNA and PEI were prepared in sterile isotonic glucose solution at pH 7.4. The preparation occurred in two steps. First, PEI solution was prepared by mixing the appropriate amount of PEI stock solution (2 mg/ml) with glucose. The DNA was gently mixed with the glucose solution to achieve a final DNA concentration of 2 µg/100 µl polyplex solution for the in vitro experiments and 26 µg/100 µl for in vivo experiments. Both solutions were then incubated for a period of ten minutes. In the second step, polymer solution was added rapidly to the DNA and mixed by vigorous pipetting. The resulting polyplexes were incubated for 10-20 minutes at room temperature prior to use. When various PEI nitrogen to DNA phosphate ratios (N/P) were investigated, the final volumes of 100 µl for in vitro transfection and 150 µl for in vivo transfection were kept constant. The concentration of PEI was adjusted to the amount of DNA in order to maintain N/P ratios of 6, 8 and 10 for BPEI and LMWPEI and N/P ratios of 8, 10 and 20 for PEGPEI.

Physico-chemical Properties

To study the physico-chemical properties of the different polyplexes, investigations of structure, particle size and charge were performed. The polyplexes were prepared as described above.

Structure and morphology of DNA and polyplexes at N/P 8 was investigated using atomic force microscopy (AFM). Images of DNA and the PEI/DNA polyplexes were obtained using a Nanoscope IIIa Multimode Atomic Force Microscope (Veeco, Santa Barbara, CA, USA), operating in tapping mode in a liquid environment. All imaging was carried out at a scan speed of approximately 3 Hz with a 512 x 512 pixel resolution. Silicon nitride oxide-sharpened cantilevers were selected, operating at resonance frequencies of approximately 10 kHz. A sample volume of 40 µl was placed onto a 1 cm^2 disk of freshly cleaved mica. 10 mM nickel chloride was added to the naked DNA solution to facilitate immobilization of the plasmid at the mica surface. To determine the mean polyplex size from these images, the diameter at about half-height of 30-50 polyplexes were analyzed.

The hydrodynamic diameters of PEI/DNA polyplexes were measured by dynamic light scattering (DLS) using an Autosizer (Malvern Instruments, Worcester, UK). The scattered light was detected at a 90° angle through a 100 µm pinhole. Measurements were performed at 25°C with count rates between 50 and 300 kCps in 5 runs of 60 sec duration each and analyzed in CONTIN mode. The z-average of the polyplexes hydrodynamic diameters and the corresponding standard deviations (SD) were calculated from three independent measurements with freshly prepared samples.

The surface-charges of PEI/DNA and naked DNA were determined by measuring the zeta-potential using the method of laser Doppler anemometry (LDA). The zeta-potentials were measured in the standard capillary electrophoresis cell of a Zetasizer 3000 HS (Malvern Instruments, Worcester, UK). The measurements were performed in pure water at pH 7.4 at 25 °C with automatic duration. The average values and the corresponding SD were calculated in three independent measurements, five runs each.

In vitro transfection

Human lung epithelial cell line (A549) was obtained from the German Collection of Microorganisms and Cell Cultures and was maintained according to the supplier's specifications. To evaluate the gene expression in A549, the transfection experiments were carried out as previously described in detail [23]. Briefly, cells in passages 6-15 were seeded at a density of 25000 cells per well on 24-well cell culture plates 24 h prior to the transfection experiments. The polyplexes were prepared as described above and 100 µl solutions were added to each well containing 900 µl fresh medium and incubated for 4 hours. The medium was then replaced and the cells were allowed to grow for a further 44 hours. The luciferase expression and protein concentration was determined in the cell lysate. All experiments were performed in triplicate and data were expressed in ng luciferase per mg protein (± SD).

Cytotoxicity

The cytotoxicity of PEI/DNA polyplexes at different N/P ratios was investigated using both LDH and MTT assays on A549 cells. The polyplex formation and administration to cell cultures was performed as described above. Furthermore, the cytotoxicity of the polymers alone at increasing concentration was studied using the MTT assay.

To evaluate the polyplexes membrane cytotoxicity, a lactate dehydrogenase (LDH) assay was performed using A549. The cells were cultured as described above and allowed to grow for 72 hours prior to the polyplex application. Four hours post application, the amount of

cytoplasmatic LDH released as a result of cell membrane damage was quantified using a LDH activity kinetic assay from Sigma Diagnostics (St. Louis, MO, USA) according to the manufacturer's protocol. The assay is based upon the enzymatic reaction of pyruvate and NADH to lactate and NAD^+ catalyzed by LDH. The reduction of NADH was spectrophotometrically determined at 340 nm (Ultrospec 1000, Pharmacia Biotech, Freiburg, Germany). Controls were performed using medium (no LDH release) and 0.1 % Triton X-100 set as maximum LDH release (100 %). The results were presented as percentage cytotoxicity calculated by the released LDH * 100 % / total LDH. All samples were run in triplicate and the experiments were repeated twice.

The MTT assay was performed using the previously reported method [27]. A549 cells were seeded in 96-well microtiter plates at a density of 4200 cells per well and allowed to grow for 72 hours prior to polyplex application. The three different polymers were mixed with medium to final concentrations of 0.001, 0.01, 0.1, 0.5 and 1.0 mg/ml and 100 µl of these were applied per well. When polyplexes cytotoxicity was studied 100 µl of the medium were replaced with 83 µl fresh medium and 17 µl polyplexes to achieve the same conditions as used in the in vitro transfection experiments. After 4 hours incubation with polymers and polyplexes respectively, the medium was replaced by 200 µl fresh medium and 20 µl (3-(4,5-dimethylthiatol-2-yl)-2,5-diphenyl tetrazolium bromide) (MTT, Sigma, Seelze). After 4 hours, the unreacted dye was removed and 200 µl DMSO was added. The absorption was measured using the ELISA reader Titertek Plus MS 212 (ICN, Eschwege, Germany) at 570 nm, with a background correction at 690 nm. The relative cell viability (%) was related to control wells containing cell culture medium without polymer or polyplexes and was calculated by: absorption test x 100 % / absorption control. Data are presented as a mean of six measurements (± SD). The values of the polymers were fitted to a Bolzmann sigmoidal function using Microcal Origin® v 7.0 (OriginLab, Northampton, USA) and IC50 was calculated.

In vivo transfection

The polyplexes were prepared as described above and 150 µl of PEI/DNA or naked DNA were instilled into the lung of C57BL/6 mice. The mice were purchased from Charles River Laboratories (Sulzfeld, Germany) aged 4-6 weeks, weighing 22-28 g. Prior to the application the animals were held for five days in the animal lab were they were fed regularly (Muskator GmbH, Düsseldorf, Germany). For in vivo transfection, the animals were lightly anesthetized with 0.06-0.08 µl mixture (1:1:3) of ketamine hydrochloride 100 mg/ml (Ketavet®,

Pharmacia, Erlangen, Germany), xylacine hydrochloride 2 % (Rompun®, Bayer, Leverkusen, Germany) and isotonic sodium chloride. For intratracheal instillation the mice were positioned in a vertical position and polyplexes were administered using a flexible needle (0.9 x 25 mm). Forty-eight hours after instillation the mice were sacrificed. After washing the lungs with isotonic sodium chloride by catheterizing the arteria pulmonalis, the lungs were removed and weighed. Per one gram of lung tissue 2 µl reporter lysis buffer (Promega, Mannheim, Germany) were added, the lung was immediately homogenized and frozen at minus 20°C. After thawing, the samples were centrifuged for 20 minutes at 4 °C and the luciferase assay was performed as described in the in vitro experiments. The transfection efficiencies and the corresponding SD were calculated as the mean value of 6 experiments and presented as pg luciferase per mg lung tissue. The use of animals in this study was approved by the local ethics committee for animal experimentation and the experiments were carried out according to the guidelines of the German law of protection of animal life.

Stability

The effect of Alveofact® and bronchial alveolar lining fluid (BALF) upon the polyplex stability was evaluated using a reverse fluorescence quenching assay [28, 29]. The fluorescence of ethidium bromide (EtBr), a DNA-intercalating agent, is enhanced upon binding to DNA and quenched when displaced by higher affinity compounds.

Polyplex preparation was carried out as described. The amount of DNA was increased to 6 µg per 100 µl and condensed with the appropriate amount of polymer to achieve N/P ratios of eight. The polyplexes were placed in a 96-well plate and 50 µl EtBr (40 µg/ml) were added. Alveofact® was dissolved in isotonic glucose solution pH 7.4 and added to the polyplexes to achieve final concentrations of 0.002, 0.02, 0.2, 1.0, 2.0 µg/µl. When stability in BALF was tested 100 µl of freshly attained BALF instead of Alveofact® was added to the polyplexes. The fluorescence measurements were began immediately after the addition of Alveofact® and BALF respectively, and were carried out over a period of 90 minutes at a temperature of 37°C (Fluorescence reader FL600, Micro plate Fluorescence BioTEK, Winooski, USA) using $?_{ex}$ = 485 nm and $?_{em}$ = 590 nm. The fluorescence is reported relative to the value obtained with naked DNA and EtBr (= 100%), as the mean ± SD of five measurements.

Statistical analysis

Statistical calculations were carried out using the software package GraphPad InStat v3.06 (GraphPad Software, Inc. San Diego, CA, USA). To identify statistically significant differences one-way ANOVA with Bonferroni's post test analysis was performed. Differences were considered significant if $P = 0.05$ (*), $P = 0.01$ (**), $P = 0.001$ (***) and marked accordingly in the figures.

RESULTS AND DISCUSSION

The delivery of genes to the airways holds considerable promise for the treatment of lung diseases, such as cystic fibrosis, asthma, cancer and pulmonary hypertension. Non-viral gene delivery systems have been shown to be safe alternatives to viral vectors in pulmonary gene therapy [30, 31]. However, there are still several problems to overcome with these systems, such as the need for a higher transfection efficiency, repeated administration, cell specific targeting and lower toxicity. The polycation PEI has been shown to hold several advantages as a non-viral gene carrier to the lung, such as a higher efficiency compared to lipid carriers, superior stability against DNase, lung surfactant and nebulization [13, 24, 28, 31]. The aim of our study was to find a PEI modification that exhibits comparable or improved transfection efficiency and is less toxic than the commonly utilized BPEI. Furthermore, by implementing a range of methods to thoroughly characterize the polyplexes, an enhanced understanding of the polymer structure-response relationship should be elucidated.

Physico-chemical properties

Plasmid and polyplex (N/P 8) morphologies in an aqueous environment were determined by AFM and representative images are shown in Figure 1. Image A displays naked plasmid DNA in a predominantly open circular form, however, some twisting of the DNA strands can also be observed. Images B-D illustrate the BPEI, LMWPEI and PEGPEI polyplexes respectively on the nanoscale. No uncomplexed strands of DNA were detected. Hence, it can be assumed that at an N/P ratio of 8 all three polymers fully condensed the plasmid forming spherical particles as shown in the AFM micrographs.
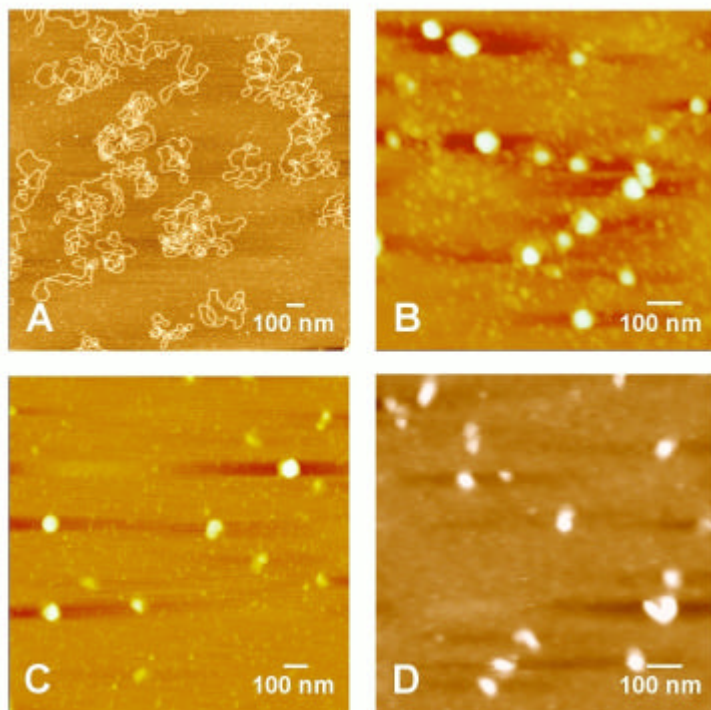
Figure 1. In situ AFM images showing the structure of naked DNA in isotonic glucose solution (A) and polyplexes formed of DNA and BPEI (B), LMWPEI (C), PEGPEI (D) at an N/P ratio of 8.

The particle sizes of PEI/DNA polyplexes were measured using DLS and AFM (Table 1). Both methods yielded the smallest particles sizes for polyplexes from BPEI and DNA. LMWPEI and PEGPEI formed the slightly larger polyplexes at all the investigated N/P ratios with particle diameters of ca. 100-140 nm.

Size of the polyplexes has been reported to be an important factor in facilitating gene transfer in cells [32-34]. An additional complication of polyplex delivery to the lung stems from the fact that two major clearance processes are seen in lung tissue, namely mucociliary and alveolar macrophage clearance. While particles > 500 nm are usually removed from the lung by mucociliary clearance, those < 250 nm may escape phagocytosis of alveolar macrophages [35]. Also, endocytotic uptake of particles is clearly affected by their size and increases with decreasing diameters [36]. Polyplexes from PEI will be taken up by endocytosis and subsequently release DNA according to the proton sponge hypothesis [37]. These considerations suggest that the PEI/DNA polyplexes studied here may have to fulfill different size requirements under cell culture conditions and in vivo.

To estimate the surface charge of the PEI/DNA polyplexes, we measured their zeta-potentials using LDA. The results for naked DNA and PEI/DNA polyplexes at different N/P

ratios are shown in Table 1. Plasmid DNA had a highly negative zeta-potential of -33 mV. All polyplexes displayed positive zeta-potentials due to an excess of the polycation. The highest zeta-potential of approximately +32 mV was obtained for BPEI polyplexes. An increase in the N/P ratio did not affect upon the BPEI polyplex surface charge. Zeta-potentials of LMWPEI polyplexes were found to be significantly lower than these of BPEI polyplexes. Furthermore, a slight potential increase (from 15 to 22 mV) at higher N/P ratios was observed. Constant low zeta-potentials of approximately 17 mV were measured for all PEGPEI polyplexes.

Table 1. Physico-chemical properties of the different polyplexes: Polyplex hydrodynamic diameters were measured using DLS and average values were determined from three measurements of five runs each. AFM was also used to make size measurements. The mean values were calculated from 30-50 polyplexes of different images. The zeta-potential mean values ± SD were determined in three independent measurements of five runs each using LDA.

polyplexes	N/P ratio	particle sizes [nm]		zeta-potential
		DLS	AFM	[mV]
BPEI	6	95.0 ± 6.7		32.9 ± 4.4
BPEI	8	102.5 ± 10.0	87.3 ± 12.6	32.3 ± 6.2
BPEI	10	90.6 ± 13.4		31.5 ± 4.5
LMWPEI	6	105.2 ± 10.7		15.2 ± 3.9
LMWPEI	8	138.4 ± 16.9	91.0 ± 39.9	18.7 ± 5.1
LMWPEI	10	136.6 ± 8.9		21.7 ± 6.5
PEGPEI	8	111.2 ± 5.7	115.1 ± 18.7	17.0 ± 1.9
PEGPEI	10	120.2 ± 20.2		17.3 ± 2.2
PEGPEI	20	104.7 ± 21.1		16.9 ± 2.3
DNA				-32.7 ± 9.48

The high zeta-potential of the BPEI polyplexes we observed here is in line with previous reports [37]. It was stated that at N/P ratios > 4, BPEI polyplexes have a zeta-potential between 30 and 35 mV, due to the complete DNA condensation and an excess of polymer. This excessive polymer covers the particle surface of the polyplexes and therefore, the zeta-potential of BPEI/DNA does not further increase with the increasing N/P ratio. This, on the other hand, led us conclude that the LMWPEI polyplexes are less compact and the particle

surface is not completely covered by the polymer at N/P ratios of 6 and 8. We believe that the zeta-potential increase with the increasing N/P ratio, provides evidence for a reduction in DNA condensation compared to that observed with BPEI, due to its lower molecular weight [22]. The low charge of PEGPEI/DNA confirmed that PEG shields the polyplex surface, also at N/P ratios > 10 [38, 39].

In vitro transfection

To evaluate the gene transfer efficiency of the three PEI modifications, polyplexes at differing N/P ratios were applied to A549 cells and luciferase gene expression was quantified after 48 hours (Figure 2). The data indicated that the transfection efficiency increases with increasing N/P ratio. This finding is consistent with previous reports [21, 39]. Among the different PEIs tested, PEGPEI was by far the most effective transfection agent. At N/P ratios of both 8 and 10, the efficiency of PEGPEI polyplexes (4.3 and 6.1 ng/mg respectively) was three times higher (P = 0.05) than observed with BPEI polyplexes (1.5 and 2.1 ng/mg respectively). At N/P 20 the transfection rate of PEGPEI polyplexes increased to approximately 52 ng/mg, which was 20 times higher than observed with the BPEI polyplexes at N/P 10 (P = 0.001). Whilst the transfection of LMWPEI polyplexes was the least efficient, its increase with an increasing N/P ratio was the highest and approximately 0.9 ng/mg was achieved using N/P 10. The transfection rate of naked DNA was negligible (0.0014 ng/mg) to the point of not being detectable in the diagram.

Apart from the PEGPEI used in this study, other PEG-grafted PEI derivatives have been extensively investigated as potential candidates for non-viral gene delivery [39]. After screening these polymers as gene vectors for A549 cells, the PEGPEI selected here was found to be by far the most efficient carrier in lung epithelial cells. Furthermore, an N/P ratio of 20 for PEG-grafted PEIs was shown to be highly efficient and less toxic than BPEI in mouse fibroblasts [39]. For this reason, we chose this N/P ratio for the experiments in this study, in addition to the N/P ratios of 8 and 10.
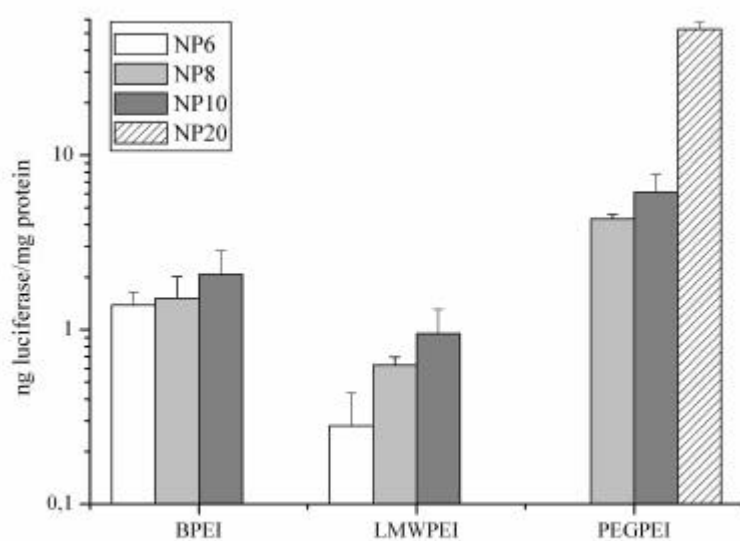
Figure 2. Transfection efficiency of PEI/DNA polyplexes at different N/P ratios in an epithelial cell culture model (A549). All results are the average ± SD of three independent experiments of three samples each.

We have demonstrated a remarkable increase in the transfection efficiency of PEGPEI/DNA compared to BPEI/DNA polyplexes in A549 alveolar epithelial cells. In contrast, the transfection efficiencies of LMWPEI polyplexes in the A549 lung cells were shown to range below that of the commercially available BPEI. However, the efficiency of LMWPEI/DNA improved with increasing N/P ratio, probably due to the increased zeta-potential. Similar results have been reported before and the gene expression of PEIs with a low molecular weight were described to range below that of high molecular weight PEIs when applied to numerous cell lines at N/P ratios < 10 [22, 27]. In this context, it was also assumed that in comparison to BPEI, the poor in vitro transfection, the low zeta-potential and the slightly larger size provide evidence for a reduction in the condensation between LMWPEI and DNA.

Cytotoxicity

The LDH assay was performed to test the cytotoxicity based upon membrane damage caused by polyplexes under transfection conditions, whereas the MTT assay was chosen to

study the cell viability over a wide range of polymer concentrations and under transfection conditions.

To assess the cell membrane damage, polyplexes at different N/P ratios were applied to A549 cells over a period of four hours and then the extracellular LDH was quantified (Figure 3). Naked DNA at a concentration of 2 µg/ml, the same concentration used in polyplex formulation, caused membrane damage as represented by a LDH release of 2.2% (P = 0.05 in comparison with medium control). No significant LDH release compared to the control cells and, therefore, no membrane toxicity was observed using polyplexes at N/P 6. Whilst the polyplexes of LMWPEI and PEGPEI did not show a significantly higher LDH release at an N/P ratio of 8, BPEI polyplexes led to an increasing LDH release of up to 4 %. At an N/P ratio of 10, BPEI/DNA caused the most sever membrane damage (5.2 % LDH release) when compared with LMWPEI/DNA (3.5 %) and PEGPEI/DNA (4 %). The highest cytotoxicity of approximately 6.5 % LDH release was observed for PEGPEI/DNA at N/P 20. When comparing polyplexes with naked DNA, we observed that only BPEI N/P 10 and PEGPEI N/P 20 led to significantly higher levels of membrane damage. Because the LDH release of these two polyplexes exceeded 5 %, they are considered to be cytotoxic [27].

Figure 3. The cell membrane damaging effect of naked DNA and PEI/DNA polyplexes at different N/P ratios was quantitated b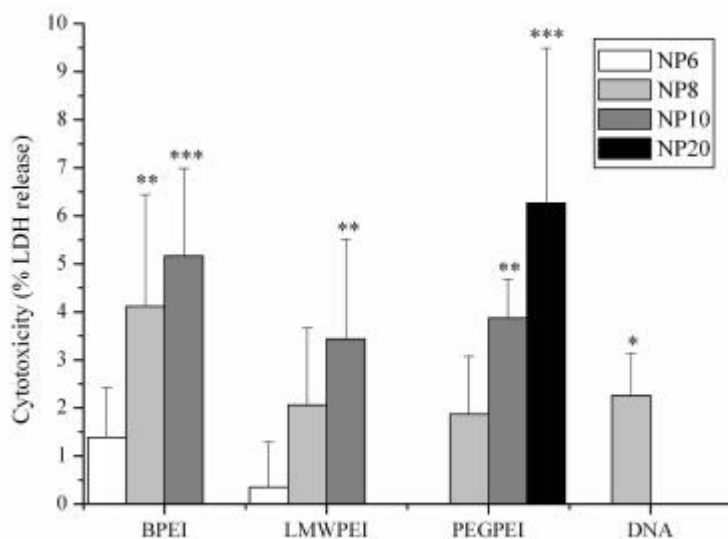y the release of the cytosolic enzyme, LDH, from A549. Each value represents the mean ± SD of three determinations of three samples each.

Statistically significant differences from the medium control are denoted with one (P = 0.05),

two (P = 0.01) or three (P = 0.001) asterisks.

The metabolic and mitochondrial activity of polymer- or polyplex-treated cells was determined using the colorimetric MTT-assay [40]. As illustrated in Figure 4A, the toxicity of all polymers was concentration dependent. Whilst both BPEI and PEGPEI reduced the cell viability dramatically at polymer concentrations of 0.01 mg/ml (~ 25 % viability), LMWPEI showed less influence upon the cells (~ 75 % viability). Considering the IC50 values, BPEI 0.071 mg/ml, PEGPEI 0.074 mg/ml and LMWPEI 0.26 mg/ml, it is clear that the metabolic activity reduction is far lower using LMWPEI compared to BPEI and PEGPEI.

After four hours of polyplex application (Figure 4B) to A549, the cell viability decreased for BPEI/DNA, LMWPEI/DNA at N/P ratios 6-10 and PEGPEI/DNA at N/P ratios 8 and 10 to approximately 85-75 %. Comparison of these polyplexes did not show significant differences in cell viability. Only PEGPEI polyplexes at an N/P ratio of 20 caused a strong reduction in the metabolic activity and the viability dropped to 65 %. Application of naked DNA alone resulted in a remaining cell viability of 95% ± 3.3 (data not shown).

PEG-grafted PEI modifications have been shown to hold distinct advantages in lung gene therapy as they are involved in fewer interactions with proteins or cells, thus they tend to exhibit a lower toxicity, due to the shielding effect of PEG [41, 42]. Reduced interactions between the polyplexes and the cell surface can be observed as a decrease in the cell membrane damage [27]. The LDH assay data obtained here for PEGPEI in comparison to BPEI polyplexes suggested a decrease in cell membrane damage at N/P ratios of 8 and 10, respectively. This observation and the lower zeta-potential of PEGPEI/DNA confirmed the shielding effect of PEG [38, 39]. However, at an N/P ratio of 20, PEGPEI polyplexes significantly increased the LDH release, thus the cell membrane was aggravated to a significant extent. We assume that at an N/P ratio of 20, free, uncomplexed polymer is present in the solution and interaction between this free PEGPEI and the cell surface increased conspicuously. Furthermore, according to the reduced cell viability observed in the MTT assay, PEGPEI showed a similar cytotoxicity as that of BPEI. This reduction in the metabolic activity indicated, that after membrane interaction the polymer was incorporated in the cell plasma and damaged the mitochondria. Taken together, the PEGPEI polyplexes have, in comparison to BPEI polyplexes, a reduced cytotoxicity at N/P ratios of 8 and 10. This finding is in agreement with the low cytotoxicity of PEGPEI polyplexes previously reported [42, 43]. However, uncomplexed PEGPEI, which probably existed at the high N/P ratio of 20, led to

significant damage of lung epithelial cells. Therefore, PEGPEI advantages, such as polyplex surface shielding and low toxicity, can only be taken into account when N/P ratios = 10 are applied to lung epithelial cells. We assume that the PEGPEI/DNA interaction with the membrane is reduced, due to the PEG shielding [39], but once inside the cell the lysosomal release is highly efficient. This would explain the high gene expression in vitro combined with low zeta-potential and reduced membrane damage.
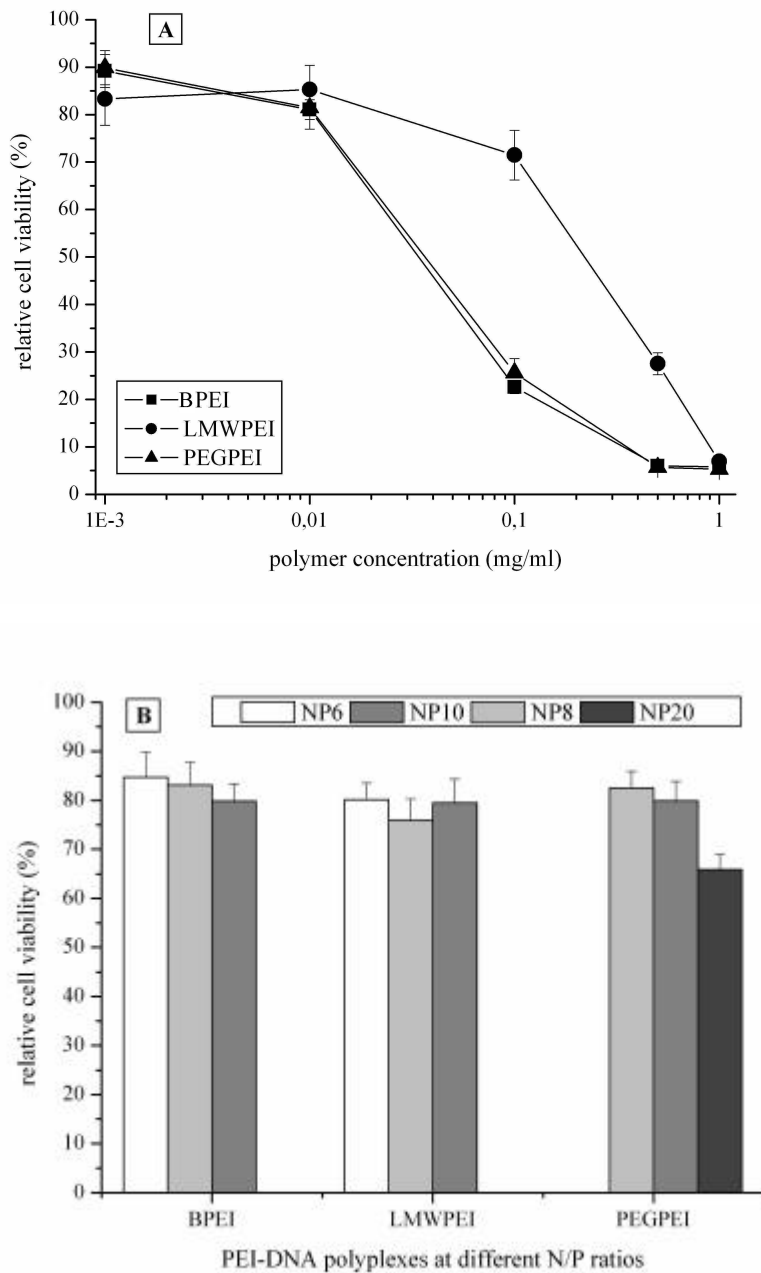
Figure 4. Cytotoxic effects were determined by MTT assay and presented as the relative cell viability (mean ± SD of six determinations). Polymer solutions (A) of 0.001, 0.01, 0.1, 0.5,

and 1.0 mg/ml and polyplexes (B) BPEI/DNA, LMW/DNA N/P 6, 8, 10 and PEGPEI/DNA N/P 8, 10, 20 were applied to A549 over a period of four hours.

Several studies performed in our laboratory have compared low and high molecular weight PEIs. Lower toxicity combined with a high transfection efficiency in differing cell lines was clearly demonstrated [22, 33]. Using human lung epithelial cells, lower toxicity, demonstrated by a reduction in membrane damage and favorable cell viability, was also observed for the LMWPEI utilized in this study. Therefore, it can be concluded, that in contrast to BPEI and PEGPEI, the interaction between the cell membrane and LMWPEI is reduced and, thus, the incorporation of the polyplexes into the cells and the mitochondrial damage are also reduced. The lower zeta-potentials of the LMWPEI polyplexes confirmed the in vitro results, i.e., the lower charge caused fewer interactions with the cell membranes, which in turn suppressed gene expression.

In vivo transfection

To determine the transfection efficiency of the PEI modifications in mice, polyplexes and DNA were delivered to the lung via an intrapulmonary route. In order to evaluate the transfection peak in the mouse lung, a time screening experiment (Figure 5) was carried out prior to the investigation of the various polyplexes. Luciferase concentrations were measured at 12, 24, 48, 72, 120 and 240 hours after LMWPEI/DNA N/P 6 instillation, with the highest transfection rate being observed at 48 hours post-administration. Therefore, all studies of the luciferase expression in the mouse lung were carried out 48 hours after the intrapulmonary administration. An equivalent incubation time for PEI/DNA treated mice via aerosol administration has been described before [31].
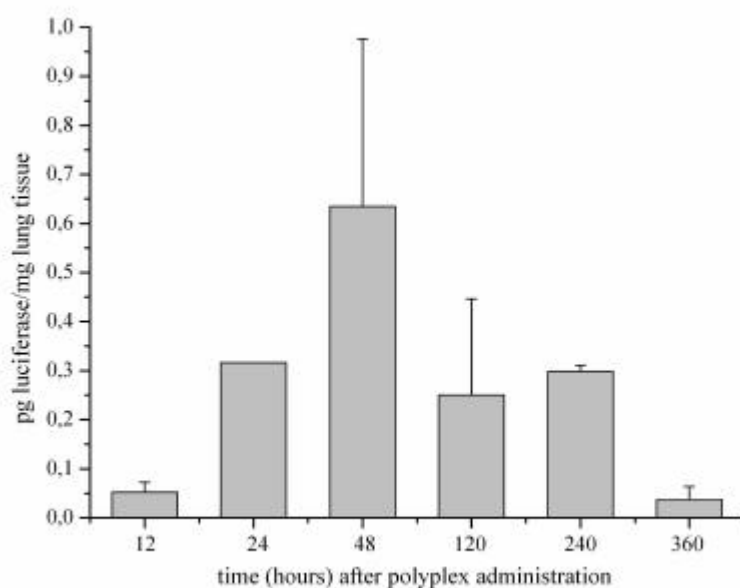
Figure 5. Transfection efficiency of LMWPEI/DNA polyplexes N/P 6 in C57BL/6 mice lung 12, 24, 48, 120, 240, 360 hours post-administration. Values are averages ± SD of three experiments.

Figure 6 presents the luciferase expression of DNA and the different polyplexes in the mouse lung 48 hours after intrapulmonary application. When administering plasmid DNA in the absence of a carrier, a transfection efficiency of approximately 0.4 pg luciferase per mg lung tissue was obtained. Marginally more luciferase was produced when polyplexes of DNA with BPEI or LMWPEI N/P 6 and PEGPEI N/P 8, 10 and 20 were administered to the lungs of mice. Thus, these polyplexes did not cause a significant increase in the transfection efficiency when compared to naked DNA. A ten fold higher efficiency was obtained when BPEI polyplexes at N/P 8 were administered. The highest luciferase accumulation (8.2 pg/mg) was observed for LMWPEI polyplexes at N/P 8. This enormous in vivo transfection efficiency significantly surpassed (P = 0.01) that of all other polyplexes investigated in this study.
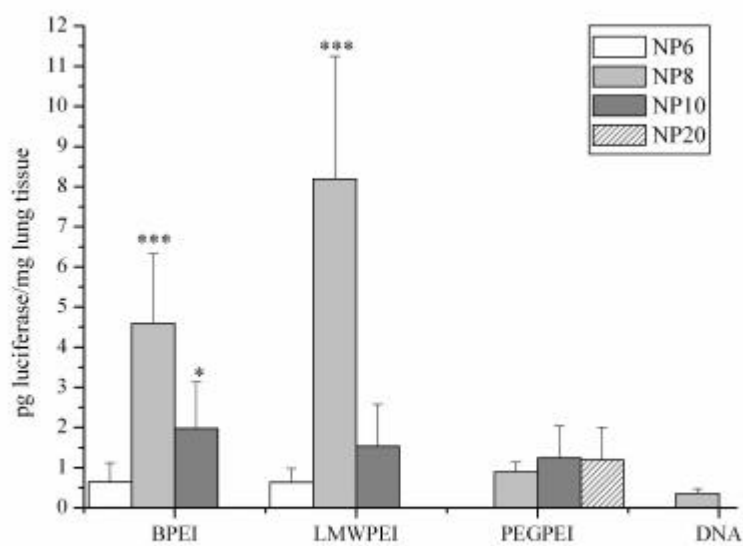
Figure 6. Transfection efficiency of PEI/DNA polyplexes at different N/P ratios in C57BL/6 mice lung. All results provided are mean ± SD of six experiments. Statistically significant differences from DNA are denoted with one (P = 0.05) or three (P = 0.001) asterisks.

Whilst PEGPEI/DNA appears to be an outstanding transfection agent in cell culture, this behavior was not confirmed in the in vivo experiments. It was found that the transfection efficiency of the PEGPEI polyplexes was at the same level as DNA applied without a carrier, independent of the N/P ratios. Also, Kichler et al [42] reported a low transfection efficiency of PEGPEI polyplexes when compared to naked DNA after instillation to the mouse lung. However, our data are still to some extent encouraging since it has been reported that PAA dendrimers or lipid based carriers show a lower transfection efficiency than naked DNA [44, 45].

The transfection efficiencies of LMWPEI polyplexes in the A549 lung epithelial cells were shown to range below that of the commercially available BPEI. An efficacious gene expression in the mouse lung was achieved after LMWPEI/DNA was administered via an intrapulmonary route. In particular at the N/P ratio of 8, LMWPEI polyplexes seem to have better properties than BPEI and PEGPEI as a gene carrier to deliver the plasmid DNA into the nucleus of lung cells in living mice.

To our knowledge, this significant transfection rate increase from the N/P ratio of 6 to 8 and then the significant transfection decrease from the N/P ratio of 8 to 10 seen for BPEI and LMWPEI polyplexes were not demonstrated before. It was particularly surprising since

Gautam et al. reported the highest gene expression in the lung of aerosol-treated mice for BPEI polyplexes at a N/P ratio of 15 [46]. However, the conditions used in this study were different from ours, e.g. the reporter gene and the amount of polyplex used were different, as well as the route of administration. Similar conditions were used by Bragonzi et al. who condensed BPEI with DNA (50 µg per mouse of a CMV controlled plasmid), administered the polyplexes via the intrapulmonary route to C57BL/6 mice and compared the transfection efficiency using a range of N/P ratios [13]. They demonstrated a luciferase expression decrease when the N/P ratio increased from 5 to 10, which is comparable to our results here. We assume that the amount of free polymer for BPEI and LMWPEI polyplexes at an N/P ratio of 6 was still too low to enhance the endosomal escape by the proton sponge effect [37]. At an N/P ratio of 10, un-complexed BPEI and LMWPEI probably enhanced endosomal escape, but also increased the in vivo toxicity. Because, high toxicity was shown to reduce transfection efficiency in vivo but not in vitro [6], we assume that this is the case in the mouse lung at an N/P ratio of 10. The cytotoxicity studies in vitro had shown a slight increase in membrane and mitochondrial damage with an increasing N/P ratio, but did not affect the transfection efficiency of the A549 cells. We assume that under the complex conditions in the lung environment, at high N/P ratios free polymer can easier escape from the polyplexes and cause cell damage and thus led to the transfection efficiency drop when the N/P ratio was increased from 8 to 10. Also Goula et al. observed stronger side effects with an increasing N/P ratio after the intra venous administration of PEI/DNA polyplexes (125 µg plasmid per mouse) [12]. Taken together, utilizing BPEI and LMWPEI as carrier for pulmonary gene delivery an N/P ratio of eight is preferable.

Stability

It was reported, that components of the bronchial alveolar lining layer affect the transfection efficiency of pulmonary gene delivery systems [47]. In an attempt to identify if similar pattern can explain the differences observed between the in vitro and in vivo transfection efficiencies, stability studies in Alveofact® and BALF were carried out using the DNA intercalation agent, EtBr (Figure 7). If the PEI condenses DNA successfully, EtBr can no longer intercalate and fluorescence intensity decreases measurably. Conversely, increasing fluorescence signal indicates decreased DNA condensation and loosing of the complex structure [29].
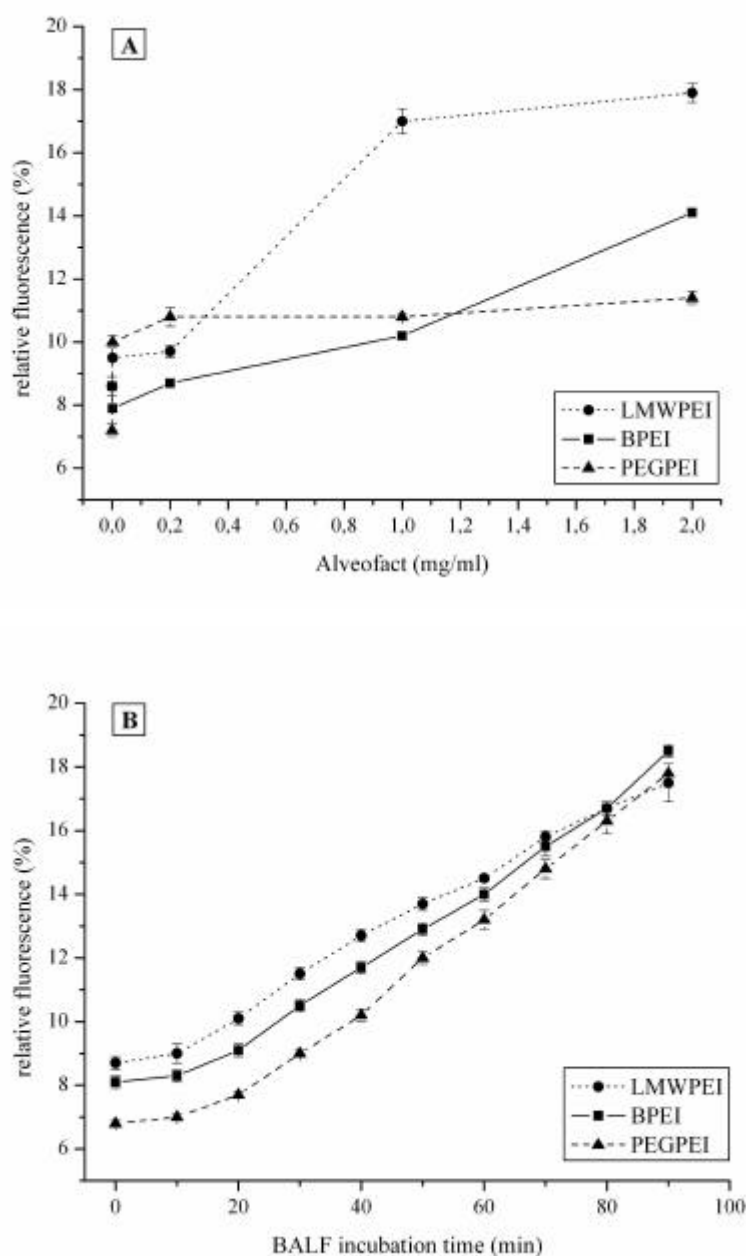
Figure 7. Polyplex (N/P = 8) stability: A) Polyplexes were treated with increasing amounts of Alveofact ® *for 90 minutes at 37°C. B) Polyplexes were treated at 37°C with freshly attained BALF. Values ± SD were determined in three independent measurements and depicted as a percentage*

When Alveofact® and BALF were not present, the polymers were able to condense the DNA (N/P 8) up to a residual fluorescence of approximately 8.5 % (BPEI and LMWPEI) and 7 % (PEGPEI), respectively. Using increasing quantities of Alveofact®, the stability of the polyplexes (N/P 8) was investigated at 37°C for 1.5 hours (Figure 7A). For all three

polyplexes, slight increases in fluorescence were observed at 0.002 µg/µl. However, at higher Alveofact® concentrations, LMWPEI/DNA displayed a lower stability, with a relative fluorescence under these conditions of 17 % (1.0 µg/µl) and 17.9 % (2 µg/µl). Whilst the relative fluorescence for PEGPEI polyplexes was highest at 0.2 µg/µl (10.8 %), the DNA release did not increase at 1 and 2 µg/µl Alveofact® (10.8 % and 11.4 % relative fluorescence). A constant fluorescence increase up to 14.2 % was observed for BPEI/DNA.

The kinetics of DNA liberation from the polyplexes in BALF (at 37°C) is presented in Figure 7B. All three polyplexes investigated showed similar increases in relative fluorescence over the observation period of 90 minutes. However, the fluorescence data obtained over a period of 60 minutes indicated that PEGPEI was superior, followed by BPEI and LMWPEI when considering the DNA condensation and encapsulation.

In comparison to BPEI and LMWPEI, the PEGPEI polyplexes were most stable in the presence of a high concentration of Alveofact® and BALF. As mentioned before, the PEG chains prevent interactions between serum cells and proteins [38, 43]. A similar reduction in the interactions probably also protects the polyplexes and, thus, the DNA against proteins, proteolipids and enzymatic degradation in the BALF and Alveofact®. Therefore, a better stability of PEGPEI polyplexes in the lung environment can be assumed. As discussed above, LMWPEI is not as efficient in condensing DNA as BPEI. Due to the denser structure of amino groups in the BPEI molecule, the compaction ability is improved and this advance BPEI compare to LMWPEI in protecting the DNA. Interestingly, it was demonstrated, that strong condensation between DNA and its carrier can reduce the gene expression [48]. Also in our study higher stability was associated lower in vivo transfection efficiency.

As a consequence, we explain the discrepancy between in vitro and in vivo transfection efficiency as follows. Firstly, different conditions in vivo and in vitro should be taken into account. These include: i) the higher concentration of polyplexes in vivo, ii) the range of different salts, proteins, proteolipids and enzymes in the mouse lung, and iii) the number of different cell types present in the mouse lung (e.g. bronchial and alveolar epithelial cells, as well as macrophages) compared to the one single type of human alveolar epithelial cell in vitro. Furthermore, it has been reported that lung cells can function differently in vitro compared to in vivo. It was observed that forty-one percent of the proteins expressed in vivo were not detected in cell culture [47].

Secondly, the superior transfection efficiency of LMWPEI polyplexes in the mouse lung was obvious and can be explained by interactions with lung surfactant, such as Alveofact®.

This destabilization of LMWPEI polyplexes suggests that transfection experiments under in vitro conditions are not predictive of experimental results in animals. Hence, other polyplex properties seem to be important for successful gene transfer in mice, rather than those anticipated from the in vitro experiments. A sufficiently high stability in the lung environment seems to be essential [1]; however, if the polymer-DNA interactions are too strong, intracellular DNA release may be compromised. For an improved in vivo gene transfer the polyplexes need to disassemble and release the DNA into the nuclear compartment, yet protect the DNA against degradation during the uptake process [4]. We assume that the DNA release from LMWPEI polyplexes is facilitated under in vivo conditions and, thus, has improved the gene expression in the mouse lung. Further investigations, e.g. lung histology studies after administration of labeled polyplexes, are necessary to confirm this hypothesis. Koeping-Hoeggård et al. studied a range of low molecular weight chitosan-DNA polyplexes and also observed differences between in vitro and in vivo transfection experiments. They reported a moderate efficiency in epithelial cells for the polyplexes with the highest transfection efficiency in the mouse lung, and, interestingly, a low stability in the presence of heparin [48].

CONCLUSION

In summary, this study has demonstrated LMWPEI to be a non-viral gene carrier combining low cytotoxicity in lung epithelial cells with a high gene delivery in the mouse lung. To our knowledge, this paper is the first to describe the use of low molecular weight PEI for pulmonary gene delivery. In essence, we have shown that the use of LMWPEI in vivo achieves a significant improvement in gene expression when compared to the commercially available BPEI. PEGPEI was also investigated and was shown to be a stable, efficacious transfection agent with low membrane toxicity. However, only moderate gene expression was observed in vivo. In conclusion, we believe that LMWPEI holds great promise as a carrier system in lung gene therapy. Indeed, the fact that LMWPEI caused significant improvements in gene expression makes this polymer an extremely promising alternative to the commonly used BPEI in pulmonary gene therapy.

REFERENCES

1. D. R. Gill, L. A. Davies, I. A. Pringle*, et al.* The development of gene therapy for diseases of the lung. *Cell Mol Life Sci* **61**: 355-368 (2004).
2. S. Ferrari, D. M. Geddes, and E. W. Alton. Barriers to and new approaches for gene therapy and gene delivery in cystic fibrosis. *Adv Drug Deliv Rev* **54**: 1373-1393 (2002).
3. T. R. Flotte. Gene therapy progress and prospects: recombinant adeno-associated virus (rAAV) vectors. *Gene Ther* **11**: 805-810 (2004).
4. E. Wagner. Strategies to improve DNA polyplexes for in vivo gene transfer: will "artificial viruses" be the answer? *Pharm Res* **21**: 8-14 (2004).
5. T. R. Flotte and B. L. Laube. Gene therapy in cystic fibrosis. *Chest* **120**: 124S-131S (2001).
6. R. K. Scheule, J. A. St George, R. G. Bagley*, et al.* Basis of pulmonary toxicity associated with cationic lipid-mediated gene transfer to the mammalian lung. *Hum Gene Ther* **8**: 689-707 (1997).
7. M. Brzoska, K. Langer, C. Coester*, et al.* Incorporation of biodegradable nanoparticles into human airway epithelium cells-in vitro study of the suitability as a vehicle for drug or gene delivery in pulmonary diseases. *Biochem Biophys Res Commun* **318**: 562-570 (2004).
8. C. Rudolph, C. Plank, J. Lausier*, et al.* Oligomers of the arginine-rich motif of the HIV-1 TAT protein are capable of transferring plasmid DNA into cells. *J Biol Chem* **278**: 11411-11418 (2003).
9. L. Vaysse, C. Guillaume, I. Burgelin*, et al.* Proteolipidic vectors for gene transfer to the lung. *Biochem Biophys Res Commun* **290**: 1489-1498 (2002).
10. I. Fajac, S. Grosse, J. M. Collombet*, et al.* Recombinant Escherichia coli as a gene delivery vector into airway epithelial cells. *J Control Release* **97**: 371-381 (2004).
11. S. Ferrari, E. Moro, A. Pettenazzo*, et al.* ExGen 500 is an efficient vector for gene delivery to lung epithelial cells in vitro and in vivo. *Gene Ther* **4**: 1100-1106 (1997).
12. D. Goula, C. Benoist, S. Mantero*, et al.* Polyethylenimine-based intravenous delivery of transgenes to mouse lung. *Gene Ther* **5**: 1291-1295 (1998).
13. A. Bragonzi, G. Dina, A. Villa*, et al.* Biodistribution and transgene expression with nonviral cationic vector/DNA complexes in the lung. *Gene Ther* **7**: 1753-1760 (2000).
14. P. Chollet, M. C. Favrot, A. Hurbin*, et al.* Side-effects of a systemic injection of linear polyethylenimine-DNA complexes. *J Gene Med* **4**: 84-91 (2002).
15. J. W. Wiseman, C. A. Goddard, D. McLelland*, et al.* A comparison of linear and branched polyethylenimine (PEI) with DCChol/DOPE liposomes for gene delivery to epithelial cells in vitro and in vivo. *Gene Ther* **10**: 1654-1662 (2003).
16. N. V. Koshkina, I. Y. Agoulnik, S. L. Melton*, et al.* Biodistribution and pharmacokinetics of aerosol and intravenously administered DNA-polyethyleneimine complexes: optimization of pulmonary delivery and retention. *Mol Ther* **8**: 249-254 (2003).
17. A. Gautam, C. L. Densmore, and J. C. Waldrep. Pulmonary cytokine responses associated with PEI-DNA aerosol gene therapy. *Gene Ther* **8**: 254-257 (2001).
18. A. Gautam, J. C. Waldrep, C. L. Densmore*, et al.* Growth inhibition of established B16-F10 lung metastases by sequential aerosol delivery of p53 gene and 9-nitrocamptothecin. *Gene Ther* **9**: 353-357 (2002).
19. A. Gautam, C. L. Densmore, S. Melton*, et al.* Aerosol delivery of PEI-p53 complexes inhibits B16-F10 lung metastases through regulation of angiogenesis. *Cancer Gene Ther* **9**: 28-36 (2002).

20. S. F Jia., L. L. Worth, C. L. Densmore, *et al.* Eradication of osteosarcoma lung metastases following intranasal interleukin-12 gene therapy using a nonviral polyethylenimine vector. *Cancer Gene Ther* **9**: 260-266 (2002).

21. D. Fischer, T. Bieber, Y. Li, *et al.* A novel non-viral vector for DNA delivery based on low molecular weight, branched polyethylenimine: effect of molecular weight on transfection efficiency and cytotoxicity. *Pharm Res* **16**: 1273-1279 (1999).

22. K. Kunath, A. von Harpe, D. Fischer, *et al.* Low-molecular-weight polyethylenimine as a non-viral vector for DNA delivery: comparison of physicochemical properties, transfection efficiency and in vivo distribution with high-molecular-weight polyethylenimine. *J Control Release* **89**: 113-125 (2003).

23. L. A. Dailey, E. Kleemann, T. Merdan, *et al.* Modified polyethylenimines as non viral gene delivery systems for aerosol therapy: Effects of nebulization on cellular uptake and transfection efficiency. *J Control Release* **100**: 425-436 (2004).

24. E. Kleemann, L. A. Dailey, H. G. Abdelhady, *et al.* Modified polyethylenimines as non-viral gene delivery systems for aerosol gene therapy: Investigations of the complex structure and stability during air-jet and ultrasonic nebulization. *J Control Release* **100**: 437-450 (2004).

25. A. von Harpe, H. Petersen, Y. Li, *et al.* Characterisation of commercially available and synthesized polyethylenimines for gene delivery. *J Control Release* **69**: 309-322 (2000).

26. H. Petersen, P. M. Fechner, D. Fischer, *et al.* Synthesis, characterisation, and biocompatibility of polyethylenimine-graft-poly(ethylene glycol) block copolymer. *Macromolecules* **35**: 6867-6874 (2002).

27. D. Fischer, Y. Li, B. Ahlemeyer, *et al.* In vitro cytotoxicity testing of polycations: influence of polymer structure on cell viability and haemolysis. *Biomaterials* **24**: 1121-1231 (2003).

28. N. Ernst, S. Ulrichskötter, W. A. Schmalix, *et al.* Interaction of liposomal and polycationic transfection complexes with pulmonary surfactant. *J Gene Med* **1**: 331-340 (1999).

29. J. Rosenecker, S. Naundorf, S. W. Gersting, *et al.* Interaction of bronchoalveolar lavage fluid with polyplexes and lipoplexes: analysing the role of proteins and glycoproteins. *J Gene Med* **5**: 49-60 (2003).

30. W. J. Gautam A, Densmore CL. Aerosol gene therapy. *Mol Biotechnol* **23**: 51-60 (2003).

31. C. L. Densmore, F. M. Orson, B. Xu, *et al.* Aerosol delivery of robust polyethylenimine-DNA complexes for gene therapy and genetic immunization. *Mol Ther* **1**: 180-188 (2000).

32. W. L. Kircheis R, Wagner E. Design and gene delivery activity of modified polyethylenimines. *Adv Drug Deliv Rev* **53**: 341-358 (2001).

33. D. Fischer, A. v. Harpe, and T. Kissel. Polyethylenimine: Polymer Structure Influences the Physicochemical and Biological Effects of Plasmid/PEI Complexes. *Biomaterials* 195-211 (2000).

34. S. P. Ogris M, Kursa M, Mechtler K, Kircheis R, Wagner E. The size of DNA/transferrin-PEI complexes is an important factor for gene expression in cultured cells. *Gene Therapy* **5**: 1425-1433 (1998).

35. W. C. Groneberg DA, Wagner U, Chung KF, Fischer A. Fundamentals of pulmonary drug delivery. *Respiratory Medicine* **97**: 382-387 (2003).

36. I. Mellman. Endocytosis and molecular sorting. *Annu Rev Cell Dev Biol* **12**: 575-625 (1996).

37.   O. Boussif, F. Lezualcho, M. A. Zanta, *et al.* A versatile vector for gene and oligonucleotide transfer into cells in culture and in vivo: polyethylenimine. *Proc Natl Acad Sci U S A* **92**: 7297-7301 (1995).

38.   M. Ogris, G. Walker, T. Blessing, *et al.* Tumor-targeted gene therapy: strategies for the preparation of ligand-polyethylene glycol-polyethylenimine/DNA complexes. *J Control Release* **91**: 173-181 (2003).

39.   H. Petersen, M. F. Fechner, A. L. Martin, *et al.* Polyethylenimine-graft-poly(ethylene glycol) copolymers: Influence of copolymer block structure on DNA complexation and biological activities as gene delivery system. *Bioconjug Chem* **13**: 845-854 (2002).

40.   T. Mosmann. Rapid colorimetric assay for cellular growth and survival: application to proliferation and cytotoxicity assays. *J Immunol Methods* **65**: 55-63 (1983).

41.   C. Rudolph, U. Schillinger, C. Plank, *et al.* Nonviral gene delivery to the lung with copolymer-protected and transferrin-modified polyethylenimine. *Biochim Biophys Acta* **1573**: 75-83 (2002).

42.   A. Kichler, M. Chillon, C. Leborgne, *et al.* Intranasal gene delivery with a polyethylenimine-PEG conjugate. *J Control Release* **81**: 379-388 (2002).

43.   M. Ogris, S. Brunner, S. Schuller, *et al.* PEGylated DNA/transferrin-PEI complexes: reduced interaction with blood components, extended circulation in blood and potential for systemic gene delivery. *Gene Ther* **6**: 595-605 (1999).

44.   J. F. Kukowska-Latallo, E. Raczka, A. Quintana, *et al.* Intravascular and endobronchial DNA delivery to murine lung tissue using a novel, nonviral vector. *Hum Gene Ther* **11**: 1385-1395 (2000).

45.   J. Zabner, S. H. Cheng, D. Meeker, *et al.* Comparison of DNA-lipid complexes and DNA alone for gene transfer to cystic fibrosis airway epithelia in vivo. *J Clin Invest* **100**: 1529-1537 (1997).

46.   A. Gautam, C. L. Densmore, B. Xu, *et al.* Enhanced gene expression in mouse lung after PEI-DNA aerosol delivery. *Mol Ther* **2**: 63-70 (2000).

47.   E. Durr, J. Yu, K. M. Krasinska, *et al.* Direct proteomic mapping of the lung microvascular endothelial cell surface in vivo and in cell culture. *Nat Biotechnol* **22**: 985-992 (2004).

48.   M. Koeping-Hoeggard, K. M. Varum, M. Issa, *et al.* Improved chitosan-mediated gene delivery based on easily dissociated chitosan polyplexes of highly defined chitosan oligomers. *Gene Ther* **11**: 1441-1452 (2004).

Chapter 4

Enhanced pulmonary gene expression using low-molecular-weight polyethylenimine polyplexes is facilitated by low in vivo toxicity and improved distribution in both conducting and respiratory airways

ABSTRACT

The non-viral vector polyethylenimine (PEI) has been intensively characterized as DNA carrier for pulmonary gene therapy. In a previous study we compared the commonly used branched PEI (BPEI) with a low molecular weight PEI (LMWPEI) and (polyethylene glycol)-graft PEI (PEGPEI) for gene delivery to the mouse lung (Chapter 3). Here we studied these vectors in terms of DNA protection and safety of the polyplexes following intrapulmonary administration into mice. As LMWPEI/DNA displayed superior transgene expression and biocompatibility in the mouse lung, we investigated the distribution of fluorescence labeled polyplexes and the nebulization employing an electric micropump nebulizer. The DNase digestion study confirmed earlier findings in that the LMWPEI polyplexes display the lowest stability, followed by BPEI and PEGPEI. All parameters investigated to assess polyplex toxicity (cell counts, percentage of neutrophils and macrophages, protein and cytokine concentrations) showed a rang order of inflammation response: naked DNA ~ LMWPEI/DNA < BPEI/DNA < PEGPEI/DNA. LMWPEI polyplexes were distributed in the cells of both the bronchi and alveoli, whereas BPEI polyplexes were mainly deposited in the conducting airways. With a Green Fluorescing Protein (GFP) encoding plasmid, the transgene expression was located, thus confirming the findings of the distribution studies. The transfection efficiency of nebulized LMWPEI polyplexes was found to decrease by a factor of 50 compared to the intratracheal instillation. Distribution studies showed an even but low level of polyplex deposition throughout the mouse lung, indicating, that further investigations are necessary to improve the efficiency of the nebulizer system. In conclusion, the excellent level of gene expression seen with LMWPEI/DNA administered via instillation can be explained by low levels of inflammation and enhanced distribution in the mouse lung. Thus LMWPEI holds great promise for safe and efficient gene delivery in the therapy of pulmonary diseases.

INTRODUCTION

The lung holds promise for gene therapy since it is easily accessible through the airways, offers a large surface area for transfection and avoids risks of systemic side effects. Polyethylenimine (PEI) and various PEI modifications have been successfully studied gene transfer to lung tissue via direct intratracheal instillation [1-3], aerosolization [4, 5] and intravenous injection [6, 7]. Serious lung inflammation, evidenced by neutrophil infiltration and reduced arterial oxygen saturation, was observed when plasmid DNA (pDNA) with the commonly used 25 kDa branched PEI (BPEI) was administered intratracheally in the mouse lung [3]. By contrast, only mild lung inflammation was reported for pDNA and BPEI polyplexes administered via aerosol inhalation [8].

Recently, we synthesized and characterized a branched low molecular weight PEI (LMWPEI) which displayed superior transgene expression in the mouse lung and low toxicity in vitro [9, 10]. Polyethylenglycol-grafted derivatives of PEI (PEGPEI) seem to be beneficial for gene therapy of the lung due to reduced interactions with proteins or cells and hence lower cytotoxicity [2, 11]. Previously, we reported superior transfection efficiency in lung epithelial cells using a PEGPEI, however, a tremendous transfection rate decrease when administered to the mouse lung [10]. Lung inflammation and cytokine release after pulmonary delivery of cationic lipid-DNA complexes was shown to decrease the level of transgene expression [12, 13]. In an attempt to clarify whether lung inflammation could explain the reduced transfection efficiency of the PEGPEI in the mouse lung, we report here the total cell numbers, the percentage of neutrophils and alveolar macrophages, and the protein, TNF-alpha and IL-2 concentrations in the bronchial alveolar lavage fluid (BALF) of polyplex treated mice.

Intra- and extracellular enzymes affect the transfection efficiency of gene delivery systems [14, 15]. In particularly, non-viral vectors protecting DNA against DNase degradation were shown to improve the transfection efficiency [16]. Polyplex stability in the extracellular lung environment was extensively studied previously [10]. In the present report, the effects of the intracellular enzyme DNase I on polyplexes stability of LMWPEI, BPEI and PEGPEI were characterised in DNase digestion studies employing atomic force microscopy (AFM). AFM is a comparatively new technique for studying events involving DNA, such as condensation or degradation, and has recently been used to visualize the morphology of gene delivery systems [17, 18].

Fluorescent markers and pDNA encoding the GFP were used to study both the distribution and the transgene expression of poly- and lipoplexes in the mouse lung [19-22].

Distribution and gene expression of BPEI polyplexes were shown mainly in the bronchial region, whereas linear PEI (22 kDa) polyplexes transferred the pDNA mainly to alveolar cells [19]. Furthermore, improved transfection efficiency of linear PEI polyplexes, was attributed to the larger surface area available in the alveolar cells. Since high transfection efficiency was also obtained for LMWPEI [10], we employed doubled-labeled polyplexes and GFP to study polyplexes distribution in the mouse lung.

To accomplish both non-toxic gene delivery systems in addition to improved lung distribution, we developed an inhalation system for the delivery of PEI/DNA polyplexes into the mouse airways. An electric micropump nebulizer, namely Aeroneb Pro®, was thought to be advantageous for drug aerosolization, due to small aerosol droplet sizes, high output and virtually no residual volume. The aerosol leaves the nebulizer through a vibrating mesh, creating a fine mist. This process significantly reduces effects upon the drug molecule due to the low frequency, constant temperature and the absence of baffles [23, 24]. Furthermore, a previous study (Chapter 6) showed reduced effects upon the stability of liposomal formulations. Therefore, we employed the nebulizer Aeroneb Pro® for the application of polyplexes into the airways of mice. To our knowledge, this is the first study employing an electric micropump nebulizer for the application of pulmonary gene delivery systems.

The aim of this study was to increase the understanding of efficacious and safe pulmonary gene delivery, the distribution in the mouse lung and the DNA protection offered by BPEI/DNA, LMWPEI/DNA and PEGPEI/DNA polyplexes.

MATERIALS AND METHODS

Polymers

The 25 kDa branched polyethylenimine (BPEI) was a gift from BASF (Ludwigshafen, Germany). The 5 kDa low molecular weight PEI (LMWPEI) was synthesised and characterized as described previously [25-27]. The (polyethylene glycol)-graft PEIs (PEGPEI), were synthesized as previously described [28]. Briefly, PEGPEIs were obtained by activating PEG-monomethyl ether with a hexamethylene diisocyanate. The coupling of PEG to the amino groups of BPEI was carried out in anhydrous chloroform at 60 °C, which led to a the PEI copolymers: $(PEG5k)_2PEI$ containing 2 PEG 5 kDa molecules per molecule of BPEI and $(PEG550)_{35}PEI$ containing 35 550 Da molecules per molecule of BPEI. For the distribution studies BPEI and LMWPEI respectively were labeled using Oregon Green® 488 carboxyl acid (Molecular probes, Leiden, the Netherlands) and labelling procedure was

carried out as described in the manufacturers protocol. All other reagents were of analytical grade.

Plasmids

The plasmid pGL3 carrying the luciferase coding region under the promoter control of cytomegalovirus (CMV) was kindly provided by J. Hänze (Department of Molecular Biology, University of Giessen, Germany). The plasmid peGFP-N1 carrying the green fluorescence coding region under the promoter control of CMV was kindly provided by C. Rudolph (Department of Paediatrics, University of Munich, Germany). Both plasmids were propagated in E. coli and purified by PlasmidFactory (Bielefeld, Germany). Labeled DNA (pGL3-Alexa Fluor®) was prepared as described in the manufacturers protocol for ARES® DNA labeling kit (Molecular probes, Leiden, the Netherlands). Briefly, the amine-modified dUTP was incorporated in the pGL3 plasmid strand by a Nick translation, followed by the addition of the amine-reactive dye Alexa Fluor®. Unreacted enzymes and dye were removed from the labeled plasmid using the QIAquick PCR purification kit (Qiagen, Hilden, Germany).

Polymplex formation

Polyplexes consisting of pDNA and a PEI modification (BPEI, LMWPEI or PEGPEI) were prepared in sterile isotonic glucose solution at pH 7.4 as described recently [29]. Briefly, the polymer solution was added rapidly to the DNA and mixed by vigorous pipetting followed by 10-20 minutes incubation at room temperature prior to use. When various nitrogen (PEI) to phosphate (DNA) ratios (N/P) were investigated, the concentration of the PEI was adjusted to the quantity of DNA in order to maintain N/P ratios of 6, 8, 10 and 20. When the transfection efficiency of different PEI mixtures was studied, the concentrations, relating to the quantity of nitrogen, were for 1:1 mixtures: 50 % BPEI or LMWPEI + 50 % (PEG5k)2PEI; for 1:2 mixtures 33.3 % BPEI or LMWPEI + 66.6 % (PEG5k)2PEI.

Atomic Force Microscopy

Images of DNA and the PEI/DNA polyplexes were obtained using a Nanoscope IIIa Multimode Atomic Force Microscope (Veeco, Santa Barbara, CA, USA), operating in tapping mode in a liquid environment. All imaging was carried out at a scan speed of approximately 3 Hz with a 512 x 512 pixel resolution. Silicon nitride oxide-sharpened cantilevers were selected, operating at resonance frequencies of approximately 10 kHz. The experiments were repeated twice to ensure reproducibility. The samples for the DNase digestion studies

contained polyplexes (N/P 8) or DNA (1.5 µg/ml) and 0.75 units/ml DNase I (Boehringer, Mannheim, Germany) in digestion buffer. The reaction was carried out over a period of 120 minutes at 37 °C. At severeal times (0, 30, 60, 90, 120 min) samples of 40 µl were taken, placed onto a 1 cm^2 disk of freshly cleaved mica and imaged immediately. Due to the fast degradation of naked DNA, its digestion was tracked at room temperature by in situ AFM imaging [18]. PBS buffer (1mM) containing 2 mM MgCl$_2$ and 1 mM NiCl$_2$ was added to the plasmid solution to facilitate immobilization of the plasmid at the mica surface. The digestion buffer for these experiments contained 0.1 M sodium acetate, 5 mM magnesium sulphate and was titrated to pH 8.0 [30].

Animals

C57BL/6 mice were purchased from Charles River Laboratories (Sulzfeld, Germany) aged 4-6 weeks, weighing 22-28 g. Prior to treatment the animals were acclimatized for five days. For polyplex application, the animals were lightly anesthetized with 0.06-0.08 µl mixture (1:1:3) of ketamine hydrochloride 100 mg/ml (Ketavet®, Pharmacia, Erlangen, Germany), xylacine hydrochloride 2 % (Rompun®, Bayer, Leverkusen, Germany) and isotonic sodium chloride. For intratracheally instillation or lung lavage the mice were positioned in a vertical position and intubated using a flexible needle (0.9 x 25 mm). The use of animals in this study was approved by the local ethics committee for animal experimentation and the experiments were carried out according to the guidelines of the German law of protection of animal life.

Polyplex toxicity in the mouse lung

Toxic effects of the polyplexes and pDNA, both containing 260 µg/ml DNA, in the mouse airways were studied similar to reports in the literature [8, 31]. Controls were performed using isotonic glucose solution at pH 7.4. Polyplexes of BPEI and LMWPEI at the N/P ratios 6, 8, 10 and polyplexes of (PEG5k)$_2$PEI at the N/P ratios 8, 10 and 20 were prepared and applied to the mouse lung via intratracheally instillation as described above. Twenty-four hours post-administration mice were sacrificed and bronchial alveolar lavages were performed with ice cold phosphate buffered saline (PBS) pH 7.4 containing 5 mM EDTA according to the following protocol: Lungs were lavaged successively with 300 µl, 300 µl, 400 µl, and 8 x 500 µl PBS to achieve a total volume of 5.0 ml. The first three lavages were pooled separately and centrifuged at 300g. The supernatant was collected and the cell pellet resuspended with cell medium. The remaining 4 ml were also centrifuged at 300g, the

supernatant discarded, the cell pellet resuspended in cell medium, and added to the cells from the first three lavages. Total cells in the bronchial alveolar lavage fluid (BALF) were counted in a Neubauer hemacytometer. Polymorph-nuclear leucocytes (PMN) recruitment and alveolar macrophages were assessed by preparing centrifuge smears and staining them with Diff® (Dade, Munich, Germany). The number of neutrophils and macrophages were expressed as the percent of the total number of cells. A quantification of total proteins in the BALF supernatant (~1 ml) was performed based on the Bradford method using a standard BCA Assay Kit from Bio-Rad Laboratories (Munich, Germany) according to the manufacturer's protocol. Protein concentrations were calculated from a standard curve made from bovine serum albumin (BSA) in concentrations ranging from 0.2 to 2.0 mg/ml. The cytokine quantification was performed using mouse-specific immunoassay kits for tumour necrosis factor alpha (TNF-a) and interleukin 2 (IL-2) respectively (R&D systems Inc., Minneapolis, USA) according to the manufacturers protocol. The values of the toxicity studies were calculated as mean ± SD of three experiments.

In vivo transfection

In vivo transfection studies were carried out as described previously [10]. Briefly, 48 hours after polyplex application the mice were sacrificed. Prior to removal and weighing, the lung was washed with isotonic sodium chloride by catheterizing the arteria pulmonalis. Homogenization was carried out in reporter lysis buffer, followed by freezing at -20°C. Luciferase assay was performed and the transfection efficiencies ± SD were calculated as the mean value of 5 experiments and presented as pg luciferase per mg lung tissue.

Nebulization

The nebulization system (Figure 1) consisted of the electronic micro-pump Aeroneb Pro®, operated at a frequency of 0.13 MHz (Aerogen, Stierlin, CA, USA), a lung ventilator for mice (MiniVent, HSE-Harvard, March-Hugstetten, Germany) and numerous pipes. The nebulizer was connected to the lung ventilator to both facilitate aerosol transport within the inspiration cycle into the mouse lung, and to ensure expiration air was removed from the nebulization system. The nebulizer was filled with 1 ml LMWPEI polyplex solution (N/P 8) containing 160 µg DNA, and the aerosolization to residual volume was performed in approximately 30-40 minutes with an inspiration volume of 250 µl per breath and a frequency of 100 min^{-1}.

Aerosol droplets that were deposited in the recycling compartment were collected and re-introduced into the nebulizer reservoir. This compartment was designed by cutting a 20 ml syringe down to 1 cm length and inserted in the Aeroneb Pro® body. The syringe tip was connected to a plastic pipe, which was closed with a clamp. On opening the clamp, the deposited aerosol was collected into an Eppendorf tube. All nebulizations were repeated four times.
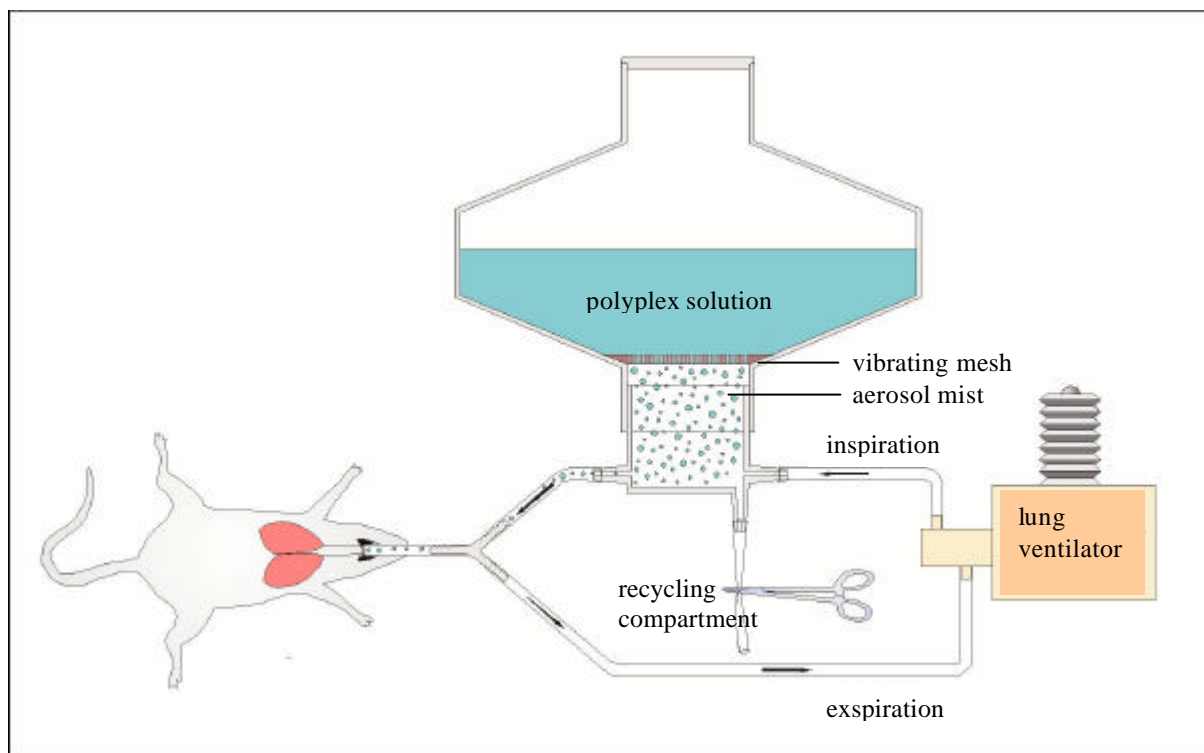
Figure 1: Schematic of the inhalation system for aerosol treatment of mice (not to scale).

Distributions of the polyplexes in the mouse lung

To evaluate polyplex distribution in the mouse lung, polyplexes at N/P 8 were formed between pDNA-Alexa Fluor® and BPEI-Oregon Green® or LMWPEI-Oregon Green®. Four hours post-administration the mice were sacrificed and perfused with PBS and 4% paraformaldehyde (PFA) in PBS via the arteria pulmonalis. The lung was then removed, and fixated in 4% PFA for approximately 1 hour. Lung immersion in PBS at 4°C was performed overnight prior to embedding in Tissue-Tek® (Sakura Finetek, Zoeterwoude, the Netherlands) and flash-freezing in liquid nitrogen [32]. Cryosections (50 µm) were cut, embedded in FluorSave® (Merck Biosciences, Darmstadt, Germany) and examined under a confocal laser scanning microscope (Axiovert™, Zeiss CLSM 501, Jena, Germany) equipped with a Zeiss Neofluor 63x/1.2 water immersion objective. Simultaneous scans for Alexa Fluor® and

Oregon Green® were performed with excitation wavelengths of 543 nm (bypass filter: 560-615 nm) and 488 nm (bypass filter: 505-550 nm plus transmission light) respectively. A gallery of optical slices (0.4 µm) was collected and xz, yz composites were processed using Zeiss LSM 510™ software.

To localize gene expression in the mouse lung, LMWPEI and BPEI polyplexes (N/P 8) were prepared using peGFP-N1 instead of pGL3. Forty-eight hours post-administration mice were sacrificed and their lungs were treated using the same procedure described above. The localization of the GFP was also examined under the confocal laser scanning microscope using an excitation wavelength of 488 nm (by pass filter: 505-550 nm) and transmission light to achieved cell membrane visualization. A gallery of optical slices (0.4 µm) was collected and xz, yz composites were processed using Zeiss LSM 510™ software

The distribution studies of both the double labeled polyplexes and the GFP were repeated twice to ensure reproducibility. Controls were performed with unlabeled pGL3 and polymer.

Statistical analysis

Statistical calculations were carried out using the software package GraphPad InStat v3.06 (GraphPad Software, Inc. San Diego, CA, USA). To identify statistically significant differences one-way ANOVA with Bonferroni's post test analysis was performed. Differences were considered significant if $P = 0.05$ (*) and marked accordingly in the figures.

RESULTS AND DISCUSSION

DNase digestion

The ability of a gene carrier to protect DNA against enzymatic degradation by DNase I, which is located in the cytoplasm, can be demonstrated by DNase digestion studies [11, 33]. In the present work we utilized, for the first time, AFM to track the effect of DNase I upon the structure of PEI polyplexes. These investigations are based upon the method of Abdelhady et al. [18].

Figure 2 depicts a control study of naked DNA that has been exposed to DNase I. This shows that DNA fragmentation begins at around 15 minutes (Figure 2B) after the DNase addition, with complete fragmentation having occurred within 30 minutes (Figure 2C). Figure 3 shows images of LMWPEI, BPEI and (PEG5k)$_2$PEI polyplexes at certain times of the DNase digestion. The images observed at 0 minutes demonstrate the morphology of the polyplexes prior to DNase application. All three polymers fully condensed the pDNA,

forming spherical particles. After the application of DNase I full DNA protection was observed for all three polyplexes within 30 minutes. The strongest influence of DNase upon the polyplex morphology was observed for LMWPEI/DNA, indicating the lowest level of DNA protection. During the first 30 minutes, LMWPEI polyplexes tended to form aggregates. As the experiment progressed, the polyplex size steadily decreased and after 120 minutes of DNase digestion, only fragments remained. This fragmentation indicates that the enzyme is able to access the plasmid at the polyplex surface sufficiently to allow the accumulation at the DNA helix, and thus complete strand breakage. Interestingly, the degradation appeared to decrease the size of the particles slowly until complete fragmentation. This observation supports the assumption of DNA being spherically distributed throughout the polyplex.

In contrast to LMWPEI, BPEI and (PEG5k)$_2$PEI seemed to be able to protect the DNA for longer periods as the particle morphologies remaining unchanged after 90 minutes. The images recorded at 120 minutes after DNase application show a gradual degradation of the polyplexes. These findings suggest that BPEI and (PEG5k)$_2$PEI are able to bind the plasmid DNA more strongly, thus forming more stable polyplexes. These higher stabilities are in agreement with the observation of our previous stability studies in lung lining fluid and surfactant [10]. Taken together, protection of the DNA against lung intra- and extra-cellular enzymes can be ranked as follow: (PEG5k)$_2$PEI > BPEI > LMWPEI.

Consequently, the results of all stability studies performed suggest that DNA release from the gene vector is an important step for effective gene expression and too strong binding between DNA and PEI can reduce the transfection rate. However, polyplex stability is just one of many prerequisite for an effective gene delivery [14].
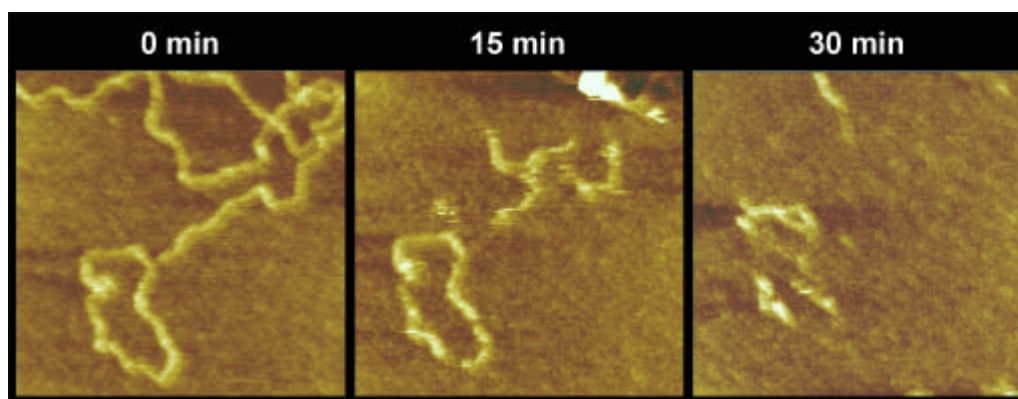
Figure 2: DNase digestion of the naked DNA. The plasmid degradation was tracked by in situ AFM imaging [18]. The x and y scales are 100 nm and z scale 5 nm.
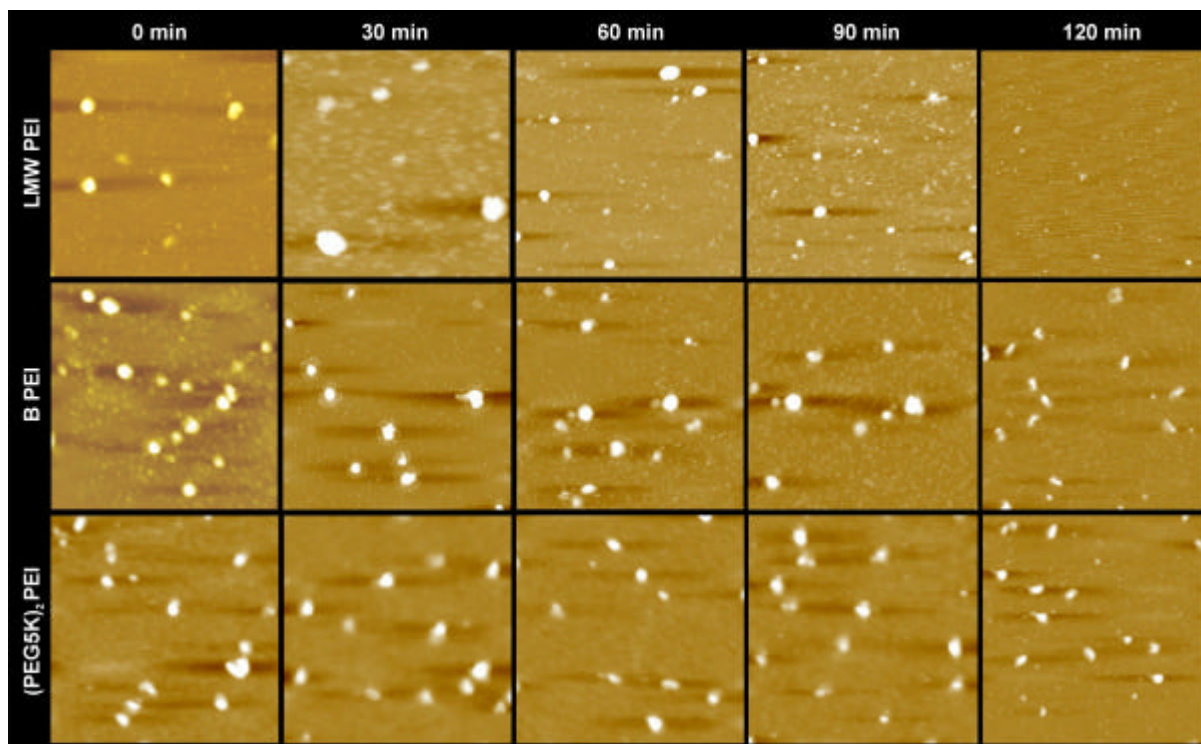
Figure 3: DNase digestion: Polyplexes were exposed to the DNase I over a period of 120 minutes at 37 °C. AFM images were taken at the time zero and then at every 30 minutes. The x and y scales are 1 µm and z scale 30-50 nm.

Polyplex toxicity in the mouse lung

Recently, the cytotoxicity of the polymers BPEI, LMWPEI and (PEG5k)$_2$PEI and their complexes with pDNA were determined by measuring the metabolic activity and membrane damage of treated lung epithelial cells in vitro [10]. The cytotoxic effects were shown to increase in the order: LMWPEI < (PEG5k)$_2$PEI < BPEI, and furthermore the toxicity was found to increase at higher polymer concentrations. To investigate the compatibility of these vectors for pulmonary gene delivery, the effects of the polyplexes in the mouse airways were characterised (Figure 4 & 5). Previous reports have demonstrated a correlation between toxicity in the mouse lung and decreased transfection efficiency [12, 13]. Here, we have investigated whether lung inflammation occurred after polyplex application, an effect that, if observed, would provide some explanations to the discrepancies noted in our previous studies [10].

The total protein concentration in the lining fluid of the lung can be consulted to characterize general alterations of the natural composition of the fluid, because proteins detected include enzymes, cytokines as well as immunoglobulins or other extracellular

proteins. As such, a significant protein increase does not necessarily indicate an inflammation process - the results have to be considered together with the values obtained for cell counts and cytokine response. Increased levels of protein (Figure 4A) were observed in the BALF for all investigated polyplexes when compared with DNA or glucose control. The Increase was, however, not significant in case of LMWPEI and BPEI polyplexes at the N/P ratio of 6. Considering the N/P ratios and thus the polymer concentration, increasing quantities of protein were observed. Comparing the three PEIs investigated, the most significant alteration of the lining fluid was observed for $(PEG5k)_2PEI/DNA$ at all N/P ratios employed.

The total number of cells and polymorph-nuclear leucocytes (PMNs) present in the BALF are two particularly reliable indicators of lung inflammation [12]. Both measurements mirrored the trends observed for protein concentration. Figures 4B demonstrate that an increasing N/P ratio led to an influx of cells. Comparing this with Figure 4C it becomes clear that the increase in cell numbers was primarily due to an increase in the number of PMN. Both the total cell counts and the PMN recruitment increased in the order LMW < BPEI < $(PEG5k)_2PEI$. By contrast to PMN, the percentage of alveolar macrophages (Figure 4D) decreased with increasing cell counts. These observations suggest a shift in the relative cellular constitution of the mouse lung from a primarily macrophage-dominated environment to one that was dominated by neutrophils. Large numbers of neutrophils in the lung serve as a source of activated oxygen species and proteolytic enzymes such as neutrophil elastase [12]. Therefore, the significant PMN increases observed for DNA (33 ± 11 %), LMWPEI/DNA (36 ± 10 % to 39 ± 3 %), BPEI/DNA (36 ± 10 % to 66 ± 15 %) and $(PEG5k)_2PEI/DNA$ (70 ± 6 % to 90 ± 6 %) compared to glucose control (0 ± 1 % PMN) suggest that acute inflammatory damage had occurred in the mouse lung. Furthermore, the inflammation was increasingly severe as higher N/P ratios were applied, probably as a consequence of the polymer excess in the polyplex formulation. The decrease of alveolar macrophages with increasing cell counts can be explained by their function as phagocytic cells of the distal lung [34]. Thus, macrophages may have taken up quantities of the polyplexes and DNA followed by autolysis or apoptosis. The degree to which macrophages and neutrophils contributed to the pulmonary inflammation remains unknown. More investigations are necessary in order to further clarify this situation, such as time scale of cytokine infiltration, inhibition of neutrophil influx into the lung or cytokine and superoxid anion release from macrophages [12].

The cytokines TNF-α and IL-2 are mediators in acute pulmonary inflammation and their appearance in the BALF of mice were found to be highest 24 hours post-application of gene vectors [8, 12]. Neutrophil influx appeared to coincide with the appearance of TNF-α and IL-

2, indicating that these mediators play a predominant role in the infiltration of PMN [12]. Our aim here was to investigate whether the PEI modifications also led to TNF-α and IL-2 response, thus causing or aggravating lung inflammation. Similar to the investigated inflammation parameters above, the cytokine concentrations (Figure 5) increased with increasing N/P ratios. These observations support the assumption of stronger cytotoxic effects upon the mouse airways due to the polymer excess at high N/P ratios. TNF-α response (Figure 5A) was observed in all investigated samples, even in the glucose control. It is likely that the stress for the mouse during the instillation caused already a TNF-α response in the mouse lung. However, the level of the control was still too low to initiate acute lung inflammation, noted previously as 0 % neutrophil infiltration. Whilst the comparison of TNF-α levels between the different gene vectors did not indicate significant differences, the IL-2 concentration increased in the rang order: LMWPEI < BPEI < (PEG5k)$_2$PEI. The results of the IL-2 concentrations mirrored almost exactly the results of the PMN recruitment, thus PMN infiltration is probably mediated predominantly by IL-2. Additionally, the observed protein values (Figure 4A) suggest that its increase was caused mainly by IL-2.

These toxicity data document severe lung inflammation when gene vectors were administered at high concentration. The pDNA itself, in particular under the promoter of CMV, has previously been reported to cause toxic side effects in numerous cells [35]. Considering the different PEI vectors, it was clear that the toxic effects upon the mouse airways increased in the order: LMWPEI < BPEI < (PEG5k)$_2$PEI. When comparing these results with our previous in vitro studies [10], the low toxicity of LMWPEI could be confirmed. Moreover, the results provide evidence for the hypothesis of decreased transfection efficiency in vivo due to severe lung inflammation.

Taken together, the LMWPEI caused the highest transfection efficiency in the mouse lung because of its low toxicity, which is at N/P 6 & 8 as low as that of naked DNA. BPEI and in particular (PEG5k)$_2$PEI caused more severe pulmonary inflammation, in turn reducing transfection efficiency in the mouse lung.

A)

B)

C)

D)

Figure 4: Polyplex toxicity in the mouse lung: Bronchial alveolar lavage fluids were obtained to determine A) the protein concentration, B) the total cell counts, C) the percentage of polymorph-nuclear leucocytes (PMN) and D) the percentage of alveolar macrophages. Data are presented as mean ± SD of 3 experiments in each group.

A)

B)

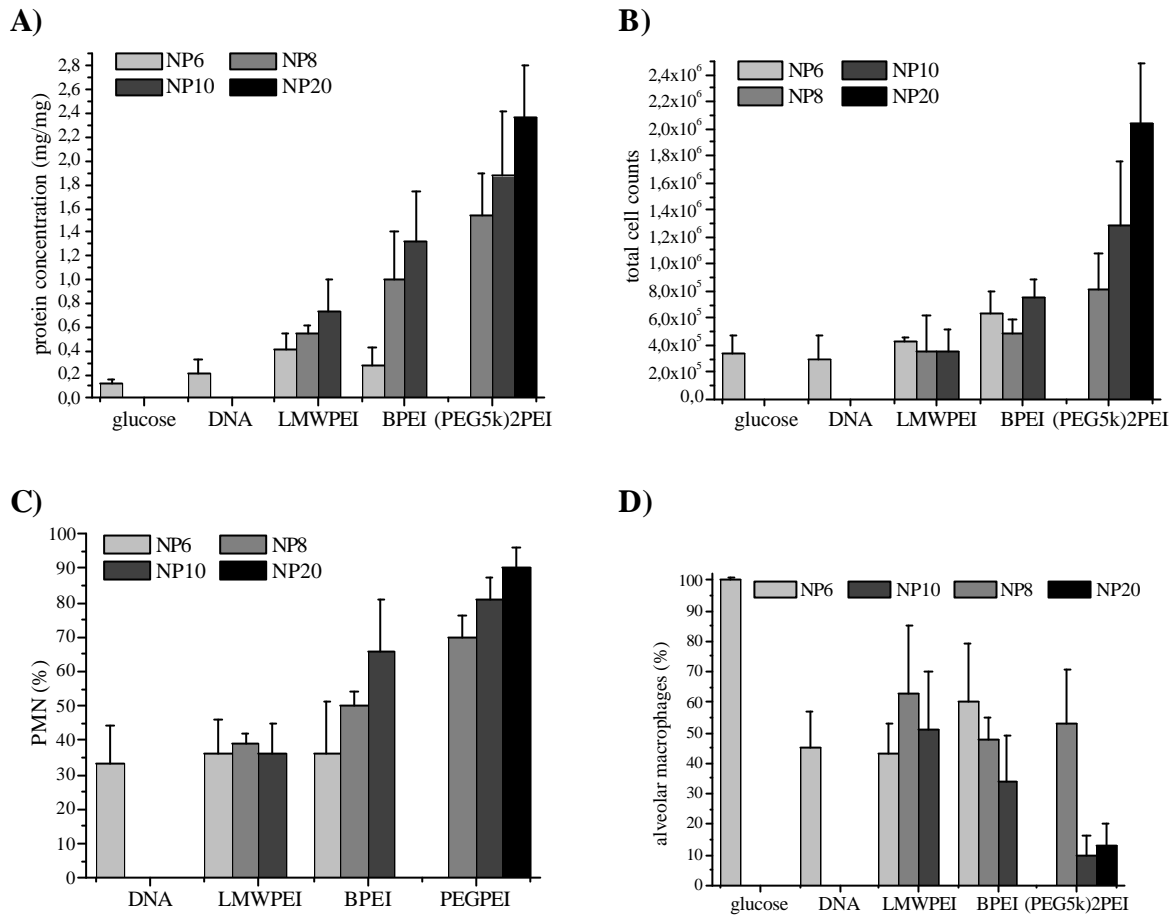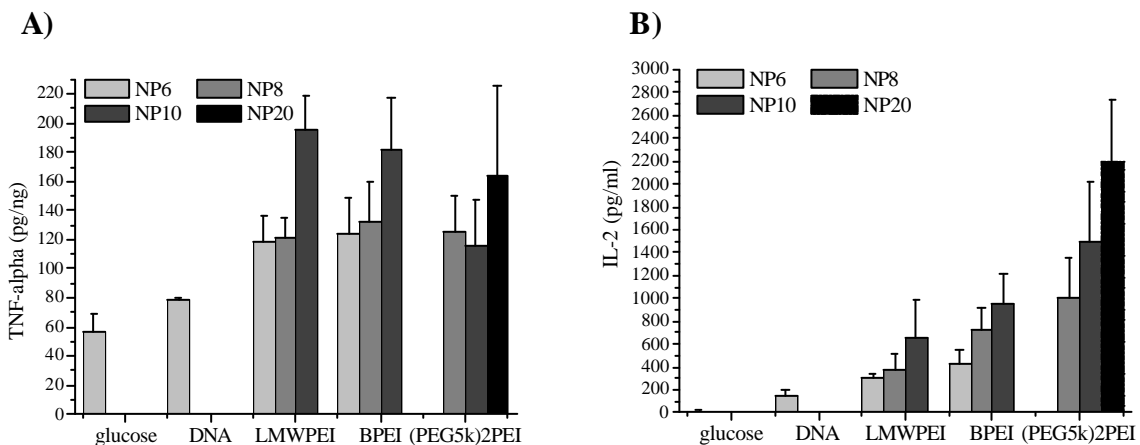*Figure 5: Polyplex toxicity in the mouse lung: Bronchial alveolar lavage fluids were obtained to determine the cytokines concentration A) TNF-a and B) IL-2. Data are presented as mean ± SD of 3 experiments in each group.*

Transfection efficiency in the mouse lung

Since poor transfection efficiency in the mouse lung for the gene vector $(PEG5k)_2PEI$ was obtained [10], our aim was to improve the efficiency and safety of PEGPEI vectors. In order to evaluate if the amount of PEG in the gene vector played a predominant role, we employed several modifications as pulmonary gene delivery systems, such as $(PEG550)_{35}PEI$, mixtures of BPEI with $(PEG5k)_2PEI$ and mixtures of LMWPEI with $(PEG5k)_2PEI$. The gene expressions of these vectors were studied in the mouse lung after intrapulmonary instillation, and compared to the previously studied BPEI, LMWPEI and $(PEG5k)_2PEI$ (Figure 6). All polyplexes were prepared at an N/P ratio of 8 since we had obtained the highest gene expression at this ratio [10].

When administering pDNA in the absence of a carrier, a transfection efficiency of approximately 0.4 pg luciferase per mg lung tissue was observed. Marginally more luciferase was produced when polyplexes of DNA with $(PEG5k)_2PEI$ or $(PEG5k)_2PEI$ /BPEI mixtures were administered. Hence, these polyplexes did not cause any significant improvement in transgene expression. By contrast, significantly increased transfection efficiency was obtained when polyplexes of BPEI, LMWPEI, $(PEG550)_{35}PEI$ or mixtures of LMWPEI with $(PEG5k)_2PEI$ were administered. The improvement observed for $(PEG550)_{35}PEI$ suggested that higher grafting of BPEI with low molecular weight PEGs improved the transfection efficiency, whereas lower grafting with high molecular weight PEGs decreased the transfection rate in the mouse lung. These findings are in agreement with previous studies [2]. They observed decreasing transfection efficiency in the mouse lung with increasing molecular weight of the PEG copolymer. Furthermore, gene expression at the level of naked plasmid DNA was reported for gene delivery systems formed with PEGPEI copolymers [2, 11]. Therefore, our findings are encouraging and $(PEG550)_{35}PEI$ should be considered for further in vivo studies, such as a coupling to targeting structures. Our results here support the advantages of high grafting with low molecular weight PEGs for an improved gene transfer to the lung. Furthermore it is worth noting that $(PEG550)_{35}PEI$ is the PEGPEI with the lowest toxicity synthesised in our laboratory [28, 36].

Mixing LMWPEI with $(PEG5k)_2PEI$ led to an improved gene expression when compared with $(PEG5k)_2PEI$ alone. However, the high level of LMWPEI transfection was not achieved. Since $(PEG5k)_2PEI$ has been demonstrated to be more toxic than LMWPEI, this polymer composition is not worth studying further. Although Ogris et al. favour mixtures of PEGPEI

copolymers with unmodified PEI [37, 38], our results do not confirm the advantages of PEI/PEGPEI mixtures when applied to the mouse airways.
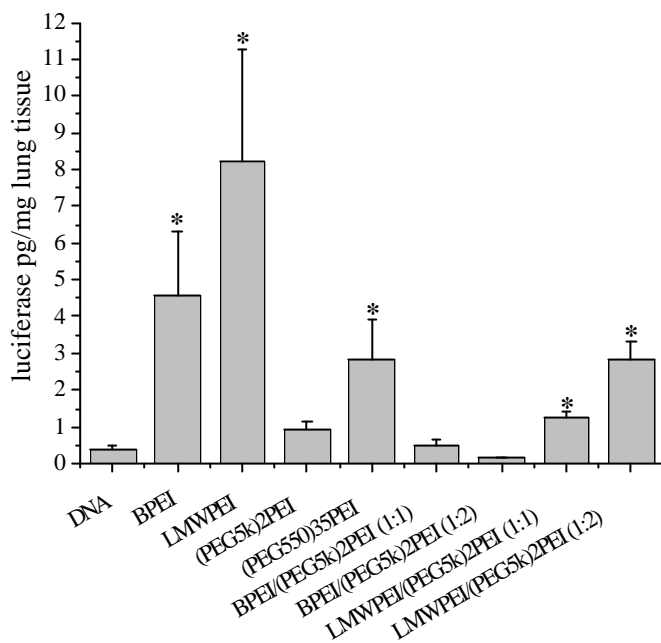
Figure 6: In vivo transfection efficiencies of several polyplexes at an N/P ratio of 8. From left to right: pDNA alone, BPEI, LMWPEI, $(PEG5k)_2PEI$, $(PEG550)_{35}PEI$, BPEI mixed with $(PEG5k)_2PEI$ (1:1) and (1:2), LMWPEI mixed with $(PEG5k)_2PEI$ (1:1) and (1:2). The in vivo results are presented as mean ± SD of 3-6 experiments, with statistically significant differences from DNA being highlighted with an asterisk (P = 0.05).

Inhalation device development

One of the most important aspects in the development of an inhalation system is the choice of the nebulizer itself. As discussed in the introduction to this thesis, the Aeroneb Pro® holds several key advantages when compared to other common air-jet and ultrasonic nebulizers. Furthermore, the high cost of plasmid DNA make the low residual volume displayed by the Aeroneb Pro® an important feature.

Unlike humans, mice are compulsive nose-breathing animals and aerosol delivery to the deeper compartment of the lung is severely impaired by the physiologic function of their nose. Only particles of diameters < 1 µm can be efficiently inhaled and deposited in the deeper airways of the mouse lung [39]. Since the mass median aerodynamic diameter

(MMAD) of the aerosol generated by Aeroneb Pro® was found to be 4 µm (Chapter 6), the majority of the aerosol would be deposited in the mouse nose. In order to bypass the nasal passage and acquire the applied dose, we have developed a new inhalation system for mice (Figure 1, page 99). In this system was the animal anaesthetized and intratracheally intubated. Constant deep breathing was achieved by employing a lung ventilator.

As the Aeroneb Pro® was designed for humans, it has a high output of approximately 400 µl per minute. While humans have a tidal volume of approximately 500 ml, the lung capacity of a mouse is approximately 0.3 ml. Thus the output of the Aeroneb Pro® is much too high for the mouse, and the majority of the generated aerosol deposit underneath the nebulizer mesh. Therefore, we have developed an "aerosol recycling compartment" which allows the deposited aerosol droplets to be collected by opening a clamp. These can subsequently be added back into the nebulizer reservoir.

The lung ventilator was employed to ensure uniform deep breathing, thus increasing deposition in the respiratory airways of the anaesthetized mouse. Results obtained from the first runs of the new nebulizer system indicated that short pipes are important to reduce the total volume between the mouse and ventilator, because a large volume caused blending of the inspiration and expiration air stream.

The new system was validated by aerosolizing 99m technetium labeled isotonic sodium chloride solution over a period of 30 minutes into the anaesthetized intubated mouse. By measuring the total counts/sec of the whole mouse lung, the aerosol deposition in the airways could be determined. In these experiments (n=4) we observed an aerosol deposition of approximately 10 µl/min (data not shown). Therefore, we calculated for the polyplex aerosolization that a nebulization period of 25 minutes would lead to the deposition of 40 µg DNA in the lung, as this was the quantity used during the intratracheal instillation. In the following transfection experiments mice were treated with polyplex solutions employing the new nebulizer system over a 30-40 minute time period, to ensure enough polyplex deposition.

Transfection efficiency of nebulized polyplexes

As we have previously seen and discussed (chapter 3), LMWPEI/DNA triggers enormous luciferase accumulation in the lung of mice (8.2 pg/mg) [10] and further reveals high biocompatibility. As such, we have attempted to further develop this gene vector for inhalation therapy. The luciferase expression of LMWPEI polyplexes in the mouse lung was measured post-administration via the new inhalation system (Figure 7). Unfortunately, the transfection efficiency in the mouse lung after the nebulization decreased dramatically and

ranged below the level of DNA. This finding is particularly disappointing since we had observed no alterations post-nebulization of LMWPEI/DNA in vitro. In terms of particle size (dynamic light scattering), structure (atomic force microscopy) and in vitro transfection (A549), the aerosolized LMWPEI polyplexes were found to be unspoiled (data not shown). Due to the polyplex stability observed in these in vitro experiments, we had hypothesized that the transfection efficiency in the mouse lung after aerosol administration should be comparable to that of instillation. Interestingly, many reports of the group of Densmore et al. documented successful gene delivery by inhalation [5, 31]. In these studies varies types of genes, complexed with BPEI, were expressed at high levels in the lungs of mice upon aerosol administration. Their experimental setup was based on a whole animal body nebulization chamber, which even resulted in the inhibition of tumour growth when plasmid DNA coding for protein p53 or cytokine IL-12 was applied with BPEI (N/P 10) [40-42]. On the other hand a recent report of Rudolph et al. highlighted the difficulties involved in aerosol delivery to the mouse lung [4]. In their experimental setup also a whole body nebulization chamber was utilized and large quantities of DNA (250 µg per mouse) were necessary to achieve even slight levels of gene expression. By interposing a spacer with silica gel between the nebulizer and the mouse chamber, the transfection efficiency could be increased significantly. The silica gel triggered the evaporation of water from the aerosol passing the spacer and thus reduced the droplet size. Consequently, utilizing such a silica-covered spacer in the setup of our nebulizer model may increase the transfection efficiency of LMWPEI polyplexes.

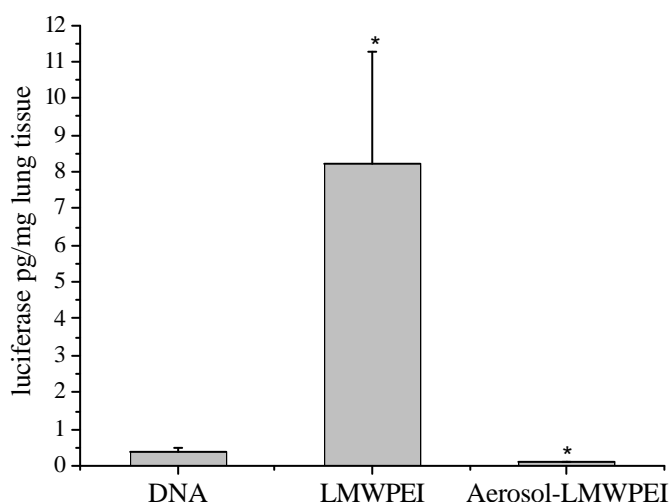*Figure 7: In vivo transfection efficiencies of pDNA and LMWPEI polyplexes post-instillation versus post-inhalation. The in vivo results are presented as mean ± SD of 5 experiments, with statistically significant differences from DNA being highlighted with an asterisk (P = 0.05).*

It is likely that gene delivery via inhalation leads to an even distribution in the bronchial and alveolar regions, whilst instillation leads to the "flooding" of only a proportion of lung bifurcations. It was demonstrated previously, that the gene expression of numerous PEI/DNA complexes in primary alveolar epithelial cells ranged four magnitudes below that of primary bronchial epithelial cells [43]. Hence, we assume a pronounced alveolar distribution in the mouse lung could have reduced the transfection efficiency of the nebulized LMWPEI polyplexes. Therefore, we investigated both the distribution of double labeled polyplexes in the mouse lung and the expression of GFP after the application of LMWPEI/peGFP-N1 via both the instillation and the inhalation route.

Distributions of the polyplexes in the mouse lung

Our main objective was to find out whether the distribution of polyplexes within the mouse lung altered the effectivity of transgene expression. The pDNA was labeled with Alexa Fluor® and subsequently complexed with the Oregon Green® labeled BPEI or LMWPEI. These polyplexes were administered to the mouse lung via instillation or inhalation (only LMWPEI/DNA). In order to evaluate the location of the polyplexes in the lung, cryosections were imaged by confocal laser scanning microscopy. Representative images are depicted in Figure 8, and co-localisation of the plasmid DNA (red) with the polymer (green) appeared yellow. Whilst aerosol administration (Figure 8C & E) resulted in a uniform fluorescent polyplex distribution throughout the entire lung, the polyplex instillation resulted in a mixture of non-fluorescing (images not shown) and fluorescing regions, as can be seen in Figures 8A, B, D & E. This observation might be the result of a "pooling" of polyplex solution in certain lung bifurcations, whilst other areas were not reached by the polyplexes during the instillation process. In contrast, the nebulization seems to promote a constant distribution throughout the entire conducting and respiratory airways. This proposed "pooling" effect observed during instillation of the gene vectors was also observed by others, and might cause additional stress to the mouse thus further aggravating lung inflammation [12].

Double labeled BPEI polyplexes (Figure 8A & D) were mainly localized in the bronchial epithelia and endothelia cells. The consideration of the bronchial tree clarifies that the polyplexes first passes the bronchial cells before reaching the respiratory tract. Due the highly positive surface of BPEI/DNA [10], it is likely, that these adhere rapidly to the cilia of the bronchi, and then undergo endocytosis into the bronchial epithelial cells. Our results concur with previous reports concerning the highly efficient gene transfer mechanism of BPEI to the bronchial cells when targeting the mouse lung [19, 20].

Unlike BPEI, LMWPEI polyplexes were equally distributed in bronchi and alveoli (Figure 8B & E). Furthermore, similar to BPEI/DNA, a significant distribution was observed in the endothelial cells. Interestingly, LMWPEI and DNA were often not co-located, which suggest a separation of polymer and DNA. Indeed, the images (Figure 8B & E) suggest that DNA was internalized into the nucleus, while LMPEI remained in the cytoplasm. We assume that LMWPEI polyplexes were released into the cytoplasm via endosomal swelling and rupture [44], followed by the release of DNA from the polyplexes. Hence it seems that the DNA alone passed into the nuclear core through pores, while the polymer remained in the cytoplasm. This finding supports our assumption that the enhanced DNA release from LMWPEI polyplexes is advantageous in pulmonary gene delivery [10]. Localization of DNA alone in the nucleus was also observed for the nebulized LMWPEI polyplexes (Figure 8C & F), albeit to a far lower extent.
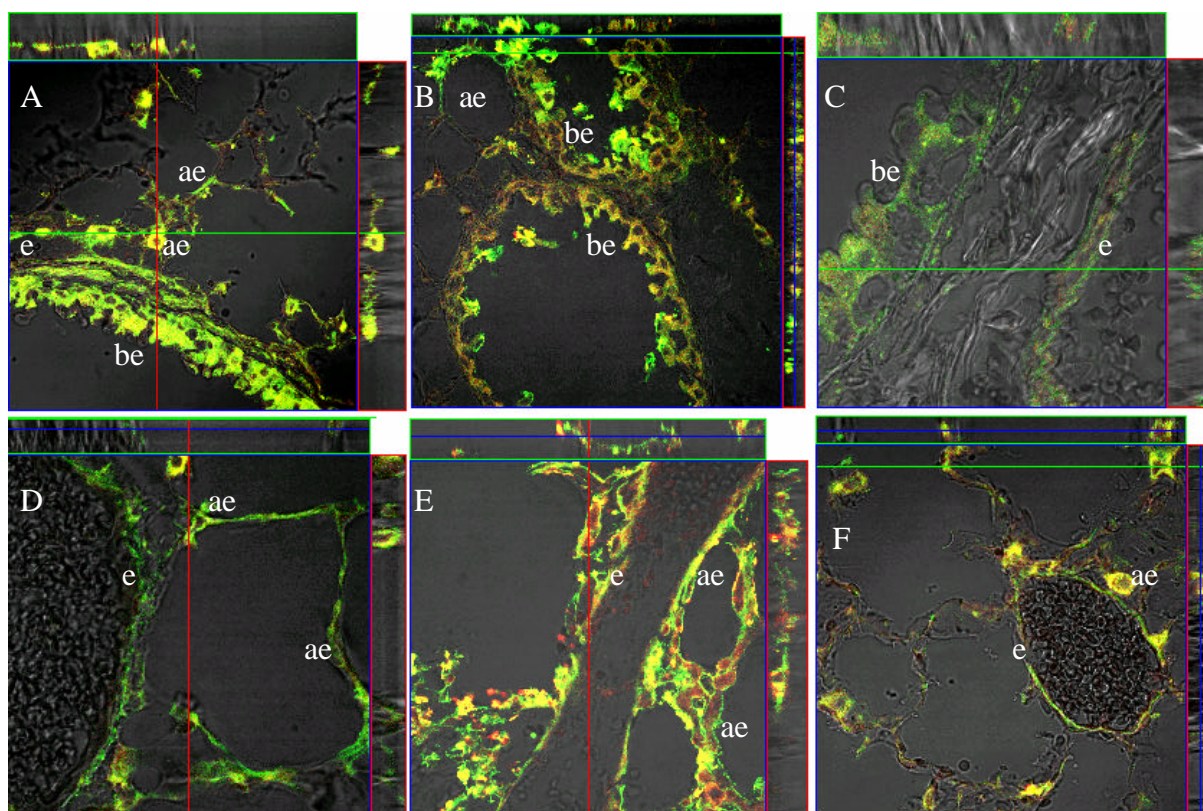
Figure 8: Distribution of double labeled fluorescent polyplexes in the mouse lung 4 hours post-administration via instillation of BPEI/DNA (A&D) or LMWPEI/DNA (B&E) and via nebulization of LMWPEI/DNA (C&F). Alexa Flour®-DNA is shown in red, Oregon Green®-polymer is green and the co-localization of both results in the appearance of yellow. DNA and polymer were found to be localized in bronchial epithelia cells (be), alveolar epithelia (ae) cells and lung endothelia cells (e).

Images recorded after the administration of GFP encoding plasmid complexed with BPEI and LMWPEI respectively, (Figure 9) confirmed the findings seen for the polyplex distribution. The application of BPEI and LMWPEI polyplexes via instillation resulted in the expression of GFP in some lung bifurcations and in others not (data not shown). In the case of BPEI polyplexes (Figure 9A & D), the majority of GFP was produced in the bronchial cells. Interestingly, the few alveolar cells that were found to express GFP were type II cells. Both nebulized (Figure 9B & E) and instilled (Figure 9C & F) LMWPEI polyplexes caused GFP expression in the bronchial and alveolar epithelial cells, as well as in the endothelial cells. The extent of GFP expression was reduced in the case of the nebulized LMWPEI/DNA, but evenly distributed throughout the lung. These data suggest uniform, but low efficient gene delivery by aerosolized polyplexes and confirm the findings of the distribution studies with double-labeled polyplexes.

Interestingly, localization of the polyplexes in both endothelial and epithelial cells was demonstrated for intravenous injection but not for intrapulmonary application. Goula et al. reported that linear PEI (22 kDa) polyplexes, when delivered intravenously, rapidly cross the endothelial barrier and transfect the pulmonary tissue, resulting in transgene expression in alveolar and bronchial epithelial as well as endothelia cells [7, 22]. Our observations suggest that such movements also took place when polyplexes were delivery into the airways. Uyechi et al. observed similar distributions for lipoplexes on administration to mice airways [21]. Consequently, LMWPEI polyplexes are conceivably useful tools for the creation of therapeutic gene delivery systems for different lung diseases [45]. For example, lung metastases could be a targeted because of the different cell population being attacked by cancer cells.
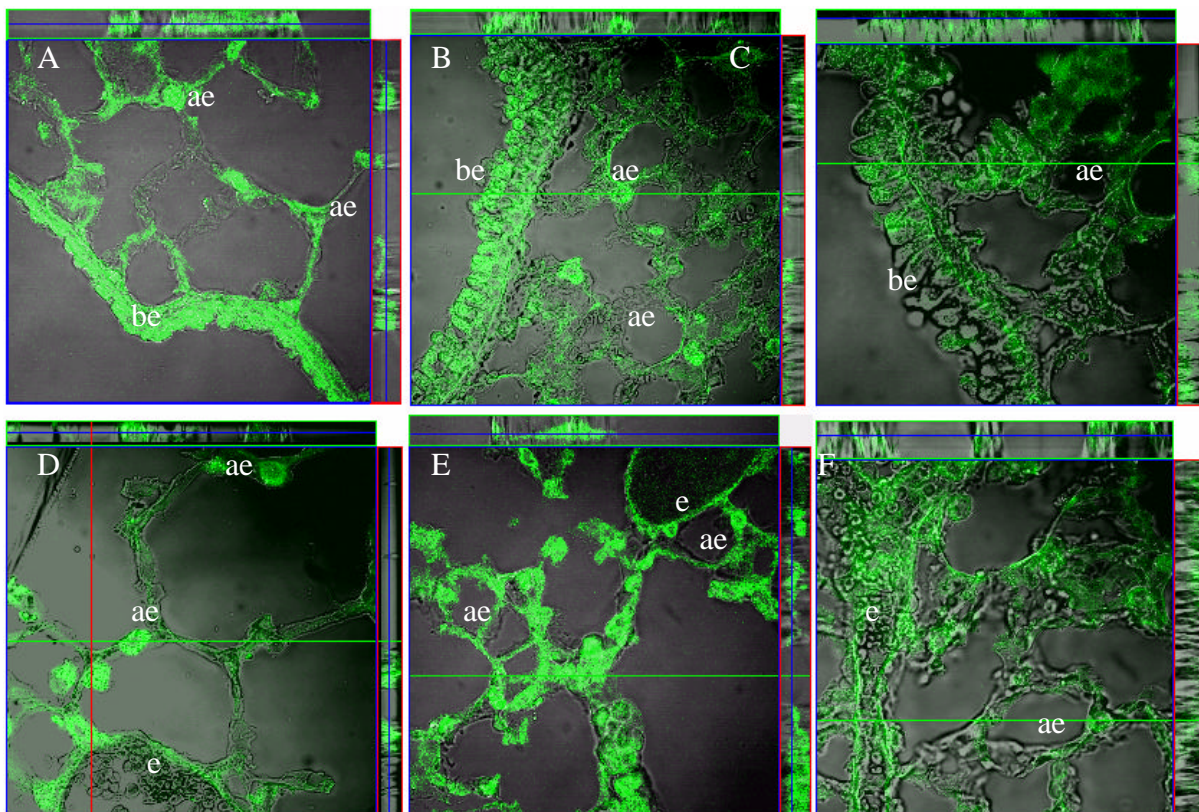
Figure 9: Cryosections of polyplex treated mouse lungs, illustrating the GFP expression determined 48 hours after the intratracheal application of BPEI/DNA (A&D) and LMWPEI/DNA (B&E) as well as LMWPEI/DNA post-application via the new nebulizer system (C&F). GFP was found to be localized in bronchial epithelia cells (be), alveolar epithelia cells (ae) and lung endothelia cells (e).

Taken together, the results presented here in suggest, that the high transfection efficiency of LMWPEI/DNA can be explained by their low toxicity and additionally due to their gene expression in both conducting and respiratory airways. In contrast, the nebulization of LMWPEI/DNA led to very low gene expression throughout the whole lung, due to the lower quantity of polyplexes deposited at the airway cells.

CONCLUSION

In summary, we were able to gain new sights in pulmonary gene delivery. The conflicting results observed for in vivo and in vitro gene expression of LMWPEI and PEGPEI polyplexes were also further elucidated here.

As a consequence of the DNase digestion and previous results, we postulate, that strong binding between DNA and polymer is an advantage in transferring genes safely into the cells. However this advantage does not necessarily increase the transfection efficiency in vivo. If gene vectors trigger toxic side effects and/or poor distribution in the targeted organ, the advantages observed in vitro could be nullified.

Pulmonary inflammation and cytokine response in polyplex treated animals was low but detectable for DNA and LMWPEI/DNA, more pronounced for BPEI/DNA, and most severe for PEGPEI. The transfection efficiency of these gene vectors in vivo has been demonstrated to follow the rank order LMWPEI > BPEI > PEGPEI. Thus we conclude that lung inflammation by high concentrations of cytotoxic PEI-based gene vectors decrease the levels of gene expression in the mouse lung. As the DNA and gene vectors themselves were the underlying source of the toxicity, it is clear that strategies to increase the safety of plasmid DNA and PEIs would reduce any initial pulmonary inflammation. LMWPEI/DNA caused the same degree of lung inflammation as DNA, hence this vector could be a step in the right direction.

With a view to achieving transient and stress free inhalation gene therapy, we have developed an aerosol inhalation system for mice. Unfortunately, this system failed to deliver sufficient doses of polyplexes into the mouse lung. Although a uniform distribution and gene expression throughout the conducting and respiratory airways was achieved, the amount of polyplexes reaching the lung cells was too little. Consequently, further studies are required to improve the nebulization efficiency of the inhalation system. Such studies may possibly include aerosol drying by silica gel, since this simple method has previously been demonstrated to optimize PEI-based gene delivery to the lung [4].

The location of the BPEI polyplexes and the resulting transgene expression were detected primarily in the bronchial cells of the mouse lung. In contrast, LMWPEI polyplexes gave high signals in both the bronchial and alveolar cells. Therefore, LMWPEI may be useful for obtaining therapeutic gene transfer in diseases involving all lung cell types, such as lung metastases or pulmonary hypertension.

In conclusion, the data presented here underline both the high transfection capacity of LMWPEI polyplexes and the relative lack of toxicity associated with their use in the mouse lung. Taken together, these results strengthen arguments favouring the use of this vector to achieve safe and efficient pulmonary gene delivery in vivo.

REFERENCES

1. S. Ferrari, E. Moro, A. Pettenazzo, *et al.* ExGen 500 is an efficient vector for gene delivery to lung epithelial cells in vitro and in vivo. *Gene Ther* **4**: 1100-1106 (1997).
2. C. Rudolph, U. Schillinger, C. Plank, *et al.* Nonviral gene delivery to the lung with copolymer-protected and transferrin-modified polyethylenimine. *Biochim Biophys Acta* **1573**: 75-83 (2002).
3. C. Rudolph, J. Lausier, S. Naundorf, *et al.* In vivo gene delivery to the lung using polyethylenimine and fractured polyamidoamine dendrimers. *J Gene Med* **2**: 269-278 (2000).
4. C. Rudolph, A. Ortiz, U. Schillinger, *et al.* Methodological optimization of polyethylenimine (PEI)-based gene delivery to the lungs of mice via aerosol application. *J Gene Med* **7**: 59-66 (2005).
5. C. L. Densmore, F. M. Orson, B. Xu, *et al.* Aerosol delivery of robust polyethylenimine-DNA complexes for gene therapy and genetic immunization. *Mol Ther* **1**: 180-188 (2000).
6. A. Bragonzi, A. Boletta, A. Biffi, *et al.* Comparison between cationic polymers and lipids in mediating systemic gene delivery to the lung. *Gene Ther* **6**: 1995-2004 (1999).
7. D. Goula, N. Becker, G. F. Lemkine, *et al.* Rapid crossing of the pulmonary endothelial barrier by polyethylenimine/DNA complexes. *Gene Ther* **7**: 499-504 (2000).
8. A. Gautam, C. L. Densmore, and J. C. Waldrep. Pulmonary cytokine responses associated with PEI-DNA aerosol gene therapy. *Gene Ther* **8**: 254-257 (2001).
9. D. Fischer, T. Bieber, Y. Li, *et al.* A novel non-viral vector for DNA delivery based on low molecular weight, branched polyethylenimine: effect of molecular weight on transfection efficiency and cytotoxicity. *Pharm Res* **16**: 1273-1279 (1999).
10. E. Kleemann, N. Jekel, L. A. Dailey, *et al.* Enhanced gene expression in mice using polyplexes of low-molecular weight poly (ethylene imine) for pulmonary gene therapy. *J Gene Med* **submitted**: (2005).
11. A. Kichler, M. Chillon, C. Leborgne, *et al.* Intranasal gene delivery with a polyethylenimine-PEG conjugate. *J Control Release* **81**: 379-388 (2002).
12. R. K. Scheule, J. A. St George, R. G. Bagley, *et al.* Basis of pulmonary toxicity associated with cationic lipid-mediated gene transfer to the mammalian lung. *Hum Gene Ther* **8**: 689-707 (1997).
13. B. D. Freimark, H. P. Blezinger, V. J. Florack, *et al.* Cationic lipids enhance cytokine and cell influx levels in the lung following administration of plasmid: cationic lipid complexes. *J Immunol* **160**: 4580-4586 (1998).
14. D. Lechardeur, A. S. Verkman, and G. L. Lukacs. Intracellular routing of plasmid DNA during non-viral gene transfer. *Adv Drug Deliv Rev* **57**: 755-767 (2005).
15. M. Ruponen, P. Honkakoski, S. Ronkko, *et al.* Extracellular and intracellular barriers in non-viral gene delivery. *J Control Release* **93**: 213-217 (2003).
16. M. Koeping-Hoeggard, K. M. Varum, M. Issa, *et al.* Improved chitosan-mediated gene delivery based on easily dissociated chitosan polyplexes of highly defined chitosan oligomers. *Gene Ther* **11**: 1441-1452 (2004).
17. H. G. Hansma. Surface Biology of DNA by Atomic Force Microskoy. *Annu Rev Phys Chem* **52**: 71-92 (2001).
18. H. G. Abdelhady, S. Allen, M. C. Davies, *et al.* Direct real-time molecular scale visualisation of the degradation of condensed DNA complexes exposed to DNase I. *Nucl Acid Res* **31**: 4001-4005 (2003).

19. A. Bragonzi, G. Dina, A. Villa, *et al.* Biodistribution and transgene expression with nonviral cationic vector/DNA complexes in the lung. *Gene Ther* **7**: 1753-1760 (2000).

20. A. Gautam, C. L. Densmore, E. Golunski, *et al.* Transgene expression in mouse airway epithelium by aerosol gene therapy with PEI-DNA complexes. *Mol Ther* **3**: 551-556 (2001).

21. L. S. Uyechi, L. Gagne, G. Thurston, *et al.* Mechanism of lipoplex gene delivery in mouse lung: binding and internalization of fluorescent lipid and DNA components. *Gene Ther* **8**: 828-836 (2001).

22. D. Goula, C. Benoist, S. Mantero, *et al.* Polyethylenimine-based intravenous delivery of transgenes to mouse lung. *Gene Ther* **5**: 1291-1295 (1998).

23. R. Dhand. Nebulizers that use a vibrating mesh or plate with multiple apertures to generate aerosol. *Respir Care* **47**: 1406-1416 (2002).

24. R. Dhand. New frontiers in aerosol delivery during mechanical ventilation. *Respir Care* **49**: 666-677 (2004).

25. A. von Harpe, H. Petersen, Y. Li, *et al.* Characterisation of commercially available and synthesized polyethylenimines for gene delivery. *J Control Release* **69**: 309-322 (2000).

26. D. Fischer, T. Bieber, Y. Li, *et al.* A novel non-viral vector for DNA delivery based on low molecular weight, branched polyethylenimine: effect of molecular weight on transfection efficiency and cytotoxicity. *Pharm Res* **16**: 1273-9 (1999).

27. K. Kunath, A. von Harpe, D. Fischer, *et al.* Low-molecular-weight polyethylenimine as a non-viral vector for DNA delivery: comparison of physicochemical properties, transfection efficiency and in vivo distribution with high-molecular-weight polyethylenimine. *J Control Release* **89**: 113-125 (2003).

28. H. Petersen, P. M. Fechner, D. Fischer, *et al.* Synthesis, Characterisation, and Biocompatibility of Polyethylenimine-graft-poly(ethylene glycol) Block Copolymer. *Macromolecules* **35**: 6867 - 6874 (2002).

29. E. Kleemann, L. A. Dailey, H. G. Abdelhady, *et al.* Modified polyethylenimines as non-viral gene delivery systems for aerosol gene therapy: Investigations of the complex structure and stability during air-jet and ultrasonic nebulization. *J Control Release* **100**: 437-450 (2004).

30. W. T. Godbey, M. A. Barry, P. Saggau, *et al.* Poly(ethylenimine)-mediated transfection: a new paradigm for gene delivery. *J Biomed Mater Res* **51**: 321-328 (2000).

31. A. Gautam, C. L. Densmore, B. Xu, *et al.* Enhanced gene expression in mouse lung after PEI-DNA aerosol delivery. *Mol Ther* **2**: 63-70 (2000).

32. L. Liu, S. Sanz, A. D. Heggestad, *et al.* Endothelial targeting of the Sleeping Beauty transposon within lung. *Mol Ther* **10**: 97-105 (2004).

33. W. T. Godbey, K. K. Wu, and A. G. Mikos. Tracking the intracellular path of poly(ethylenimine)/DNA complexes for gene delivery. *Proc Natl Acad Sci USA* **96**: 5177-5181 (1999).

34. E. R. Weibel. Morphology of the human lung. *Springer-Verlag, Berlin* (1963)

35. G. McLachlan, B. J. Stevenson, D. J. Davidson, *et al.* Bacterial DNA is implicated in the inflammatory response to delivery of DNA/DOTAP to mouse lungs. *Gene Ther* **7**: 384-392 (2000).

36. H. Petersen, M. F. Fechner, A. L. Martin, *et al.* Polyethylenimine-graft-poly(ethylene glycol) copolymers: influence of copolymer block structure on DNA complexation and biological activities as gene delivery system. *Bioconjug Chem* **13**: 845-854 (2002).

37. M. Ogris, S. Brunner, S. Schuller, *et al.* PEGylated DNA/transferrin-PEI complexes: reduced interaction with blood components, extended circulation in blood and potential for systemic gene delivery. *Gene Ther* **6**: 595-605 (1999).

38. M. Ogris, G. Walker, T. Blessing, *et al.* Tumor-targeted gene therapy: strategies for the preparation of ligand-polyethylene glycol-polyethylenimine/DNA complexes. *J Control Release* **91**: 173-181 (2003).

39. M. G. Menache, F. J. Miller, and O. G. Raabe. Particle inhalability curves for humans and small laboratory animals. *Ann Occup Hyg* **39**: 317-328 (1995).

40. A. Gautam, C. L. Densmore, and J. C. Waldrep. Inhibition of experimental lung metastasis by aerosol delivery of PEI-p53 complexes. *Mol Ther* **2**: 318-323 (2000).

41. A. Gautam, C. L. Densmore, S. Melton, *et al.* Aerosol delivery of PEI-p53 complexes inhibits B16-F10 lung metastases through regulation of angiogenesis. *Cancer Gene Ther* **9**: 28-36 (2002).

42. S. F. Jia, L. L. Worth, C. L. Densmore, *et al.* Aerosol gene therapy with PEI: IL-12 eradicates osteosarcoma lung metastases. *Clin Cancer Res* **9**: 3462-3468 (2003).

43. L. A. Dailey, E. Kleemann, T. Merdan, *et al.* Modified polyethylenimines as non viral gene delivery systems for aerosol therapy: effects of nebulization on cellular uptake and transfection efficiency. *J Control Release* **100**: 425-436 (2004).

44. O. Boussif, F. Lezualcho, M. A. Zanta, *et al.* A versatile vector for gene and oligonucleotide transfer into cells in culture and in vivo: polyethylenimine. *Proc Natl Acad Sci U S A* **92**: 7297-7301 (1995).

45. D. R. Gill, L. A. Davies, I. A. Pringle, *et al.* The development of gene therapy for diseases of the lung. *Cell Mol Life Sci* **61**: 355-368 (2004).

Chapter 5

Nano-Carriers for DNA delivery to the lung

based upon TAT peptide covalently coupled to PEG-PEI

ABSTRACT

Gene therapy aimed at the respiratory epithelium holds therapeutic potential for diseases such as cystic fibrosis and lung cancer. Polyethylenimine (PEI) is commonly utilized for gene delivery to the airways. In this study, we describe a new modification of PEI, in which a protein transduction domain (TAT) was covalently coupled to 25 kDa branched PEI (BPEI) through a heterobifunctional polyethylenglycol (PEG) spacer resulting in a TAT-PEG-PEI conjugate. Improved plasmid DNA complexation and protection was observed for the polyplexes formed between plasmid DNA and TAT-PEG-PEI/DNA. These small polyplexes (~ 90 nm) evidenced significantly improved stability against polyanions, Alveofact®, bronchial alveolar lining fluid and DNase. In order to determine the polyplex toxicity in vitro, MTT assays were performed. In vivo investigations were also performed, with the mice bronchial alveolar lavage being tested for total cell counts, quantity of neutrophils and the total protein and TNF-alpha concentrations. All parameters suggested significantly lower levels of toxicity for TAT-PEG-PEI. Transfection efficiencies of both BPEI and TAT-PEG-PEI polyplexes with DNA were studied under in vitro conditions (A549) and in the mouse lung after intratracheal instillation. While luciferase expression in A549 cells was significantly lower for TAT-PEG-PEI/DNA (0.2 ng/mg protein) than for BPEI/DNA (2 ng/mg), higher transfection efficiencies for TAT-PEG-PEI/DNA were detected in the mouse lung. Confocal laser scanning microscopy studies demonstrated that transgene expression was distributed through bronchial and alveolar tissue. Thus, TAT-PEG-PEI represents a new approach to non-viral gene carriers for lung therapy, comprising protection for plasmid DNA, low toxicity and significantly enhanced transfection efficiency under in vivo conditions.

INTRODUCTION

Intensive efforts have been devoted to pulmonary gene medicine trying to address diseases such as cystic fibrosis and lung cancer [1, 2]. Of crucial importance in this context are vectors or carrier systems for genetic information among which non-viral vectors based on polyethylenimine (PEI), have shown some promise due to their stability under in vivo conditions and transfection efficiency after nebulization [3]. Polyethylenglycol-grafted derivatives of PEI (PEG-PEI) seem to be beneficial for gene therapy of the lung due to reduced interactions with proteins or cells and hence lower cytotoxicity [4, 5]. Polyplexes of DNA and branched 25 kDa PEI (BPEI) transfected preferably bronchial cells, a feature considered to be important in the treatment of cystic fibrosis and lung cancer [6, 7]. Normally different sub-populations of lung cells are involved in pulmonary diseases. Thus, vectors transfecting both bronchial as well as alveolar tissue would be of general interest.

To improve the transfection efficiency of non-viral carriers, new strategies were put forward to enhance cellular uptake of PEI based polyplexes, amongst which peptides enhancing cell adhesion and internalization reached a prominent position [8]. Peptide sequences, also designated as protein transduction domains (PTD) or membrane translocalization signals, were identified as potentially useful labels for intracellular delivery of proteins, oligonucleotides, plasmid DNA (pDNA) and colloidal carrier systems [9]. Peptides derived from the TAT protein sequence of human immune deficiency virus (HIV) have been reported to show unusual translocation abilities by direct crossing biological membranes due to its strong cell surface adherence, independent from receptors and temperature [10]. Recently, however, several reports have challenged this view, suggesting a cell uptake via endocytic pathways for liposomal [11] and for cationic polymer based TAT conjugates [12]. Chloroquin influencing adsorptive endocytosis, [13] as well as fluid-phase macropinocytosis [14, 15], a receptor- and caveolar-/clathrin-independent specialized form of endocytosis, have recently been suggested as part of the translocation mechanism. In this context, cell fixation techniques need to be taken into account to avoid misinterpretation of cell uptake studies due to artefacts [16].

Apart from the uptake mechanism, sequence and the structure of the PTD have been the subjects of intensive investigations. Basis amino acid sequences seems to play an important role in translocation, as demonstrated for arginine [17] or guanidine rich peptides [18, 19]. Higher molecular weight peptide sequences consisting of multimers enhanced only the in vitro transfection of PEI/DNA polyplexes, but failed in increasing the in vivo expression in

the mouse lung [20]. Recently, polymerisation of HIV-TAT peptides resulted in high molecular weight polycations which displayed elevated DNA complexation and transfection efficiency in vitro [13].

Peptides derived from the TAT protein sequence of HIV type 1 have been utilized to deliver nanoparticles into cells. Particularly, TAT conjugates have been employed in cationic gene delivery vehicles, either with [21] or without [20, 22] covalent attachment to the carrier. Consequently, TAT peptide in combination with a PEG-PEI copolymer could be a promising candidate as gene delivery vehicle intended for pulmonary administration.

Here we report the synthesis and characterization of polymer conjugates in which a oligopeptide sequence derived from HIV-1 TAT modified by a C-terminal cysteine residue is covalently coupled to BPEI using a hetero-bifunctional linker based upon PEG. The aim of this study was to combine the favorable characteristics of PEG-grafted BPEI with the HIV-TAT oligopeptide to yield a vector capable of mediating gene transfection after local administration to the airways. Furthermore, an ideal vector in the treatment of pulmonary diseases such as lung cancer would be able to mediate gene transfer to both bronchial and alveolar epithelial cell combined with lower toxicity than BPEI. The PEG linker is intended to reduce unwanted interactions of the polpylex with protein, cell or other components of the airways, thereby providing enhanced polyplex stability and lowered toxicity. Coupling of the oligopeptide to the cationic BPEI should help to overcome restrictions of pure oligopeptide based polyplexes, such as low plasmid complexation ability [23, 24] or the decrease of their potential biological effects due to interaction with the complexed DNA [25]. The PEG linker, additionally, provides a steric shielding of the cationic BPEI core from the oligopeptide sequence and, thereby, facilitates the coupling reaction of the two cationic moieties. In the resulting TAT-PEG-PEI conjugate, the TAT sequence is separated from the BPEI core by the hydrophilic PEG, thus enabling the presentation of the TAT oligopeptide moieties on the surface of TAT-PEG-PEI/DNA polyplexes [26].

MATERIALS AND METHODS

Materials

The synthetic decapeptide sequence GRKKKRRQRC was synthesized by Bachem (Bubendorf, Switzerland), α-vinyl sulfone-?-N-hydroxysuccinimide ester poly(ethylene glycol) (NHS-PEG-VS) was purchased from Nektar Therapeutics (Huntsville, USA). The 25 kDa branched polyethylenimine (BPEI) was a gift from BASF (Ludwigshafen, Germany).

The plasmid pGL3 carrying luciferase coding region under the promoter control of cytomegalovirus (CMV) was kindly provided by J. Hänze (Department of Molecular Biology, University of Giessen, Germany) and was propagated in E. coli and purified by Plasmid Factory (Bielefeld, Germany). Herring testes DNA was obtained from Sigma (Seelze, Germany). The plasmid peGFP-N1 carrying green fluorescence coding region under the promoter control of cytomegalovirus (CMV-N1) was kindly provided by C. Rudolph (Department of Pediatrics, University of Munich, Germany), was propagated in E. coli and purified by Plasmid Factory (Bielefeld, Germany). The natural surfactant Alveofact® was purchased from Boehringer-Ingelheim (Germany). Bronchial alveolar lavage fluid (BALF) was freshly obtained form C57BL/6 mice via intra-tracheal instillation 1 hour prior to use. For removal of the cells, the BALF was centrifuged at 300 g at 4°C, and the pellet was discarded. All other reagents used were of analytical purity.

Activation of BPEI

19.2 mg (565 µmol) of bifunctional PEG (3.4 kDa), containing both an α-vinyl sulfone and an ω-N-hydroxysuccinimide ester group, was weighed into a glass flask 4.293 µl of a BPEI solution (corresponding to 12.15 mg/0.486 µmol BPEI; 282.4 µmol total amines) in 0.1M borate buffer at pH 5.5 were added and stirred. The activation reaction was carried out for 4 hours at room temperature, followed by pH adjustment to 7 with 1N chloride acid and additionally incubated for 2 hours at room temperature.

Coupling of the oligopeptide onto activated PEG-PEI

For coupling, 2.98 mg (2.26 µmol) of the oligopeptide TAT dissolved in 866 µl pure water were added to the activated PEG-PEI yielding a theoretical degree of substitution of approximately 1% based upon amine functions. The mixture was stirred for additional 2 hours at room temperature.

Purification of TAT-PEG-PEI

Removal of unreacted PEG and low molecular weight residues was performed with an ultrafiltration cell (Amicon, Bedford, USA) equipped with a 10 kDa molecular weight cut-off membrane (Millipore, Bedford, USA) and 0.1 M borate buffer at pH 7.5 as eluent.

Amine concentration of the conjugate was determined by a recently described copper assay [27].

Polyplex formation

The polyplexes consisting of plasmid DNA and either BPEI or TAT-PEG-PEI, were prepared in sterile isotonic glucose solution at pH 7.4 as described recently [28]. Briefly, the polymer solution was added rapidly to the DNA and mixed by vigorous pipetting followed by 10-20 minutes incubation at room temperature prior to use. When various polymer nitrogen to DNA phosphate ratios (N/P) were investigated, the concentration of the BPEI or TAT-PEG-PEI solution was adjusted to the amount of DNA (20 µg/ml polyplex solution for the in vitro experiments and 260 µg/ml for in vivo experiments) in order to maintain N/P ratios between 0.5 and 10.

Ethidium bromide exclusion assay

DNA condensation was measured by quenching of ethidium bromide (EtBr) fluorescence as described earlier [29]. Briefly, quadruplicates of 8 µg of herring testes DNA were complexed with increasing amounts of BPEI or TAT-PEG-PEI in 96-well plates in 60 mM Tris buffer at pH 7.4. After 10 min incubation time, 20 µl EtBr solution (0.1 mg/ml) were added. The fluorescence was measured on a Perkin Elmer LS 50 B fluorescence plate reader (Perkin Elmer, Rodgau, Germany) at λ_{ex} = 518 nm and λ_{em} = 605 nm. Results are given as relative fluorescence (rel. F) and the value of 100% is attributed to the fluorescence of DNA with ethidium bromide (rel. F = F sample/F DNA solution).

Physico-chemical properties

To study the physico-chemical properties of the polyplexes, investigations of particle charge, size and aggregation tendency were performed. The surface-charges were determined by measuring the zeta-potential in the standard capillary electrophoresis cell of a Zetasizer 3000 HS (Malvern Instruments, Worchester, U.K.). The measurements were performed in isotonic glucose solution at pH 7.4 at 25 °C with automatic duration. The average values and the corresponding SD were calculated in three independent measurements, five runs each.

For dynamic light scattering, polyplexes were prepared in a total volume of 50 µl with isotonic glucose or sodium chloride solution at pH 7.4. Polyplex size measurements were carried out with a Nanosizer Lo-C from Malvern Instruments (Worchester, U.K.) at 25 °C (HeNe laser, 633 nm). For data analysis, the viscosity (0.8905 mPa s) and refractive index (1.333) of pure water at 25 °C were used. Results are given as mean values of three runs of 120 sec duration each.

Polyplex stability in heparin, bronchial alveolar lavage fluid and surfactant

Increasing amounts of heparin in 10 µl pure water were added to 100 µl polyplex solution, yielding heparin concentrations of 0.1 to 2.0 IU per µg DNA, and incubated for 10 minutes. 25 µl of this mixture was applied to a 1% agarose gel containing EtBr. Gels were run for 60 minutes at 70 V, prior to the scanning with a transilluminometer (Biometra, Göttingen, Germany).

The effect of surfactant (Alveofact®) and bronchial alveolar lavage fluid (BALF) upon the polyplex stability was evaluated using a reverse fluorescence quenching assay [30, 31]. For polyplex preparation, the amount of DNA was increased to 60 µg/ml and condensed with the appropriate amount of BPEI and TAT-PEG-PEI respectively, to achieve an N/P ratio of eight. Hundred µl of the polyplex solution were placed in 96-well plate and 50 µl EtBr (40 µg/ml) were added. Alveofact® was dissolved in isotonic glucose solution pH 7.4 and added to the polyplexes to achieve final concentrations of 0.002, 0.02, 0.2, 1.0, 2.0 µg/µl. When stability in BALF was tested 100 µl of freshly attained BALF instead of Alveofact® was added to the polyplexes. The fluorescence measurement (Fluorescence reader FL600, Micro plate Fluorescence BioTEK, Winooski, USA) was started immediately after BALF or Alveofact® addition and carried out over a period of 90 minutes at 37°C using λ_{ex} = 485 nm and λ_{em} = 590 nm. The fluorescence is reported relative to the value obtained with naked DNA and EtBr (= 100%), as mean ± SD of five measurements.

DNase stability assay

Polyplexes were prepared at N/P 6 in isotonic glucose using 5 µg of DNA in a total volume of 25 µl, as previously described [32]. Aliquots of 5 µl corresponding to 1 µg of DNA were incubated with 0.01, 0.1, 1, 2.5 and 5 international units (I.U.) of DNase I in 1 µl digestion buffer (0.1 M sodium acetate, 5 mM $MgSO_4$ pH 7.4) for 15 minutes at 37 °C. To stop the DNase digestion, 6 µl termination buffer (equal volumes of 0.5 M EDTA, 2 M NaOH and 0.5 M NaCl) were added, followed by 2 µl of a heparin solution containing 1000 I.U. per ml. To separate the polymer form DNA, the resulting mixtures were applied to a 1 % agarose gel and electrophoresed at 70 V for 1 hour. The resulting gel was visualized and photographed with a transilluminometer (Biometra, Göttingen, Germany).

In vitro transfection

Human lung epithelial cell line (A549) was obtained from the German Collection of Microorganisms and Cell Cultures and was maintained according to the supplier's

specifications. To evaluate the gene expression in A549, the transfection experiments were carried out as previously described in detail [28]. Briefly, cells in passages 8-15 were seeded at a density of 25 000 cells per well on 24-well cell culture plates, 24 h prior to the transfection experiments. The polyplexes were prepared as described above and 100 µl solutions were added to each well containing 900 µl fresh medium and incubated for 4 hours. The medium was replaced and the cells were allowed to grow for a further 44 hours. The luciferase expression (luciferase assay reagent, Promega, Mannheim, Germany) and protein concentration (see below) were determined in the cell lysate. All experiments were performed in triplicate and data were expressed in ng luciferase per mg protein (± SD).

In vivo transfection

To study the luciferase expression in the mouse lung 150 µl polyplexes or DNA alone were instilled into the lung of C57BL/6 mice. The mice were purchased from Charles River Laboratories (Sulzfeld, Germany) aged 4-6 weeks, weighing 22-28 g. Prior to the treatment, the animals were hold for five days in the animal lab were they were fed regularly (Muskator GmbH, Düsseldorf, Germany). For intratracheal instillation, the mouse was lightly anesthetized with 0.06-0.08 µl mixture (1:1:3) of ketamine hydrochloride 100 mg/ml (Ketavet®, Pharmacia, Erlangen, Germany), Xylacine hydrochloride 2 % (Rompun®, Bayer, Leverkusen, Germany) and isotonic sodium chloride. Then the mouse was positioned in a vertical position and polyplexes were administered using a flexible needle (0.9 x 25 mm). Forty-eight hours after instillation the animal was sacrificed using an overdose of anesthesia. The mouse lung was washed with isotonic sodium chloride by catheterizing the arteria pulmonalis, and then the lung was removed and weighed. Per one gram of lung tissue 2 µl of ice cold reporter lysis buffer (Promega, Mannheim, Germany) was added, the lung was immediately homogenized and frozen at -20°C. After thawing, the samples were centrifuged for 20 minutes at 4 °C and luciferase assay was performed as described in the in vitro experiments. The transfection efficiencies and the corresponding SD were calculated as the mean value of 5 experiments and presented as pg luciferase per mg lung tissue. The use of animals in this study was approval by the local ethics committee for animal experimentation and the experiments were carried out according to the guidelines of the German law of protection of animal life.

Cytotoxic effects of polymers on lung epithelial cells

To evaluate the toxicity of BPEI and TAT-PEG-PEI, MTT assays were performed as previously reported [31, 33]. A549 cells were seeded in 96-well microtiter plates at a density of 4200 cells per well and allowed to grow for 72 hours prior to the application of the polymer solution (final concentrations: 0.001, 0.01, 0.1, 0.5 and 1.0 mg/ml in cell media). After 4 hours of incubation, the medium was replaced with 200 µl fresh medium and 20 µl (3-(4,5-dimethylthiatol-2-yl)-2,5-diphenyl tetrazolium bromide) (MTT, Sigma, Seelze). After 4 hours, the unreacted dye was removed and 200 µl DMSO was added. The absorption was measured using the ELISA reader Titertek Plus MS 212 (ICN, Eschwege, Germany) at 570 nm, with a background correction at 690 nm. The relative cell viability (%) was related to control wells containing cell culture medium without polymer and was calculated by: absorption test x 100 % / absorption control. Data are presented as a mean of six measurements ($\pm$ SD). The values of the polymers were fitted to a Bolzmann sigmoidal function using Microcal Origin® v 7.0 (OriginLab, Northampton, USA) and IC50 was calculated.

Polyplex toxicity in the mouse lung

Toxic effects of the polyplexes at an N/P ratio of 10 and of the naked DNA in the mouse airways were studied based upon the experiments of Gautam et al. [34, 35]. Controls were performed using isotonic glucose solution at pH 7.4. Animals were treated as described for in vivo transfection. Twenty-four hours post-administration mice were sacrificed and lavages of the bronchial alveolar lining fluid (BALF) were performed with ice cold phosphate buffered saline (PBS) pH 7.4 containing 5 mM EDTA according to the following protocol: Lungs were lavaged successively with 300 µl, 300 µl, 400 µl, and 8 x 500 µl PBS to achieve a total volume of 5.0 ml. The first three lavages were pooled separately and centrifuged at 300g. The supernatant was collected and the cell pellet resuspended with cell medium. The remaining 4 ml were also centrifuged at 300g, the supernatant discarded, the cell pellet resuspended in cell medium, and added to the cells from the first three lavages. Total cells in the BALF were counted in a Neubauer hemacytometer. Polymorph-nuclear leucocytes (PMN) recruitment was assessed by preparing centrifuge smears and staining them with DiffQuick® (Dade, Munich, Germany) according to the manufacturer's protocol. A quantification of total proteins in the BALF supernatant (1 ml) was performed based on the Bradford method using a standard BCA Assay Kit from Bio-Rad Laboratories (Munich, Germany) according to the

manufacturer's protocol. Protein concentrations were calculated from a standard curve made from bovine serum albumin (BSA) in concentrations ranging from 0.2 to 2.0 mg/ml. tumor necrosis factor alpha (TNF-α) quantification was performed using mouse-specific immunoassay kits for TNF-α (R&D systems Inc., Minneapolis, USA) according to the manufacturers protocol. The values of the toxicity studies were calculated as mean $\pm$ SD of three experiments.

Distributions of the polyplexes in the mouse lung

Labeled DNA (pGL3-Alexa Fluor®) was prepared as described in the manufacturer's protocol for ARES® DNA labeling kit (Molecular probes, Leiden, the Netherlands). Briefly, the amine-modified dUTP was incorporated in the pGL3 plasmid strand by a Nick translation, followed by the addition of the amine-reactive dye Alexa Fluor®. Unreacted enzyme and dye, respectively, were removed from the plasmid DNA using the QIAquick PCR purification kit (Qiagen, Hilden, Germany). TAT-PEG-PEI was labeled using Oregon Green® 488 carboxyl acid (Molecular Probes, Leiden, the Netherlands) and labeling procedure was carried out as described in the manufacturer's protocol.

To evaluated polyplex distribution in the mouse lung, polyplexes at N/P ratio of 10 were formed between pGL3-Alexa Fluor® and TAT-PEG-PEI-Oregon Green® and applied to the mouse lung as described above. Four hours post-administration the mouse was sacrificed, and then perfused with PBS and then with 4% paraformaldehyde (PFA) in PBS via the arteria pulmonalis. The lung was removed and fixation in 4% PFA was performed for 1 hour. Lung immersion in PBS at 4°C was performed overnight prior to embedding in Tissue-Tek® (Sakura Finetek, Zoeterwoude, the Netherlands) and flash-freezing in liquid nitrogen. Cryosections (50 µm) of the mouse lung were cut and embedded in FluorSave® (Merck Biosciences, Darmstadt, Germany). The distribution of the double labeled polyplexes was examined under a confocal laser scanning microscope (Axiovert™, Zeiss CLSM 501, Jena, Germany) equipped with a Zeiss Neofluor 63x/1.2 water immersion objective. Simultaneous scans for Alexa Fluor® and Oregon Green® were carried out with an excitation wavelengths of 543 nm (by pass filter: 560-615 nm) and 488 nm (by pass filter: 505-550 nm and transmission light) respectively. A gallery of optical slices (0.4 µm) was collected and xz, yz composites were processed using Zeiss LSM 510™ software.

To localize the expression of green fluorescence protein (GFP) in the mouse lung, TAT-PEG-PEI polyplexes (N/P 10) were prepared using pDNA encoding GFP instead of

luciferase, and administered to the mouse lung as described above. Forty-eight hours post-application the mice were sacrificed and their lungs were treated in the same procedure as described for the distribution studies of double labeled polyplexes. The localization of the GFP was also examined under the confocal laser scanning microscope as described above. Scans for the GFP was carried out with an excitation wavelengths of 488 nm (by pass filter: 505-550 nm) and 1 % transmission light to visualize the cell membranes and nuclei. A gallery of optical slices (0.4 µm) was collected and xz, yz composites were processed using Zeiss LSM 510™ software

The distribution studies of both the double labeled polyplexes and the GFP were repeated twice to ensure reproducibility. Controls were performed with unlabeled pDNA and TAT-PEG-PEI at an N/P ratio of 10.

Statistical analysis

Statistical calculations were carried out using the software package GraphPad InStat v3.06 (GraphPad Software, Inc. San Diego, CA, USA). To identify statistically significant differences one-way ANOVA with Bonferroni's post test analysis was performed. Differences were considered significant if $P = 0.05$ (*) and marked accordingly in the figures.

RESULTS AND DISCUSSION

TAT-PEG-PEI conjugate synthesis

The TAT-PEG-PEI conjugate is composed of a BPEI core, a 3.4 kDa PEG linker and an oligopeptide sequence. The two-step reaction was performed as shown in Scheme 1. Bifunctional NHS-PEG-VS was used to activate BPEI via the primary amine reactive ω-N-hydroxysuccinimide ester moiety at pH 5.5, thus avoiding the conjugation and cross-linking of the α-vinyl sulfone groups to the amine functions of BPEI, which occurs at higher pH [36]. ^{1}H-NMR was used to confirm that the vinyl sulfone protons remained intact (data not shown). Additionally, the competing hydrolysis reaction of the N-hydroxysuccinimide ester is suppressed at acidic pH [37]. Reaction was carried out for 4h at pH 5.5, after adjusting the pH to 7; the solution was stirred for additional 2 hours to allow hydrolysis of eventually unreacted reagent.

The vinyl sulfone group has been reported to selectively react with sulfhydryl groups at neutral pH [38]. Thus, after activation of the BPEI core, the oligo-peptide containing a cysteine moiety at the C terminus was coupled to the α-vinyl sulfone group at pH 7. The

composition of the conjugates was calculated by assuming that NHS-PEG-VS completely coupled to BPEI (containing 581 amine functions) and that the oligopeptide TAT coupled to 80% of the PEG blocks (only 80% of PEG blocks of NHS-PEG-VS were substituted with vinyl sulfone as indicated by the manufacturer). The degree of PEG substitution was calculated to be 2.0% for PEG and 0.8% for TAT of all amines present in BPEI.

Scheme 1. Reaction scheme for the activation of BPEI with PEG vinyl sulfone followed by the addition of the oligopeptide TAT.

TAT = GRKKKRRQRC
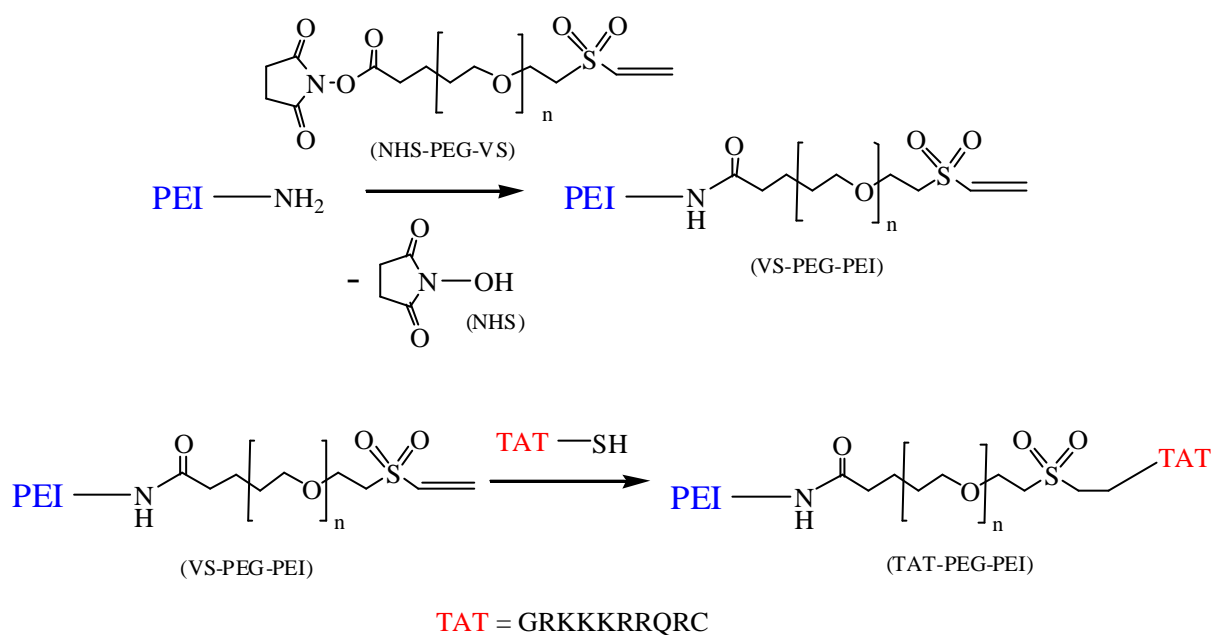
Ethidium bromide exclusion assay

The quenching of ethidium bromide fluorescence was used to compare the DNA condensation ability of TAT-PEG-PEI versus BPEI. While free ethidium bromide shows only weak fluorescence, its fluorescence increases strongly when intercalated into DNA [29]. As shown in Figure 1, TAT-PEG-PEI displays an enhanced DNA condensation ability compared to the poor condensation of BPEI, both significantly improved at the N/P ratio of 3. The stronger DNA condensation ability may be attributed to the enhanced cationic charge density of the conjugate due to the cationic amino acids, which exceeds the loss of positive charges due to the coupling. Additionally, these results indicate that there is no significant steric hindrance from the PEG shielding, as it was observed for similar peptide-PEG-PEI conjugates [39]. Taken together, it can be assumed that the BPEI core as well as the oligopeptide plays a role in DNA compaction.
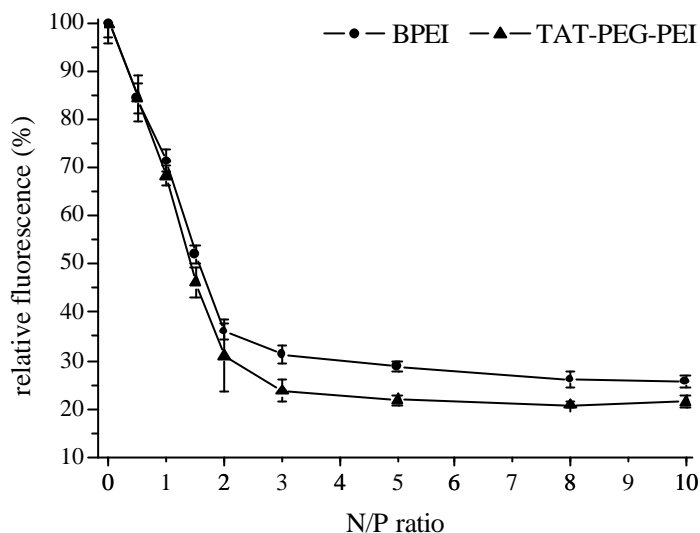
Figure 1. Ethidium bromide fluorescence quenching assay of the BPEI polyplexes and TAT-PEG-PEI polyplexes respectively, formed with salmon testes DNA. Values are given as mean $\pm$ SD (n = 4).

Physico-chemical properties

To determine the surface charge of the polyplexes their corresponding zeta-potentials were measured using laser Doppler anemometry. While naked DNA had a highly negative zeta-potential of -33 mV, the polyplexes displayed positive zeta-potentials due to an excess of the polycation. For TAT-PEG-PEI polyplexes at an N/P ratio of 8 a zeta-potential of 15 ± 3 mV was observed, which increased to 20 ± 3 mV at an N/P ratio of 10. However, it was significantly lower than the zeta-potential observed for BPEI polyplexes, which displayed a potential of 32 mV for both N/P ratio 8 and 10. Investigations of TAT peptide oligomers and monomers, respectively, had shown that the complexation between TAT and pDNA leads to the formation of highly positive charged ($\sim$ 30-40 mV) particles [13, 20]. These observations suggest that the reduced positive zeta-potentials observed for the TAT-PEG-PEI/DNA was neither caused by BPEI or TAT alone. It is likely that both BPEI and TAT are involved in the DNA condensation process and, thus, BPEI as well as TAT and PEG might appear at the particle surface. Therefore, we assume that the PEG spacer in the TAT-PEG-PEI molecule contributed to surface shielding as it was described before for PEG-PEI copolymers [40, 41].

The size of the resulting polyplexes between TAT-PEG-PEI and pDNA is shown in Figure 2. Depending on the preparation medium and its ionic strength, the polyplex sizes

ranged from 135 to 176 nm in isotonic sodium chloride and from 89 to 107 nm in isotonic glucose at pH 7.4. A decrease in the particle size was observed for TAT-PEG-PEI/DNA in glucose solution when the N/P ratio increased from 3 to 10, most likely due to the enhanced condensation of DNA. In sodium chloride solution, the dependency of the size from the N/P ratio was less pronounced. Generally, polyplexes prepared at N/P ratio of 3 displayed the largest size, and the polydispersity index pointed to some aggregation (data not shown).

Generally, polyplexes prepared at low N/P ratios with neutral surface charges tend to aggregate. Additionally, also polyplexes prepared with excess of polymer, thus leading to particles with a net positive surface charges, display enhanced aggregation tendency in high ionic strength media [42]. To overcome both problems, a hydrophilic shielding component, such as PEG, is commonly introduced into the complexes to reduce aggregation [43]. It was recently shown that the PEG chains in PEG-PEI copolymers must have a minimum molecular weight of about 5 kDa to prevent complex aggregation [44]. In contrast, in the case of TAT-PEG-PEI, a 3.4 kDa PEG chain seems to be enough for efficient aggregation prohibition, presumably due to the unique structure of the conjugate having two cationic moieties linked together with a PEG chain. As depicted in Figure 2B, the TAT-PEG-PEI polyplexes prepared in high ionic strength medium (150 mM NaCl) remained stable over a period of 20 minutes, whereas BPEI polyplexes prepared as a control showed a drastic increase in size due to aggregation (as confirmed by polydispersity index, data not shown).
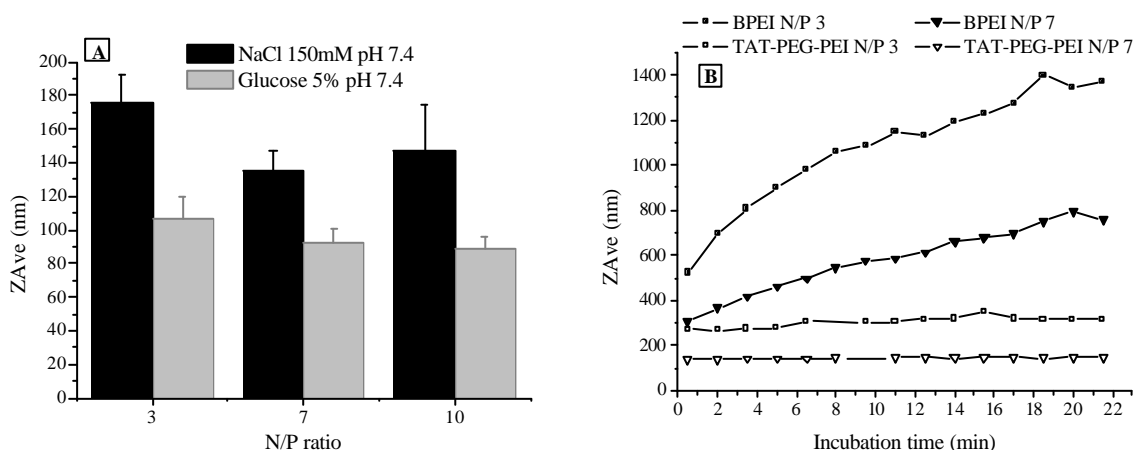

Figure 2. Particle size: A) Hydrodynamic diameters of TAT-PEG-PEI polyplexes in different media. B) Comparison of TAT-PEG-PEI polyplexes to BPEI polyplexes in their tendency to form aggregates in high ionic strength medium (NaCl 150 mM at pH 7.4).

Zeta-potential and size of the polyplexes have been reported to be important factors in facilitating gene transfer in cells [45, 46]. Endocytotic uptake of particles increases with increasing zeta-potential, but also enhances toxic side effects due to unspecific interactions between the gene delivery systems and cell membranes. Therefore, efforts have been undertaken to shield the highly positive particle surface of BPEI polyplexes to produce gene carriers with lower cytotoxicity [40, 47]. The reduced zeta-potential and the absence of aggregate formation of TAT-PEG-PEI polyplexes indicate a certain particle surface shielding, providing an enhanced stability and lower cytotoxicity. Beside the complications of gene delivery to the lung cells, such as mucociliary clearance and phagocytosis by alveolar macrophages, endocytotic uptake of particles is clearly affected by their size and increases with decreasing diameters [48, 49]. The TAT-PEG-PEI polyplexes obtained here were small and stable at numerous N/P ratios in several media. Therefore, prevention of mucociliary and macrophage clearance can be assumed and endocytotic uptake by the epithelial cells is pronounced.

Polyplex stability

To investigate whether the enhanced condensation ability of TAT-PEG-PEI also enhances the protection of the complexed DNA against polyanion exchange and enzymatic degradation in the lung environment, the polyplexes stability were studied in the presence of heparin, Alveofact®, BALF and DNase I (Figure 3-5).

The polyplexes (N/P 8) were challenged with increasing amounts of the model polyanion heparin (Figure 3). BPEI was able to protect pDNA against heparin exchange up to 0.2 IU heparin. An amount of 0.5 IU heparin resulted in a release of the DNA from the BPEI polyplexes. In contrast, TAT-PEG-PEI was able to complex pDNA up to 0.5 IU with only minor release. And 1.0 IU heparin was necessary to completely release the DNA from these polyplexes, indicating enhanced DNA condensation ability.
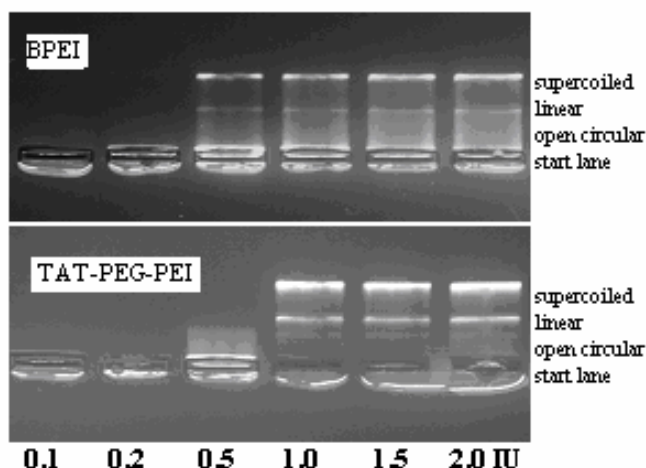
Figure 3. Polyplex stability in heparin: BPEI and TAT-PEG-PEI polyplexes (N/P 8) were challenged with increasing amounts of heparin (0.1, 0.2, 0.5, 1, 1.5, 2, IU heparin per 1 µg pDNA).

Stability studies using Alveofact[®] and BALF were carried out with a reverse EtBr exclusion assay [31] (Figure 4). In the absence of Alveofact[®] and BALF both polycations were able to condense DNA up to a residual fluorescence of approximately 8 % (BPEI) and 5 % (TAT-PEG-PEI), respectively. Addition of Alveofact[®] increased the residual fluorescence for both polyplexes in a concentration dependent manner. The relative fluorescence after the addition of 2 mg/ml Alveofact[®] indicated BPEI/DNA displayed a lower stability (14.1 %) compared to TAT-PEG-PEI polyplexes (11.8 %). The relative fluorescence of the polyplexes in BALF indicating DNA release from the BPEI polyplexes increased in a linear fashion from 8 % (0 min) up to 18.5 % relative fluorescence (90 min), while DNA liberation from the TAT-PEG-PEI polyplexes was negligible (1.4 % increase over the 90 min observation). Consequently, protection of DNA against extracellular pulmonary enzymes was more pronounced for TAT-PEG-PEI compared to BPEI.
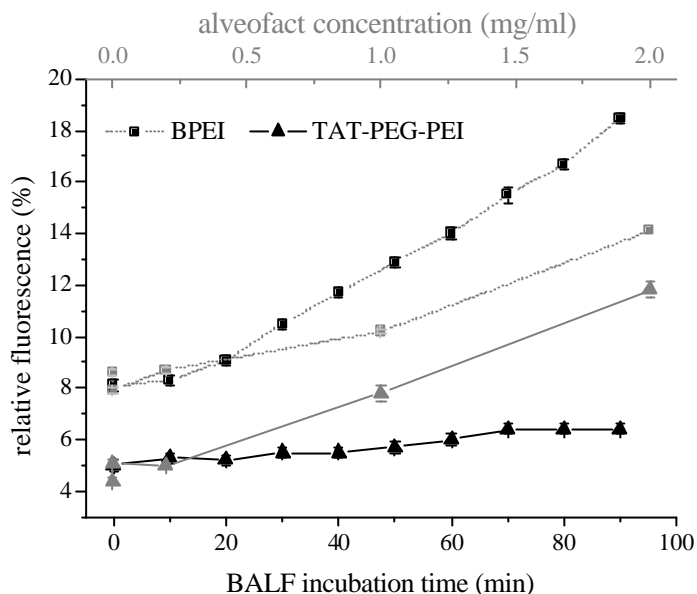
Figure 4. BPEI and TAT-PEG-PEI polyplexes (N/P 8) were treated with increasing amount of Alveofact® (grey scale) and BALF (black scale), respectively. Values ± SD were determined in three independent measurements and depicted as percentage of maximum fluorescence (100 %: naked DNA).

Representative image of the DNase digestion assay is shown in Figure 5. When TAT-PEG-PEI polyplexes were incubated with increasing concentrations of DNase I over a period of 15 minutes, DNA digestion occurred at a concentration of 2.5 IU DNase I per 1 µg DNA. Further increase of DNase I concentration up to 5 IU led to the complete degradation of pDNA. In the case of BPEI polyplexes, DNA degradation was observed at a significantly lower enzyme concentration (0.1 IU DNase I per 1 µg DNA). The denser structure of the TAT-PEG-PEI complexes could explain these differences. The structure of DNA seems to be complexed more loosely in BPEI polyplexes and hence DNase I partially degraded the plasmid over a vast range of enzyme concentrations, whereas TAT-PEG-PEI provides a complete protection up to more than 1 IU DNase per 1 µg pDNA.
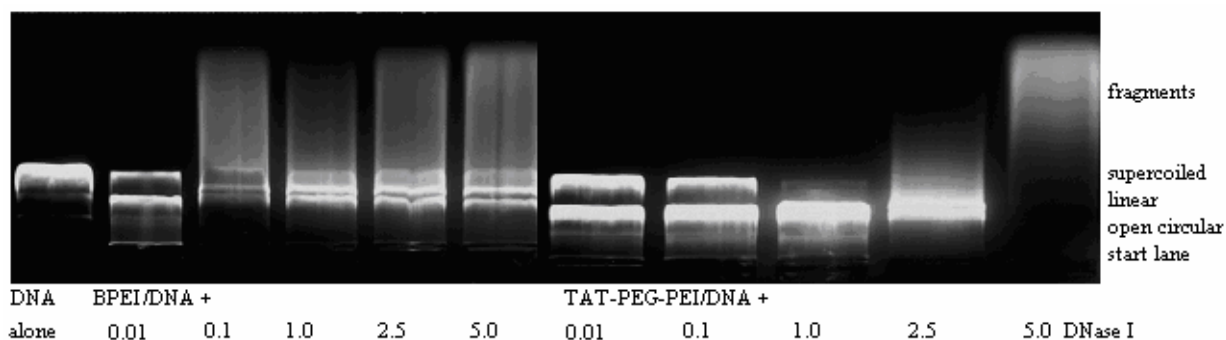
Figure 5. BPEI/DNA (lane 2-6) and TAT-PEG-PEI/DNA (lane 7-11) were challenged with increasing amounts of DNase I (0.01, 0.1, 1, 2.5 and 5 IU per 1 µg pDNA). Lane 1 shows free, undigested pDNA.

Apart from the protection of pDNA against intracellular enzymes (e.g. endo/lysosome), also a sufficiently high stability of gene delivery systems in the extracellular environment of the lung seems to be essential for an efficient pulmonary gene delivery [1, 50]. Compared to BPEI, the stability of TAT-PEG-PEI polyplexes was significantly higher in the presence of high concentration of heparin, Alveofact®, BALF as well as DNase I. This improved stability profile of TAT-PEG-PEI/DNA against anion exchange, is indicative of increased complexation and condensation properties of TAT-PEG-PEI for pDNA. Similarly, Soundara Manickam et al. demonstrated also an improved DNA condensation utilizing a polymerized TAT peptide in comparison to TAT monomers [13]. PEGylation of PEI has been shown to prevent interactions between the polyplexes and serum cells, proteins or enzymes [4, 44]. The modification of BPEI with TAT-PEG may have contributed to the reduced zeta-potential and increased polyplex stability by steric shielding through mobile PEG chains.

Transfection efficiency

Plasmid DNA was complexed with BPEI or TAT-PEG-PEI at N/P ratios of 8 and 10 to examine the transfection efficiency in vitro (Figure 6A) and in the mouse lung (Figure 6B). While the transfection efficiency of TAT-PEG-PEI polyplexes in the lung epithelial cells A549 was shown to range far below that of BPEI, an efficacious gene expression in the mouse lung was achieved after administration by intratracheal instillation. At N/P ratio of 10, a significant improvement in gene expression mediated by the TAT-PEG-PEI carrier (12.6 pg luciferase/mg lung tissue) was observed in comparison to BPEI (2 pg luciferase/mg lung tissue).

Since efficient gene transfer of non-covalently coupled TAT oligepeptides under in vitro was demonstrated in the literature [13, 20], we investigated whether TAT alone also mediates efficient gene expression in the mouse lung under in vivo conditions. Therefore, complexes between unmodified TAT peptide and pDNA were prepared and administered under the same conditions as the other polyplexes. The transfection efficiency in the mouse lung was negligible and ranged at background level (data not shown). This observation suggests that the oligopeptide alone is not sufficient to mediate transfection of lung cells under in vivo conditions. Numerous other studies also failed to support gene transfer by TAT oligopeptides (11- and 17 amino acid respectively) alone. Reduced stability of complexes and lower electrostatic interactions between the TAT and pDNA were put forward as explanation [22, 51]. To overcome these problems, Soundara Manickam et al. used high molecular weight polymerisates of TAT to complex plasmids [13].
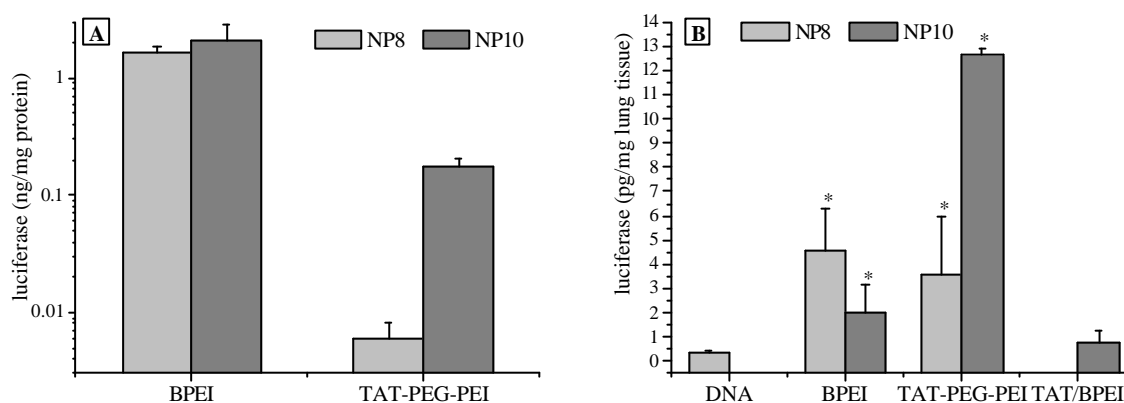
Figure 6. Transfection efficiency of the polyplexes at N/P ratios of 8 & 10: A) luciferase expression in A549, B) luciferase expression in C57BL/6 mice lung. The in vivo results are provided as mean ± SD of five experiments and statistically significant differences from DNA are denoted with an asterisk (P = 0.05).

To probe whether the covalent linkage between TAT and BPEI was essential for improved transfection efficiency of our TAT conjugate in the mouse lung, we prepared polyplexes between DNA and the TAT peptide followed by the addition of BPEI (N/P 10), as described by Rudolph et al. [20]. We did not detect an improved transfection rate for TAT/PEI polyplexes (0.75 pg luciferase/mg lung tissue) compared with BPEI polyplexes (2 pg luciferase/mg lung tissue), indicating that the PEG linker in the TAT-PEG-PEI conjugate is required to facilitate gene transfer in the mouse lung. Torchilin et al. studied the transfection and cell uptake of liposomes that were covalent liked to TAT oligopeptide and

postulated that the peptide increases the cell membrane permeability only if it is attached to the liposome membrane and accessible for cell surface interaction [52]. In contrast to our results, Rudolph et al. demonstrated that covalent linkage is not necessary to improve the efficiency of a TAT vector [20]. They obtained a 390-fold transfection rate increase when a mixture of BPEI with a TAT dimer was studied in vitro; however, no significant improvement could be detected in vivo. The different TAT structures used in our (GRKKKRRQRC) and Rudolph`s study (dimeric C(YGRKKRRQRRRG)$_2$) might explain these conflicting results.

The in vivo transfection results obtained with TAT-PEG-PEI polyplexes demonstrated unexpected differences of a ca. 600% higher transfection efficiency compared to BPEI which is not reflected in the in vitro experiments. Similar discrepancies were reported before for both TAT-DNA and chitosan-DNA polyplexes [51, 53]. The success or failure of a gene delivery system to mediate gene expression in the lung may be related to cell membrane specific differences and extracellular environment. Thus, the multidimensional tissue structure of the lung and extra-cellular protein/enzyme network reveal difficulties in extrapolation of in vitro results to successful gene delivery into the complex lung systems [54]. Furthermore, aggregated particles have been reported to increase transfection efficiency in cell culture, simply by sedimentation onto the cell surface [55]. As shown above, BPEI polyplexes formed aggregates in sodium chloride and these large aggregates easily sediment on the surface of cells in culture resulting in improved cell uptake. In contrast much less of the small and stable TAT-PEG-PEI polyplexes could reach the cell surfaces at the bottom of the well plates, resulting in lower in vitro gene expression compared to BPEI.

A significant increase in transfection efficiency was observed for TAT-PEG-PEI polyplexes in comparison to TAT/PEI polyplexes under in vivo conditions, suggesting that covalent coupling of TAT to BPEI via PEG led to significant advantages in mediating efficient gene delivery into lung epithelial cells of mice. Recent studies also reported that in both, polyplexes and liposomes, consisting of pDNA and TAT, the peptide needs to be freely accessible for cell membrane interactions [13, 22, 56]. It is tempting to speculate that the PEG spacer between TAT and BPEI provides both, shielding of the highly cationic BPEI surface charge and free, un-hindered interaction for TAT with the cell membrane. The high gene expression in vivo and the enhanced DNA condensation as well as the protection by TAT-PEG-PEI led us to the conclusion, that TAT is involved in both, the DNA compactation process and the cell uptake. A schematic representation of the gene delivery system reflecting our results is depicted in scheme 2.

Scheme 2. Schematic pattern of the interactions between TAT-PEG-PEI and pDNA forming polyplexes, and the interaction of those with cell membranes.
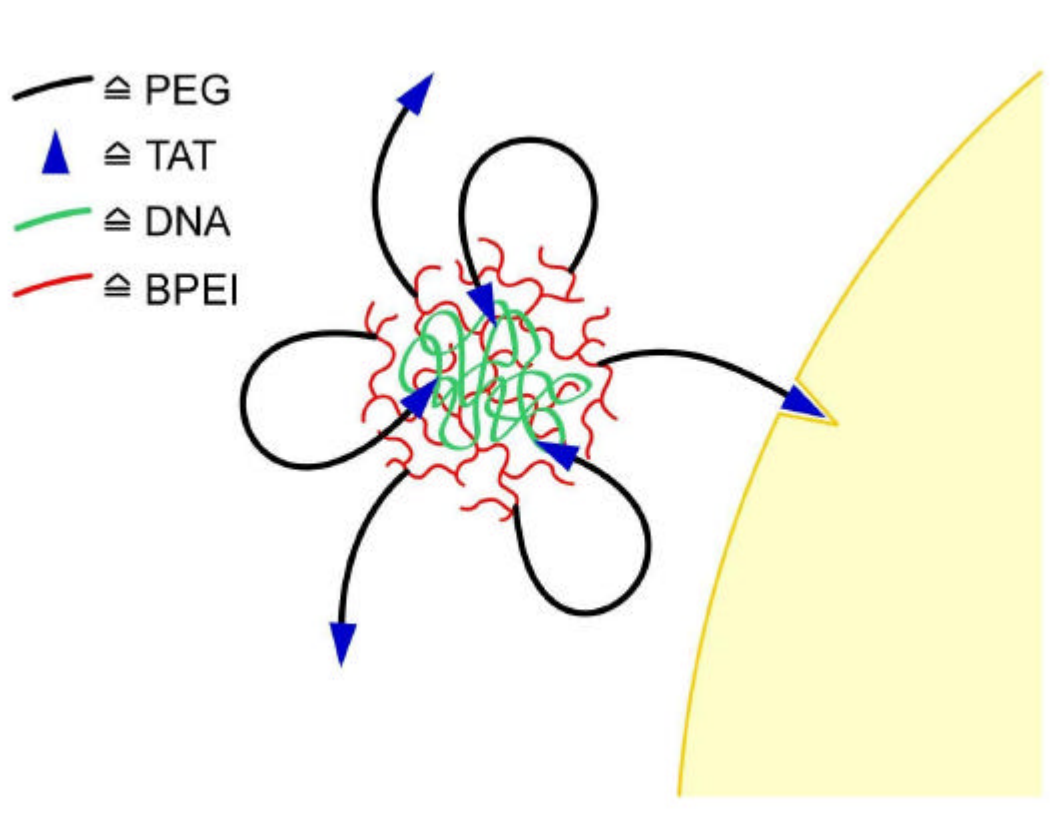
Toxicity

The metabolic and mitochondrial activity of polymer treated cells was determined using the colorimetric MTT-assay [57]. As illustrated in Figure 7A, the toxicity of the polymers was concentration dependent. Whilst BPEI reduced the cell viability dramatically at concentrations of 0.01 mg/ml (~ 23 % viability), TAT-PEG-PEI showed less influence upon the cells (~ 70 % viability). Considering the IC_{50} values (BPEI: 0.071 mg/ml, and TAT-PEG-PEI: 0.2 mg/ml), the reduction in metabolic activity is far lower with TAT-PEG-PEI compared to BPEI. Less toxic effects were also reported for both monomer and polymerized TAT oligopeptides in comparison to BPEI polyplexes [13]. In general, in vitro studies of PTDs have demonstrated their non-toxicity in numerous cell lines [58]. Furthermore, modification of BPEI with PEG led to a reduction of toxic side effects in vitro as well as in vivo [40, 47, 50]. Hence, we assume that the TAT peptide as well as the PEG shielding together are responsible for the reduced in vitro cytotoxicity.

The total numbers of cells in the BALF, as well as polymorph-nuclear leucocytes (PMN), are two reliable hallmarks of lung inflammation [35, 59]. The cell counts (Figure 7B) of BPEI

polyplexes treated lungs was higher than that of both DNA and glucose control. In contrast, TAT-PEG-PEI polyplexes did not cause significantly higher cell counts in the BALF.

PMN (Figure 7B) were not observed after the application of glucose control, indicating that the isotonic solution did not provoke neutrophil infiltration into the lung and thus no inflammatory process was activated. DNA and both polyplex formulations caused an increased PMN recruitment indicating a slight inflammation in the mouse lung. Whereas BPEI polyplexes displayed a significantly higher PMN recruitment (66 ± 15 % of the entire cell population) compared to plasmid DNA (33 ± 11%), TAT-PEG-PEI polyplexes (47 ± 17 %) did not increase the PMN proportion significantly.

The total protein concentration (Figure 7C) in BALF characterizes general alterations of the natural composition of the lining fluid and detects enzymes, cytokines as well as other proteins. Thus, significant increases in the protein concentrations do not necessarily suggest an inflammation reaction. These results have to be considered in conjunction with PMN and cell counts. The amount of protein measured in the BALF generally mirrored the trends observed for cell counts, although the differences between polyplexes and both DNA and glucose was more pronounced. Significant increased levels of protein were observed in the BALF for both BPEI and TAT-PEG-PEI polyplexes when compared with pDNA and glucose control. However, the values obtained for total cell counts and PMN indicated that the acute inflammatory reaction caused by TAT-PEG-PEI/DNA is not significantly different from DNA, in contrast to BPEI/DNA. Therefore we assume that the high protein level of TAT-PEG-PEI/DNA might be the result of other mediators, such as interleukins, which were not measured here in.

Cytokine response to aerosol delivery of BPEI polyplexes has also been documented [34]. Hence, our aim was to investigate whether TAT-PEG-PEI polyplexes delivered to the mouse lung led to a TNF-α response, as mediator of an acute inflammatory reaction. Whilst the TNF-α level (Figure 7D) was significantly increased after administration of BPEI polyplexes, TAT-PEG-PEI polyplexes did not cause a significant increased in TNF-α level.
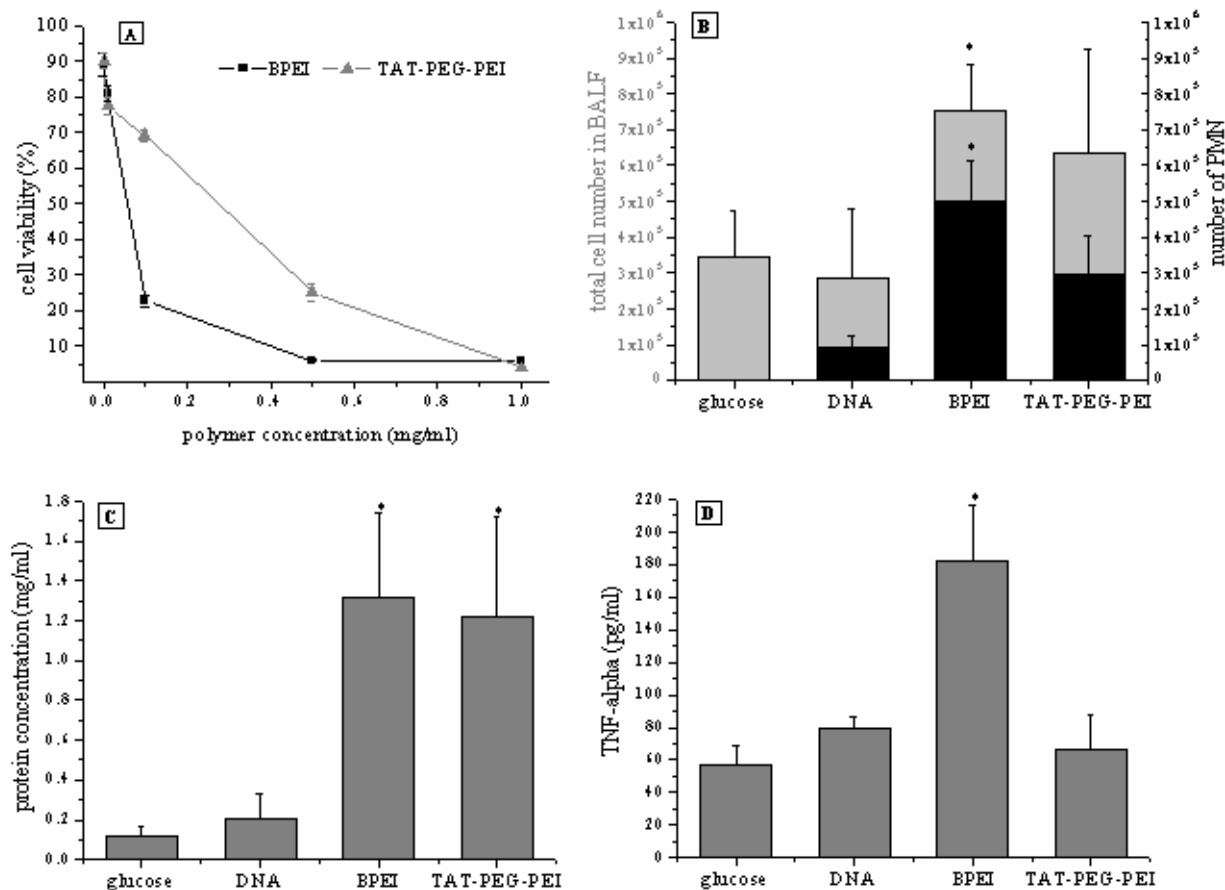
Figure 7. Toxicity studies: A) Cytotoxic effects of the polymers at concentrations of 0.001, 0.01, 0.1, 0.5, and 1.0 mg/ml on A549 cells were determined by MTT assay and presented as the relative cell viability (mean ± SD of six determinations). Indicators of pulmonary inflammation (mean ± SD of three experiments) in the BALF 24 hour post-application of polyplexes (N/P 10) in the mouse lung: B) Total cell number (grey scale) and PMN number (black scale), C) Total protein concentration, D) TNF-α concentration.

Taken together, the toxicity data indicate inflammatory reactions almost at the level of naked DNA when TAT-PEG-PEI was administered in the mouse lung. Plasmid DNA itself, in particular under the promoter of CMV, has been reported to cause toxic side effects in numerous cells [60]. The inflammatory mediator and indicators studied here were significantly higher for BPEI than for TAT-PEG-PEI. Therefore, TAT-PEG-PEI represents a more suitable gene carrier and thus an improvement to the common used BPEI in respect of toxicity in the lung. These in vivo results as well as the in vitro results are in line with previous reports, where low cytotoxicity for TAT peptides and TAT modified liposomes was reported [13, 52].

Distributions of the polyplexes in the mouse lung

The final aim of our study was to localize the polyplex distribution 4 hours post-administration and the site of gene expression 48 hours post-administration. In this attempt, double-labeled TAT-PEG-PEI polyplexes were applied to the mouse lung and the polyplex location in the lung was evaluated. Well aware of the problems involved in cell fixation causing artefacts, which have been reported to influence the cell entry of TAT oligopeptides [16], we used cryosections obtained by paraformaldehyde fixation via the endothelial route. Representative confocal laser scanning microscopy images are shown in Figure 8A & B. The pDNA (red) and the polymer (green) were mainly co-localized, seen as yellow overlapping. The double-labeled polyplexes were localized in the bronchial epithelia cells, since those are the first cells to come to pass on the way in the deeper respiratory tract (Figure 8A). More interesting, polyplexes could also be observed in the alveolar region (Figure 8B). Images taken post-administration of GFP coding plasmid complexed with TAT-PEG-PEI confirmed these findings, since GFP was observed in both the bronchial as well as the alveolar epithelia cells (Figure 8C & D). These findings indicate successful gene transfer followed by transgene expression in the conducting as well as respiratory airways.

Until now, it was demonstrated that BPEI polyplexes are capable of targeting bronchial cells [6, 7], which could be confirmed by our studies (data not shown). In contrast, TAT-PEG-PEI was able to mediate transfection to bronchial as well as alveolar cells. It is likely, that BPEI/DNA polyplexes, due to their highly positive surface charge and aggregation, "stick" at the bronchial ciliated cells and are unable the reach the respiratory tract. By contrast, the small, shielded particles of TAT-PEG-PEI/DNA are able to pass the bronchial region, hence depositing also in the alveolar region. Due to the larger surface area of the alveolar sacs, a more extensive transfection of lung tissue was achieved.
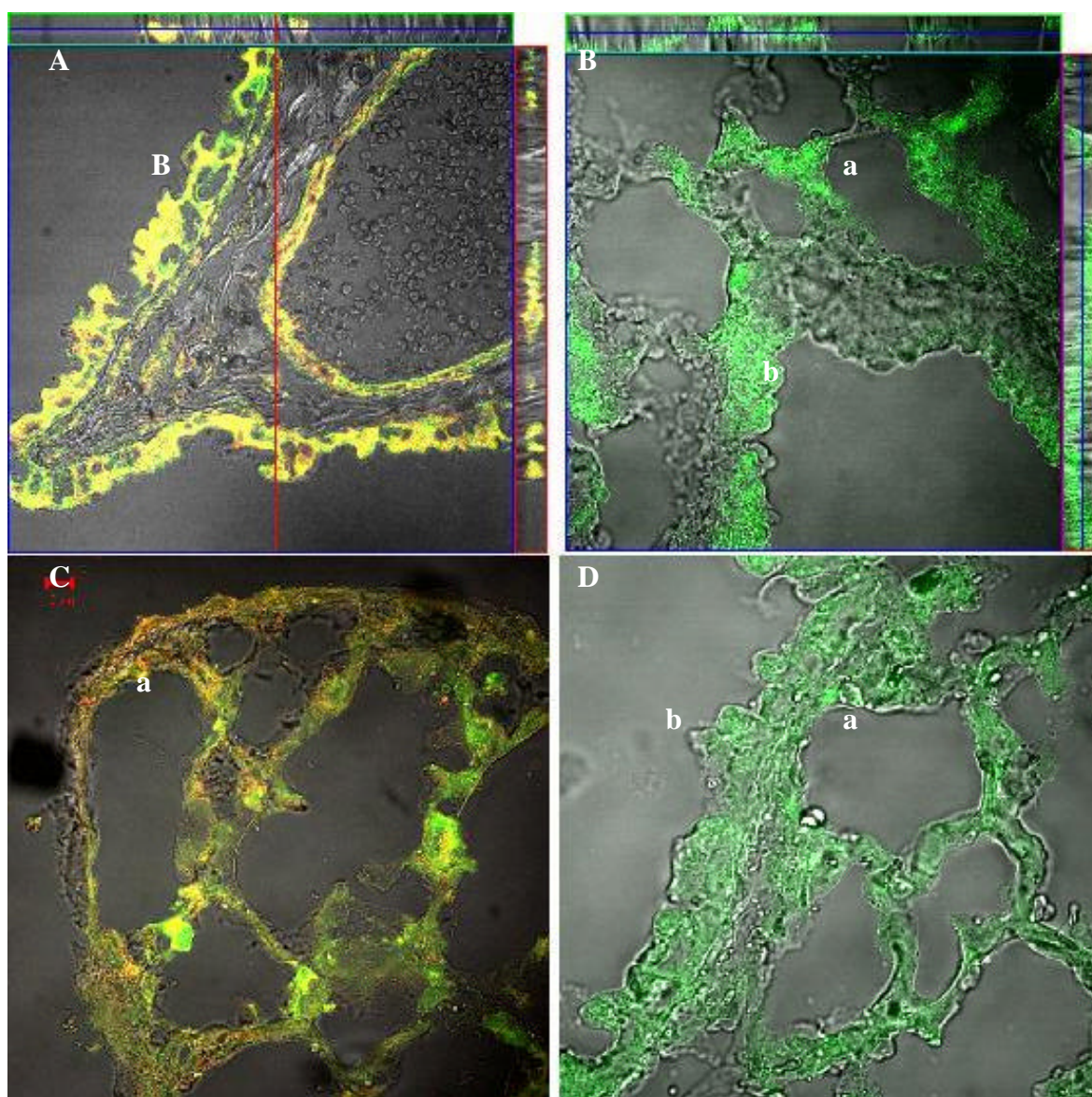
Figure 8. Polyplex distribution in the mouse lung: Localization of double-labeled TAT-PEG-PEI/DNA 4 hours post-application in A) bronchial and C) alveolar cells. Localization of the GFP expression 48 hours post-administration in B) bronchial and D) alveolar epithelial cells. (a) indicates alveolar region, (b) indicates bronchial region.

CONCLUSION

In summary, TAT-PEG-PEI conjugates are a new delivery system for pDNA to the lung that displays several beneficial features in comparison to unmodified BPEI: (i) The use of TAT-PEG-PEI led to enhanced polyplex stability and DNA protection in pulmonary environment. (ii) The zeta-potential of the TAT-PEG-PEI polyplexes was reduced due to PEG shielding of the surface charge, leading to decreased aggregation tendency in high ionic strength media. (iii) The lower surface charge and the PEG shielding also significantly reduced cytotoxicity in the lung epithelial cells in both in vitro and in vivo studies. (iv) TAT-PEG-PEI/DNA demonstrated a 600% increase in transfection efficiency in vivo when compared to BPEI. (v) TAT-PEG-PEI directed pDNA into the epithelial cells of the bronchi and alveoli.

The enhanced transfection efficiency under in vivo conditions is most likely due to the increased DNA condensation, the improved polyplex stability and the TAT mediated cell uptake. The PEG spacer seems to be essential for both the enhanced gene expression and the reduced toxicity. Further experiments exploring the polyplex composition and the uptake mechanism are currently under way in our laboratory.

Taken collectively, these data suggest that TAT-PEG-PEI could be an interesting pulmonary delivery system for pDNA, potentially offering new treatment modalities for a variety of lung diseases, depending on the cell population to be targeted. TAT-PEG-PEI offers the possibility of transfecting both alveolar and bronchial tissue through inhalation.

Non-viral gene delivery systems, such as PEI, have not reached the same transfection efficiencies as viral vectors, but this study demonstrates that potential modifications of polycations have not yet been exhausted. TAT-PEG-PEI may provide an interesting addition to the spectrum of polycationic delivery systems since it enhances gene expression in conducting and respiratory airways, and also improves the biocompatibility and polyplex stability in the extra and intra-cellular lung environment, features which are highly sought after in a gene carrier system for local therapy to the lung.

REFERENCES

1. D. R. Gill, L. A. Davies, I. A. Pringle*, et al.* The development of gene therapy for diseases of the lung. *Cell Mol Life Sci* **61**: 355-368 (2004).
2. S. Ferrari, D. M. Geddes, and E. W. Alton. Barriers to and new approaches for gene therapy and gene delivery in cystic fibrosis. *Adv Drug Deliv Rev* **54**: 1373-1393 (2002).
3. A. Gautam, J. C. Waldrep, and C. L. Densmore. Aerosol gene therapy. *Mol Biotechnol* **23**: 51-60 (2003).
4. C. Rudolph, U. Schillinger, C. Plank*, et al.* Nonviral gene delivery to the lung with copolymer-protected and transferrin-modified polyethylenimine. *Biochim Biophys Acta* **1573**: 75-83 (2002).
5. A. Kichler, M. Chillon, C. Leborgne*, et al.* Intranasal gene delivery with a polyethylenimine-PEG conjugate. *J Control Release* **81**: 379-388 (2002).
6. A. Bragonzi, G. Dina, A. Villa*, et al.* Biodistribution and transgene expression with nonviral cationic vector/DNA complexes in the lung. *Gene Ther* **7**: 1753-1760 (2000).
7. A. Gautam, C. L. Densmore, E. Golunski*, et al.* Transgene expression in mouse airway epithelium by aerosol gene therapy with PEI-DNA complexes. *Mol Ther* **3**: 551-556 (2001).
8. M. Lundberg, S. Wikstrom, and M. Johansson. Cell surface adherence and endocytosis of protein transduction domains. *Mol Ther* **8**: 143-150 (2003).
9. C. H. Tung and W. R. Arginine containing peptides as delivery vectors. *Adv Drug Deliv Rev* **55**: 281-294 (2003).
10. E. Vives, P. Brodin, and B. Lebleu. A truncated HIV-1 Tat protein basic domain rapidly translocates through the plasma membrane and accumulates in the cell nucleus. *J Biol Chem* **272**: 16010-16017 (1997).
11. M. M. Fretz, G. A. Koning, E. Mastrobattista*, et al.* OVCAR-3 cells internalize TAT-peptide modified liposomes by endocytosis. *Biochim Biophys Acta* **1665**: 48-56 (2004).
12. H. Hashida, M. Miyamoto, Y. Cho*, et al.* Fusion of HIV-1 Tat protein transduction domain to poly-lysine as a new DNA delivery tool. *Br J Cancer* **90**: 1252-1258 (2004).
13. D. Soundara Manickam, H. S. Bisht, L. Wan*, et al.* Influence of TAT-peptide polymerization on properties and transfection activity of TAT/DNA polyplexes. *J Control Release* **102**: 293-306 (2005).
14. I. M. Kaplan, J. S. Wadia, and S. F. Dowdy. Cationic TAT peptide transduction domain enters cells by macropinocytosis. *J Control Release* **102**: 247-253 (2005).
15. J. S. Wadia, R. V. Stan, and S. F. Dowdy. Transducible TAT-HA fusogenic peptide enhances escape of TAT-fusion proteins after lipid raft macropinocytosis. *Nature Medicine* **10**: 310-315 (2004).
16. J. A. Leifert, S. Harkins, and J. L. Whitton. Full-length proteins attached to the HIV tat protein transduction domain are neither transduced between cells, nor exhibit enhanced immunogenicity. *Gene Ther* **9**: 1422-1428 (2002).
17. S. Futaki. Arginine-rich peptides: potential for intracellular delivery of macromolecules and the mystery of the translocation mechanisms. *Int J Pharm* **245**: 1-7 (2002).
18. J. Fernandez-Carneado, M. Van Gool, V. Martos*, et al.* Highly efficient, nonpeptidic oligoguanidinium vectors that selectively internalize into mitochondria. *J Am Chem Soc* **127**: 869-874 (2005).

19. A. M. Funhoff, C. F. van Nostrum, M. C. Lok, *et al.* Poly(3-guanidinopropyl methacrylate): a novel cationic polymer for gene delivery. *Bioconjug Chem* **15**: 1212-1220 (2004).

20. C. Rudolph, C. Plank, J. Lausier, *et al.* Oligomers of the arginine-rich motif of the HIV-1 TAT protein are capable of transferring plasmid DNA into cells. *J Biol Chem* **278**: 11411-11418 (2003).

21. H. Hashida and M. Miyamoto. Fusion of HIV-1 Tat protein transduction domain to poly-lysine as a new DNA delivery tool. *Br J Cancer* **90**: 1252-1258 (2004).

22. L. Hyndman, J. L. Lemoine, L. Huang, *et al.* HIV-1 Tat protein transduction domain peptide facilitates gene transfer in combination with cationic liposomes. *J Control Release* **99**: 435-444 (2004).

23. T. Reschel, C. Konak, D. Oupicky, *et al.* Physical properties and in vitro transfection efficiency of gene delivery vectors based on complexes of DNA with synthetic polycations. *J Control Release* **81**: 201-217 (2002).

24. D. L. McKenzie, K. Y. Kwok, and K. G. Rice. A potent new class of reductively activated peptide gene delivery agents. *J Biol Chem* **275**: 9970-9977 (2000).

25. K. H. Bremner, L. W. Seymour, A. Logan, *et al.* Factors influencing the ability of nuclear localization sequence peptides to enhance nonviral gene delivery. *Bioconjug Chem* **15**: 152-161 (2004).

26. A. Eguchi, T. Akuta, H. Okuyama, *et al.* Protein transduction domain of HIV-1 Tat protein promotes efficient delivery of DNA into mammalian cells. *J Biol Chem* **276**: 26204-26210 (2001).

27. K. Kunath, A. v. Harpe, and H. Petersen. The structure of PEG-modified poly(ethylene imines) influences biodistribution and pharmacokinetics of their complexes with NF-kB decoy in mice. *Pharm Res* **19**: 810-817 (2002).

28. L. A. Dailey, E. Kleemann, T. Merdan, *et al.* Modified polyethylenimines as non viral gene delivery systems for aerosol therapy: Effects of nebulization on cellular uptake and transfection efficiency. *J Control Release* **100**: 425-436 (2004).

29. H. Petersen, K. Kunath, A. L. Martin, *et al.* Star-shaped poly(ethylene glycol)-block-polyethylenimine copolymers enhance DNA condensation of low molecular weight polyethylenimines. *Biomacromolecules* **3**: 926-936 (2002).

30. N. Ernst, S. Ulrichskötter, W. A. Schmalix, *et al.* Interaction of liposomal and polycationic transfection complexes with pulmonary surfactant. *J Gene Med* **1**: 331-340 (1999).

31. J. Rosenecker, S. Naundorf, S. W. Gersting, *et al.* Interaction of bronchoalveolar lavage fluid with polyplexes and lipoplexes: analysing the role of proteins and glycoproteins. *J Gene Med* **5**: 49-60 (2003).

32. W. T. Godbey, M. A. Barry, P. Saggau, *et al.* Poly(ethylenimine)-mediated transfection: a new paradigm for gene delivery. *J Biomed Mater Res* **51**: 321-328 (2000).

33. D. Fischer, Y. Li, B. Ahlemeyer, *et al.* In vitro cytotoxicity testing of polycations: influence of polymer structure on cell viability and hemolysis. *Biomaterials* **24**: 1121-1131 (2003).

34. A. Gautam, C. L. Densmore, and J. C. Waldrep. Pulmonary cytokine responses associated with PEI-DNA aerosol gene therapy. *Gene Ther* **8**: 254-257 (2001).

35. A. Gautam, C. L. Densmore, B. Xu, *et al.* Enhanced gene expression in mouse lung after PEI-DNA aerosol delivery. *Mol Ther* **2**: 63-70 (2000).

36. K. Sagara and S. W. Kim. A new synthesis of galactose-poly(ethylene glycol)-polyethylenimine for gene delivery to hepatocytes. *J Control Release* **79**: 271-281 (2002).

37. A. J. Lomant and G. Fairbanks. Chemical probes of extended biological structures: synthesis and properties of the cleavable protein cross-linking reagent [35S]dithiobis(succinimidyl propionate). *J Mol Biol* **104**: 243-261 (1976).

38. L. Li, S. W. Tsai, and A. L. Anderson. Vinyl sulfone bifunctional derivatives of DOTA allow sulfhydryl- or amino-directed coupling to antibodies. Conjugates retain immunoreactivity and have similar biodistribution. *Bioconjug Chem* **13**: 110-115 (2002).

39. K. Kunath and T. Merdan. Integrin targeting using RGD-PEI conjugates for in vitro gene transfer. *J Gene Med* **5**: 588-599 (2003).

40. H. Petersen, P. M. Fechner, D. Fischer, *et al.* Synthesis, characterisation, and biocompatibility of polyethylenimine-graft-poly(ethylene glycol) block copolymer. *Macromolecules* **35**: 6867-6874 (2002).

41. M. Ogris, G. Walker, T. Blessing, *et al.* Tumor-targeted gene therapy: strategies for the preparation of ligand-polyethylene glycol-polyethylenimine/DNA complexes. *J Control Release* **91**: 173-181 (2003).

42. V. S. Trubetskoy and A. Loomis. Caged DNA does not aggregate in high ionic strength solutions. *Bioconjug Chem* **10**: 624-628 (1999).

43. S. J. Sung and S. H. Min. Effect of polyethylene glycol on gene delivery of polyethylenimine. *Biol Pharm Bull* **26**: 492-500 (2003).

44. H. Petersen, M. F. Fechner, A. L. Martin, *et al.* Polyethylenimine-graft-Poly(ethylene glycol) Copolymers: Influence of Copolymer Block Structure on DNA Complexation and Biological Activities as Gene Delivery System. *Bioconjug Chem* **13**: 845-854 (2002).

45. D. Fischer, A. v. Harpe, and T. Kissel. Polyethylenimine: Polymer Structure Influences the Physicochemical and Biological Effects of Plasmid/PEI Complexes. *Biomaterials* 195-211 (2000).

46. R. Kircheis, T. Blessing, S. Brunner, *et al.* Tumor targeting with surface-shielded ligand-polycation DNA complexes. *J Control Release* **72**: 165-170 (2001).

47. M. Ogris, S. Brunner, S. Schuller, *et al.* PEGylated DNA/transferrin-PEI complexes: reduced interaction with blood components, extended circulation in blood and potential for systemic gene delivery. *Gene Ther* **6**: 495-605 (1999).

48. D. A. Groneberg, C. Witt, U. Wagner, *et al.* Fundamentals of pulmonary drug delivery. *Respir Med* **97**: 382-387 (2003).

49. I. Mellman. Endocytosis and molecular sorting. *Annu Rev Cell Dev Biol* **12**: 575-625 (1996).

50. E. Wagner. Strategies to improve DNA polyplexes for in vivo gene transfer: will "artificial viruses" be the answer? *Pharm Res* **21**: 8-14 (2004).

51. Z. Siprashvili, F. A. Scholl, S. F. Oliver, *et al.* Gene transfer via reversible plasmid condensation with cystein-flanked, internal spaced arginine-rich peptides. *Hum Gene Ther* **14**: 1225-1233 (2003).

52. V. P. Torchilin, T. S. Levchenko, R. Rammohan, *et al.* Cell transfection in vitro and in vivo with non-toxic TAT peptide-liposome-DNA complexes. *Proc Natl Acad Sci U S A* **100**: 1972-1977 (2003).

53. M. Koeping-Hoeggard, K. M. Varum, M. Issa, *et al.* Improved chitosan-mediated gene delivery based on easily dissociated chitosan polyplexes of highly defined chitosan oligomers. *Gene Ther* **11**: 1441-1452 (2004).

54. E. Durr, J. Yu, K. M. Krasinska, *et al.* Direct proteomic mapping of the lung microvascular endothelial cell surface in vivo and in cell culture. *Nat Biotechnol* **22**: 985-992 (2004).

55. M. Ogris, P. Steinlein, M. Kursa, *et al.* The size of DNA/transferrin-PEI complexes is an important factor for gene expression in cultured cells. *Gene Ther* **5**: 1425-1433 (1998).

56. V. P. Torchilin, R. Rammohan, V. Weissig, *et al.* TAT peptide on the surface of liposomes affords their efficient intracellular delivery even at low temperature and in the presence of metabolic inhibitors. *Proc Natl Acad Sci U S A* **98**: 8786-8791 (2001).

57. T. Mosmann. Rapid colorimetric assay for cellular growth and survival: application to proliferation and cytotoxicity assays. *J Immunol Methods* **65**: 55-63 (1983).

58. E. Vives, B. Brodin, and B. Lebleu. A truncated HIV-1 Tat protein basic domain rapidly translocates through the plasma membrane and accumulates in the cell nucleus. *J Biol Chem* **272**: 16010-16017 (1997).

59. R. K. Scheule, J. A. St George, R. G. Bagley, *et al.* Basis of pulmonary toxicity associated with cationic lipid-mediated gene transfer to the mammalian lung. *Hum Gene Ther* **8**: 689-707 (1997).

60. G. McLachlan, B. J. Stevenson, D. J. Davidson, *et al.* Bacterial DNA is implicated in the inflammatory response to delivery of DNA/DOTAP to mouse lungs. *Gene Ther* **7**: 384-392 (2000).

61. U. Griesenbach, S. Ferrari, D. M. Geddes, *et al.* Gene therapy progress and prospects: cystic fibrosis. *Gene Ther* **9**: 1344-1350 (2002).

Chapter 6

Effect of nebulization on novel iloprost-containing liposomes for the treatment of pulmonary arterial hypertension

ABSTRACT

Pulmonary arterial hypertension (PAH) is a severe and progressive disease. The treatment with the aerosolized prostacyclin analogue iloprost presents an approved therapeutic approach with 6-9 inhalations per day, indicating the need of a sustained release formulation. Liposomal formulations consisted of dipalmitoyl-phosphatidylcholin (DPPC), cholesterol (CH) and polyethylenglycol-dipalmitoyl-phosphatidylethanolamin (DPPE-PEG) were prepared. Their physico-chemical properties were investigated using techniques such as dynamic light scattering, atomic force microscopy and differential scanning calorimetry. Their stabilities during aerosolization using three different types of nebulizers (air-jet, ultrasonic and electronic micro pump) were investigated by means of drug loading and particle size, pre- and post-nebulization. Depending upon the lipid components diameters of approximately 200-400 nm were observed. The highest drug loading (12µg/ml iloprost) combined with high liposomal stability (70% drug encapsulation post-nebulization) was observed for the DPPC/CH liposomes. The relatively high phase transition temperature (53°C) and unchanged particle sizes confirmed their high stability. The incorporation of DPPE-PEG in the liposomes resulted in decreased stability (20-50% drug encapsulation post-nebulization) and 28°C lower phase transition temperature. The electronic micro pump offered a number of significant advantages over the other nebulizers including the production of small aerosol droplets (~ 4µm), high output and the lowest deleterious physical influence upon all investigated liposomes. Iloprost-loaded liposomes containing DPPC and CH display a novel formulation, which is well suited to aerosolization by the electronic micro pump, and offers considerable promise as sustained release formulation for the treatment of PAH.

INTRODUCTION

Pulmonary arterial hypertension (PAH) is a disease that both severely confines the life quality of the patient and has a poor prognosis for survival. The disease pattern is characterized by an increased pulmonary arterial pressure due to vasoconstriction, hypertrophy and intimal fibrosis [1, 2]. Two drugs are currently available for use in the treatment of the advanced state of PAH (NYHA III & IV): the oral endothelin-antagonist Bosentan®, and intravenous, subcutaneous, oral or inhalative prostacyclin and its analogues [3].

Over the past decade intravenous prostacyclin (Eprostenol®) has been the therapy of choice for patients with PAH [4]. Prostacyclin is a short-living vasodilator, which acts to modestly reduce both the patient's systemic blood pressure and the mean pulmonary arterial pressure [5]. Prostacyclin's most potent effect seems to be through positive inotropism, by raising the cardiac output [6]. However, the long-term use of intravenous prostacyclin has potential for side effects, such as marked flushing, diarrhoea, thrombocytopenia and unremitting foot pain [7]. Additionally, the continuous venous catheter infusions of drug significantly increase the risk of potentially life-threatening infections in the patient.

While prostacyclin is clearly a potent and efficacious drug for the treatment of PAH, the relative severity of the side-effects led to the development of prostacyclin analogues. As such iloprost (Ventavis®), which was recently approved by the EMEA for inhalative treatment of PAH, minimises the systemic side effects and can be administered as aerosol in lower doses to the patient's lung [8]. Long-term treatment of nebulized iloprost was demonstrated to cause strong pulmonary vasodilatation and decompensate right heart failure. Furthermore, this non-invasiveness permits improved patience compliance. Unfortunately, the short half-life requires frequent inhalation, ranging from six up to twelve times a day [9]. Therefore, a sustained-release formulation for iloprost would be desirable.

Currently, two types of nebulizer can be used in medical aerosolization - air-jet or ultrasonic nebulizers. Air-jet nebulizers are based on the venturi principle, whereas ultrasonic nebulizers use the converse piezoelectric effect to convert alternating current to high-frequency acoustic energy [10]. Both types of nebulizer offer various advantages and disadvantages. The main disadvantages of air-jet nebulizers are the lower output, and the deleterious effect upon some drug formulations as a result of the high shear forces applied during nebulization. Ultrasonic energy is notorious for altering or damaging some aerosolized drug substances [10, 11]. A new nebulizer technology is the electronic micro pump, whose

operation is based upon the electric oscillation of a cavity disc. The predominant advantage of electronic micro pumps is that the drug solution is transported directly through the cavity disc and does not re-enter the liquid compartment as is the case in standard ultrasonic and air-jet nebulizers [12].

Pulmonary administration of aerosolized liposomes represents a valid alternative route for the treatment of lung disorders via topical drug delivery [13-15]. The advantages of such an administration route are numerous, and include the facilitated administration of sustained-release formulations to maintain therapeutic drug levels in the lungs, aqueous compatibility and facilitated intracellular delivery [16]. In this respect a major challenge is the liposomes membrane stability during the aerosolization, since shear forces (air-jet) and high frequencies (ultrasonic) can alter the nebulizing content. Considering the alternative therapeutic application, reduced side effects of inhaled iloprost and the formulations stability, we have developed novel liposomal formulations as potential iloprost carriers for the efficacious aerosol therapy of PAH.

The aim of this study was to investigate the physicochemical characteristics of lipid-based nanoparticles in order to assess their suitability as inhalative iloprost carriers. This was achieved by preparing and studying a number of liposomes, containing carboxyfluorescein as a model drug and in a second experimental series containing iloprost. The lipids used for these formulations were dipalmitoyl-phosphatidylcholin (DPPC), cholesterol (CH) and [methoxy (polyethylglycol)-2000]-dipalmitoyl-phosphatidylethanolamin (DPPE-PEG) [17]. All formulations were characterized in terms of their ability to encapsulate the drug, stability during air-jet, ultrasonic and micro-pump nebulization, size (by dynamic light scattering), morphology (using atomic force microscopy) and thermotropic behaviour (employing differential scanning calorimetry). Furthermore, the nebulizers PariBoy® (air-jet), Optineb® (ultrasonic) and Aeroneb® (electric micro pump) were characterized by means of their output (by loss of weight) and aerosol particle size (using laser light diffraction) when nebulizing liposome dispersions.

MATERIALS AND METHODS

Materials

The lipids dipalmitoyl-phosphatidylcholin (DPPC), cholesteol (CH) and [methoxy (polyethylenglycol)-2000]-dipalmitoyl-phosphatidylethanolamin (DPPE-PEG) were purchased from Avestin (Ottawa, Canada). 5(6)-carboxyfluorescein (COF) was purchased

from Fluka BioChemika (Neu-Ulm, Germany). ^{3}H-labeled iloprost and iloprost trometamol (ILO) as well as the chromatographic column and the Sephadex 50 medium gel were purchased from Amersham Bioscience (Freiburg, Germany).

Liposome preparation

DPPC/CH liposomes (PC) were prepared at a molar ratio of 70:30 and DPPC/CH/PEG liposomes (PCP) at a molar ratio of 50:45:5. The corresponding quantities of lipids were dissolved in a chloroform methanol mixture (70:30). A thin lipid film was created by rotary evaporation at 60 °C under reduced pressure, and subsequently dried for further 60 minutes in a vacuum cabinet [18]. This film was rehydrated with the drug solution to reach a total lipid concentration of 3.15 mg/ml (5 mM). The solution medium for the COF containing liposomes was PBS buffer (pH 7.4) and the final drug concentration was 10 mg COF/ml (26.5 mM). The drug solution for iloprost loaded liposomes were prepared by diluting ^{3}H-labeled iloprost with iloprost trometamol at a ratio of 1:500 in either PBS buffer (pH 7.4) or 0.1 M acetate buffer (pH 4.7) and a final drug concentration of 0.25 mg iloprost/ml (2.75 mM) was used. For drug encapsulation the rehydrated film was rotated at 60 °C for 2 hours and, after cooling, was stored for one hour at 4°C. The size of the resulted large multilamellar vesicles was reduced by extruding the liposomal dispersion through a 400 nm polycarbonate membrane filter (Liposofast, Avestin, Ottawa, Canada) 21 times at the same operating temperature employed during the hydration process [19]. The samples obtained were allowed to stabilize for 24 hours at 4°C. Non-encapsulated COF was separated from the liposomes using gel chromatography (FPLC AEKTA prime, Amersham Pharmacia Biotech, Freiburg, Germany) packed with Sephadex G-50 medium gel in a 25 cm column at a flow rate of 1.0 ml/min. The non-encapsulated iloprost/^{3}H-iloprost was removed from the liposomal dispersion by three-time centrifugation and resuspension.

All experiments described here were carried out three times using freshly prepared lipid preparations.

Nebulization

The nebulization of 4 ml liposomal preparation was carried out for 10 minutes. The liposomes were aerosolized at 10 l/min airflow rate using the electronic micro pump Aeroneb®, operated with a frequency of 0.13 MHz (Aerogen, Stierlin, CA, USA), the ultrasonic nebulizer Optineb® (Nebutec, Elsenfeld, Germany) operated with a frequency of 2.4 MHz and the air-jet nebulizer Pari LC® star (Pari, Starnberg, Germany) operated with the

Pari Boy® compressor. The nebulized samples were collected by aerosol deposition on a glass plate and subsequent collection in 1.5 ml Eppendorf tubes.

Physico-chemical properties of the nebulizer output

The mass median aerodynamic diameters (MMAD) of the aerosol droplets produced from the different nebulizers when filled with liposomal dispersion or isotonic sodium solution were determined using laser light scattering (Sympatec, Clausthal-Zellerfeld, Germany). The measurements were performed with aerosol concentrations of 5 to 30 %, in 6 runs of 5 ms duration each and analyzed in MIE mode. The density of the aqueous dispersion and solution respectively, was set equal that of pure water and thus the MMAD is equal the volume aerodynamic diameter. The geometric standard deviation (GSD) was calculated from the laser diffraction values according to the following equation: GSD = $\sqrt{}$ 84 % undersize / 16 % undersize.

To calculate the nebulizer mass output, the nebulizers were weighed before and after each aerosolization experiment. The resulting difference in weight was used to calculate the mass output in µg per minute.

Atomic force microscopy

All experiments were performed using a DI multimode atomic force microscope equipped with a Nanoscope IIIa controller (Veeco, Santa Barbara, CA). The instrument was equipped with an E-scanner with a maximum scan size of 13 µm x 13 µm. Images were collected in Tapping Mode, using oxide sharpened silicon nitride cantilevers (Veeco, Santa Barbara, CA) operating at resonant frequencies of approximately 8 kHz. All images were recorded with 512 x 512 pixel resolution. Scan speeds varied between applications. To reduce sample distortion, all data were acquired using optimum set-points and drive amplitudes aimed at minimising tip-sample interaction. Gains and scan-rate were continually adjusted to optimize the data obtained. Post-imaging analysis was carried out on NanoScope IIIa™ software, version 5.12b48.

Dynamic light scattering

The hydrodynamic diameters of the non-nebulized and nebulized liposomes were measured using a Zetasizer 3000 HS (10 mW HeNe laser, 633 nm) from Malvern Instruments (Worcestershire, UK). The scattered light was detected at a 90° angle through a 100 µm pinhole. Measurements were performed at count rates between 100 and 300 kCps, at 25°C in

5 runs of 60 sec duration each and analyzed in CONTIN mode. The instrument was calibrated with nanosphere size standards (polymer microspheres in water, 220 nm +/- 6 nm) from Duke Scientific (Palo Alto, CA, USA).

Differential scanning calorimetry

Phase transition temperatures of the lipids and the liposomal formulations, respectively, were determined using a differential scanning calorimeter (DSC7, PerkinElmer, Rodgau-Jügesheim, Germany). A 5 mg sample of the lipid powders or the COF loaded liposomes were sealed in standard aluminium pans and scanned in two heating/cooling cycles at a rate of 10 °C/min from -20 °C to 95 °C in a nitrogen atmosphere. Data from the first scan were always discarded to avoid mixing artefacts. The phase transition temperatures (Tc) were calculated using the Pyris Software (PerkinElmer, Rodgau-Jügesheim, Germany).

Drug loading efficiency

The quantity of drug encapsulated pre- and post-nebulization was evaluated by measuring the total drug (D_{total}) and the non-encapsulated drug (D_{free}) concentration.

The drug loading of the liposomes containing the model drug COF was determined fluorometrically (Fluoreszenzreader FL600, Microplate Fluorescence BioTEK, Winooski, USA) [18]. Primarily, aliquots of 100 µl COF loaded liposomes were diluted 100 times with PBS buffer (pH 7.4) and samples of 100 µl were placed in a 96 black well plate to measure the concentration of free COF. For lipid membrane lyses, further 100 µl of the diluted liposomes were diluted 10 times with Triton X-100 1% / PBS and incubated under agitation (100 r/min) for 10 minutes. Hundred µl samples of the lysed liposomes were placed in a 96-well plate to measure the total COF concentration. The amount of free and total COF was determined fluorometrically at an excitation wavelength of 485 nm and an emission wavelength of 530 nm. The calibration curve was prepared with COF concentrations between 1 and 2000 ng/ml in both PBS buffer (pH 7.4) and Triton X-100 1% / PBS.

During the second investigation series the drug loading of the iloprost containing liposomes was determined by radioactivity measurements. In order to evaluate the quantity of non-encapsulated iloprost, liposome dispersions were centrifuged for 30 min at 15,000g and the supernatant collected. Aliquots (250 µl) of the supernatant and the non-centrifuged liposomes, respectively, were transferred into separate 6 ml polyethylene vials prior to the addition of 5 ml aliquots of the Ultima Gold® scintillation cocktail (Packard Bioscience, Rodgau-Jügesheim, Germany). The radio activities of all samples were determined in a

Tricarb 2100 (Packard Bioscience, Rodgau-Jügesheim, Germany) liquid scintillation counter with a pre-count delay of 60 sec and a count time of five minutes per sample. A calibration curve was prepared with iloprost concentrations between 0.01 and 500 µg/ml in both PBS buffer (pH 7.4) and acetate buffer (pH 4.7). For counter calibration ^{3}H Standards (Packard Bioscience, Rodgau-Jügesheim, Germany) were measured before each run.

The encapsulation efficiency (EE) of the liposomal preparations was calculated by comparing the concentration of encapsulated drug ($D_{encap} = D_{total} - D_{free}$) to the quantity of drug (D_{start}) present in the liposomal dispersion prior to the removal of the non-encapsulated drug:

$$EE\ [\%] = 100\ \%\ *\ (D_{total} - D_{free})\ /\ D_{start}$$

To evaluate the nebulization stability the percentage of encapsulated drug (D_{encap}), pre- and post-nebulization, was calculated by comparing the amount of encapsulated drug ($D_{total} - D_{free}$) to that of total drug concentration (D_{total}):

$$D_{encap}\ [\%] = 100\ \%\ *\ (D_{total} - D_{free})\ /\ D_{total}$$

Statistical analysis

Statistical calculations were carried out using the software package GraphPad InStat v3.06 (GraphPad Software, Inc. San Diego, CA, USA). All values are presented as the mean ± standard deviation (SD) unless otherwise stated. The average values of all measurements were calculated from three freshly prepared liposomal formulations, and three runs each preparation. To identify statistically significant differences one-way ANOVA with Bonferroni's post test analysis was performed. Probability values $p < 0.05$ were considered significant and marked with an asterisk in the figures.

RESULTS

All liposomal formulations investigated in this study are listed in Table 1. A series of COF loaded liposomes were initially prepared in order to evaluate a stable formulation suitable to undergo nebulization. Besides the listed lipid combinations several other formulations were investigated, using the components Dimyristoyl-Phosphatidylcholin and Stearylamine. However, formulations incorporating these components exhibited very poor stabilities during nebulization (~ 10 % encapsulated drug post-aerosolization) and low drug

loading efficiencies (~ 0.5 %) (data not shown). Hence the more stable PC and PCP liposomes were chosen for the preparation of iloprost containing drug delivery systems.

Table 1. Terms and lipid components (mM) of liposomal formulations used throughout this study. PC denotes DPPC/CH liposomes (molar ratio 70:30) and PCP denotes DPPC/CH/DPPE-PEG liposomes (molar ratio 50:45:5). The second term COF and ILO, respectively, denotes the drug encapsulated in the liposomes. The term 4.7 indicates the use of acetate buffer pH 4.7 as dispersion medium, if no number is used in the term, the liposomes were prepared in PBS buffer pH 7.4.

liposome term / components	PC-COF	PCP-COF	PC-ILO	PCP-ILO	PC4.7-ILO	PCP4.7-ILO
dipalmitoyl-phosphatidylcholin (DPPC)	3.5	2.5	3.5	2.5	3.5	2.5
cholesterol (CH)	1.5	2.25	1.5	2.25	1.5	2.25
[methoxy (polyethylenglycol)-2000]-dipalmitoyl-phosphatidylethanol-amin (DPPE-PEG)		0.25		0.25		0.25
Carboxyfluorescein (COF) in PBS, pH 7.4	26.5	26.5				
Iloprost (ILO) in PBS, pH 7.4			2.75	2.75		
ILO in acetate buffer, pH 4.7					2.75	2.75

Physico-chemical properties of the nebulizer output

The aerosols produced by the three nebulizers were characterized, and the results are summarized in Table 2. For these experiments isotonic sodium chloride solution and COF loaded liposomes were nebulized. Apart from the increased MMAD of the air-jet nebulized

PCP-COF liposomes none of the nebulizers showed significant differences regarding MMAD, GSD or mass output when PC, PCP liposomes or sodium chloride were aerosolized in comparison. The MMADs of the aerosols were approximately 4 µm for all three investigated nebulizers. The differences in MMADs and GSDs between the nebulizers were negligible. Significant differences were observed when comparing the GSD values of Aeroneb[®] to that of Pari LC[®]. This means the droplet size range of the Aeroneb[®] is smaller than that of Pari LC[®].

The mass output (which dictates the total delivered dose) was approximately 400 mg per minute for both the Optineb[®] and the Aeroneb[®] and approximately 100 mg per minute for the air-jet nebulizer Pari LC[®].

Table 2. Aerosol Characterization: Mass median aerodynamic diameter (MMAD), geometric standard deviation (GSD) and mass output of the nebulizer, aerosolizing COF loaded PC and PCP liposomes or isotonic sodium chloride solution. Statistically significant differences between sodium chloride and liposomes nebulization are marked by an asterisk.

	Aeroneb[®]	Optineb[®]	Pari LC[®]
MMAD [µm]			
PC	4.3 ± 0.04	4.1 ± 0.42	4.5 ± 0.23
PCP	4.3 ± 0.28	4.6 ± 0.41	4.6 ± 0.12 *
NaCl	4.3 ± 0.21	4.0 ± 0.36	4.3 ± 0.06
GSD			
PC	1.8 ± 0.04	1.9 ± 0.14	2.1 ± 0.13
PCP	1.9 ± 0.05	2.0 ± 0.05	2.1 ± 0.03
NaCl	1.8 ± 0.09	1.9 ± 0.07	2.0 ± 0.1
output [mg/min]			
PC	375 ± 31	382 ± 21	110 ± 13
PCP	401 ± 18	395 ± 15	98 ± 18
NaCl	390 ± 22	398 ± 30	101 ± 25

Liposome morphology

Liposome morphologies when loaded with COF were determined by AFM and representative images are shown in Figure 1. Image A & B (three dimension) display PC liposomes as predominantly smooth spherical particles. The liposome diameters varied from

approximately 100 nm to 500 nm. However, despite the high concentration of liposomes in the relatively small area under observation, no merging was observed over the imaging period of two hours. In contrast, imaging the PCP liposomes was problematic due to the tendency of these liposomes to coalesce. The diameters of the PCP liposomes, obtained from AFM images (Figure 1C & D) captured soon after the application of liposomes to the silicon surface, ranged from approximately 200 nm to 300 nm. Whilst the liposome surface was not as smooth as seen for the PC liposomes, they still existed as spherical particles in a narrow size range.
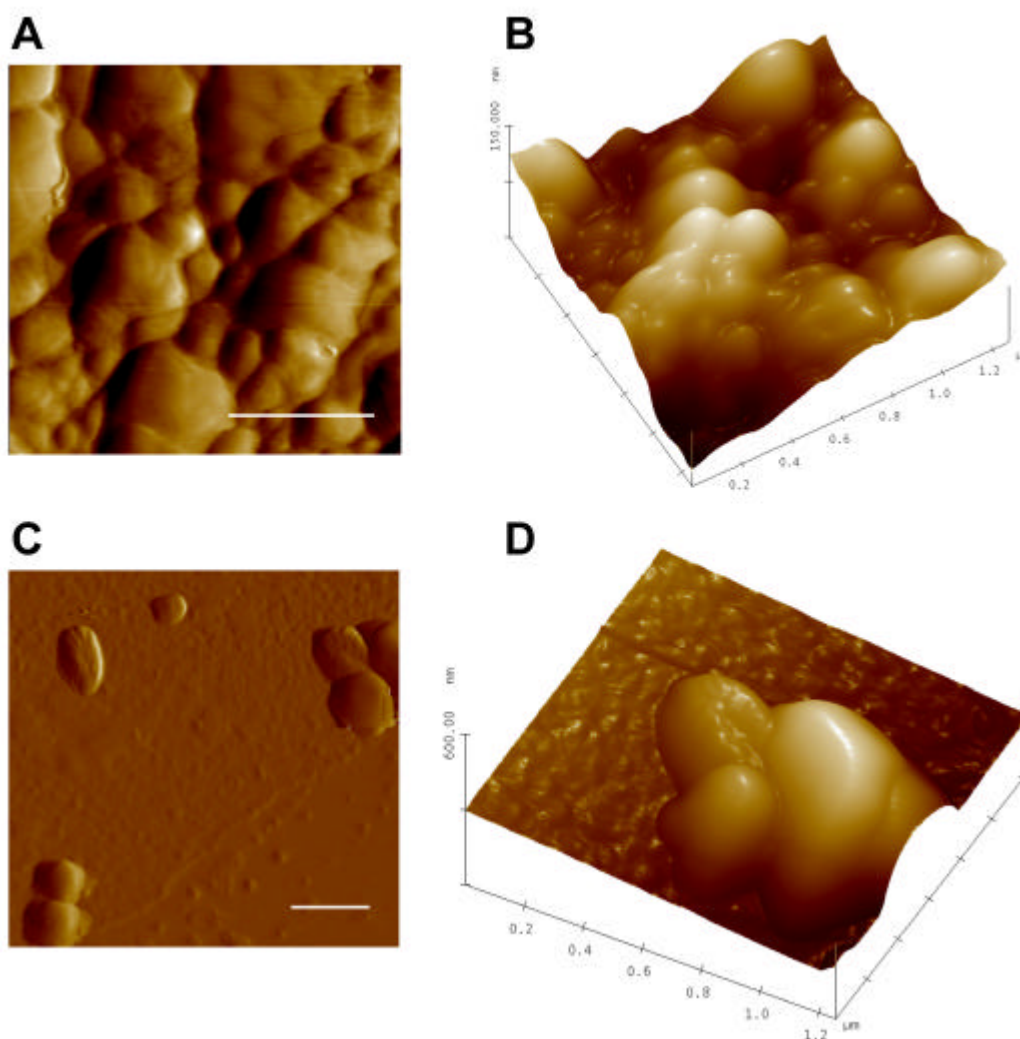

Figure 1. AFM Images showing the morphology of COF containing PC (A & B) and PCP liposomes (C & D) in two dimensions and three dimensions, respectively. The size bars represent 500 nm in the images.

Size and polydispersity of nebulized and non-nebulized liposomes

The hydrodynamic diameters and the polydispersity index (PDI) of COF loaded liposomes (Figure 2) and iloprost loaded liposomes (Figure 3) were determined using DLS pre- and post-nebulization. Both the COF loaded and the iloprost loaded PCP liposomes were shown to be significantly smaller than the PC liposomes. The PDI as a dimension of particle uniformity was approximately 0.15 for all non-nebulized PCP liposomes. This indicates that PCP liposomes exhibit a greater degree of uniformity than the PC liposomes, which displayed a polydispersity index of approximately 0.3.

The diameter of the non-nebulized PC-COF liposomes was approximately 400 nm, while the PCP-COF liposomes exhibited diameters of approximately 225 nm. A significant decrease in hydrodynamic diameter and polydispersity was observed for both the Pari LC$^{®}$-nebulized and the Optineb$^{®}$-nebulized PC-COF liposomes, but in the case of the Aeroneb$^{®}$-nebulized PC-COF liposomes such a decrease was not apparent.

When compared to the COF loaded liposomes, the iloprost loaded liposomes exhibited slightly different physical properties. Whereas the PC-ILO liposomes were approximately 380 nm in diameter (PDI ~ 0.3), the PCP-ILO liposomes were around 275 nm (PDI ~ 0.17). Using PBS buffer (pH 7.4) or acetate buffer (pH 4.7) as dispersion medium for the preparation of ILO liposomes did not appear to have a major influence upon these physical properties. Apart from air-jet nebulized PC-ILO liposomes, the hydrodynamic diameter of all iloprost liposomes decreased significantly as a consequence of the nebulization process. Furthermore, nebulization appeared to influence the polydispersity of the iloprost loaded liposomes to a greater extent than that of the COF loaded liposomes.

Figure 2. Size (A) and polydispersity index (B) of the non-nebulized and nebulized COF loaded liposomes measured by DLS. The mean particle sizes are given as z-average in nm ± SD and were determined by measuring 3 samples and repeating the measurement 5 times. Significant differences (p = 0.05) between pre- and post-nebulized liposomes are marked with an asterisk.

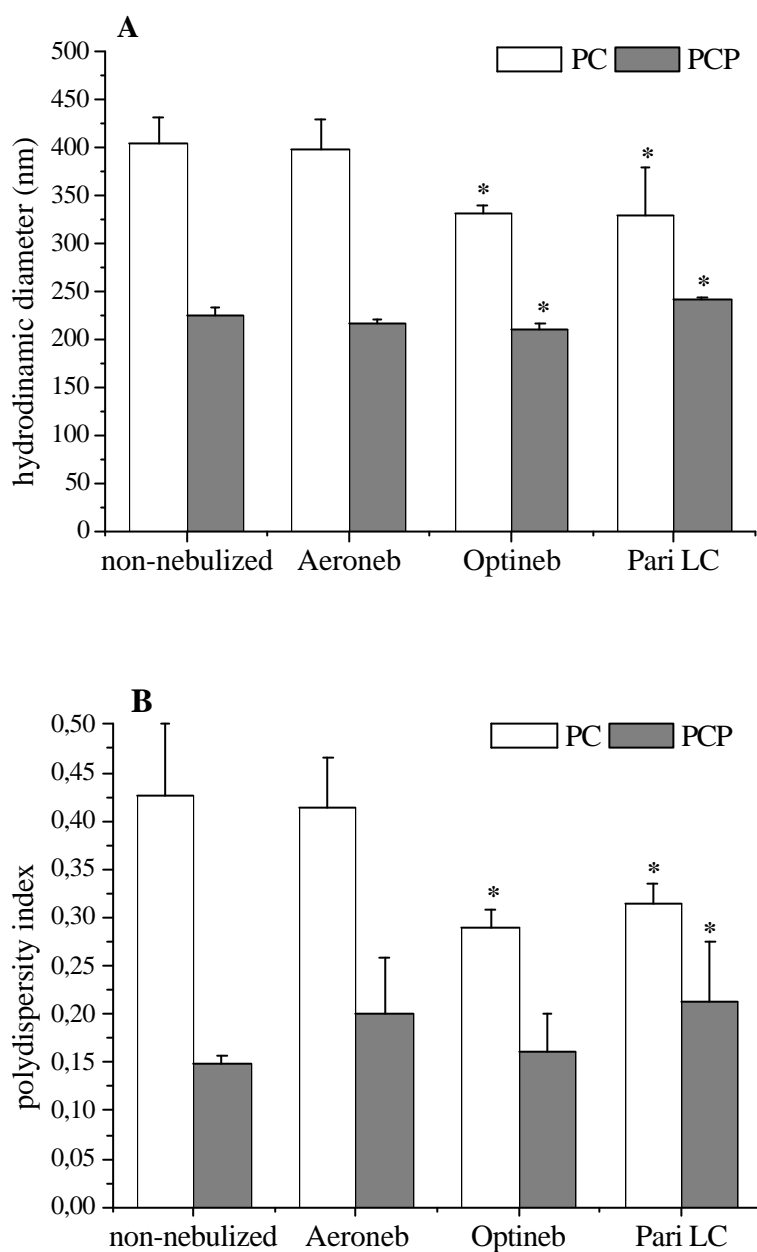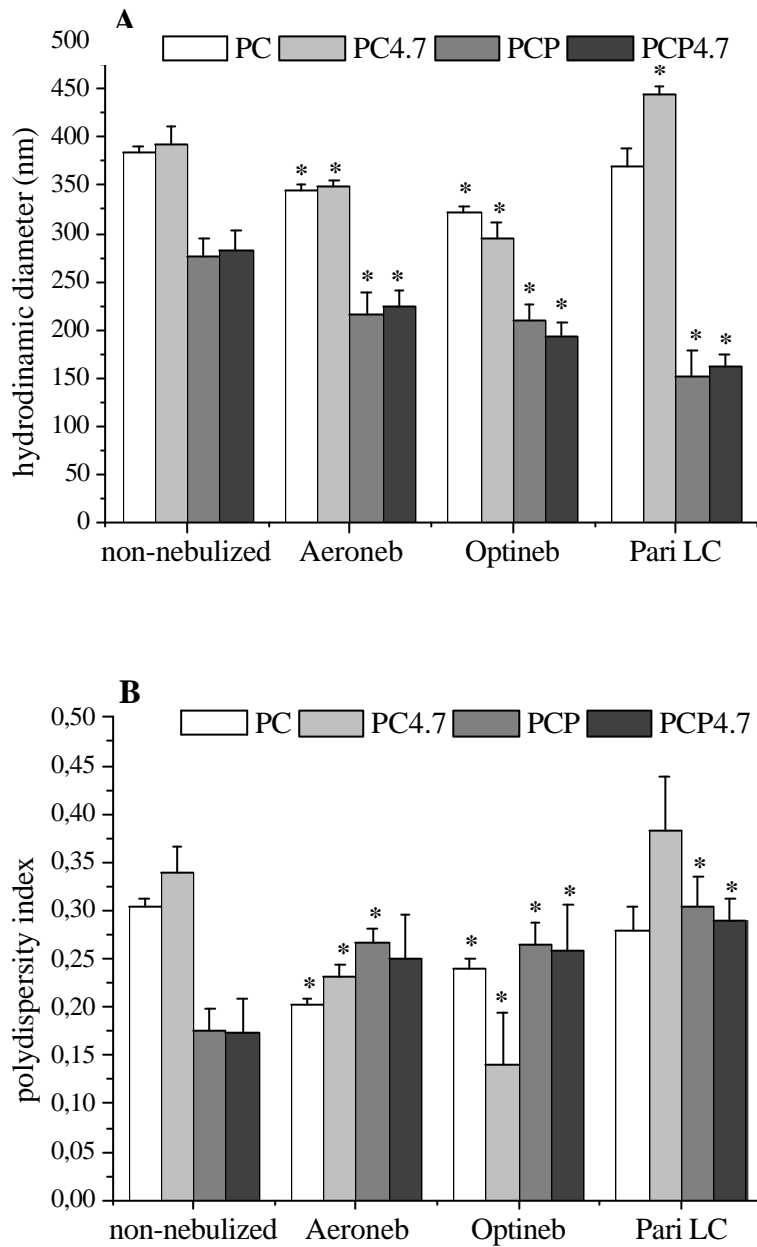*Figure 3. Size and polydispersity index of the non-nebulized and nebulized iloprost loaded liposomes measured by DLS. The mean particle sizes are given as z-average in nm ± SD and were determined by measuring 3 samples and repeating the measurement 5 times and significant differences (p = 0.05) between pre- and post-nebulized liposomes are marked with an asterisk.*

Transition temperature

The phase transition temperate (Tc) of the lipids and the COF loaded PC/PCP liposomes were determined using DSC and the values are displayed in Table 3. For the powdered lipid mixtures investigated here, phase transitions for each separate lipid could be identified, whereas for the liposomal formulations just one Tc could be observed, indicating the uniform distribution of the lipids throughout the bilayer membranes [20]. The phase transition of PC liposomes (Tc ~ 53 °C) appeared at a much higher temperature than observed with the PCP liposomes (Tc ~ 35 °C).

Table 3. Phase transition temperatures (Tc) of COF liposomes and lipid components determined by DSC. The values are given as mean of three measurement ± SD.

lipids	liposomes	Tc in °C
	PC-COF	52.8 ± 0.8
	PCP-COF	35.3 ± 0.6
DPPC		41.6 ± 0.3
CH		76.0 ± 0.5
DPPE-PEG		35.1 ± 1.0

COF and iloprost encapsulation

The percentages of drug encapsulated in the different liposomes are presented in Table 4. High encapsulation efficiency (4.6 %) was observed with the PC-COF liposomes, whilst the figure was lower for the PCP-COF liposomes (1.6 %).

Loading the PC liposomes with iloprost instead of COF led to a decreased encapsulation efficiency of 1.7 %. However, when the iloprost loaded PC liposomes were prepared with acetate buffer (pH 4.7) in place of PBS (pH 7.4), the loading efficiency increased considerably to 4.4 %. Loading the PCP liposomes with iloprost an encapsulation efficiency of 0.6 % was obtained using the common PBS or acetate buffer.

Table 4. Drug loading of the different liposomes: Encapsulation efficiency of COF and iloprost in liposomes in percent of the total quantity of drug initially used. Quantity of iloprost loaded in the liposomal formulations in µg/ml.

Liposomal formulation	drug loading efficiency COF liposomes [%]	drug loading efficiency iloprost liposomes [%]	drug loading iloprost liposomes [µg/ml]
PC	4.6 ± 0.3	1.7 ± 0.5	4.2 ± 1.2
PC4.7		4.4 ± 0.3	11.0 ± 0.7
PCP	1.6 ± 0.6	0.6 ± 0.08	1.4 ± 0.3
PCP4.7		0.6 ± 0.1	1.7 ± 0.5

Stability of COF liposomes

The percentage of COF encapsulated in the non-nebulized and nebulized liposomes refers to the total amount of drug in the dispersion, are presented in Figure 4. The PC-COF liposomes were considerably more stable than the PCP-COF liposomes during the nebulization process. Pre-nebulization, 99 % of COF was encapsulated in the PC-COF liposomes. During the nebulization process, the proportion of encapsulated COF decreased to 70 %, with no significant differences being observed between the three different nebulization methods. In the case of the PCP-COF liposomes, also 99 % of COF was encapsulated pre-nebulization. However, less than a half of this remained within the liposomes post-nebulization (47 % post-Aeroneb®, 45 % post-Optineb® and 39 % post-Pari®).

Figure 4. Percentage of COF encapsulated in the liposomes: 100 % represents the total quantity of COF in the liposomal dispersion. Significant differences (p = 0.05) between pre- and post-nebulized liposomes are marked with an asterisk.

Stability of iloprost liposomes

The proportions of iloprost encapsulated within the nebulized and non-nebulized liposomes are detailed in Figure 5. Similar to the PC-COF liposomes, the PC-ILO liposomes displayed an improved stability during the nebulization process when compared to the PCP liposomes. Altering the dispersion medium did not appear to lead to significant differences in the stability. A proportion of 98 % of encapsulated iloprost was observed in the non-nebulized PC-ILO liposomes. During the nebulization process this figure decreased to ~70 % for the Aeroneb® and the Optineb® nebulizers and to approximately 50 % for the Pari LC® nebulizer. The encapsulated iloprost within the PCP liposomes decreased from approximately 85 % pre-nebulization to 45 % post-Aeroneb®, 30 % post-Optineb® and 20 % post-Pari® nebulization.
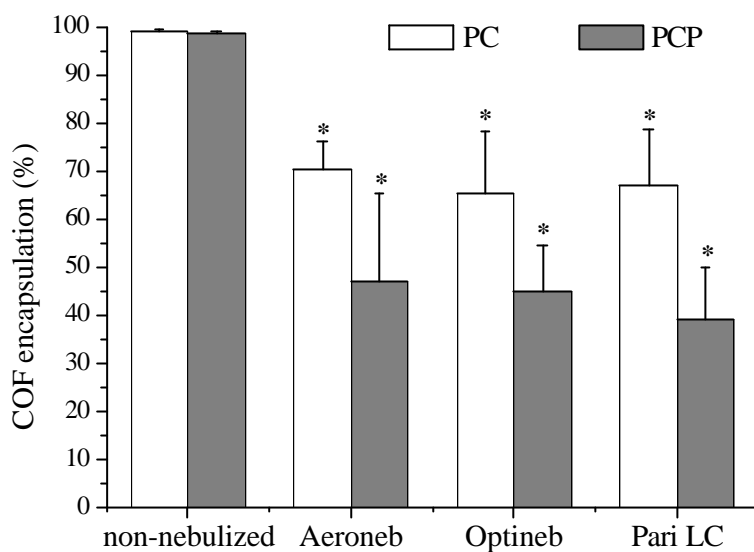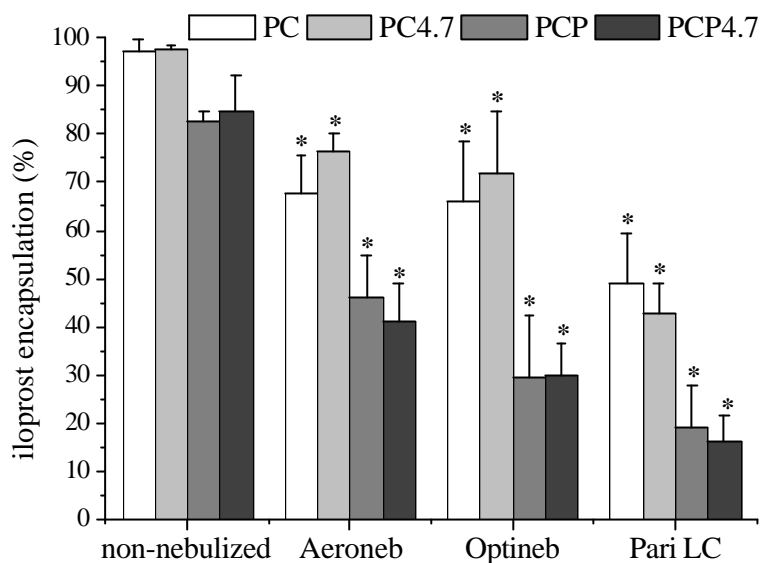
Figure 5. Percentage of iloprost encapsulated in the liposomes: 100 % represents the total quantity of iloprost in the liposomal dispersion. Significant differences (p = 0.05) between pre- and post-nebulized liposomes are marked with an asterisk.

DISCUSSION

In order to successfully treat PAH with iloprost it is vital that the drug is delivered to the alveolar region of the lung at a therapeutically effective concentration. Because the intraacinar pulmonary arteries are tightly surrounded by alveolar surfaces, it is possible to vasodilate these vessels by alveolar deposition of iloprost [21]. In general, aerosol droplets of 1-5 µm are considered optimal for penetrating to the lower respiratory tract [22, 23]. Particles of this size have been demonstrated to deposit in the lung via gravimentational sedimentation, inertial impactation or by diffusion into terminal alveoli by Brownian motion [24]. As such, the selection of the most suitable aerosolization device is a vitally important consideration. In this study we have investigated three types of nebulizer as prospective devices for the aerosolization of iloprost loaded liposomes. The air-jet nebulizer Pari LC[®] is a commonly used nebulizer and has been the focus of several studies concerning the delivery of drugs and lipid- or polymer-based nanoparticles [10, 25-27]. Ultrasonic nebulizers, such as the Optineb[®], have also been employed for the aerosolization of several drugs, liposomes, nanoparticles and DNA-complexes [28-31]. The Aeroneb[®] nebulizer has been used for the nebulization of liposomal formulations and has shown a significantly improved drug output when compared to the standard air-jet nebulizer [32]. The studies presented here indicate that

the three nebulizers are able to generate small aerosol droplets of both sodium chloride solutions and liposomal dispersions. As such, a substantial deposition of aerosol particles to the alveolar region can be assumed. The drug output of the Aeroneb® and Optineb® nebulizers were approximately 4 times higher than that of the Pari LC®. This represents a significant advantage when considering patient compliance for clinical purposes, since the inhalation time for a patient would be significantly reduced when using the Aeroneb® or the Optineb®.

Suitable drug delivery systems for the PAH therapy must satisfy several requirements, such as efficient drug loading, stability during aerosolization and small particle size. Hence, the aim of this study was to develop liposomal formulations that efficiently encapsulate iloprost, and show little or no alterations in particle size and drug encapsulation post-nebulization. To satisfy these requirements, the components used for the liposomal formulations play a predominant role. It has been reported that two major factors control the liposomal membrane stability, both of which are related to structural discontinuities and membrane defects in the lipid bilayer [33]. It was demonstrated that the utilization of long chain saturated acyl chains such as DPPC combined with optimal levels of CH in the liposomal membrane act to minimize both types of membrane defect, and the lipid bilayer is presented homogeneously [34]. Thus, using DPPC and CH appears to encourage the formation of more stable liposomes with regard to reduced permeability and increased liposome elasticity. Furthermore, the integration of grafted PEG lipids in the liposomal formulation (at a molar concentration of 5 to 7 %) reportedly increases liposomal stability in biological systems and decreases macrophage clearance [33, 35].

The lipid compositions used throughout this work were carefully selected by considering both our need for stable liposomes suitable for inhalation therapy, and previous findings from the literature. With regards to the liposome structure, thermotropic behaviour, size and encapsulation efficiency, the PC liposomes did indeed achieve our expectations. However, the PCP liposomes did not. This is discussed at length below.

The phase transition temperature (Tc) is particularly important when considering liposomal stability. Whereas below the Tc most lipids exist in a gel phase with hydrocarbon chains in a parallel order, above the Tc the lipids are conversed to the liquid crystalline phase. At the Tc the carbon chains disorder and defects in the lipid membrane occur. It has previously been demonstrated that phospholipids with Tc values greater than body temperature form more stable liposomes than those with lower Tc [36, 37]. Therefore, we expected to produce stable liposomes as a consequence of the high concentrations of DPPC (Tc ~ 41 °C) and CH (Tc ~ 76 °C) present in both liposomal formulations investigated.

However, we obtained an unexpectedly low value of approximately 35°C for the PCP liposomes and a much higher Tc of circa 53°C for the PC liposomes.

It is well known that numerous variables can influence the thermotropic behaviour of a lipid system. These include the interactions of foreign molecules (such as drugs or salt) with the bilayer, and the interactions between the lipid molecules themselves [20, 38]. As such, we believe that the incorporation of DPPE-PEG into the liposomal membrane brought about some change within the lipid bilayer, to such an extent that structural discontinuities or membrane defects occurred. This disordered membrane acted to lower the Tc as less energy was required to achieve transition. Membrane defects could also explain the poor stability of the PCP liposomal formulations observed during the nebulization. This finding is in agreement with a number of other studies that reported a decrease in stability as the liposomes Tc declined [20, 37-39]. In addition, our AFM images revealed the PC liposomes exhibited a smoother particle surface in comparison to the PCP liposomes, which may indicate a change in the bilayer structure.

Substances that are transported into the respiratory tract undergo two major clearance processes, the mucociliary and the alveolar macrophage clearance. Thus, the lung represents a particularly challenging system for the successful delivery and cellular uptake of liposomes. Particles of diameter larger than 5 µm are deposited mainly in the upper airways and bronchioles, and are hence susceptible to removal by the beating cilia. In order to prevent this, both the liposome and aerosol particulate diameters play important roles. A compromise must be found between the drug loading efficiency (which is enhanced with increasing liposomal size) and transport to the lower airways (which increases with decreasing particle diameter) [40]. The liposome diameters reported here were adjusted to 400 nm by extrusion. The hydrodynamic diameter observed for the PC liposomes were found to range around the adjusted size. The nebulization of those liposomes appeared to have little effect on the hydrodynamic diameter, particularly when using the Aeroneb®. Such a marginal alteration in the liposome size indicates a high stability of the PC liposomes during the nebulization process, which in turn is in agreement with the high phase Tc of these liposomes. In the case of the PCP liposomes, we observed a hydrodynamic diameter approximately 150 nm below the adjusted size of 400 nm. Such phenomenon has been reported before and smaller liposome sizes than the actual filter pore diameters were obtained when preparing eggPC/CH liposomes [19, 29]. When PCP-COF liposomes were nebulized, there was no size alteration observed. For the iloprost loaded PCP liposomes, nebulization using the Aeroneb® apparatus again encouraged minimal alteration in particle size and polydispersity measurements. This is a strong indication that the electric micro

pump Aeroneb® offers far milder aerosolization conditions in comparison to the ultrasonic or air-jet nebulizers.

The brought size range of the PC liposomes might be explained when considering the Tc. Taylor et al. reported for DPPC/CH liposomes: below the Tc in the presence of CH, phospholipid chains are more mobile and elastic than in the absence of CH as the CH prevents the hydrocarbon chain crystallising into the rigid crystalline gel phase [20]. In the present study the liposomal size adjustment by extrusion was performed at 60 °C, which is just above the Tc of PC liposomes. As such, the size extrusion process of the PC liposomes may well have been affected by the more elastic bilayer that would have existed at that temperature. Hence, rather than simply having any excess bilayers excoriated from the outer surface of the liposome, these more elastic liposomes will undergo some oval deformation whilst passing through the filter pores [20]. However, this does not occur with the PCP liposomes probably due to the membrane discontinuities resulting form DPPE-PEG incorporation, and extrusion of these liposomes resulted in particle sizes smaller than the adjusted 400 nm.

Carboxyfluorescein is a commonly used model drug for the investigation of liposomal formulations loaded with hydrophilic compounds [25, 41]. Therefore, we selected COF in order to evaluate suitable formulations for further studies with the ^{3}H-labeled iloprost. PC-COF liposomes offered relatively high encapsulation efficiency and their stability during aerosolization was significantly better than the PCP-COF liposomes. When PC liposomes were loaded with iloprost at pH 7.4 the encapsulation efficiency dropped. However when these liposomes were loaded with iloprost at pH 4.7, they regained their high encapsulation efficiency and they retained their good stability during nebulization. Iloprost has a pKa value of 4.7, indicating that at pH 4.7, 50 % of iloprost exists in the uncharged form whilst 50 % carries a proton. An acetate buffer with a pH close to the drug's pKa was selected for the iloprost encapsulation as the uncharged iloprost is more lipophilic and can be better incorporated into the bilayers. This method allowed us to develop an efficient iloprost loading procedure for PC liposomes. In general the remarkable lower encapsulation efficiency of PCP liposomes in comparison to PC liposomes might be related to the membrane defects in the lipid bilayers. Since the DPPE-PEG affected the lipid packing of the bilayer, the PCP liposome's Tc decreased remarkable and the drug loss increased significantly.

The moderate encapsulation efficiency of 1.6 % observed when COF was introduced into the PCP liposomes was not obtained when iloprost was encapsulated, even when the pH 4.7 acetate buffer was used, the efficiency ranged below 1 %. We believe a feasible explanation for this observation is that the hydrophilic PEG chains, which arise from the presence of DPPE-PEG

lipid in the formulation, extend into the liposomes aqueous interior. As such, the encapsulation efficiency of hydrophilic substances such as COF is enhanced in comparison to more amphiphilic molecules like iloprost (log P O/W = 1.6) [42].

The improved stability alongside the diminished drug loading of the PC liposomes is in agreement with a number of previous reports concerning liposomes containing DPPC and CH [39, 40]. As discussed above, we expected that the PCP liposomes would be stable during the nebulization process. However, these liposomes lost approximately double the quantity of drug when compared to the PC liposomes. The review by Lasic *et al.* concerning the integration of DPPE-PEG lipids in liposome bilayer implies that from a biological viewpoint, there is an increase in stability when these components are present within the formulation, whilst the increase in bilayer leakage caused by DPPE-PEG integration can be viewed as a decrease in stability [40]. This confirms our findings of low stability of PCP liposomes during nebulization.

PEG-ylated liposomes are currently used in numerous intravenous formulations, however, to the best of our knowledge, they have not yet been used in inhalation therapy. From the findings presented herein it can be concluded that PEG-ylated liposomes consisting of DPPC, CH and DPPE-PEG (in a molar ratio of 50:45:5) are not suitable for aerosolization, due to the high drug loss observed during nebulization.

Traditionally, air-jet nebulization has been employed to administer liposomes to the lung, but the high shear stresses generated during this process can cause the release of the drug encapsulated in the liposomes [43]. Desai *et al* reported a drug release of up to 50 % when ciprofloxacin or salbutanol containing liposomes were nebulized using the Pari LC$^{®}$ apparatus [44]. These results are comparable with our findings in the case of the PCP liposomes. However, the drug losses observed when nebulizing the PC liposomes with the Pari LC$^{®}$ apparatus were smaller, indicating these liposomes are a more convenient formulation for inhalation therapy.

An increased damage caused by the ultrasonic nebulizer in comparison to air-jet has previously been reported [29, 45]. Here we observed the opposite, both liposomal formulations displayed a higher stability when using the ultrasonic nebulizer Optineb$^{®}$ in comparison to the air-jet nebulizer Pari LC$^{®}$. A probably explanation for this controversial results is, that in the Optineb$^{®}$ apparatus the ultrasonic waves are not directly meet the drug content, they first have to pass a water contact medium. Hence the heating in our ultrasonic nebulizer is much reduced compared to the most commercial ultrasonic nebulizers. Therefore,

the Optineb® displays a more suitable aerosolizer than the majority of common used ultrasonic nebulizers.

We observed both the highest liposomal drug loss and alteration of particle size when the Pari LC® was employed for the liposomal aerosolization. The smallest loss of encapsulated drug was observed for PC liposomes when aerosolized with the Aeroneb®, making this the most stable formulation/nebulizer combination. Furthermore, the use of this nebulizer did not alter the hydrodynamic diameter of PC liposomes. A recent report also suggested the Aeroneb® apparatus is most suitable for the nebulization of sensitive drug compounds, such as proteins or peptides [32]. The authors pointed out that in contrast to common ultrasonic nebulizers, the temperature increase in the Aeroneb® is minimized because of the lower operating frequency and the energy required for nebulization is applied to the vibrational element rather than to the drug solution.

Liposomal aerosols have proven to be non-toxic in human and animal studies [46, 47]. In contrast to the rapid clearance of soluble drug from the lung, 50–60 % of phosphatidylcholine liposomes are retained in the lung for up to 24 hours after inhalation [48, 49]. Beside this, in the treatment of PAH patients a daily dose of inhaled iloprost is approximately 30 µg. Those are distributed into 6-12 inhalations per day due to the short half live of iloprost [1]. Here we have developed a liposomal formulation (PC4.7) containing 12 µg iloprost per ml. Assuming the liposomes are both retained for 24 hours in the lung and release all of the iloprost over this period of time, PAH patients would have to inhale 2.5 to 3 ml iloprost loaded PC liposomes once a day.

CONCLUSION

We conclude that iloprost encapsulated in liposomal formulation consisting of DPPC/CH (molar ratio 70:30) has the potential to become an effective sustained release drug delivery system for the inhalation therapy of PAH. Furthermore, we have observed improved liposomal stability, high mass output and small aerosol droplets when the ultrasonic or the electric micro pump nebulizer was employed. Additionally, the Aeroneb® features several other practical advantages as previously reported: it is small, portable, battery operated and leaves a, minimal residual volume [50]. Therefore, the nebulizer of choice for the application of iloprost liposomes should be the Aeroneb®. Further studies are required to prove the pharmacokinetics of liposomal drug release in vitro and in vivo, and will be performed in our laboratory.

REFERENCES

1. H. Olschewski and W. Seeger. Pulmonary hypertension: Pathophysiology, diagnosis, treatment, and development of a pulmonary-selective therapy. *UNI-MED Verlag AG, Bremen* (2002).
2. S. Archer and S. Rich. Primary pulmonary hypertension: a vascular biology and translational research "Work in progress". *Circulation* **102**: 2781-2791 (2000).
3. D. B. Badesch, S. H. Abman, G. S. Ahearn, *et al.* Medical therapy for pulmonary arterial hypertension - ACCP evidence-based clinical practice guidelines. *Chest* **126**: 35S-62S (2004).
4. V. V. McLaughlin, A. Shillington, and S. Rich. Survival in primary pulmonary hypertension - The impact of epoprostenol therapy. *Circulation* **106**: 1477-1482 (2002).
5. B. R. Vane JR. Pharmacodynamic profile of prostacyclin. *Am J Cardiol* **75**: 3A-10A (1995).
6. S. Rich and V. V. McLaughlin. The effects of chronic prostacyclin therapy on cardiac output and symptoms in primary pulmonary hypertension. *J Am Coll Cardiol* **34**: 1184-1187 (1999).
7. S. Kesten, J. Dainauskas, V. V. McLaughlin, *et al.* Development of nonspecific interstitial pneumonitis associated with long-term treatment of primary pulmonary hypertension with prostacyclin. *Chest* **116**: 566-569 (1999).
8. H. A. Ghofrani, F. Rose, R. T. Schermuly, *et al.* Amplification of the pulmonary vasodilatory response to inhaled iloprost by subthreshold phosphodiesterase types 3 and 4 inhibition in severe pulmonary hypertension. *Crit Car Med* **30**: 2489-2492 (2002).
9. H. Olschewski, H. A. Ghofrani, T. Schmehl, *et al.* Inhaled iloprost to treat severe pulmonary hypertension. *Ann Intern Med* **132**: 435-443 (2000).
10. J. L. Rau. Design principles of liquid nebulization devices currently in use. *Respir Care* **47**: 1257-1275 (2002).
11. O. N. M. McCallion, K. M. G. Taylor, M. Thomas, *et al.* Nebulization of fluids of different physicochemical properties with air-Jet and ultrasonic nebulizers. *Pharm Res* **12**: 1682-1688 (1995).
12. J. B. Fink, D. Schmidt, and J. Power. Comparison of a nebulizer using a novel aerosol generator with a standard ultrasonic nebulizer designed for use during mechanical ventilation. In I. Aerogen (ed), *ATS 2001* (2001).
13. R. N. Niven, T. M. Carvajal, and H. Schreier. Nebulization of liposomes III The effects of operating conditions and local environment. *Pharm Res* **9**: 515-520 (1992).
14. H. Schreier. Liposome Aerosols. *J Liposome Res* **2**: 145-184 (1992).
15. K. M. Taylor and J. M. Newton. Liposomes for controlled delivery of drugs to the lung. *Thorax* **47**: 257-259 (1992).
16. W. S. Hung OR, Varvel JR, Shafer SL, Mezei M. Pharmacokinetics of inhaled liposome-encapsulated fentanyl. *Anesthesiology* **83**: 277-284 (1994).
17. T. Schmehl, T. Gessler, and E. Waschkowitz. WO 2003/084507A3 Atomizable liposomes and the use for the pulmonary administration of active substances. (2003).
18. V. P. Torchilin and V. Weissig. Liposomes - A practical approach, *Oxford University Press, Oxford*, 2003.
19. R. C. MacDonald, R. I. MacDonald, B. P. M. Menco, *et al.* Small-volume extrusion apparatus for preparation of large, unilamellar vesicles. *Biochim Biophys Acta* **1061**: 297-303 (1991).

20. K. M. G. Taylor and R. M. Morris. Thermal-analysis of phase-transition behaviour in liposomes. *Thermochim Acta* **248**: 289-301 (1995).

21. H. Olschewski, B. Rohde, J. Behr, *et al.* Pharmacodynamics and pharmacokinetics of inhaled iloprost, aerosolized by three different devices, in severe pulmonary hypertension. *Chest* **124**: 1294-1304 (2003).

22. D. A. Groneberg, C. Witt, U. Wagner, *et al.* Fundamentals of pulmonary drug delivery. *Respir Med* **97**: 382-387 (2003).

23. P. W. Barry and C. O'Callaghan. Inhalational drug delivery from seven different spacer devices. *Thorax* **51**: 835-840 (1996).

24. A. J. Hickey, T. B. Martonen, and Y. Yang. Theoretical relationship of lung deposition to the fine particle fraction of inhalation aerosols. *Pharm Acta Helv* **71**: 185-190 (1996).

25. R. Abu-Dahab, U. F. Schäfer, and C. M. Lehr. Lectin-functionalized liposomes for pulmonary drug delivery: effect of nebulization on stability and bioadhesion. *Eur J Pharm Sci* **14**: 37-46 (2001).

26. P. A. Bridges and K. M. G. Taylor. An investigation of some of the factors influencing the jet nebulization of liposomes. *Int J Pharm* **204**: 69-79 (2000).

27. S. T. Dailey LA, Gessler T, Wittmar M, Grimminger F, Seeger W, Kissel T. Nebulization of biodegradable nanoparticles: impact of nebulizer technology and nanoparticle characteristics on aerosol features. *J Control Release* **86**: 131-144 (2003).

28. K. M. G. Taylor and O. N. M. McCallion. Ultrasonic nebulizers for pulmonary drug delivery. *Int J of Pharm* **153**: 93-104 (1997).

29. K. K. M. Leung, P. A. Bridges, and K. M. G. Taylor. The stability of liposomes to ultrasonic nebulization. *Int J Pharm* **145**: 95-102 (1996).

30. L. A. Dailey, T. Schmehl, T. Gessler, *et al.* Nebulization of biodegradable nanoparticles: impact of nebulizer technology and nanoparticle characteristics on aerosol features. *J Control Release* **86**: 131-144 (2003).

31. E. Kleemann, L. A. Dailey, H. G. Abdelhady, *et al.* Modified polyethylenimines as non-viral gene delivery systems for aerosol gene therapy: Investigations of the complex structure and stability during air-jet and ultrasonic nebulization. *J Control Release* **100**: 437-450 (2004).

32. R. Dhand. New frontiers in aerosol delivery during mechanical ventilation. *Respir Care* **49**: 666-677 (2004).

33. Y. Barenholz. Liposome application: problems and prospects. *Current Opinion in Colloid & Interface Science* **6**: 66-77 (2001).

34. O. G. Mouritsen and K. Jorgensen. A New Look at Lipid-Membrane Structure in Relation to Drug Research. *Pharm Res* **15**: 1507-1519 (1998).

35. D. D. Lasic and D. Needham. The Stealth Liposomes: A Prototypical Biomaterial. *Chem Rev* **95**: 2601-2627 (1995).

36. D. Crommelin and H. Schreier. Liposomes in colloidal drug delivery systems. *Marcel Dekker, New York* (1994).

37. M. Anderson and A. Omri. The effect of different lipid components on the in vitro stability and release kinetics of liposome formulations. *Drug Deliv* **11**: 33-39 (2004).

38. S. C. Semple, A. Chonn, and P. R. Cullis. Influence of cholesterol on the association of plasma proteins with liposomes. *Biochem* **35**: 2521-2525 (1996).

39. M. Grit and D. J. Crommelin. Chemical stability of liposomes: implications for their physical stability. *Chem Phys Lipids* **64**: 3-18 (1993).

40. D. D. Lasic. Novel applications of liposomes. *Trends Biotechnol* **16**: 307-321 (1998).

41. M. Brandl, M. Drechsler, D. Bachmann, *et al*. Preparation and characterization of semi-solid phospholipid dispersions and dilutions thereof. *Int J Pharm* **170**: 187-199 (1998).
42. Schering AG. Sicherheitsdatenblatt Iloprost, Berlin, 1-5 (1997).
43. R. N. Niven and H. Schreier. Nebulization of liposomes I Effects of lipid composition. *Pharm Res* **7**: 1127-1133 (1990).
44. T. R. Desai, R. E. Hancock, and W. H. Finlay. A facile method of delivery of liposomes by nebulization. *J Control Release* **84**: 69-78 (2002).
45. P. A. Bridges and K. M. G. Tayler. Nebulizers for the generation of liposomal aerosols. *Int J Pharm* **173**: 117-125 (1998).
46. M. A. Myers, D. A. Thomas, L. Straub, *et al*. Pulmonary effects of chronic exposure to liposome aerosols in mice. *Exp Lung Res* **19**: 1-19 (1993).
47. J. C. Waldrep, B. E. Gilbert, C. M. Knight, *et al*. Pulmonary delivery of beclomethasone liposome aerosol in volunteers. Tolerance and safety. *Chest* **111**: 316-323 (1997).
48. Y. Morimoto and Y. Adachi. Pulmonary uptake of liposomal phosphatidylcholine upon intratracheal administration to rats. *Chem Pharm Bull (Tokyo)* **30**: 2248-2251 (1982).
49. A. Pettenazzo, A. Jobe, M. Ikegami, *et al*. Clearance of phosphatidylcholine and cholesterol from liposomes, liposomes loaded with metaproterenol, and rabbit surfactant from adult rabbit lungs. *Am Rev Respir Dis* **139**: 752-758 (1989).
50. R. Dhand. Nebulizers that use a vibrating mesh or plate with multiple apertures to generate aerosol. *Respir Care* **47**: 1406-1416 (2002).

Chapter 7

Summary and Perspectives

SUMMARY AND PERSPECTIVES

This thesis describes the development and characterization of a variety of polymeric and liposomal drug delivery systems for use in pulmonary aerosol therapy. A variety of polyethylenimines (PEIs) were studied in depth in an attempt to develop biocompatible gene vectors for efficient non-viral gene therapy for the lung (Chapter 2-5). Another study (Chapter 6) investigates a number of lipid-based nanoparticles that were specifically designed to act as sustained release formulations for pulmonary drug delivery.

The investigations presented in Chapter 2 form the foundations of this thesis by evaluating the general suitability of PEI as a gene vector in an aerosol therapy. Four different PEI modifications (branched, linear, polyethylenglycol-grafted and biodegradable PEI) copolymer were utilized as carriers for plasmid DNA (pDNA), with the resulting polyplexes displaying diameters of approximately 100 nm. These were extensively characterized with respect to identifying any structural and/or physico-chemical alterations that occurred during aerosolization with both air-jet and ultrasonic nebulizer. A number of techniques including atomic force microscopy (AFM), dynamic light scattering (DLS) and laser Doppler anemometry (LDA) were employed to determine the various morphologies, diameters and zeta-potentials of the polyplexes pre- and post-aerosolization. The PEI modifications and displaying stronger DNA condensation were shown to form more stable polyplexes, due to the reduced level of damage observed post- aerosolization. The poly (ethylene glycol) PEI copolymer (PEGPEI) was shown to have the superior carrier properties regarding DNA condensation and protection. Furthermore, our results suggested that improved stability for PEI/DNA polyplexes can be attained using the ultrasonic nebulizer in preference to the air-jet apparatus. Thus, we concluded that ultrasonic nebulization is a milder aerosolization method for PEI-based gene delivery systems. Additionally, PEGPEI appeared to display the most promising properties as a pulmonary gene carrier, due to its stability. Therefore, we decided to employ the PEGPEI copolymer in addition to the commonly used branched 25 kDa PEI (BPEI) in the subsequent studies.

Our primary aim in Chapter 3 was the development of a gene vector that achieves both high transgene expression and biocompatibility in the pulmonary epithelium. To accomplish this aim, a low molecular weight (5 kDa) PEI (LMWPEI) and a PEGPEI copolymer were employed as pDNA vectors and compared with the commonly utilized BPEI. Investigations of the polyplex morphologies (using AFM), sizes (by DLS) and zeta-potentials (using LDA) revealed that all three polymers are able to condense pDNA, forming small, positively charged particles of approximately 100 nm diameter. Cytotoxicity studies, performed using

the MTT- and LDH-assay, indicated LMWPEI had the superior biocompatibility of the three polymers investigated. The transfection efficiencies of the three polyplexes were studied both in vitro (cell cultured lung epithelia) and in vivo (intratracheally instillation to the mouse lung). Whilst LMWPEI polyplexes were shown to be inefficient in transfecting lung epithelial cells in vitro, they caused the highest transfection rate in the mouse lung. Interestingly, the opposite behaviour was observed when PEGPEI polyplexes were investigated, with a high gene expression in vitro not being reproduced in vivo. We hypothesized that the polyplexes relative stability in the lung environment might explain this observation. In order to investigate the polyplex stability, natural lung lining fluid and lung surfactant were utilized, and a decreasing trend of DNA encapsulation in the order: PEGPEI > BPEI > LMWPEI was observed. Therefore, we concluded that stronger interactions between the carrier and the pDNA may hinder the DNA release under in vivo conditions, thus reducing the transfection efficiency. Our results indicated that LMWPEI fulfils the key requirements of low cytotoxicity and high gene expression in the mouse lung.

Based upon the promising results of Chapter 3 the biocompatibility of LMWPEI/DNA in the mouse lung was further investigated, and the results are presented in Chapter 4. Polyplexes were applied via instillation, and after 48 hours lung lavages were performed. The bronchial alveolar lining fluid (BALF) obtained was subsequently investigated for total cell counts, quantity of neutrophils and macrophages as well as total protein and cytokine concentrations. These parameters are hallmarks of acute lung inflammation, and increased values were observed for all investigated systems in comparison to the control mice. In the case of pDNA and LMWPEI/DNA, only minor alterations were detected whereas BPEI/DNA caused stronger inflammation and surprisingly PEGPEI/DNA led to the most severe inflammation. When considering these findings together with the transfection results obtained in vivo (Chapter 3), we concluded that increasing cytotoxicity in the mouse lung (LMWPEI < BPEI < PEGPEI) causes decreasing transfection efficiency (LMWPEI > BPEI > PEGPEI). As such, LMWPEI was chosen as our preferred pDNA carrier for inhalation therapy. In parallel to this work, we developed a novel aerosol inhalation device for mice. Unfortunately, the transfection rate in the mouse lung decreased dramatically post- LMWPEI/DNA aerosolization in comparison to the instilled polyplexes. In an attempt to identify the reasons for this failure, we employed double-labeled polyplexes in order to compare the lung distribution of inhaled versus instilled polyplexes. The nebulized LMWPEI polyplexes were shown to be uniformly localized throughout the mouse lung in small quantities. In contrast, the instilled polyplexes were detected in much higher concentrations, in bronchial and

alveolar regions, but were not evenly distributed. Interestingly, polyplexes were observed in epithelial and endothelial cells. Consequently, LMWPEI represents a highly efficient and biocompatible gene vector for the lung and is superior to the more commonly used BPEI.

Another study (Chapter 5) describes the development and characterisation of a novel gene vector that is based upon BPEI covalently linked to a TAT peptide (a protein transduction domain) via a PEG spacer. The oligopeptide TAT was chosen to enhance cell uptake into lung cells, since reports had demonstrated high translocation ability of TAT by direct crossing biological membranes. In keeping with the two previous studies, the TAT-PEG-PEI conjugate was extensively investigated in terms of DNA condensation, DNA protection in the intra- and extracellular lung environment, polyplex size, stability, zeta-potential, in vitro and in vivo toxicity, transfection efficiency and polyplex distribution in the mouse lung. Since our key aim had been to develop a non-toxic, highly efficient carrier for the epithelial cells of the conducting and respiratory airways, this new carrier fulfilled the majority of our requirements. It was able to form very small and stable particles with pDNA. A ~600% improved gene expression in the mouse lung was observed for TAT-PEG-PEI polyplexes in comparison to BPEI and a ~300% improved gene expression in comparison to LMWPEI. Furthermore, only minor effects upon the lung function were observed, with no additional inflammation compared to pDNA instillation alone. A particular advantage of this carrier is its ability to transport DNA safely into the different cell types of the lung. Hence, it could be employed in the treatment of pulmonary diseases that attack the entire lung, such as lung cancer.

Consequently, the TAT-PEG-PEI conjugate and to a lower extend also LMWPEI represent promising new approaches in pulmonary gene therapy of various lung disorders. Further work is necessary to decrease the cytotoxicity to a level where no inflammation is observed. This might be achieved by using either a highly branched PEGPEI copolymer or a LMWPEI in place of BPEI for the synthesis of TAT-PEG-PEI. Since a number of recent studies have reported conflicting results regarding the cellular uptake and pathway of TAT peptides, a study should be performed in order to track the pathway of TAT-PEG-PEI polyplexes into the cells and nucleus. Further work should focus on the development of a cell specific gene vector for pulmonary gene therapy. In this respect, the synthesis of LMWPEI modifications carrying target moieties such as lectin, folate, peptides (e.g. RGD) or antibodies would be of particular interest. The next major set of experiments should focus on the delivery of therapeutic genes such as IL-12, p53, prostacyclin or nitric oxide synthase, via optimized TAT-PEG-PEI or LMWPEI vehicles. Additionally, the challenge of efficient

polyplex administration to mice via aerosol inhalation remains. Improvements of the nebulization system developed here may be achieved by employing a so called 'drying spacer', a development recently reported by Rudolph et al.

Currently the drug iloprost is approved for the aerosol therapy of pulmonary hypertension. However, the effectiveness of this formulation is limited by the short half live of iloprost in vivo. As such, the aim of the study presented in Chapter 6 was to develop a sustained releasing formulation for iloprost. A variety of lipid combinations were studied in order to find a formulation that accomplish both, encapsulate high quantities of iloprost and is stable throughout the aerosolization process. Initially, the model drug Carboxyfluorescein was encapsulated in liposomes consisting of Dipalmitoyl-phosphatidylcholin (DPPC) and Cholesterol (CH), or DPPC, CH and PEG-dipalmitoyl-phoshatidylethanolamine (DPPE-PEG). Liposomal morphology was studied using AFM and the liposome phase transition temperatures were investigated using differential scanning calorimetry. Their stability during aerosolization was investigated using air-jet, ultrasonic and micro pump nebulizers. These nebulizers were compared in terms of mass output, aerosol droplet size and their effects upon the liposome stability. Regarding liposome size and drug loading pre- and post-nebulization, the DPPC/CH liposomes were shown to be the most stable formulation, particularly during ultrasonic and micro pump nebulization. In a second study, Iloprost-loaded liposomes were prepared and we were able to show that the DPPC/CH liposomes again displayed the highest encapsulation efficiency and stability during ultrasonic and micro pump nebulization. We concluded that DPPC/CH liposomes are well suited to act as a sustained release formulation for the treatment of pulmonary hypertension.

This study highlights the clear possibilities that exist for the development of a pulmonary sustained release formulation for the treatment of pulmonary hypertension. The next steps would focus on drug release and cellular uptake studies in lung epithelial cells, followed by pharmacokinetic studies in an ex vivo animal model. The effectiveness of the liposomal iloprost formulation should be further investigated by employing an animal pulmonary hypertension model, e.g. holding mice under hypoxia conditions.

The novel approaches and technologies described in this thesis represent small but important advances in the application of aerosol therapy to the treatment of acquired diseases. Hopefully formulations similar to those described here will one day offer significantly improved treatments for people suffering from a range of illnesses.

ZUSAMMENFASSUNG UND AUSBLICK

Inhalt dieser Arbeit war die Entwicklung und Charakterisierung verschiedener polymer- und lipid-basierter nanopartikulärer Formulierungen mit dem Ziel, diese bei der inhalativen Behandlung von Lungenerkrankungen einzusetzen zu können. Eine Reihe von Polyethyleniminen (PEI) wurde auf ihre Verwendbarkeit als nicht-virale biokompatible DNA-Transporter für eine Lungen-Gentherapie untersucht (Kapitel 2-5). Eine weitere Studie (Kapitel 6) verfolgte das Ziel Liposomen zu entwickeln, die für eine kontrollierte Wirkstofffreigabe nach Inhalation geeignet sind.

Die Untersuchungen des Kapitels 2 stellen in dieser Dissertation, die Grundlage der Evaluierung von PEI als inhalierbare DNA Transporter zu dienen, dar. Es wurden vier verschiedene PEI-Modifikationen (verzweigtes, lineares, bioabbaubares & Polyethylenglycol-modifiziertes PEI) ausgewählt, die mit plasmidischer DNA (pDNA) Partikel in der Größenordnung von ca. 100 nm formten. Diese so genannten Polyplexe wurden hinsichtlich ihrer strukturellen und physikochemischen Veränderung während der Vernebelung mit einem Düsen- bzw. einem Ultraschallvernebler charakterisiert. Für diese Untersuchungen fanden verschiedene Techniken Anwendung, wie die Rasterkraftmikroskopie, die dynamische Lichtstreuung und die Laser Doppler Anemometrie. Damit konnten die Parameter Polyplex-Morphologie, Größe bzw. Zeta-Potential vor und nach den Vernebelungen bestimmt werden. Die Ergebnisse dieser Untersuchungen zeigten, dass die PEI Modifikationen, die am stärksten die pDNA komplexierten, die geringsten Veränderungen während der Vernebelung erfuhren. Dabei hatte das Polyethylenglycol-PEI (PEGPEI) die besten Eigenschaften hinsichtlich, DNA Komplexierung und Schutz bei der Vernebelung. Ein Vergleich der beiden Verneblersysteme ergab, dass alle Polyplexe am stabilsten während der Ultraschallverneblung waren. Als Schlussfolgerung dieser Studie, stellten wir die Ultraschall-Vernebelung als die geeignetere Methode für die Verabreichung von PEI-basierten Gentransfersystemen in die Lunge heraus. Des Weiteren sind die guten Stabilitätseigenschaften des PEGPEI hervorzuheben, auf Grund dessen wir in den darauf folgenden Studien PEGPEI als Vektor, neben dem Standartvektor verzweigtes 25 kDa PEI (BPEI), für die Pulmonale DNA Applikation verwendeten.

Das Ziel der zweiten Studie (Kapitel 3) war die Entwicklung eines biokompatiblen und effizienten Systems für den Gentransport in die Lungen Epithelzellen. Dafür wurden zwei PEI Modifikationen verwendet, ein niedermolekulares PEI (LMWPEI) und das schon beschriebene PEGPEI, die mit dem Standart-Vektor BPEI verglichen wurden. Die Untersuchungen der Polyplex Morphologie (Rasterkraftmikroskopie), Größe (Dynamischer Lichtstreuung) und Zeta-Potential (Laser Doppler Anemometrie) zeigten, dass alle drei

Polymere die pDNA vollständig kondensierten und mit dieser kleine, positiv geladene Partikel von ca. 100 nm formten. Zur Untersuchung der Polymer-Toxizität in vitro wurden MTT- und LDH-Assays durchgeführt. Dabei stellte sich heraus, dass das LMWPEI die beste Biokompatibilität aufweist. Die Transfektionseffizienz der drei verschiedenen Vektoren wurde in vitro an einer Lungenepithelzelllinie und in vivo in Mäuselungen nach intratrachealer Instillation untersucht. Dabei wurde für LMWPEI im Vergleich zu BPEI und PEGPEI in vitro die geringste Genexpression detektiert, während die Transfektionsrate in der Mäuselunge für das LMWPEI am höchsten war. Interessanterweise beobachteten wir für PEGPEI ein genau gegensätzliches Verhalten und die sehr hohe Genexpression in der Zellkultur konnte in den Tierversuchen nicht reproduziert werden. Auf Grund dieser Beobachtungen stellten wir die Hypothese auf, dass eine gute Stabilität der Polyplexe im Mucus, im Surfactant und im Zellplasma, die Transfektion in vivo verändern könnten. Um dies zu untersuchen, wurden die Polyplexe mit Lavagen von Mäuselungen und mit natürlichem Surfactant inkubiert. Es konnte eine abnehmende Stabilität der Polyplexe in der Reihenfolge: PEGPEI > BPEI > LMWPEI beobachtet werden. Daraus schlussfolgerten wir, dass starke Wechselwirkungen zwischen dem Polymer und der DNA in vivo zu einer schlechteren Freigabe der DNA führt und somit die Transfektionseffizienz verringert. Die Ergebnisse der Studie in Kapitel 3 zeigten, dass mittels LMWPEI im Tiermodel ein biokompatibler und effizienter Genvektor für die Lungentherapie entwickelt werden konnte.

Diese viel versprechenden Ergebnisse gaben Anlass zu weiterführenden Studien über die Verträglichkeit von LMWPEI in der Mäuselunge (Kapitel 4). Dazu wurden die Polyplexe von LMWPEI im Vergleich zu BPEI und PEGPEI via Instillation in die Mäuselunge verabreicht und nach 48 Stunden wurden die Lungen lavagiert. Diese Lavagen wurden dann hinsichtlich Entzündungsfaktoren wie Gesamtzellzahl, Anzahl der Neutrophilen und der Makrophagen, Konzentration der Gesamtproteine und der Zytokine untersucht. Dabei wurden sowohl für die pDNA als auch die Polyplexe erhöhte Werte gemessen, diese konnten eingestuft werden in leichte Entzündungen bei der DNA und LMWPEI/DNA, mittlere Lungenentzündung bei BPEI/DNA und starke Lungenentzündung bei PEGPEI/DNA. Die Betrachtung dieser Ergebnisse im Zusammenhang mit den Transfektionsraten führte uns zu der Schlussfolgerung, dass mit zunehmender Toxizität in der Mäuselunge (LMWPEI < BPEI < PEGPEI) die Transfektionseffizienz (LMWPEI > BPEI > PEGPEI) abnimmt. Folglich wählten wir das LMWPEI für weitergehende Versuche zur Aerosolapplikation in die Lunge aus. Dafür entwickelten wir ein neues Inhalationssystem für Mäuse. Bedauerlicherweise nahmen die Transfektionsraten von LMWPEI/DNA nach der Vernebelung im Vergleich zur

Instillation um den Faktor 50 ab. Um den Grund für diese drastische Abnahme zu erkunden, stellten wir Polyplexe her, bei denen sowohl die pDNA als auch das LMWPEI fluoreszenzmarkiert waren und verglichen deren Lungenverteilung nach Instillation mit der nach Inhalation. In den Konfocale Fluoreszenzmikroskopischen Untersuchungen der Lungenschnitte zeigte sich, dass die vernebelten Polyplexe gleichmäßig in der Lunge verteilt waren, jedoch in sehr geringen Mengen. Im Gegensatz dazu waren die Polyplexe nach der Instillation in sehr hohen Konzentrationen sowohl in den Bronchien als auch in den Alveolen vorhanden, jedoch wurden nicht alle Abschnitte der Lunge erreicht. Des Weiteren beobachteten wir erstmalig, dass LMWPEI/DNA auch in die Lungenendothelzellen aufgenommen wurde. Zusammenfassend ergibt sich, dass LMWPEI ein sehr effizienter sowie biokompatibler Genvektor für die Lungentherapie ist, und diesbezüglich auch viel bessere Eigenschaften als das häufig eingesetzte BPEI aufweist.

In einer weiteren Studie (Kapitel 5) ist die Entwicklung eines neuen Genvektors beschrieben, der mit einem TAT-Peptid (eine Proteintransduktionsdomaine) modifiziert wurde. Dazu wurde das TAT Peptid an BPEI über eine PEG-Kette kovalent gebunden. Dieses neue PEI Konjugat wurde, wie schon die zuvor beschriebenen Vektoren, hinsichtlich Kondensation der pDNA, Schutz der pDNA im extra- und intrazellulärem Lungenmilieu, Polyplexgröße, Stabilität, Zeta-Potential, in vitro und in vivo Transfektionseffizienz sowie Toxizität und Verteilung der Polyplexe in der Mäuselunge untersucht. Unser Ziel war es gewesen, einen nicht toxischen und sehr effizienten Genvektor zu entwickeln. Dies konnte mit dem neuem TAT-PEG-PEI weitgehend erreicht werden. Dieses Konjugat war in der Lage, sehr kleine und stabile Partikel mit pDNA zu formen. In der Mäuselunge wurde für die TAT-PEG-PEI Polyplexe ein Anstieg der Genexpression von ~600 % im Vergleich zu BPEI und ~300 % im Vergleich zu LMWPEI beobachtet. Weiterhin konnten wir eine hervorragende Verträglichkeit in vivo feststellen, und die Werte der Indikatoren eine Entzündungsrektion lagen im Bereich derer von pDNA. Ein weiterer Vorteil von TAT-PEG-PEI war der sichere Transport der pDNA in die verschiedenen Zellentypen der Lunge. Aus diesem Grund könnte dieser neu Genvektor für die Behandlung verschiedener Lungenerkrankungen eingesetzt werden, bei der verschiedenste Zelltypen betroffen sind, wie z.B. beim Lungenkrebs.

Das wichtigste Ergebnis dieser vier beschriebenen Studien ist, dass TAT-PEG-PEI und im geringerem Maße auch LMWPEI als gut verträgliche und effiziente Vektoren das Potential besitzen, in der Gentherapie verschiedener Lungenerkrankungen Anwendung zu finden. Selbstverständlich sind weitergehende Studien notwendig, um die zwar geringe aber doch vorhandene Toxizität der Polyplexe weiter zu reduzieren. Dieses Ziel könnte beispielsweise

erreicht werden, indem man für die Synthese von TAT-PEG-PEI das LMWPEI oder ein hochsubstituiertes PEGPEI verwendet. Des Weiteren sollte die Aufnahme von TAT-PEG-PEI Polyplexen in die Zelle genauer untersucht werden, da bisher widersprüchliche Studien über die Aufnahme und den Weg des TAT Peptides in der Zelle existieren. Weitergehende Studien hinsichtlich zellspezifischer Genvektoren sollten durchgeführt werden. Es wäre z.B. möglich, das LMWPEI mit einer zielgerichteten Struktur zu modifizieren, wie z.B. Lectin, Folat, einem Antikörper oder Peptiden wie z.B. das RGD. Der nächste Schritt sollte dann darin bestehen, therapeutische Gene (IL-12, p53, NO oder Prostacyclin Produzenten) mittels der optimierten Vektoren TAT-PEG-PEI und LMWPEI in die Lungenzellen zu transportieren. Des Weitern sollte versucht werden, das Vernebelungssystem für die in vivo Versuche zu verbessern, z.B. durch einen so genannten „Trocknenden Spacer", wie er kürzlich von Rudolph et al. (2005) beschrieben wurde.

Die fünfte Studie dieser Arbeit (Kapitel 6) beschreibt lipid-basierte Formulierungen als inhalierbare Drug Delivery Systeme. Der Wirkstoff Iloprost ist zugelassen in der Aerosoltherapie der Arteriellen Pulmonalen Hypertonie. Jedoch ist die Wirksamkeit dieses Stoffes begrenzt durch seine kurze Halbwertszeit. Infolgedessen war das Ziel der Studie die Entwicklung einer Formulierung, die Iloprost über einen verlängerten Zeitraum freisetzt. Solch eine Formulierung sollte beides gewährleisten: eine hohe Wirkstoffverkapselung und Stabilität während der Vernebelung. Dazu wurden verschiedene Lipidkombinationen für die Herstellung von Liposomen untersucht. Zuerst wurde die Modellsubstanz Carboxyfluorescein in Liposomen verkapselt, die aus Dipalmitoyl-phosphatidylcholin (DPPC) und Cholesterol (CH), oder aus DPPC, CH und PEG-dipalmitoyl-phoshatidylethanolamine (DPPE-PEG), bestanden. Die Stabilität dieser Liposomen wurde an drei verschiedenen Verneblern untersucht: Düsen-, Ultraschall- und Mikropumpenvernebler. Diese Systeme wurden hinsichtlich der Menge an produziertem Aerosol, der Aerosoltropfengröße und deren Einfluss auf die Liposomen verglichen. Dabei wurde die Stabilität der Liposomen in Bezug auf Liposomengröße und der Wirkstoffverkapselung, jeweils vor und nach der Vernebelung beurteilt. Es stellte sich heraus, dass die DPPC/CH Liposomen am stabilsten waren, insbesondere nach der Vernebelung mit dem Ultraschall- und dem Mikropumpenverneblern. In einer zweiten Versuchsreihe wurden die Liposomen mit Iloprost beladen. Dabei wurde die höchste Stabilität und Verkapselungseffizienz ebenfalls für die DPPC/CH Liposomen vor allem nach der Mikropumpenverneblung gefunden. Demzufolge schlussfolgerten wir, DPPC/CH Liposomen sind als eine Formulierung mit verlängerter Wirkstofffreigabe in der

Behandlung der pulmonalen Hypertonie gut geeignet. Bis dieses Ziel erreicht werden kann, sind jedoch noch viele weiterführende Untersuchungen notwendig, und die hier präsentieren Ergebnisse stellen erst den Grundstein dafür dar. Als nächste Schritte sollten die Aufnahme der Liposomen in Lungenepithelzellen bzw. die Wirkstofffreisetzung untersucht werden, gefolgt von pharmakokinetischen ex vivo Studien. Danach sollte die Wirksamkeit der Iloprost-Liposomen an einem Tiermodel untersucht werden, bei dem, z.B. ausgelöst durch die Haltung in Hypoxie, eine pulmonale Hypertonie besteht.

Die neuen Formulierungen und Technologien, die in dieser Dissertation beschrieben sind, stellen zwar nur einen kleinen, aber dennoch wichtigen Fortschritt in der Entwicklung von neuen Therapieformen für die Behandlung von Lungenerkrankungen dar. Derartige Formulierungen geben Anlass zur Hoffnung eines Tages die Behandlung von schwerkranken Patienten deutlich zu verbessern.

Appendices

ABBREVENTIONS

AAV	Adenoassociated Virus
AFM	Atomic force microscopy
ARDS	Acute respiratory distress syndrome
BALF	Bronchial alveolar lining fluid
bioPEI	Poly(ethylenimine-co-L-lactamide-co-succinamide) (8 kDa)
BPEI	Branched polyethyleneimine (25 kDa)
CF	Cystic fibrosis
COF	5(6)-Carboxyfluorescein
CH	Cholesterol
CLSM	Confocal laser scanning microscopy
COPD	Chronic obtrusive pulmonary disease
DLS	Dynamic light scattering
DPI	Dry powder inhaler
DPPE-PEG	Polyethylenglycol-dipalmitoyl-phosphatidylethanolamin
DPPC	Dipalmitoyl-phosphatidylcholin
DSC	Differential scanning calorimeter
EtBr	Ethidium bromide
GFP	Green fluorescence protein
GnRH	Gonadotropin releasing hormone
GSD	Geometric standard deviation
Hgh	Human growth hormone
HIV	Human immunodeficiency virus
IL	Interleukin
ILO	Iloprost
LDA	Laser Doppler anemometry
LDH	Lactat dehydrogenase
linPEI	Linear polyethyleneimine (22 kDa)
LMWPEI	Low molecular weight polyethylenimine
MDI	Metered dose inhaler
MMAD	Mass median aerodynamic diameter
MTT	(3-(4,5-Dimethylthiatol-2-yl)-2,5-diphenyl tetrazolium bromide)
NHS-PEG-VS	Alpha-vinyl sulfone-? -N-hydroxysuccinimide ester poly(ethylene glycol)

N/P	Ratio of nitrogen to phosporous
PAH	Pulmonary arterial hypertension
PAI	Pseudomonas aeruginosa infection
PCP	Pneumocystis-carinii-pneumonia
PDI	Polydispersity index
pDNA	Plasmid deoxyribonucleic acid
PEG	Poly(ethylene glycol)
PEGPEI	Poly(ethylene glycol)-graft-polyethyleneimine
$(PEG5k)_2PEI$	[5 kDa Poly(ethylene glycol)]$_2$-graft-polyethyleneimine
$(PEG550)_{35}PEI$	[550 Da Poly(ethylene glycol)]$_{35}$-graft-polyethyleneimine
PEI	Polyethyleneimine
PMN	Polymorph-nuclear leucocytes
PTD	Protein transduction domain
SD	Standard deviation
TAT	Decapeptide GRKKKRRQRC
TAT-PEG-PEI	Conjugate of BPEI and TAT linked via NHS-PEG-VS
Tc	Phase transition temperatures
TNF-α	Tumour necrosis factor alpha

CURRICULUM VITAE

Persönliche Daten

Elke Kleemann

geboren am 21.02.1977 in Leipzig

ledig

Studium und Schulbildung

10/2001	Approbation als Apothekerin
01/2001 – 08/2001	Diplompharmazie an der Martin-Luther-Universität Halle während des Praktikums bei der Jenapharm GmbH & Co. KG
10/1995 – 04/2000	Studium der Pharmazie an der Ernst-Moritz-Arndt-Universität Greifswald
07/1995	Abitur am Ehrenberg-Gymnasium Delitzsch

Praktika und berufliche Tätigkeiten

01/2002 – heute	Wissenschaftlicher Mitarbeiter der Philipps-Universität Marburg. Anfertigungen der vorliegenden Dissertation unter Leitung von Herrn Prof. Dr. Thomas Kissel, Institut für Pharmazeutische Technologie und Biopharmazie, Marburg.
01/2001 – 07/2001	Praktikum bei der Jenapharm GmbH & Co. KG, Abteilung Galenische Entwicklung,
05/2000 – 10/2000	Pharmaziepraktikum in der Kaufpark Apotheke, Dresden

LIST OF PUBLICATIONS

Publications

E. Kleemann, L. A. Dailey, H. G. Abdelhady, T. Gessler, T. Schmehl, C. J. Roberts, M. C. Davies, W. Seeger & T. Kissel. Modified polyethylenimines as non-viral gene delivery systems for aerosol gene therapy: Investigations of the complex structure and stability during air-jet and ultrasonic nebulization. *Journal of Controlled Release* **100(3)**: 437-450 (2004).

E. Kleemann, N. Jekel, L. Fink, T. Gessler, T. Schmehl, C. J. Roberts, W. Seeger & T. Kissel. Enhanced pulmonary gene expression is facilitated by low toxicity of low-molecular-weight polyethylenimine under in vivo conditions. *Journal of Gene Medicine:* revised (2005).

E. Kleemann, M. Neu, N. Jekel, L. Fink, T. Schmehl, T. Gessler, W. Seeger & T. Kissel. Nano-carriers for DNA delivery to the lung based upon TAT peptide covalently coupled to PEG-PEI. *Journal of Controlled Release*: submitted (2005).

C. Brus, E. Kleemann, A. Aigner, F. Czubayko & T. Kissel. Stabilization of oligonucleotide-polyethylenimine complexes by freeze-drying: physicochemical and biological characterization. *Journal of Controlled Release* **95(1)**:119-31 (2004).

L.A. Dailey, E. Kleemann, T. Merdan, H. Petersen, T. Gessler, T. Schmehl, W. Seeger & T. Kissel. Modified polyethylenimines as non viral gene delivery systems for aerosol therapy: Effects of nebulization on cellular uptake and transfection efficiency. *Journal of Controlled Release* **100(3)**: 425-436 (2004).

L.A. Dailey, E. Kleemann, M. Widmar, T. Gessler, T. Schmehl, C. Roberts, W. Seeger & T. Kissel. Surfactant-free, biodegradable nanoparticles for aerosol therapy based upon the branched polyesters, DEAPA-PVAL-g-PLGA. *Pharmaceutical Research* **20(12)**: 2011-20 (2003).

Poster presentations

E. Kleemann, N. Jekel, L. Fink, T. Schmehl, T. Gessler, W. Seeger & T. Kissel. Modified polyethylenimines as non viral gene delivery systems for the lung: Investigations of physico-chemical properties and transfection efficiency. *12th Annual Congress of the European Society of Gene Therapy* Nov. 2004, Tampere, Finland

E. Kleemann, N. Jekel, L. Fink, T. Schmehl, T. Gessler, T. Kissel & W. Seeger. Comparison of in vitro and in vivo gene expression of three different PEI-DNA-complexes. *100th International Conference of the American Thoracic Society* May 2004, Orlando, USA

T. Gessler, L.A. Daily, E. Kleemann, T. Schmehl, J. Hänze, T. Kissel & W. Seeger. Einfluss der Verneblung auf die in vitro Transfektion von polymeren nanopartikulären DNA-Komplexen. *VIII. Deutsches Aerosol Therapie Seminar* Nov. 2003 Marburg, Germany

E. Kleemann, L.A. Dailey, H. Petersen, H.G. Abdelhady, C.J. Roberts, M.C. Davies, T. Schmehl, T. Gessler, W. Seeger & T. Kissel. Polyethylenimine as non-viral carrier for aerosol gene therapy: Investigations of the complex stability and characterisation by AFM. *30th Annual Meeting and Exposition of the Controlled Release Society* Jul. 2003, Glasgow, UK

E. Kleemann, T. Gessler, T. Schmehl, T. Kissel & W. Seeger. Inhalativ applizierbare Liposomen zur retardierten Freisetzung von Wirkstoffen. *VII. Deutsches Aerosol Therapie Seminar* Nov. 2002 Kassel, Germany

Oral presentations

Comparison of in vitro and in vivo gene expression of three different PEI-DNA-complexes. *100th International Conference of the American Thoracic Society* May 2004, Orlando, USA

Characterization of PEI-DNA polyplexes for lung gene therapy. *DPhG Doktorandentagung* Mar. 2004, Freudenstadt, Germany

A low molecular weight polyethylenimine as a non-viral carrier for aerosol gene therapy: Investigations of transfection and complex stability. *Socrates Intensive Programme: Innovative Therapeutics from molecules to drugs* Jul. 2003, London, UK

Polyethylenimine-DNA-complexes: Non-Viral carrier for aerosol gene therapy. *School of Pharmaceutical Science, University of Nottingham* Oct. 2002, Nottingham, UK